STOCHASTIC GEOMETRY:

Selected Topics

Viktor Beneš
Jan Rataj

KLUWER ACADEMIC PUBLISHERS

STOCHASTIC GEOMETRY:
Selected Topics

STOCHASTIC GEOMETRY:
Selected Topics

by

Viktor Beneš
Faculty of Mathematics and Physics
Charles University, Prague

Jan Rataj
Faculty of Mathematics and Physics
Charles University, Prague

KLUWER ACADEMIC PUBLISHERS
NEW YORK, BOSTON, DORDRECHT, LONDON, MOSCOW

eBook ISBN: 1-4020-8103-0
Print ISBN: 1-4020-8102-2

Created in the United States of America

Visit Springer's eBookstore at: http://www.ebooks.kluweronline.com
and the Springer Global Website Online at: http://www.springeronline.com

Contents

Preface

Since the seventies years of the past century, stimulated namely by the ingenious collection edited by Harding and Kendall [47] and Matheron's monograph [69], stochastic geometry is a field of rapidly increasing interest. Based on the current achievements of geometry, probability and measure theory, it enables modeling of two- and three-dimensional random objects with interactions as they appear in microstructure of materials, biological tissues, macroscopically in soil, geological sediments, etc. In combination with spatial statistics it is used for the solution of practical problems such as description of spatial arrangement and estimation of object characteristics. A related field is stereology which makes inference on the structures based on lower-dimensional observations.

The subject of stochastic geometry and stereology is nowadays broadly developed so that it can be hardly covered by a single monograph. This was successfuly tried in the eighties by Stoyan et al. [109] (the first edition appeared in 1987), recently, however, specialized books appear more frequently, as those by Schneider & Weil [103], Vedel-Jensen [116], Howard & Reed [54], Van Lieshout [115], Barndorff-Nielsen et al. [2], Ohser & Mücklich [86] and Møller & Waagepetersen [80]. This list might be followed by volumes on the shape theory and random tessellations. We tried to continue this series by collecting several recently studied topics of stochastic geometry and stereology, with accents on fibre and surface systems, particle systems, estimation of intensities, anisotropy analysis and statistics of particle characteristics.

Like in all applied areas, a close cooperation between theoretical mathematicians working in stochastic geometry and related fields and scientists doing applied research is necessary, and there are several activities aiming at a satisfaction of this need. Among them, we may mention regular stereological congresses organized by International Society for Stereology, where biologists, medical doctors, material scientists and

mathematicians meet together, further the joint workshops of mathematitians and physicists interested in stochastic geometry organized by D. Stoyan (see [74]).

The present book is an attempt to present the theory in a concise mathematical way, but illustrated with a number of practical demonstrations on simulated or real data.

After the first chapter presenting necessary background from measure theory, convex geometry, probability and statistics, Chapter 2 is devoted to an overview of the basic notions and results on random sets, random measures and point processes in the euclidean space (we refer here frequently to the monograph of Daley & Vere-Jones [23]). Section 3 deals with stationary random fibre and surface systems and the estimation of their intensities. In our terminology, a random fibre (surface) system is a random closed set, whereas the notion of a fibre (surface) process is reserved for genuine processes of fibres (surfaces). Using an approach of geometric measure theory, fibres (surfaces) are modelled by Hausdorff rectifiable sets, as suggested by Zähle [125] already in 1982, but not widely accepted in stochastic geometry so far.

Chapter 4 is devoted to an important method of geometric sampling called "vertical" and originated in the eighties by Baddeley, Cruz-Orive and Gundersen (see [1, 4]). Vertical sampling is a promising alternative to isotropic uniform random (IUR) sampling which is hardly applicable to real structures. Vertical sampling designs are applied to the intensity estimation of random fibre and surface systems and following the joint research with Gokhale [39], [51] to the estimation of some other characteristics as particle mean width or integral mixed curvature. We use both model- and design-based approaches in this chapter.

The analysis of anisotropy of a random fibre or surface system is the contents of Chapter 5. We focus on both planar and spatial fibre systems and spatial surface systems. An overview is presented of different methods solving the inversion of the well-known formula connecting the rose of intersections with the rose of directions (see (5.10)). The estimation of the orientation-dependent rose of normal directions (for the boundary of a full-dimensional body in the space) is considered as well.

Section 6 deals with the stereology of particle systems, reviewing and developing some classical methods of unfolding of particle parameters using data from planar sections. Including particle orientations among parameters requires again vertical sections to be employed for sampling. Finally, applying the statistical theory of extremes it is shown how to detect extremal characteristics of particles.

Acknowledgments

The research work included was supported by several grants, most recently by the Czech Ministery of Education project MSM 113200008, the Grant Agency of the Czech Republic, project 201/03/0946, Grant Agency of the Academy of Sciences of the Czech Republic, project IAA 1057201 and Grant Agency of Charles University, project No. 283/2003 /B-MAT/MFF. PhD students and post-doctorands from the Faculty of Mathematics and Physics, Charles University in Prague, participated on the solution of grants and parts of their papers are reported. This concerns D. Hlubinka, P. Krejčíř, T. Mrkvička, M. Hlawiczková, K. Bodlák, Z. Pawlas and M. Prokešová. Particular thanks are addressed to Zbyněk Pawlas and Josef Machek for corrections and comments to the book. Zbyněk Pawlas moreover edited most of the figures.

Chapter 1

PRELIMINARIES

1.1. Geometry and measure in the Euclidean space

Let $\mathbb{R}^d$ denote the d-dimensional Euclidean space with Euclidean norm $\|\cdot\|$ and scalar product $\langle\cdot,\cdot\rangle$. By $B_r(x)$ we shall denote the closed ball with centre x and radius r and we shall write briefly $B_r \equiv B_r(0)$. The symbol $\mathbb{S}^{d-1} = \{u \in \mathbb{R}^d : \|u\| = 1\}$ denotes the unit sphere, $\mathrm{SO}(d)$ the group of rotations in $\mathbb{R}^d$ and $\mathcal{L}_k$ the Grassmannian of k-dimensional linear subspaces of $\mathbb{R}^d$, $k = 0, 1, \ldots, d$. The space $\mathcal{L}_k$ is equipped with the unique rotation invariant (uniform) probability distribution denoted by U.

For two subsets A, B of $\mathbb{R}^d$, we denote by

$$A \oplus B = \{a + b : a \in A, b \in B\}$$

the Minkowski sum of A and B and we write shortly $A + b$ instead of $A \oplus \{b\}$ (the translate of A by the vector b). Further,

$$A \ominus B = \bigcap_{b \in B} (A + b)$$

denotes the Minkowski subtraction of A and B. By $\check{B} = \{-b : b \in B\}$ we denote the central reflection of B and the set $A \oplus \check{B}$, $A \ominus \check{B}$ is called the dilation, erosion of A with B, respectively. It follows from the definition that $z \in A \oplus \check{B}$ if and only if the translate $z + B$ hits A, whereas $z \in A \ominus \check{B}$ if and only if $z + B$ is contained in A.

The symbol $[x, y]$ denotes the segment with end-points $x, y \in \mathbb{R}^d$.

1.1.1 Measures

Under a *measure* we always understand a nonnegative and σ-additive set functional. A *Borel measure* in $\mathbb{R}^d$ is a measure defined on the σ-algebra $\mathcal{B}^d$ of Borel subsets of $\mathbb{R}^d$. The symbol δ_x denotes the Dirac measure concentrated in $x \in \mathbb{R}^d$, i.e., $\delta_x(B) = \mathbf{1}_B(x)$, where $\mathbf{1}_B$ is the characteristic function of the set B (i.e., $\mathbf{1}_B(x) = 1$ for $x \in B$ and $\mathbf{1}_B(x) = 0$ otherwise).

If μ is a measure on a measurable space $(A, \mathcal{A})$ and $f : (A, \mathcal{A}) \to (E, \mathcal{E})$ a measurable mapping, then μf^{-1} denotes the f-image of μ, i.e., a measure on $(E, \mathcal{E})$ given by

$$\mu f^{-1}(B) = \mu(f^{-1}(B)), \quad B \in \mathcal{E}. \tag{1.1}$$

For two measures μ, ν on $(A, \mathcal{A})$ we say that ν is *absolutely continuous* with respect to μ (written as $\nu \ll \mu$) if any μ-null set is also a ν-null set. If this holds for σ-finite measures μ, ν, then there exists a μ-almost everywhere unique measurable function $f : A \to \mathbb{R}_+$ (called a density of ν with respect to μ) such that $\nu(A) = \int_A f d\mu$.

The *support* of a measure μ on $(\mathbb{R}^d, \mathcal{B}^d)$ is defined as

$$\operatorname{supp} \mu = \bigcap \{F \subset \mathbb{R}^d \text{ closed } : \mu(\mathbb{R}^d \setminus F) = 0\},$$

$\operatorname{supp} \mu$ is the smallest closed set such that μ vanishes on its complement.

The *convolution* of two measures μ, ν on $(\mathbb{R}^d, \mathcal{B}^d)$ is the Borel measure in $\mathbb{R}^d$

$$\mu * \nu = (\mu \times \nu)+^{-1}, \tag{1.2}$$

where $\mu \times \nu$ is the product measure in $\mathbb{R}^d \times \mathbb{R}^d$ and $+ : (x, y) \mapsto x + y$ is the usual operation af addition. Using (1.1) and the Fubini theorem, we get the standard formula

$$\begin{aligned} (\mu * \nu)(B) &= (\mu \times \nu)(+^{-1}(B)) \\ &= (\mu \times \nu)(\{(x, y) : x + y \in B\}) \\ &= \int \nu(B - x)\mu(\mathrm{d}x). \end{aligned}$$

The definition of the convolution can be applied analogously for any two measures on a measurable space equipped with the addition operation which should be measurable.

By ν_d we shall always denote the Lebesgue measure in $\mathbb{R}^d$ and $\omega_d = \nu_d(B_1)$ denotes the volume of the unit ball in $\mathbb{R}^d$. For the integration with respect to the Lebesgue measure we shall sometimes write only "$\mathrm{d}x$" instead of "$\nu_d(\mathrm{d}x)$".

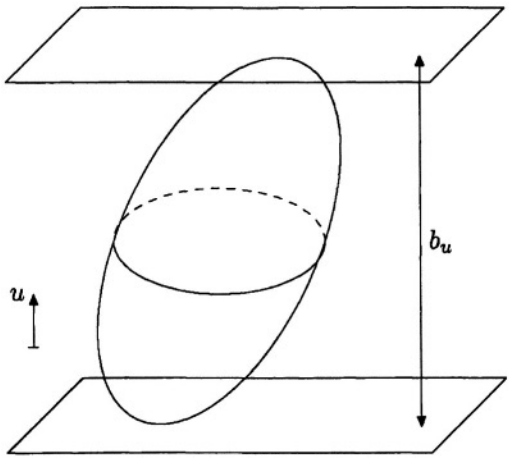

Figure 1.1. **Definition of the width of a convex body.**

1.1.2 Convex bodies

Let $\mathcal{C}, \mathcal{C}'$ be the system of all compact convex sets, nonempty compact convex sets in $\mathbb{R}^d$, respectively. A set $K \in \mathcal{C}'$ is called a convex body. If $K \in \mathcal{C}'$ then for each $u \in \mathbb{S}^{d-1}$ there is exactly one number $h(K,u)$ such that the hyperplane (line in $\mathbb{R}^2$, plane in $\mathbb{R}^3$)

$$\{x \in \mathbb{R}^d : \langle x,u\rangle - h(K,u) = 0\} \tag{1.3}$$

intersects K and $\langle x,u\rangle - h(K,u) \leq 0$ for each $x \in K$. This hyperplane is called the *support hyperplane* and the function $h(K,u)$, $u \in \mathbb{S}^{d-1}$, is the *support function* (restricted to $\mathbb{S}^{d-1}$) of K. Equivalently, one can define

$$h(K,u) = \sup\{\langle x,u\rangle, x \in K\}, \quad u \in \mathbb{R}^d. \tag{1.4}$$

Its geometrical meaning is the signed distance of the support hyperplane from the origin of coordinates. The sum $h(K,u) + h(K,-u) = b_u(K)$, $u \in \mathbb{S}^{d-1}$, is the *width* of K - the distance between the parallel support hyperplanes, see Fig. 1.1. An important property of $h(K,u)$ is its additivity in the first argument: $h(K_1 \oplus K_2, u) = h(K_1,u) + h(K_2,u)$. A convex body K is *centrally symmetric* if $K' = \check{K}'$ for some translate K' of K, i.e., if K has a centre of symmetry. In what follows, mostly convex bodies that possess a centre of symmetry will be considered.

The Minkowski sum of finitely many centred line segments is called a *zonotope*. Besides of being centrally symmetric, in $\mathbb{R}^3$ also its two-dimensional faces are centrally symmetric. Consequently, regular octahedron, icosahedron and pentagonal dodecahedron are not zonotopes.

On the other hand, in $\mathbb{R}^2$, all centrally symmetric polygons are zonotopes.

Consider a zonotope

$$Z = \bigoplus_{i=1}^{k} a_i[v_i, -v_i], \tag{1.5}$$

where $a_i > 0$, $v_i \in \mathbb{S}^{d-1}$. Its support function is given by

$$h(Z, u) = \sum_{i=1}^{k} a_i |\langle u, v_i \rangle| \tag{1.6}$$

and, conversely, a body $Z \in \mathcal{C}'$ with the support function (1.6) is a zonotope with the centre in the origin.

We shall use the standard notation $\mathcal{K}'$ for the space of all nonempty compact subsets of $\mathbb{R}^d$ equipped with the *Hausdorff metric* (see [69, 43])

$$d_H(K, L) = \max \left\{ \sup_{x \in K} \operatorname{dist}(x, L), \sup_{y \in L} \operatorname{dist}(y, K) \right\} \tag{1.7}$$

($\operatorname{dist}(x, L) = \inf_{z \in L} \|x - z\|$ is the distance of a point x from the set L).

The corresponding convergence is denoted as d_H-convergence. A set $Z \in \mathcal{C}'$ is called a *zonoid* if it is a d_H-limit of a sequence of zonotopes.

A convex body Z is a zonoid if and only if its support function has a representation

$$h(Z, u) = \int_{\mathbb{S}^{d-1}} |\langle u, v \rangle| \mu(\mathrm{d}v), \tag{1.8}$$

for an even measure μ on $\mathbb{S}^{d-1}$ (see [41, Theorem 2.1]). The measure μ is called the *generating measure* of Z and it is unique as shown in [69, Theorem 4.5.1], see also [41]. For the zonotope (1.5) we have the generating measure

$$\mu = \sum_{i=1}^{k} a_i \epsilon_{v_i}, \tag{1.9}$$

where $\epsilon_{v_i} = \frac{1}{2}(\delta_{v_i} + \delta_{-v_i})$.

Zonotopes and zonoids have several interesting properties and wide applications (see [41], [101]), e.g. the polytopes filling (tiling) $\mathbb{R}^3$ by translations are obligatory zonotopes (cubes, rhombic dodecahedrons, tetrakaidecahedrons).

EXERCISE 1.1 *Express the support function of a line segment in* $\mathbb{R}^2$ *in polar coordinates.*

EXERCISE 1.2 *Verify the additivity formula*

$$h(K \oplus L, \cdot) = h(K, \cdot) + h(L, \cdot).$$

EXERCISE 1.3 *Verify the following formula for the Hausdorff distance of two convex bodies:*

$$d_H(K, L) = \sup_{u \in \mathbb{S}^{d-1}} |h(K, u) - h(L, u)|.$$

EXERCISE 1.4 *Show that the family $\mathcal{C}'$ of convex bodies is closed in $\mathcal{K}'$ with respect to the Hausdorff metric.*

1.1.3 Hausdorff measures and rectifiable sets

In this subsection we give a survey of some notions and results from geometric measure theory which can be found in Federer [31] or Mattila [70]. An instructive treatment of the area and coarea formulae for smooth sets with applications in stochastic geometry was presented by Vedel-Jensen [116].

Let $k \in \{0, 1, \ldots, d\}$ be fixed. The *Hausdorff measure* $\mathcal{H}^k$ of order k in $\mathbb{R}^d$ is defined as

$$\mathcal{H}^k(A) = \lim_{\delta \to 0+} \inf_{\substack{A \subset \bigcup_i G_i \\ \operatorname{diam} G_i \leq \delta}} \sum_i \omega_k \left(\frac{\operatorname{diam} G_i}{2} \right)^k, \tag{1.10}$$

where $\operatorname{diam} G_i$ denotes the diameter of G_i and the infimum is taken over all at most countable coverings of A with (any) sets of diameters less or equal to δ. Equation (1.10) may be applied to any subset A of $\mathbb{R}^d$, defining $\mathcal{H}^k$ as an outer measure (called a measure in [31, §2.1.2]). The outer measure $\mathcal{H}^k$ becomes a measure when restricted to the family of $\mathcal{H}^k$-**measurable** sets which encompass the family of Borel sets. It can be shown that $\mathcal{H}^k$ is Borel regular (i.e., for any $A \subseteq \mathbb{R}^d$ there exists a Borel set $B \supseteq A$ with $\mathcal{H}^k(B) = \mathcal{H}^k(A)$), motion invariant, homogeneous of order k and, in particular, $\mathcal{H}^0$ is the counting measure and $\mathcal{H}^d = \nu_d$. Note that $\mathcal{H}^k$ extends the standard k-**dimensional** differential-geometric measure defined on C^1 smooth k-**dimensional** submanifolds of $\mathbb{R}^d$, see e.g. [97].

We call a subset $A \subset \mathbb{R}^d$ k-***rectifiable*** if it is a Lipschitz image of a bounded subset of $\mathbb{R}^k$ (a mapping f is *Lipschitz* if there exists a constant M such that $\|f(x) - f(y)\| \leq M\|x - y\|$ for any x, y from the domain of f). A set $A \subset \mathbb{R}^d$ is $(\mathcal{H}^k, k)$-***rectifiable*** if

1) A is $\mathcal{H}^k$-**measurable**,

2) $\mathcal{H}^k(A) < \infty$,

3) $A = \bigcup_{i=0}^{\infty} W_i$ with $\mathcal{H}^k(W_0) = 0$ and W_i k-rectifiable for $i \geq 1$.

Finally, $A \subset \mathbb{R}^d$ is *$\mathcal{H}^k$-rectifiable* if $A \cap K$ is $(\mathcal{H}^k, k)$-rectifiable for any $K \subset \mathbb{R}^d$ compact.

Any piecewise C^1-smooth k-dimensional manifold in $\mathbb{R}^d$ is $\mathcal{H}^k$-rectifiable, but the class of $\mathcal{H}^k$-rectifiable sets is substantially larger. For example, the distance function from any subset of $\mathbb{R}$ (even a fractal one) is Lipschitz and, hence, its graph is even 1-rectifiable. For the purposes of stochastic geometry, $\mathcal{H}^k$-rectifiable sets have the important property that the rectifiability is inherited by sections almost surely (cf. Theorems 1.11, 1.12).

Unlike the case of (piecewise) smooth manifolds, $\mathcal{H}^k$-rectifiable sets need not possess k-dimensional tangent planes in the usual sense at almost all points. Nevertheless, this property is true with a suitably adjusted definition of tangent vectors.

The *tangent cone* of a set $A \subset \mathbb{R}^d$ at $a \in \mathbb{R}^d$ is the closed cone in $\mathbb{R}^d$, $\operatorname{Tan}(A, a)$, defined by the following property: $0 \in \operatorname{Tan}(A, a)$, and a vector $u \neq 0$ belongs to $\operatorname{Tan}(A, a)$ if and only if for any $\varepsilon > 0$ there exists $b \in A$ with $0 < \|b - a\| < \varepsilon$ and

$$\left| \frac{u}{\|u\|} - \frac{(b-a)}{\|b-a\|} \right| < \varepsilon.$$

The *k-approximate tangent cone* of A at a is then given by

$$\operatorname{Tan}^k(A, a) = \bigcap \{\operatorname{Tan}(B, a) : \Theta^k(A \setminus B, a) = 0\},$$

where

$$\Theta^k(E, a) = \limsup_{\varepsilon \to 0+} \frac{\mathcal{H}^k(E \cap B_\varepsilon(a))}{\omega_k \varepsilon^k}$$

is the (upper) k-dimensional density of E in a. The set $\operatorname{Tan}^k(A, a)$ is again a closed cone in $\mathbb{R}^d$ which is in general a subset of $\operatorname{Tan}(A, a)$. Roughly speaking, we can say that $\operatorname{Tan}^k(A, a)$ neglects the "lower than k-dimensional components" of A, see Fig. 1.2. If A is a k-dimensional C^1-manifold, $\operatorname{Tan}^k(A, a) = \operatorname{Tan}(A, a)$ coincides with the classical tangent k-plane at a. The importance of the approximate tangent cones follows from the following theorem.

THEOREM 1.5 ([31, §3.2.19]) *If A is $(\mathcal{H}^k, k)$-rectifiable, then for $\mathcal{H}^k$-almost all $a \in A$, $\operatorname{Tan}^k(A, a)$ is a k-dimensional subspace of $\mathbb{R}^d$.*

Let $A \subset \mathbb{R}^d$ be $(\mathcal{H}^k, k)$-rectifiable and let $f : A \to \mathbb{R}^n$ be Lipschitz. It is not difficult to show that $f(A)$ is $(\mathcal{H}^k, k)$-rectifiable (in $\mathbb{R}^n$) as well. It

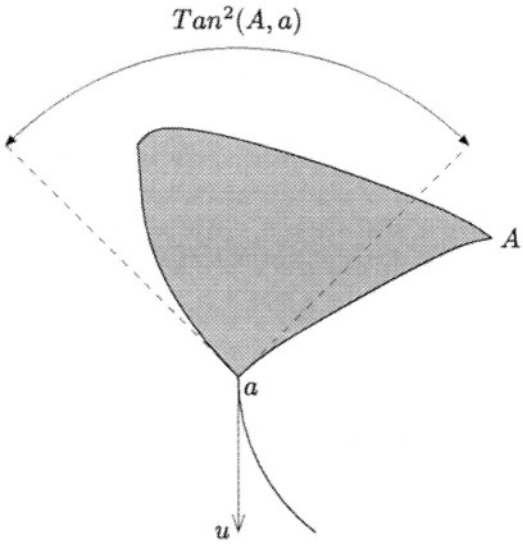

Figure 1.2. $\operatorname{Tan}^k(A,a)$ neglects the lower than k-dimensional components of A: $u \in \operatorname{Tan}(A,a)$ but $u \notin \operatorname{Tan}^2(A,a)$.

can further be shown that f can be approximated by a C^1-differentiable mapping g on $\mathbb{R}^d$ such that $\Theta^k(\{f \neq g\}, a) = 0$ for $\mathcal{H}^k$-almost all $a \in A$. If $a \in A$ is such a point and if, furthermore, $\operatorname{Tan}^k(A,a)$ is a k-dimensional subspace, we define the *approximate differential* of f at a, $\operatorname{ap} \mathrm{D} f(a)$, as the restriction of the differential $\mathrm{D}g(a)$ to the approximate tangent subspace $\operatorname{Tan}^k(A,a)$ (the correctness can be shown). For $m \leq k$, the *m-dimensional approximate Jacobian* of f at a is then defined as

$$\operatorname{ap} J_m f(a) = \sup_C \nu_m(\operatorname{ap} \mathrm{D} f(a)(C)),$$

where the supremum is taken over all unit m-cubes C in $\operatorname{Tan}^k(A,a)$. Note that, if A is a C^1-submanifold and f is differentiate on A, $\operatorname{ap} \mathrm{D} f(a)$ is the classical differential and $\operatorname{ap} J_k f(a)$ the classical Jacobian of f at a.

Now we can formulate the general area-coarea formula:

THEOREM 1.6 ([31, §§3.2.20,22]) *Let $A \subset \mathbb{R}^d$ be $(\mathcal{H}^k, k)$-rectifiable and $B \subset \mathbb{R}^n$ $(\mathcal{H}^m, m)$-rectifiable, $k \geq m$, let $f : A \to B$ be a Lipschitz mapping and let $h : A \to \mathbb{R}$ be a nonnegative measurable function. Then*

$$\int_A \operatorname{ap} J_m f(a)\, h(a)\, \mathcal{H}^k(\mathrm{d}a) = \int_B \int_{f^{-1}\{z\}} h(x) \mathcal{H}^{k-m}(\mathrm{d}x) \mathcal{H}^m(\mathrm{d}z).$$

EXERCISE 1.7 *If $g : \mathbb{R}^d \to \mathbb{R}^n$ is differentiable at a and $d \geq n$ then*

$$\operatorname{ap} J_n g(a) = \sqrt{\det(\mathrm{D}g(a)^T \mathrm{D}g(a))},$$

where $\mathrm{D}g(a)$ represents the matrix of partial derivatives of g at a.

EXERCISE 1.8 *If $f = g \mid A$ is the restriction of a differentiable mapping to a $(\mathcal{H}^k, k)$-rectifiable set $A \subset \mathbb{R}^d$ then $\operatorname{ap} \mathrm{D}f(a) = \mathrm{D}g(a) \mid \operatorname{Tan}^k(A, a)$ for $\mathcal{H}^k$-almost all $a \in A$.*

EXERCISE 1.9 *Show that the boundary of a convex body in $\mathbb{R}^d$ is $(d-1)$-rectifiable.*

EXERCISE 1.10 *Let Γ be a C^1-smooth curve in $\mathbb{R}^d$ of finite length and let p_L denote the orthogonal projection onto a subspace $L \in \mathcal{L}_{d-1}$. Assume that the projection p_L is injective $\mathcal{H}^1$-almost everywhere on Γ. By using Theorem 1.6, show that*

$$\mathcal{H}^1(p_L(\Gamma)) = \int_\Gamma \cos \sphericalangle(t(x), L) \mathcal{H}^1(\mathrm{d}x),$$

where $t(x) = \operatorname{Tan}^1(\Gamma, x)$ is the tangent direction of Γ at $x \in \Gamma$.

1.1.4 Integral geometry

The object of integral geometry are mainly formulas involving kinematic (translative) integrals of some geometric quantities. As classical reference, the book of Santaló [97] serves, whereas for our purposes, later treatment using the measure theoretic language is more appropriate (e.g. [104, 102]).

One of the simplest integral-geometric formulas follows directly from the Fubini theorem. If A is a measurable subset of $\mathbb{R}^d$ and F a k-flat in $\mathbb{R}^d$ (a k-dimensional affine subspace), then

$$\nu_d(A) = \int_{F^\perp} \nu_k(A \cap (F + y)) \nu_{d-k}(\mathrm{d}y), \tag{1.11}$$

where $F^\perp$ denotes the subspace perpendicular to F. Including an additional integration over rotations, one obtains

$$\nu_d(A) = \int_{\mathcal{F}_k} \nu_k(A \cap F) \mu_k(\mathrm{d}F), \tag{1.12}$$

where $\mathcal{F}_k$ is the space of all k-flats in $\mathbb{R}^d$ and μ_k the motion invariant measure on $\mathcal{F}_k$ normed as the product of the uniform probability distribution on $\mathcal{L}_k$ with $(d-k)$-dimensional Lebesgue measure (i.e., we can

write $\mu_k(\mathrm{d}F) = \nu_{d-k}(\mathrm{d}y)U(\mathrm{d}L)$, if $F = L+y$ is the unique decomposition of $F \in \mathcal{F}_k$ into a linear subspace L and a shift $y \in L^\perp$). An analogous formula for the volume of the intersection of two bodies follows again from the Fubini theorem:

$$\int_{\mathcal{G}_d} \nu_d(A \cap gB)\vartheta_d(\mathrm{d}g) = \nu_d(A)\nu_d(B), \tag{1.13}$$

where $\mathcal{G}_d$ is the group of all euclidean motions in $\mathbb{R}^d$ (i.e., compositions of rotations and translations) and ϑ_d the invariant measure corresponding to the product of the rotation invariant probability distribution over the group of rotations and the d-dimensional Lebesgue measure over translations.

Kinematic formulas can be written also for the Hausdorff measure of lower-dimensional (rectifiable) sets. We present here, for illustration, a result of this type due to Zähle [125, §1.5.1].

THEOREM 1.11 *Let $m+n \geq d$ be natural numbers and let A be an $\mathcal{H}^m$-rectifiable and B an $\mathcal{H}^n$-rectifiable subsets of $\mathbb{R}^d$ such that their cartesian product $A \times B$ is $\mathcal{H}^{m+n}$-rectifiable. Then $A \cap gB$ is $\mathcal{H}^{m+n-d}$-rectifiable for ϑ_d-almost all motions g and we have*

$$\int_{\mathcal{G}_d} \mathcal{H}^{m+n-d}(A \cap gB)\vartheta_d(\mathrm{d}g) = \gamma_{d,m,n}\mathcal{H}^m(A)\mathcal{H}^n(B),$$

where (denoting $\Gamma(\cdot)$ the Euler gamma function)

$$\gamma_{d,m,n} = \frac{\Gamma\left(\frac{m+1}{2}\right)\Gamma\left(\frac{n+1}{2}\right)}{\Gamma\left(\frac{m+n-d+1}{2}\right)\Gamma\left(\frac{d+1}{2}\right)}.$$

Translation formulas for the Hausdorff measure are more involved, including integration over Jacobians. We present a particular version here which will be used later. To do this, we need some notation. Let M, N be two linear subspaces of $\mathbb{R}^d$ of dimensions m, n, respectively, with $m+n \geq d$, and let $\{u_1, \ldots, u_m\}$, $\{v_1, \ldots, v_n\}$ be orthonormal bases of M, N such that $\{u_1 = v_1, \ldots, u_k = v_k\}$ is a basis of $M \cap N$. We shall denote by $[M, N]$ the (d-dimensional) volume of the parallelepiped spanned by $u_1, \ldots, u_m, v_{k+1}, \ldots, v_n$. Note that if $m = n = d-1$ then $[M, N] = \sin \sphericalangle(M^\perp, N^\perp)$.

THEOREM 1.12 *Let m, n, A, B be as in Theorem 1.11. Then $A \cap (B-z)$ is $\mathcal{H}^{m+n-d}$-rectifiable for ν_d-almost all $z \in \mathbb{R}^d$ and we have*

$$\int_{\mathbb{R}^d} \mathcal{H}^{m+n-d}(A \cap (B-z))\,\mathrm{d}z = \int_A \int_B [\mathrm{Tan}^m(A,a), \mathrm{Tan}^n(B,b)]\mathcal{H}^n(\mathrm{d}b)\mathcal{H}^m(\mathrm{d}a).$$

The theorem can be proved by applying the coarea formula (Theorem 1.6) to the function $(a, b) \mapsto b - a$ defined on $A \times B$ (for details, see [123, 125]).

More important are integral-geometric formulas for "second-order" (depending on second derivatives) quantities as quermassintegrals, intrinsic volumes or curvature measures. In order to define meaningfully these notions, we have to restrict ourselves to a smaller class of sets, e.g. to convex or polyconvex bodies, sets with smooth (C^2) boundaries, or some generalizations of these. We start for simplicity with convex bodies.

Given a convex body $K \subset \mathbb{R}^d$ and $k \in \{0, 1, \dots, d\}$, we define the **kth** *intrinsic volume* of K by

$$V_k(K) = \binom{d}{k} \frac{\omega_d}{\omega_k \omega_{d-k}} \int_{\mathcal{L}_k} \nu_k(p_L K) U(\mathrm{d}L)$$

(here p_L stands for the orthogonal projection to L). After renorming and reindexing, we get the classical quermassintegrals

$$W_{d-k}^d(K) = \frac{\omega_{d-k}}{\binom{d}{k}} V_k(K)$$

(the additional upper index at W indicates the dependence on the dimension of the embedding space). The intrinsic volumes can be defined also by means of the

$$\nu_d(K \oplus B_r) = \sum_{k=0}^{d} \omega_k r^k V_{d-k}(K). \tag{1.14}$$

A local version of the Steiner fomula makes it possible to introduce curvature measures of K as local variants of the intrinsic volumes (see [99]). If the boundary of K, ∂K, is C^2-smooth, we can also express the intrinsic volumes as integrals of certain functions of principal curvatures. We shall illustrate this fact only on the example of a smooth convex body in $\mathbb{R}^3$: let $k_1(x)$, $k_2(x)$ denote the principal curvatures of K at $x \in \partial K$ and denote

$$K(x) = k_1(x) k_2(x), \quad H(x) = \frac{k_1(x) + k_2(x)}{2} \tag{1.15}$$

the Gauss, mean (respectively) curvature of K at x. Then we have

$$V_0(K) = \frac{1}{\pi} \int_{\partial K} K(x) \mathcal{H}^{d-1}(\mathrm{d}x), \tag{1.16}$$

$$V_1(K) = \frac{1}{2\pi} \int_{\partial K} H(x) \mathcal{H}^{d-1}(\mathrm{d}x), \tag{1.17}$$

$$V_2(K) = \frac{1}{2} \int_{\partial K} \mathcal{H}^{d-1}(\mathrm{d}x). \tag{1.18}$$

Formulas (1.16), (1.17) and (1.18) can be applied as definitions of intrinsic volumes for sets with C^2 smooth boundaries (not necessarily convex). Note that local curvatures can be defined also for certain nonsmooth bodies (e.g. convex sets), but the integrals should be performed then over the unit normal bundle instead of the boundary only (see [126]).

On the other hand, formulas (1.17) and (1.18) together with our definition of intrinsic volumes can be rewritten in the form

$$S(K) = 4\int_{\mathcal{L}_2} \mathrm{area}(p_L K)U(\mathrm{d}L), \tag{1.19}$$

$$M(K) = \pi\int_{\mathcal{L}_1} \mathrm{length}(p_\ell K)U(\mathrm{d}\ell) = \int_{\mathcal{L}_2} \mathrm{perimeter}(p_L K)U(\mathrm{d}L), \tag{1.20}$$

which are known as *Cauchy* (or *Kubota*) *formulas;* here we use the classical notations $M(K)$ for the integral of mean curvature over ∂K and S for the surface area content.

Intrinsic volumes can be extended to polyconvex sets (finite unions of convex bodies) by additivity (i.e., the property $V_k(K\cup L)+V_k(K\cap L) = V_k(K) + V_k(L)$). Even after the extension, the following characteristic properties remain valid: V_0 is the Euler-Poincaré characteristic, V_{d-1} one half of the surface content (in case of a full-dimensional set), and V_d is the volume (Lebesgue measure). Of course, the Cauchy formulae are not valid for general polyconvex sets.

The basic integral-geometric relation for intrinsic volumes is

THEOREM 1.13 (PRINCIPAL KINEMATIC FORMULA) *Let K, L be polyconvex sets in* $\mathbb{R}^d$. *Then for* $k = 0, 1, \dots d$ *we have*

$$\int_{\mathcal{G}_d} V_k(K\cap gL)\vartheta_d(\mathrm{d}g) = \sum_{\substack{r+s=d+k\\ 0\le r,s\le d}} \gamma_{d,r,s}V_r(K)V_s(L)$$

(the constant $\gamma_{d,r,s}$ *is defined in Theorem 1.11).*

We remark that the principal kinematic formula holds for all reasonable extensions of intrinsic volumes and also that an appropriate generalization is true for the local versions (curvature measures). Replacing the second polyconvex set with a flat we obtain

THEOREM 1.14 (CROFTON FORMULA) *For a polyconvex set K in* $\mathbb{R}^d$ *and for* $j, k = \{0, 1, \dots d\}$ *with* $k \le j$ *we have*

$$\int_{\mathcal{F}_j} V_k(K\cap gF)\mu_j(\mathrm{d}F) = \gamma_{d,d+k-j,j}V_{d+k-j}(K).$$

EXERCISE 1.15 *Let M, N be linear subspaces of $\mathbb{R}^d$ of dimensions m, n, respectively. Then $[M, N]$ can equivalently be defined as the $(2d-m-n)$-dimensional volume of the parallelepiped spanned by any orthonormal bases of the complements $M^\perp$ and $N^\perp$.*

EXERCISE 1.16 *Applying Theorem 1.11, show that the translative integral of the number of intersection points of a curve ($(\mathcal{H}^1, 1)$-rectifiable set) Γ with a unit circle in $\mathbb{R}^2$ equals $4\mathcal{H}^1(\Gamma)$.*

EXERCISE 1.17 *Compute the intrinsic volumes of a two- and three-dimensional ball.*

EXERCISE 1.18 *Using mathematical induction, show the following iterative version of the principal kinematic formula valid for $p \geq 2$ convex bodies $K_1, \ldots, K_p$ in $\mathbb{R}^d$:*

$$\int_{\mathcal{G}_d} \cdots \int_{\mathcal{G}_d} V_k(K_1 \cap g_2 K_2 \cap \cdots \cap g_p K_p) \vartheta_d(\mathrm{d}g_p) \cdots \vartheta_d(\mathrm{d}g_2)$$
$$= \sum_{r_1+\cdots+r_p=(p-1)d+k} \gamma_{d,r_1,\ldots,r_p} V_{r_1}(K_1) \cdots V_{r_p}(K_p)$$

with the constants

$$\gamma_{d,r_1,\ldots,r_p} = \frac{\Gamma\left(\frac{r_1+1}{2}\right) \cdots \Gamma\left(\frac{r_p+1}{2}\right)}{\Gamma\left(\frac{r_1+\cdots+r_p-d}{2}\right) \Gamma\left(\frac{d+1}{2}\right)^{p-1}}.$$

1.2. Probability and statistics

In this section, $(\Omega, \mathcal{A}, \Pr)$ will denote a (fixed) abstract probability space, i.e., $\mathcal{A}$ is a σ-algebra of subsets of Ω and $\Pr$ a probability measure on $\mathcal{A}$. A measurable mapping X of Ω into a measurable space $(T, \mathcal{T})$ is called a random element in T. The distribution of X is a probability measure $\Pr X^{-1}$ on $\mathcal{T}$, cf. (1.1). Specially, if $T = \mathbb{R}$ we call X a random variable. Standard symbols are used for the expectation of a random variable $\mathrm{E}X = \int X \mathrm{d}\Pr$, variance $\mathrm{var}\, X = \mathrm{E}(X - \mathrm{E}X)^2$, covariance $\mathrm{cov}\,(X, Y) = \mathrm{E}(X - \mathrm{E}X)(Y - \mathrm{E}Y)$ of two random variables. For any random vector $X = (X_1, \ldots, X_n)$ the distribution function is defined as

$$F(x_1, \ldots, x_n) = \Pr\Big(\bigcap_{1 \leq k \leq n} [X_k \leq x_k]\Big), \quad (x_1, \ldots, x_n) \in \mathbb{R}^n.$$

A sequence of random elements (X_n) converges to a random element X *almost surely* (a.s.) if

$$\Pr\{\omega \in \Omega;\ \lim_{n\to\infty} X_n(\omega) = X(\omega)\} = 1.$$

For random elements $X, X_1, X_2, \ldots$ in a metric space (T, ρ) we say that the sequence (X_n) converges *in probability* to X (denoted $X_n \xrightarrow{\Pr} X$) if for any $\varepsilon > 0$

$$\lim_{n\to\infty} \Pr[\rho(X_n, X) > \varepsilon] = 0.$$

Almost sure convergence implies convergence in probability. A sequence (X_n) of random variables with partial sums $S_n = \sum_{i=1}^{n} X_i$ is said to obey the strong (weak) *law of large numbers* if $\frac{S_n}{n}$ converges almost surely (in probability) to a constant.

Let $\mathcal{T}$ be the Borel σ-algebra on a metric space (T, ρ). A sequence (μ_n) of probability measures on $\mathcal{T}$ *converges weakly* to a probability measure μ (we write $\mu_n \xrightarrow{w} \mu$) if $\int f \mathrm{d}\mu_n \to \int f \mathrm{d}\mu$ for every bounded continuous function $f : T \to \mathbb{R}$. A sequence (X_n) of random elements *converges in distribution* to a random element X (denoted $X_n \xrightarrow{d} X$) if $\Pr X_n^{-1} \xrightarrow{w} \Pr X^{-1}$. Convergence in probability implies convergence in distribution and both concepts coincide if X is almost surely a constant.

We shall denote by $N(a, \sigma^2)$ the Gaussian distribution with mean a and variance σ^2. Instead of $X_n \xrightarrow{d} X$ where X is Gaussian we sometimes write $X_n \xrightarrow{d} N(a, \sigma^2)$. We recall the classical central limt theorem for a sequence of independent identically distributed (i.i.d.) random variables, see e.g. [58, Proposition 4.9].

PROPOSITION 1.1 (LÉVY-LINDEBERG) *Let $X_1, X_2, \ldots$ be i.i.d. random variables with $\mathrm{E}X_1 = 0$ and $\mathrm{var}\, X_1 = 1$. Then*

$$n^{-\frac{1}{2}} \sum_{k=1}^{n} X_k \xrightarrow{d} N(0, 1).$$

For $p \geq 1$, let L^p be the class of random variables X with

$$\|X\|_p = (\mathrm{E}|X|^p)^{1/p} < \infty.$$

A sequence (X_n) of random variables converges to X in L^p if $\lim_{n\to\infty} \|X_n - X\|_p = 0$. Convergence in L^p implies convergence in probability. The converse implication is not true in general but it holds under an additional assumption. A system $(X_j,\ j \in J)$ of random variables is said to be *uniformly integrable* if

$$\lim_{q\to\infty} \sup_{j\in J} \int_{|X_j|>q} |\ X_j\ | \,\mathrm{d}\Pr = 0. \tag{1.21}$$

For the proof of the following result, see e.g. [58, Proposition 3.12].

PROPOSITION 1.2 *Let $X, X_1, X_2, \ldots$ be in L^p and let $X_n \xrightarrow{\Pr} X$. Then $X_n \to X$ in L^p if and only if the sequence $(|X_n|^p,\ n \in \mathbb{N})$ is uniformly integrable.*

In the following subsection on Markov chains we shall need the notion of a probability kernel.

DEFINITION 1.19 *Let $(T, \mathcal{T})$, $(E, \mathcal{E})$ be measurable spaces. A (probability) kernel from $(T, \mathcal{T})$ to $(E, \mathcal{E})$ is a mapping $\rho : T \times \mathcal{E} \to [0, \infty)$ such that (i) $t \mapsto \rho(t, A)$ is measurable for each $A \in \mathcal{E}$, (ii) $A \mapsto \rho(t, A)$ is a (probability) measure for all $t \in T$.*

1.2.1 Markov chains

The background of Markov chains on arbitrary state spaces is briefly described. All the notions and statements mentioned in this subsection can be found in [75].

Let $(E, \mathcal{E})$ be a Polish space (i.e., separable complete metric space) with Borel σ-algebra. Let μ be a probability measure on $\mathcal{E}$ and P a probability kernel from $(E, \mathcal{E})$ to $(E, \mathcal{E})$.

A collection $Y = \{Y_i\}_{i=0}^{\infty}$ of random elements in E is called a (*homogeneous*) *Markov chain* with transition kernel P and initial distribution μ if for any integer n and for any $A_i \in \mathcal{E}$, $i = 0, \ldots, n$, it holds

$$\Pr[Y_0 \in A_0, \ldots, Y_n \in A_n] = \int_{A_0} \cdots \int_{A_{n-1}} P(y_{n-1}, A_n) P(y_{n-2}, \mathrm{d}y_{n-1}) \ldots P(y_0, \mathrm{d}y_1) \mu(\mathrm{d}y_0).$$

The n-th power of the kernel P is defined by the recursive formula

$$P^n(x, A) = \int_E P^{n-1}(y, A) P(x, \mathrm{d}y), \tag{1.22}$$

where we set $P^0(x, A) = \delta_x(A)$. The value $P^n(x, A)$ is interpreted as the probability that the chain gets from state x to A in n steps.

The random variable $\tau_A = \min\{n \geq 1 :\ Y_n \in A\}$ is called the *return time* to a set $A \in \mathcal{E}$. A Markov chain Y is *ϕ-irreducible* with a probability measure ϕ on $(E, \mathcal{E})$ if $\phi(A) > 0$ implies $\Pr[\tau_A < \infty \mid Y_0 = x] > 0$ for all $x \in E$. According to [75, p. 88], for Y ϕ-irreducible there exists a maximal (w.r.t. partial ordering $\ll$) probability measure ψ such that Y is ψ-irreducible. Denote $\mathcal{E}^+ = \{A \in \mathcal{E} :\ \psi(A) > 0\}$.

A set $C \in \mathcal{E}$ is a *small set* if there exist $m > 0$, $\delta > 0$ and a probability measure ν such that for all $x \in C$ and $B \in \mathcal{E}$ it holds

$$P^m(x, B) \geq \delta \nu(B). \tag{1.23}$$

A ψ-irreducible Markov chain is called *aperiodic* if for some small set $C \in \mathcal{E}^+$, the greatest common divisor of those m's for which (1.23) holds for some δ is 1. Denote $\eta_A = \sum_{n=1}^{\infty} \mathbf{1}_{[Y_n \in A]}$. A set $A \in \mathcal{E}$ is *Harris recurrent* if

$$\Pr[\eta_A = \infty \mid Y_0 = x] = 1, \; x \in A.$$

A ψ-irreducible Markov chain Y is *Harris recurrent* if each $A \in \mathcal{E}^+$ is Harris recurrent.

A σ-finite measure π on $\mathcal{E}$ is *invariant* (w.r.t. the kernel P) if

$$\pi(A) = \int P(x, A)\pi(\mathrm{d}x)$$

for each $A \in \mathcal{E}$. A ψ-irreducible Markov chain Y is called *positive* if it has an invariant probability measure.

The Markov chain Y with an invariant probability measure π is called *ergodic* if

$$\lim_{n\to\infty} \sup_{A\in\mathcal{E}} |P^n(x, A) - \pi(A)| = 0$$

for all $x \in E$. An aperiodic Harris recurrent Markov chain is ergodic if and only if it is positive. Further equivalent conditions for ergodicity are stated in [75, p. 309].

A Markov chain Y with invariant probability measure π is called *geometrically ergodic* if there exists a finite measurable function M on E and $r \in (0, 1)$ such that

$$\sup_{A\in\mathcal{E}} |P^n(x, A) - \pi(A)| \leq r^n M(x) \tag{1.24}$$

for any integer n and all $x \in E$. If, in addition, $M(x)$ is bounded, Y is said to be *uniformly ergodic*. The chain Y is uniformly ergodic if and only if E is a small set. Characterizations of geometric ergodicity can be found in [75].

Let Y be a positive Markov chain and f a real measurable function on E. Denote

$$\bar{f}_n = \frac{1}{n} \sum_{i=1}^{n} f(Y_i)$$

and let $\mathrm{E}_\pi f$, $\mathbf{var}_\pi f$ be the expectation, variance of $f(X)$, respectively, where X is a random element with distribution π.

A Harris recurrent positive chain Y satisfies the strong law of large numbers:

$$\Pr\left[\lim_{n\to\infty} \bar{f}_n = \mathrm{E}_\pi f\right] = 1.$$

A positive Markov chain Y is *reversible* if for any $A, B \in \mathcal{E}$ it holds

$$\int_A P(x, B)\pi(\mathrm{d}x) = \int_B P(x, A)\pi(\mathrm{d}x).$$

If Y is geometrically ergodic, reversible and $\mathrm{var}_\pi f < \infty$ then the central limit theorem holds:

$$n^{\frac{1}{2}}(\bar{f}_n - \mathrm{E}_\pi f) \xrightarrow{d} N(0, t_f \mathrm{var}_\pi f) \quad n \to \infty, \tag{1.25}$$

where $t_f = \sum_{-\infty}^{\infty} \rho_k$ is finite and

$$\rho_k = \frac{\mathrm{cov}\,(f(Y_0), f(Y_k))}{\mathrm{var}_\pi f};$$

the initial variable Y_0 is assumed to have the distribution π.

1.2.2 Markov chain Monte Carlo

Let $(E, \mathcal{E})$ be a Polish state space with Borel σ-algebra and π a target probability measure on $\mathcal{E}$. For the case when it is impossible to simulate directly from the target distribution we discuss methods of the construction of an ergodic Markov chain Y with invariant measure π. Corresponding simulation techniques are called Markov chain Monte Carlo (MCMC). In fact, we restrict ourselves to one of them called the Metropolis-Hastings algorithm, for other methods such as Gibbs sampler, see [34].

Let the target distribution π have a density $\pi(x)$ with respect to a reference measure μ and denote $E^+ = \{x \in E;\ \pi(x) > 0\}$. Let Q be a probability kernel with density q, i.e., $Q(x, \mathrm{d}y) = q(x, y)\mu(\mathrm{d}y)$, $Q(x, E^+) = 1$ for $x \in (E^+)^c$. Define

$$\alpha(x, y) = \min\left\{\frac{\pi(y)q(y, x)}{\pi(x)q(x, y)}, 1\right\} \tag{1.26}$$

for $\pi(x)q(x, y) > 0$, $\alpha(x, y) = 1$ otherwise. The algorithm starts in an arbitrary initial state $x_0 \in E^+$. If the Markov chain state at n is $Y_n = x$, a candidate $Y_{n+1} = y$ is simulated from the distribution $Q(x, \cdot)$. With probability $\alpha(x, y)$ the candidate is accepted, otherwise it is rejected and we set $Y_{n+1} = x$. The algorithm almost surely does not leave E^+, the knowledge of $\pi(x)$ up to a multiplicative constant is sufficient.

Define $p(x, y) = q(x, y)\alpha(x, y)$ for $x \neq y$, $p(x, y) = 0$ otherwise. Put $r(x) = 1 - \int p(x, y)\mu(\mathrm{d}y)$ (probability that the chain does not leave x in a single step). Then the transition kernel of the simulated chain is

$$P(x, \mathrm{d}y) = p(x, y)\mu(\mathrm{d}y) + r(x)\delta_x(\mathrm{d}y). \tag{1.27}$$

The detailed balance condition

$$\pi(x)p(x,y) = \pi(y)p(y,x),\ x,y \in E$$

is fulfilled which implies reversibility, it follows that π is an invariant distribution for the chain Y.

EXAMPLE 1.20 *Let $E = \mathbb{R}^k$, $\mu = \nu_k$ be the Lebesgue measure and f a probability density on E. If Z is simulated from the distribution f and $Y = x + Z$, then the proposal density is $q(x,y) = f(y-x)$ and Q is a kernel of a random walk. Therefore it is called the Metropolis random walk algorithm. In the case of symmetry (i.e., $f(x) = f(-x)$ for all $x \in \mathbb{R}^k$) it holds $\alpha(x,y) = \min\{\frac{\pi(y)}{\pi(x)}, 1\}$, therefore a candidate with $\pi(y) > \pi(x)$ is always accepted.*

EXAMPLE 1.21 *The Langevin-Hastings variant of the algorithm makes use of the information from the gradient of the density Π of the target distribution. In $E = \mathbb{R}^d$ it is e.g.*

$$q(x,y) = (2\pi)^{-\frac{d}{2}}\sigma^{-d}\exp\left(-\frac{1}{2\sigma^2}\|y - x - \sigma^2 \mathrm{grad}\log\Pi(x)/2\|^2\right).$$

1.2.3 Point estimation

In this subsection, some notions from the statistical estimation theory will be recalled (see [66]).

Let an experiment $(\mathcal{X}, \mathcal{A}, \mathcal{P})$ be given, where $\mathcal{X}$ is the *sample space*, $\mathcal{A}$ a σ-algebra on $\mathcal{X}$ and $\mathcal{P} = \{P_\theta : \theta \in \Theta\}$ a parametric system of probability measures on $\mathcal{A}$, the parameter space Θ being a Polish space. A random observable X is taking values on $\mathcal{X}$ according to the distribution P_θ, a realization x of X is called *data*. A standard example is when $X = (X_1, \ldots, X_n)$ are i.i.d. random variables, $\mathcal{X} = \mathbb{R}^n$. In spatial statistics, however, observations are typically dependent.

Let $\tau : \Theta \to \mathbb{R}$ be a function of the *parameter* θ. An *estimator* of $\tau(\theta)$ is a measurable function $e : \mathcal{X} \to \mathbb{R}$. The quality of an estimator e is measured by its *risk function*

$$\mathrm{Risk}(\theta, e) = \mathrm{E}_\theta \mathrm{Loss}(\theta, e(X)),$$

where $\mathrm{Loss} : \Theta \times \mathbb{R} \to \mathbb{R}$ is the *loss function* and E_θ denotes the expectation with respect to P_θ, $\theta \in \Theta$. The *bias* of e is given by $\mathrm{E}_\theta e(X) - \tau(\theta)$; we say that e is an *unbiased estimator* of $\tau(\theta)$ if

$$\mathrm{E}_\theta e(X) = \tau(\theta), \quad \theta \in \Theta. \tag{1.28}$$

In the following we consider the quadratic loss function

$$\text{Loss}(\theta, y) = (\tau(\theta) - y)^2. \tag{1.29}$$

Then, if e is unbiased we have

$$\text{Risk}(\theta, e) = \text{E}_\theta(\tau(\theta) - e(X))^2 = \text{var}_\theta e(X).$$

An unbiased estimator e is a *uniformly best unbiased estimator* (*UBUE*) of $\tau(\theta)$ if

$$\text{var}_\theta e \le \text{var}_\theta \bar{e}, \quad \theta \in \Theta, \tag{1.30}$$

for any unbiased estimator $\bar{e}$ of $\tau(\theta)$. Thus a UBUE minimizes the risk for all values θ (uniformly) among unbiased estimators.

Let $\mathcal{T}$ be a Polish space. A measurable function $T : \mathcal{X} \to \mathcal{T}$ is called a *sufficient statistic* for the parameter θ if the conditional distribution P_θ under the condition $T = t$ is independent of the parameter θ.

In the *dominated case* (i.e., if the distributions P_θ are absolutely continuous with respect to some σ-finite measure), the property of sufficiency can be expressed by means of densities.

THEOREM 1.22 ([66]) *Let the probability distributions P_θ have densities $f(\theta, x)$ on $\mathcal{X}$ with respect to a σ-finite measure ζ. A statistic $T : \mathcal{X} \to \mathcal{T} \subset \mathbb{R}^n$ is sufficient for θ if and only if there exists a nonnegative measurable function $g : \Theta \times \mathcal{T} \to \mathbb{R}$ and a nonnegative measurable function $h : \mathcal{X} \to \mathbb{R}$ (independent of θ) such that*

$$f(\theta, x) = g(\theta, T(x)) \cdot h(x) \tag{1.31}$$

for all $\theta \in \Theta$ and for ζ-almost all $x \in X$.

Further, a statistic $T : \mathcal{X} \to \mathcal{T}$ is *complete* if the following implication holds: If v is a real measurable function on $\mathcal{T}$ such that $\text{E}_\theta v(T) = 0$ for any $\theta \in \Theta$, then $v(t) = 0$ almost surely with respect to all distributions $P_\theta T^{-1}$.

THEOREM 1.23 (RAO-BLACKWELL) *Let the experiment $(\mathcal{X}, \mathcal{A}, \mathcal{P})$ be given, $\tau(\theta)$ be a real parameter function on Θ and let T be a sufficient statistic for θ. If e is an arbitrary unbiased estimator of $\tau(\theta)$ and T is complete then*

$$e(T) := \text{E}_\theta[e \mid T] \tag{1.32}$$

is a UBUE of $\tau(\theta)$. The estimator $e(T)$ is uniquelly determined a.s. in the following sense: if $\bar{e}$ is any unbiased estimator of $\tau(\theta)$ with $\text{var}_\theta \bar{e} = \text{var}_\theta e(T)$ for any $\theta \in \Theta$, then $\bar{e} = e(T)$ P_θ-almost surely for any $\theta \in \Theta$.

REMARK 1.1. In view of the uniqueness assertion, we shall speak about *the UBUE estimator* of a parameter function $\tau(\theta)$ if the uniqueness a.s. in the sense as described in the end of Theorem 1.23 holds.

The density $f(\theta, x)$ of P_θ (cf. Theorem 1.22) taken for fixed x as a function of variable $\theta \in \Theta$ enables us to define the *likelihood function* as $\mathcal{L}(x \mid \theta) = f(\theta, x)$. Its maximum with respect to $\theta \in \Theta$ is called the maximum likelihood estimator of θ. Given the data $x = (x_1, \ldots, x_n)$ corresponding to a random sample X from $\mathcal{X}$, the likelihood function is factorized as

$$\mathcal{L}(x \mid \theta) = \prod_{i=1}^{n} q(\theta, x_i),$$

q being the marginal densities of f.

In Bayesian statistics, the parameter θ is considered as a random variable with *prior distribution* $p(\theta)\nu(d\theta)$, where ν is a fixed reference Borel measure on Θ. Assume that data x have been observed. The *posterior distribution* is then the conditional distribution of θ given $X = x$ and the *Bayes estimator* of $\tau(\theta)$ is any number $e^{\mathcal{B}}(x)$ which minimizes (with respect to $e(x)$) the posterior risk $\mathrm{E}[\mathrm{Loss}(\theta, e(x)) \mid x]$ (this expectation is taken with respect to the prior distribution). For the quadratic loss function (1.29), the Bayes estimator is the posterior mean $e^{\mathcal{B}}(x) = \mathrm{E}[\tau(\theta) \mid x]$.

Let $\mathcal{L}(x \mid \theta)$ be the likelihood function and $p(\theta)$ a prior density. The Bayes theorem yields the posterior density in the form

$$\pi(\theta \mid x) = \frac{\mathcal{L}(x \mid \theta)p(\theta)}{\int \mathcal{L}(x \mid \theta')p(\theta')\,\nu(\mathrm{d}\theta')},$$

briefly $\pi(\theta \mid x) \propto \mathcal{L}(x \mid \theta)p(\theta)$.

Statistical inference based on the posterior distribution requires evaluation of integrals $\int \tau(\theta)\mathcal{L}(x \mid \theta)p(\theta)\nu(\mathrm{d}\theta)$. Besides direct methods, the MCMC approach (cf. Subsection 1.2.2) consists in an indirect evaluation based on the simulation of the posterior. E.g., the posterior mean of $\tau(\theta)$ is estimated from

$$\mathrm{E}\tau(\theta \mid x) \approx \frac{1}{m}\sum_{i=1}^{m} \tau(\theta_i),$$

where (θ_i) is the generated Markov chain. For further applications, see [34].

In the large sample theory, the sample X and estimator $e = e(X)$ are considered as functions of the sample size n. Such a sequence (e_n) of

estimators of $\tau(\theta)$ is said to be *consistent* if

$$e_n \xrightarrow{P_\theta} \tau(\theta),\ n \to \infty, \tag{1.33}$$

for every $\theta \in \Theta$. The sequence (e_n) is said to be *strongly consistent* if almost sure convergence takes place in (1.33) instead of convergence in probability. A sequence of Bayes estimators $(e_n^{\mathcal{B}})$ is called consistent if condition (1.33) holds for $p(\theta)-$almost all $\theta \in \Theta$.

One often speaks about the (strong) consistency of a single estimator if its dependence on the size of data (n) is clear. Finally consider $\Theta \subset \mathbb{R}^d$.

LEMMA 1.24 *Let* (e_n) *be a sequence of estimators of* $\theta \in \Theta$ *with risk function*

$$\mathrm{Risk}(\theta, e_n) = \mathrm{E}_\theta \,||\, e_n - \theta \,||^2 .$$

If

$$\lim_{n\to\infty} \mathrm{Risk}(\theta, e_n) = 0 \tag{1.34}$$

for all $\theta \in \Theta$, *then* (e_n) *is consistent, as well as the sequence* $(e_n^{\mathcal{B}})$ *of Bayes estimators with the same risk function.*

Proof. The first assertion follows from the fact that convergence in probability is implied by the L^2-convergence. From (1.34) we have

$$0 \le \int \mathrm{E}_\theta \mathrm{Loss}(\theta, e_n^{\mathcal{B}}(X))p(\mathrm{d}\theta) \le \int \mathrm{E}_\theta \mathrm{Loss}(\theta, e_n(X))p(\mathrm{d}\theta) \longrightarrow 0$$

when $n \to \infty$, therefore $\lim_{n\to\infty} \mathrm{Risk}(\theta, e_n^{\mathcal{B}}) = 0$ $p(\theta)-$almost surely and the second assertion follows analogously to the first one. □

LEMMA 1.25 *Let* $\Theta \subset \mathbb{R}^d$ *be a compact parametric space and* $(e_n) \in \Theta$ *a consistent sequence of estimators of the parameter* θ. *Then* (1.34) *holds.*

Proof. By the compactness,

$$||\, e_n - \theta \,||^2 \tag{1.35}$$

is uniformly bounded by a constant $M > 0$. Since $e_n \xrightarrow{P_\theta} \theta$ in probability, following the proof of the Lebesgue dominated convergence theorem applied to the random variable (1.35), the assertion follows. □

Chapter 2

RANDOM MEASURES AND POINT PROCESSES

The purpose of this chapter is to survey basic facts about point processes, processes of particles and associated random measures which will be needed in the following chapters. The basic notion is that of a random measure, a point process is a particular case of a random measure which takes only integer values. This approach is rather unusual when dealing with point processes on the real line, where we frequently interpret the point process as a special case of a random function (a piecewise constant function with jumps at the points of the process). In higher dimension such an interpretation is no more possible. One can consider a point process either as a locally finite collection of points (i.e., a special random set), or as an integer valued random measure (measure with atoms at the points of the process). Whereas the first approach seems to be more illustrative and simpler, the second one has many technical advantages when using the additivity of measures. We shall prefer the second approach but we shall use the convention to interpret a point process simultaneously as a collection of particles if this is more advantageous.

An outstandingly important tool in connection with point processes and random measures is that of local conditioning known as the Palm theory; we refer here namely to the monographs by Kallenberg [57], Kerstan, Matthess and Mecke [60] and Daley and Vere-Jones [23]. Local conditioning is, in fact, a special kind of disintegration.

Throughout the book, random structures generated as union sets of processes of "particles" (which may be convex bodies, fibres, lines, flats etc.) are considered. This chapter provides the necessary background for these objects. The concepts of stationarity and isotropy are extremely important here.

Besides of the references given above, we mention the monographs by Stoyan, Kendall and Mecke [109] and Schneider and Weil [103] as basic reference sources on random measures and point processes.

2.1. Basic definitions

Throughout this section, (X, ρ) is a Polish space which is locally compact, i.e., to each $x \in X$ there exists a neighbourhood with a compact closure, and $\mathcal{B} = \mathcal{B}(X)$ is the Borel σ-algebra on X. We denote by $\mathcal{F} = \mathcal{F}(X)$, $\mathcal{K} = \mathcal{K}(X)$ the system of all closed, compact subsets of X, respectively.

A measure μ on $(X, \mathcal{B}(X))$ is said to be *locally finite* if it is finite on bounded Borel sets. By $\mathcal{M} \equiv \mathcal{M}(X)$ we denote the set of all locally finite measures on $(X, \mathcal{B})$. Further denote

$$\mathcal{N} \equiv \mathcal{N}(X) = \{\mu \in \mathcal{M} : \mu(B) \in \mathbb{N} \cup \{0, \infty\} \text{ for each } B \in \mathcal{B}\} \quad (2.1)$$

the set of all locally finite integer-valued measures.

Let $\mathfrak{M}$ be the smallest σ-algebra on $\mathcal{M}$ with respect to which the function $\mu \mapsto \mu(B)$ is measurable for all $B \in \mathcal{B}$. Further, let $\mathfrak{N}$ be the trace of $\mathfrak{M}$ on $\mathcal{N}$, i.e., $\mathfrak{N} = \{M \cap \mathcal{N} : M \in \mathfrak{M}\}$.

We say that a sequence $\mu_n \in \mathcal{M}$ of measures *converges vaguely* to $\mu \in \mathcal{M}$ if $\int f \, \mathrm{d}\mu_n \to \int f \, \mathrm{d}\mu$ for each continuous function f with compact support.

The following result can be found e.g. in [23, Theorem A.2.6].

THEOREM 2.1 *The space $\mathcal{M}$ with the topology of vague convergence is a Polish space and its Borel σ-algebra coincides with $\mathfrak{M}$.*

DEFINITION 2.2 *Let $(\Omega, \mathcal{A}, \Pr)$ be a probability space. A random measure on X is a measurable mapping*

$$\Psi : (\Omega, \mathcal{A}, \Pr) \to (\mathcal{M}, \mathfrak{M}).$$

A point process on X is a measurable mapping

$$\Phi : (\Omega, \mathcal{A}, \Pr) \to (\mathcal{N}, \mathfrak{N}).$$

The probability measure $\Pr\Psi^{-1}$ $(\Pr\Phi^{-1})$ is the distribution of the random measure Ψ (point process Φ) and the measure $\Lambda(\cdot) = \mathrm{E}\Psi(\cdot)$ $(\Lambda(\cdot) = \mathrm{E}\Phi(\cdot))$ is called the intensity measure of Ψ (Φ, respectively). The point process Φ is simple if $\Pr[\Phi \in \mathcal{N}^*] = 1$, where

$$\mathcal{N}^* = \{\nu \in \mathcal{N} : \nu(\{x\}) \le 1 \text{ for each } x \in X\}. \quad (2.2)$$

Note that the intensity measure Λ need not be locally finite in general.

Let us call a set $S \subset X$ *locally finite* if its intersection with an arbitrary bounded set is finite.

REMARK 2.1. It is clear that almost all realizations of a simple point process Φ are characterized by their support $\operatorname{supp}\Phi$ which is a locally finite subset of X. Therefore, simple point processes are often interpreted as locally finite random subsets of X. We shall sometimes use this interpretation and write e.g. "$x \in \Phi$" instead of "$\Phi\{x\} > 0$" or "$\Phi\{x\} = 1$".

THEOREM 2.3 ([23, PROPOSITIONS 7.1.II,III]) *For each $\nu \in \mathcal{N}$ the support $\operatorname{supp}\nu$ is a locally finite subset of X. Further, $\mathcal{N}^* \in \mathfrak{N}$ and $\nu \mapsto \operatorname{supp}\nu$ is a one-to-one mapping of $\mathcal{N}^*$ onto the set of all locally finite subsets of X.*

We shall demonstrate now the connection between simple point processes and random sets.

DEFINITION 2.4 *A random closed set in X is a measurable mapping*

$$\Xi : (\Omega, \mathcal{A}, \Pr) \to (\mathcal{F}(X), \mathfrak{F}(X)),$$

where the σ-algebra $\mathfrak{F}(X)$ on $\mathcal{F}(X)$ is generated by all families $\mathcal{F}^K = \{F \in \mathcal{F}(X) : F \cap K = \emptyset\}$, $K \in \mathcal{K}$.

It can be shown that the family of locally finite sets in X belongs to $\mathfrak{F}(X)$ (cf. Exercise 2.11).

THEOREM 2.5 *If Φ is a point process on X then $\operatorname{supp}\Phi$ is a random closed set. On the other hand, if Ξ is a locally finite random closed set in X (i.e., a random closed set in X such that $\Xi(\omega)$ is locally finite for any $\omega \in \Omega$) then $\Phi(\cdot) = \operatorname{card}(\Xi \cap \cdot)$ is a simple point process on X.*

Proof. It is enough to verify the measurability of the mapping $\nu \mapsto \operatorname{supp}\nu$ from $\mathcal{N}^*$ to $\{F \in \mathcal{F} : F$ locally finite$\}$ and of its inverse, which is left to the reader as an exercise. □

THEOREM 2.6 (CHOQUET, MATHERON) *The distribution of a random closed set Ξ is uniquelly determined by the probabilities $\Pr[\Xi \cap K = \emptyset]$, $K \in \mathcal{K}$.*

Proof. Note that the system $(\mathcal{F}^K : K \in \mathcal{K})$ is closed under finite intersections. The result follows from the well known fact that a probability measure is uniquely determined by its values on a generator closed w.r.t. finite intersections. □

COROLLARY 2.7 *The distribution of a simple point process Φ is uniquely determined by the "void probabilities"* $\Pr[\Phi(K) = 0]$, $K \in \mathcal{K}$.

DEFINITION 2.8 *Let Ψ be a random measure on (X, ρ) with distribution P and $k \in \mathbb{N}$. The measure*

$$M_k(\cdot) = \mathrm{E}\Psi^k(\cdot) = \int \mu^k(\cdot)\, P(\mathrm{d}\mu)$$

on $(X^k, \mathcal{B}(X)^k)$ is called the moment measure of k-th order of Ψ. Specially $M_1 \equiv \Lambda$ is the intensity measure of Ψ. If Φ is a point process and $k \geq 2$ we define also the factorial moment measure of k-th order

$$\alpha_k(\cdot) = \int \mu^{[k]}(\cdot)\, P(\mathrm{d}\mu),$$

where $\mu^{[k]} = \mu^k|_{X^{[k]}}$ is the restriction of μ^k to the set

$$X^{[k]} = \{(x_1, \ldots, x_k) \in X^k : x_i \neq x_j \text{ for } i \neq j\}$$

of all k-tuples of points of X with pairwise different coordinates.

REMARK 2.2. For two Borel sets $A, B \subset X$ we can write

$$M_2(A \times B) = \mathrm{E}\Psi(A)\Psi(B)$$

and if Φ is a simple point process then

$$M_2(A \times B) = \mathrm{E} \sum_{x,y \in \Phi} \mathbf{1}_A(x)\mathbf{1}_B(y)$$

and

$$\alpha_2(A \times B) = \mathrm{E} \sum_{\substack{x,y \in \Phi \\ x \neq y}} \mathbf{1}_A(x)\mathbf{1}_B(y),$$

using the convention explained in Remark 2.1.

EXERCISE 2.9 *Verify the measurability of the mapping in the proof of Theorem 2.5.*

EXERCISE 2.10 *Show that the families*

$$\mathcal{F}^B = \{F \in \mathcal{F}(X) : F \cap B = \emptyset\}$$

and

$$\mathcal{F}_B = \{F \in \mathcal{F}(X) : F \cap B \neq \emptyset\}$$

belong to $\mathfrak{F}(X)$ *for any Borel set* $B \subset X$.

EXERCISE 2.11 *Show that the family of locally finite subsets of* X *belongs to* $\mathfrak{F}(X)$. *Hint: Fix a bounded set* $B \subset X$, $k \in \mathbb{N}$, *and show that* $\mathcal{F}_{B,k} = \{F \in \mathcal{F} : \operatorname{card}(F \cap B) \leq k\} \in \mathfrak{F}(X)$. *To this end, use a sequence* $(\mathcal{A}_n, n \in \mathbb{N})$ *of refining partitions of* B *into relatively compact sets with diameters tending to* 0 *as* $n \to \infty$, *and use the representation*

$$\mathcal{F}_{B,k} = \bigcap_{n=1}^{\infty} \{F \in \mathcal{F} : \operatorname{card}\{A \in \mathcal{A}_n : F \cap A \neq \emptyset\} \leq k\}.$$

EXERCISE 2.12 *Show that for any nonnegative measurable function* f *on* X^2,

$$\int\int f(x,y)\, M_2(\mathrm{d}(x,y)) = \int\int f(x,y)\alpha_2(\mathrm{d}(x,y)) + \int f(x,x)\Lambda(\mathrm{d}x).$$

EXERCISE 2.13 *Show that* $\operatorname{var}\Psi(B) = M_2(B \times B) - (\Lambda(B))^2$, $B \in \mathcal{B}$.

2.2. Palm distributions

THEOREM 2.14 (CAMPBELL) *Let* Ψ *be a random measure on* X *with distribution* P *and a locally finite intensity measure* Λ. *Then*

$$\mathrm{E}\int_X f(x)\Psi(\mathrm{d}x) = \int_{\mathcal{M}}\int_X f(x)\mu(\mathrm{d}x)P(\mathrm{d}\mu) = \int_X f(x)\Lambda(\mathrm{d}x) \qquad (2.3)$$

for an arbitrary nonnegative measurable function f *on* X. *More generally, for* $k \in \mathbb{N}$ *and for any nonnegative measurable function* f *on* X^k *we have*

$$\mathrm{E}\int_X \cdots \int_X f(x_1,\ldots,x_k)\Psi(\mathrm{d}x_1)\cdots\Psi(\mathrm{d}x_k) = \int_{X^k} f(x_1,\ldots,x_k)M_k(\mathrm{d}x_1,\ldots,\mathrm{d}x_k). \qquad (2.4)$$

Proof. If f is the characteristic function of a measurable set then the results follow directly from the definitions. For nonnegative measurable functions, we can use the standard approximation by simple functions (see also [120, Theorem 5.2]). □

DEFINITION 2.15 *Let* Ψ *be a random measure on* X *with distribution* P *and intensity measure* Λ. *The Campbell measure* C *corresponding to* Ψ *is a measure on* $X \times \mathcal{M}$ *defined by*

$$\int_{X\times\mathcal{M}} f(x,\mu)C(\mathrm{d}(x,\mu)) = \int_{\mathcal{M}}\int_X f(x,\mu)\mu(\mathrm{d}x)P(\mathrm{d}\mu),$$

where f is an arbitrary nonnegative measurable function on $X \times \mathcal{M}$.

Note that the Campbell measure C can also be characterized by the property

$$C(A \times \mathcal{U}) = \mathrm{E}\Psi(A)\mathbf{1}_{\mathcal{U}}(\Psi),$$

where A is a bounded Borel subset of X and $\mathcal{U}$ a measurable subset of $\mathcal{M}$.

An important tool in the theory of random measures and point processes are the Palm distributions which are, in fact, certain types of conditional distributions. They are defined by means of a disintegration of the Campbell measure as expressed in the following theorem (for its proof see e.g. [23, Property 12.1.IV]).

THEOREM 2.16 *Let Ψ be a random measure on X with distribution P and a locally finite intensity measure Λ. Then there exists a probability kernel $x \mapsto P_x$ from $(X, \mathcal{B})$ to $(\mathcal{M}, \mathfrak{M})$ such that*

$$\int_{\mathcal{M}} \int_X f(x, \mu)\mu(\mathrm{d}x)P(\mathrm{d}\mu) = \int_X \int_{\mathcal{M}} f(x, \mu)P_x(\mathrm{d}\mu)\Lambda(\mathrm{d}x) \qquad (2.5)$$

for an arbitrary nonnegative measurable function f on $X \times \mathcal{M}$. If $(P'_x : x \in X)$ is another probability kernel satisfying (2.5) then for any measurable set $\mathcal{U} \subset \mathcal{M}$,

$$P_x(\mathcal{U}) = P'_x(\mathcal{U}) \text{ for } \Lambda \text{ almost all } x \in X.$$

The distribution P_x is called the Palm distribution of the random measure Ψ at the point $x \in X$.

REMARK 2.3. In fact, it has no sense to speak about the Palm distribution P_x in one particular point x since this can be defined arbitrarily. The uniqueness assertion from Theorem 2.16 nevertheless assures that the family $\{P_x : x \in X\}$ is uniquely determined for Λ-almost all x.

Let $(P_x : x \in \mathbb{R}^d)$ be the Palm distributions of the random measure Ψ. We shall sometimes use the notation Pr_x for the Palm (conditional) probability, which is formally defined as

$$\mathrm{Pr}_x[\Psi \in \cdot] = P_x(\cdot).$$

Analogously, we shall write E_x for the expectation with respect to the Palm distribution at x.

In the case of a point process Φ, the Palm distribution P_x can be interpreted as the conditional distribution of Φ under condition $x \in \Phi$

(see [109, §4.4] or [57, Theorem 12.8]). In particular, the Campbell measure C of a point process Φ is concentrated on the set

$$\{(x, \nu) \in X \times \mathcal{N} : \nu\{x\} \geq 1\}.$$

Therefore, the following definition makes sense.

DEFINITION 2.17 *If Φ is a point process the reduced Campbell measure $C^!$ is defined as*

$$\int_{X \times \mathcal{N}} f(x, \nu) C^!(\mathrm{d}(x, \nu)) = \int_{\mathcal{N}} \int_X f(x, \mu - \delta_x) \nu(\mathrm{d}x) P(\mathrm{d}\mu),$$

where f is an arbitrary measurable function on $X \times \mathcal{N}$. The reduced Palm distributions $P_x^!$ of Φ $(x \in X)$ are then defined again by means of the disintegration

$$\int f(x, \nu) C^!(\mathrm{d}(x, \nu)) = \int_X \int_{\mathcal{N}} f(x, \nu) P_x^!(\mathrm{d}\nu) \Lambda(\mathrm{d}x). \tag{2.6}$$

Sometimes, Palm distributions of higher order are needed. These can be interpreted, in the case of a point process, as conditional distributions under condition that a given finite number of points belong to the process. The formal definition is based again on the Campbell measure, now of a higher order.

Let Ψ be a random measure on X with distribution P and an intensity measure Λ and let k be a natural number. The *Campbell measure* C_k of order k corresponding to Ψ is a measure on $X^k \times \mathcal{M}$ defined by

$$\begin{aligned} &\int_{X^k \times \mathcal{M}} f(x_1, \ldots, x_k, \mu) C_k(\mathrm{d}(x_1, \ldots, x_k, \mu)) \\ &\quad = \int_{\mathcal{M}} \int_X \cdots \int_X f(x_1, \ldots, x_k, \mu) \mu(\mathrm{d}x_1) \cdots \mu(\mathrm{d}x_k) P(\mathrm{d}\mu), \end{aligned} \tag{2.7}$$

where f is an arbitrary nonnegative measurable function on $X^k \times \mathcal{M}$. Assume now that the k-th moment measure M_k of Ψ is locally finite. The *Palm distributions of order k* are defined as a probability kernel $P_{x_1, \ldots, x_k}$ from $(X^k, \mathcal{B}^k, M_k)$ to $(\mathcal{M}, \mathfrak{M})$:

$$\begin{aligned} &\int f(x_1, \ldots, x_k, \nu) C_k(\mathrm{d}(x_1, \ldots, x_k, \nu)) \\ &\quad = \int_{X^k} \int_{\mathcal{M}} f(x, \nu) P_{x_1, \ldots, x_k}(\mathrm{d}\nu) M_k(\mathrm{d}(x_1, \ldots, x_k)). \end{aligned} \tag{2.8}$$

If Φ is a point process, the *reduced Campbell measure of order* k, $C_k^!$, is given by

$$\int_{X^k \times \mathcal{M}} f(x_1, \ldots, x_k, \nu) C_k^!(\mathrm{d}(x_1, \ldots, x_k, \nu)) = \int_{\mathcal{M}} \int_X \cdots \int_X f(x_1, \ldots, x_k, \mu - (\delta_{x_1} + \cdots + \delta_{x_k})) \mu(\mathrm{d}x_1) \cdots \mu(\mathrm{d}x_k) P(\mathrm{d}\mu), \tag{2.9}$$

and the *reduced Palm distributions of order* k, $P^!_{x_1,\ldots,x_k}$, are determined by

$$\int f(x_1, \ldots, x_k, \mu) C_k^!(\mathrm{d}(x_1, \ldots, x_k, \mu)) = \int_{X^k} \int_{\mathcal{M}} f(x_1, \ldots, x_k, \mu) P^!_{x_1,\ldots,x_k}(\mathrm{d}\mu) M_k(\mathrm{d}(x_1, \ldots, x_k)). \tag{2.10}$$

EXERCISE 2.18 *Let* $\Phi = \sum_{i=1}^n \delta_{Z_i}$ *be the point process in* $\mathbb{R}^d$ *generated by* n *independent identically distributed random vectors* $Z_1, \ldots, Z_n$. *Show that the Palm distribution of* Φ *at* x *is that of* $\delta_x + \sum_{i=1}^{n-1} \delta_{Z_i}$.

2.3. Poisson process

The most familiar model of a point process is the Poisson process which is introduced in analogy to the commonly known one-dimensional case ($X = \mathbb{R}$). The basic property of the Poisson process is the mutual independence of its behavior in disjoint domains.

DEFINITION 2.19 *Let* Λ *be a locally finite measure on a Polish space X,* $\mathcal{B}_0$ *the system of bounded Borel subsets of X. A point process* Φ *on X such that*

1) *for any* $n \in \mathbb{N}$ *and* $B_1, \ldots, B_n \in \mathcal{B}_0$ *disjoint, the random variables* $\Phi(B_1), \ldots, \Phi(B_n)$ *are independent,*

2) $\Phi(B)$ *has the Poisson distribution with parameter* $\Lambda(B)$ *for any* $B \in \mathcal{B}_0$,

is called the Poisson process on X with intensity measure Λ.

The existence and uniqueness of the Poisson process follows from general existence and uniqueness results on random measures, see [23, Theorems 6.2.IV, 6.2.VII].

REMARK 2.4. It can be shown that if the intensity measure Λ is diffuse (i.e., if it has no atoms) then the corresponding Poisson process is simple,

see [23, §7.2]. According to Corollary 2.7, Φ is in this case also uniquely determined by the condition of being simple and the property

$$\Pr[\Phi(K) = 0] = e^{-\Lambda(K)}, \quad K \in \mathcal{K}. \tag{2.11}$$

One can show directly from the definition that the factorial moment measures of a Poisson process are product measures, i.e.,

$$\alpha_n = \Lambda^n. \tag{2.12}$$

As a consequence one gets the following lemma which will be used later on. The proof follows from Theorem 2.14, Exercise 2.12 and (2.12).

LEMMA 2.20 ([82, LEMMA 2]) *Let Φ be a stationary Poisson point process on a Polish space X with intensity measure Λ. Denote $F(\Phi) = \int f(x)\Phi(\mathrm{d}x)$, $G(\Phi) = \int g(x)\Phi(\mathrm{d}x)$ for nonnegative measurable functions f, g on X. Then*

$$\operatorname{cov}(F(\Phi), G(\Phi)) = \int f(x)g(x)\Lambda(\mathrm{d}x).$$

An important property of the Poisson process is that its reduced Palm distribution coincides with its ordinary distribution. This fact is known as the Slyvniak theorem, see e.g. [109, §4.4.6] or [23, Proposition. 12.1.VI]. Recall that $*$ denotes the convolution of measures, cf. (1.2).

THEOREM 2.21 (SLYVNIAK) *If P is the distribution of a Poisson point process on X with locally finite intensity measure then*

$$P_x = P * \delta_{(\delta_x)}, \text{ equivalently } P_x^! = P, \tag{2.13}$$

for Λ-almost all $x \in X$.

Let Ψ be a random measure on X with distribution Q. A point process Φ on X is called a *Cox process with driving measure* Ψ if conditionally on $\Psi = \psi$ it is a Poisson process with intensity measure ψ. In other words, the distribution of the Cox process Φ is

$$P = \int P^{\Lambda} Q(\mathrm{d}\Lambda),$$

where P^{Λ} is the distribution of a Poisson process with intensity Λ. Of course, the Cox process does not retain the independence property of the Poisson process. The most common example is the Cox process in $\mathbb{R}^d$ with driving measure $Z\nu_d$, where Z is a positive random variable.

EXERCISE 2.22 *Show that* $\alpha_2 = \Lambda \times \Lambda$ *for the Poisson point process.*

EXERCISE 2.23 *Let* Φ *be a Poisson process (not necessary stationary) on a Polish space X with the intensity measure* Λ. *Let f be a measurable function on X. Show that then*

$$\mathrm{E}e^{it\int f(K)\,\Phi(\mathrm{d}K)} = \exp\Big\{\int (e^{itf(K)} - 1)\,\Lambda(\mathrm{d}K)\Big\}. \tag{2.14}$$

Hint: Start with the functions of the form $f = \sum_{j=1}^{n} a_j \mathbf{1}_{U_j}$, *where* $a_j > 0$ *and the* U_j*'s are pairwise disjoint Borel subsets of X.*

EXERCISE 2.24 *Show that the void probabilities of the Cox process are* $\Pr[\Phi(B) = 0] = \mathrm{E}\exp(-\Lambda(B))$.

EXERCISE 2.25 *Let* Φ *be the Cox process with driving measure* Ψ *of distribution Q and with locally finite intensity measure* $\mathrm{E}\Psi$. *Then the Palm distributions* P_x *of* Φ *are the mixtures*

$$P_x = \int (P^{\Lambda} * \delta_{\delta_x})\, Q_x(\mathrm{d}\Lambda),$$

i.e., P_x *is the distribution of a Cox process with driving measure* Q_x *(the Palm distribution of Q at x).*

2.4. Finite point processes

Let $X \subset \mathbb{R}^d$ be a Borel set, μ a measure on $\mathcal{B}(X)$ with $\mu(X) < \infty$ and P the distribution of a Poisson point process Φ' with intensity measure μ. Using Definition 2.19 and Exercise 2.29, we can write the distribution P in the following way. Let $\mathcal{U} \in \mathfrak{N}(X)$ be a set of (finite) point configurations in X.

$$\begin{aligned}
P(\mathcal{U}) &= \Pr[\Phi' \in \mathcal{U}] \\
&= \sum_{n=0}^{\infty} \Pr[\Phi'(X) = n]\,\Pr[\Phi' \in \mathcal{U} \mid \Phi'(X) = n] \\
&= \sum_{n=0}^{\infty} e^{-\mu(X)} \frac{\mu(X)^n}{n!} \int_X \cdots \int_X \mathbf{1}_{[\{x_1,\ldots,x_n\}\in\mathcal{U}]} \frac{\mu(\mathrm{d}x_1)}{\mu(X)} \cdots \frac{\mu(\mathrm{d}x_n)}{\mu(X)} \\
&= e^{-\mu(X)} \Big(\mathbf{1}_{\mathcal{U}}(\emptyset) + \sum_{n=1}^{\infty} \frac{1}{n!} \int_X \cdots \int_X \mathbf{1}_{\mathcal{U}}(\{x_1,\ldots,x_n\}) \\
&\qquad\qquad \mu(\mathrm{d}x_1)\ldots\mu(\mathrm{d}x_n)\Big).
\end{aligned} \tag{2.15}$$

A point process Φ has *density* q on $\mathcal{N}(X)$ with respect to P if

$$\Pr(\Phi \in \mathcal{U}) = \int_{\mathcal{U}} q(\phi) P(\mathrm{d}\phi).$$

A sufficient condition for the integrability of a nonnegative function h on $\mathcal{N}$ with respect to P is its *local stability,* i.e., existence of a constant $K \in \mathbb{R}_+$ such that for all $\phi \in \mathcal{N}(X)$, $x \in X$ it holds

$$h(\phi \cup \{x\}) \leq Kh(\phi).$$

EXAMPLE 2.26 *Let* $h(\phi) = b^{\phi(X)}$ *for a constant* $b > 0$. *It holds* $h(\phi \cup \{x\}) \leq bh(\phi)$, *hence* h *is P–integrable and using (2.15) we obtain*

$$\int_N h(\phi)P(\mathrm{d}\phi) = \sum_{n=0}^{\infty} \frac{(b\mu(X))^n}{n!} \exp(-\mu(X)) = \exp[(b-1)\mu(X)]$$

which is the normalizing constant for h *to become a probability density. The distribution of the corresponding point process is*

$$\Pr[\Phi \in \mathcal{U}] = \mathrm{e}^{-b\mu(X)} \Big(\mathbf{1}_{\mathcal{U}}(\emptyset) + \sum_{n=1}^{\infty} \frac{1}{n!} \int_X \dots \int_X \mathbf{1}_{\mathcal{U}}(\{x_1, \dots, x_n\}) (b\mu)(\mathrm{d}x_1) \dots (b\mu)(\mathrm{d}x_n) \Big),$$

i. e., Φ *is a Poisson point process with intensity measure* $b\mu$.

EXAMPLE 2.27 *A frequent case is that X is bounded and* $\mu = \nu_d$ *is the Lebesgue measure. Let* g *be a measurable function on X. Then*

$$h(\phi) = \prod_{x_i \in \phi} g(x_i)$$

is locally stable if and only if g *is bounded. In such a case we have*

$$\begin{aligned} \int h(\phi)P(\mathrm{d}\phi) &= \mathrm{e}^{-\nu_d(X)} \sum_{n=0}^{\infty} \frac{1}{n!} \int \dots \int \prod_{i=1}^{n} g(x_i)\mathrm{d}x_1 \dots \mathrm{d}x_n \\ &= \mathrm{e}^{-\nu_d(X)} \sum_{n=0}^{\infty} \frac{(\int g(x)\mathrm{d}x)^n}{n!} \\ &= \exp\left(-\nu_d(X) + \int g(x)\mathrm{d}x\right), \end{aligned}$$

thus

$$q(\phi) = \exp(\nu(X)) \exp\left(-\int g(x)\mathrm{d}x\right) \prod_{x_i \in \phi} g(x_i) \tag{2.16}$$

is a probability density on $\mathcal{N}(X)$. *Since*

$$\begin{aligned} &\int_{\mathcal{U}} q(\phi)P(\mathrm{d}\phi) \\ &= \mathrm{e}^{-\int g(x)dx} \sum_{n=0}^{\infty} \frac{1}{n!} \int \dots \int \mathbf{1}_{\mathcal{U}}(\{x_1, \dots, x_n\}) g(x_1)\mathrm{d}x_1 \dots g(x_n)\mathrm{d}x_n, \end{aligned}$$

q is a density of a Poisson point process with intensity function (density of intensity measure w.r.t. Lebesgue measure) $g(x)$.

EXAMPLE 2.28 *The processes in Examples 2.26 and 2.27 are still of Poisson type, they do not exhibit interactions among points. A simple model with interactions, widely discussed in the literature, is the Strauss process with density*

$$q(\phi) = ab^{\phi(X)}\gamma^{S(\phi)}, \tag{2.17}$$

where $a, b, R > 0$, $0 \le \gamma \le 1$ are parameters and

$$S(\phi) = \sum_{i<j} \mathbf{1}_{[\|x_i - x_j\| < R]}, \quad \phi = (x_1, \ldots, x_n).$$

For $\gamma = 1$ it is a Poisson process, for $\gamma < 1$ there are repulsive interactions. The limiting case $\gamma = 0$ is called a hard-core process, with probability one there do not appear pairs of points with distance less than R. The Strauss process belongs to a large class of Markov point processes [115] which are intensively studied.

EXERCISE 2.29 *Show that the conditional distribution of a Poisson process Φ on X with finite intensity measure μ under condition $\Phi(X) = n$ is that of a binomial distribution of n i.i.d. points in X with distribution $\mu/\mu(X)$. Hint: The distribution of a point process (random measure) is determined by its finite dimensional distributions of numbers of points in pairvise disjoint sets (see [23, Proposition 6.2.III]). Let $k \in \mathbb{N}$ and let $A_1, \ldots, A_k$ be k pairwise disjoint Borel subsets of X. Let $j_1, \ldots, j_k$ be nonnegative integers with $j_1 + \cdots + j_k \le n$ and denote $j_{k+1} = n - \sum_{i=1}^{k} j_i$, $A_{k+1} = X \setminus \bigcup_{i=1}^{k} A_i$. Then, by using the Poisson property (Definition 2.19), show that*

$$\begin{aligned} &\Pr[\Phi(A_1) = j_1, \ldots, \Phi(A_k) = j_k \mid \Phi(X) = n] \\ &\quad = (\Pr[\Phi(X) = n])^{-1} \Pr[\Phi(A_1) = j_1, \ldots, \Phi(A_{k+1}) = j_{k+1}] \\ &\quad = \frac{n!}{j_1! \ldots j_{k+1}!} \prod_{i=1}^{k+1} \left(\frac{\mu(A_i)}{\mu(X)}\right)^{j_i}. \end{aligned}$$

EXERCISE 2.30 *Show that for $\gamma > 1$ the function q in (2.17) is not integrable and thus cannot serve as a probability density.*

2.5. Stationary random measures on $\mathbb{R}^d$

Let Ψ be a random measure on $\mathbb{R}^d$. We shall denote for brevity $\mathcal{M}^d = \mathcal{M}(\mathbb{R}^d)$, $\mathfrak{M}^d = \mathfrak{M}(\mathbb{R}^d)$. For $z \in \mathbb{R}^d$, let t_z denote the corresponding shift operator on $\mathcal{M}^d$ defined by

$$t_z\mu(B) = \mu(B - z), \quad B \in \mathcal{B}^d.$$

The random measure Ψ is called *stationary* if its distribution is shift invariant, i.e., if $t_z\Psi$ has the same distribution as Ψ for any $z \in \mathbb{R}^d$.

Further, given a rotation $\rho \in \mathrm{SO}(d)$, we define the corresponding rotation operator r_ρ on $\mathcal{M}^d$ by

$$r_\rho\mu(B) = \mu(\rho^{-1}B), \quad B \in \mathcal{B}^d. \tag{2.18}$$

The random measure Ψ is called *isotropic* if its distribution is invariant under r_ρ for any $\rho \in \mathrm{SO}(d)$.

A well-known measure-theoretic fact implies that if the intensity measure Λ of a stationary random measure Ψ is locally finite then it is a multiple of the Lebesgue measure, say $\Lambda = \lambda\nu_d$. The constant $\lambda \geq 0$ is called the *intensity* of the stationary random measure Ψ.

The stationarity implies obviously the shift covariance of the Palm distributions. The following theorem presents a possible choice of the Palm distributions for a stationary random measure.

THEOREM 2.31 *A stationary random measure Ψ on $\mathbb{R}^d$ with intensity $\lambda > 0$ has Palm distributions ($\mathcal{U} \in \mathcal{M}^d$)*

$$\begin{aligned} P_0(\mathcal{U}) &= (\lambda\nu_d(A))^{-1}\mathrm{E}\int_A \mathbf{1}_{\mathcal{U}}(t_{-x}\Psi)\Psi(\mathrm{d}x), \\ P_x(\mathcal{U}) &= P_0(t_x^{-1}\mathcal{U}), \quad x \in \mathbb{R}^d, \end{aligned}$$

where A is an arbitrary Borel set in $\mathbb{R}^d$ with positive and finite Lebesgue measure.

To prove the theorem, one has to verify that the family of distributions $(P_x : x \in \mathbb{R}^d)$ satisfies (2.5), see also [23, Theorem 12.2.II].

Theorem 2.31 provides an explicit formula for calculating the Palm distribution at the origin. Whenever talking about the Palm distribution P_0 at the origin of a stationary random measure, we shall always mean by this that $P_x = P_0t_x^{-1}$, $x \in \mathbb{R}^d$, is a family of Palm distributions of the random measure.

Some further characteristics are often used for stationary random measures. The *reduced second moment measure* $\mathcal{K}$ is defined by

$$\mathcal{K}(B) = \lambda^{-1}\int \mu(B \setminus \{0\})P_0(\mathrm{d}\mu), \quad B \in \mathcal{B}_0. \tag{2.19}$$

Note that if, in particular, Φ is a point process we have

$$\mathcal{K}(B) = \lambda^{-1}\int \mu(B)P_0^!(\mathrm{d}\mu), \quad B \in \mathcal{B}_0.$$

If there exists a density p of $\mathcal{K}$ w.r.t. ν_d, p is called the *pair correlation function.* The *K-function* is defined by

$$K(r) = \mathcal{K}(B_r), \quad r > 0. \tag{2.20}$$

If Φ is a stationary point process and $P_x^!$ the reduced Palm distribution it holds

$$\begin{aligned} \alpha_2(A \times B) &= \mathrm{E} \sum_{x \in \Phi} 1_A(x) \Phi(B \setminus \{x\}) \\ &= \lambda \int_A \int_{\mathcal{N}} \mu(B) P_x^!(\mathrm{d}\mu)\, \mathrm{d}x \\ &= \lambda^2 \int_A \mathcal{K}(B - x)\, \mathrm{d}x, \end{aligned}$$

$A, B \in \mathcal{B}_0$. Thus in the stationary case the second order moment measures can be expressed by means of λ and $\mathcal{K}$.

Consider again a stationary random measure Ψ with intensity λ. If $0 \notin B$ we can write by using Theorem 2.31

$$\mathcal{K}(B) = \frac{1}{\lambda^2 \nu_d(A)} \mathrm{E} \int_A \Psi(B - x) \Psi(\mathrm{d}x), \tag{2.21}$$

with an arbitrary bounded Borel set A of positive Lebesgue measure.

Let now Ψ_1, Ψ_2 be two stationary random measures with intensities λ_1, λ_2, respectively. Assume that Ψ_1, Ψ_2 are *jointly stationary,* i.e., that the joint distribution of $(t_z \Psi_1, t_z \Psi_2)$ is the same as that of (Ψ_1, Ψ_2), for any shift $z \in \mathbb{R}^d$. In analogy to (2.21), we define the *cross correlation measure* $\mathcal{K}_{1,2}$ of Ψ_1 and Ψ_2 as

$$\mathcal{K}_{1,2}(B) = \frac{1}{\lambda_1 \lambda_2 \nu_d(A)} \mathrm{E} \int_A \Psi_2(B - x) \Psi_1(\mathrm{d}x) \tag{2.22}$$

(the set A is as above), cf. [110, 111]. The *cross-correlation function* $p_{1,2}(x)$ of Ψ_1 and Ψ_2 is then the density of $\mathcal{K}_{1,2}$ w.r.t. Lebesgue measure (if it exists).

REMARK 2.5. If two random measures Ψ_1, Ψ_2 are independent, their cross-correlation measure is the Lebesgue measure and, hence, $p_{1,2}(x) = 1$ for (almost) all $x \in \mathbb{R}^d$.

EXERCISE 2.32 *Show that the pair correlation function of a stationary Poisson process is* $p(x) = 1$, $x \in \mathbb{R}^d$. *If* Φ *is a stationary Cox process with driving measure* $Z\nu_d$ *(i.e., a stationary "Poisson" process with random*

intensity Z), its intensity is EZ *and pair correlation function is again constant,* $p(x) = \mathrm{E}Z^2/(\mathrm{E}Z)^2$, $x \in \mathbb{R}^d$.

EXERCISE 2.33 *Let* $Y = \{Y(x),\ x \in \mathbb{R}^d\}$ *be a stationary Gaussian random field (almost surely continuous) with mean* μ, *variance* σ^2 *and correlation function* $r(x)$. *The Cox process with driving measure* $\Psi(B) = \int_B \exp(Y(x))\mathrm{d}x$ *is called a log-Gaussian Cox process (LGCP). Show that the* $n-th$ *factorial measure of a LGCP* Φ *on* $\mathbb{R}^d$ *has a density* $\lambda^{(n)}$ *(called a product density) w.r.t.* ν^d *of form*

$$\lambda^{(n)}(x_1, \ldots, x_n) = \mathrm{E}\exp(Y(x_1) + \cdots + Y(x_n)).$$

The distribution of a LGCP is determined by the intensity $\lambda = \exp(\mu + \frac{\sigma^2}{2})$ *and the pair correlation function* $p(x) = \exp(\sigma^2 r(x))$. *(Hint: Use Corollary 2.7.)*

EXERCISE 2.34 *Show that any two jointly stationary random measures* Ψ_1, Ψ_2 *in* $\mathbb{R}^d$ *with intensities* λ_1, λ_2 *fulfill*

$$\mathrm{E}\Psi_1(A)\Psi_2(B) = \lambda_1\lambda_2 \int_A \mathcal{K}_{1,2}(B - x)\mathrm{d}x = \lambda_1\lambda_2 \int_B \mathcal{K}_{2,1}(A - y)\mathrm{d}y$$

for any $A, B \in \mathcal{B}^d$. *Further, if the cross-correlation functions* $p_{1,2}$ *and* $p_{2,1}$ *exist they are symmetric in the sense that*

$$p_{1,2}(z) = p_{2,1}(-z) \quad \textit{for a.a. } z \in \mathbb{R}^d,$$

cf. [110].

2.6. Application of point processes in epidemiology

The aim of statistical disease mapping is to characterize the spatial variation of cases of a disease and to study connections with covariates. In the present example tick-borne encephalitis (TBE), an infection illness which is transmitted by parasitic ticks and which occasionally afflicts humans, is a disease in question. Epidemiologists and medical practitioners making decision on prophylactic measures deal with the problem of estimating the risk that a human gets infected by TBE at a specific location. Usually the data for statistical analysis consist of case locations and a population map. Moreover, explanatory variables of geographical nature which may influence the risk of infection are often given from geographical information systems.

The data were collected by Zeman [127]. A point pattern of locations of 446 reported cases of TBE in Central Bohemia (region denoted by

S in the following) during 1971-93 is available, see Fig. 2.1. Different covariates are considered: the locations of forests of areas between 10-50 and 50-150 ha, respectively, the subareas of three different forest types (conifer, foliate, and mixed forest) and a map of altitudes.

Finally, population data for the Central Bohemia consist of the number of inhabitants in 3582 administrative units.

The modelling of the TBE data in [7] is motivated by the following simplifying considerations. In the observation period 1971-93 a number $m = 1,112,717$ of inhabitants are living at home locations $h_1, \ldots, h_m \in S$, and the i-th person makes a number N_i of visits to the surroundings of h_i. The N_i's are assumed to be independent and Poisson distributed with mean $\lambda > 0$ independent of i. Given the N_i, the location of each visit of the ith person is distributed according to some density g_{h_i} (with respect to ν_2), and the locations of visits of all persons are assumed to be independent. For a visit to a location $s \in S$, there is associated a probability $\pi(s)$ for getting an infection during the visit. The point process of locations where persons have been infected (cases) is then a Poisson process with intensity function

$$\Lambda(s) = \rho(s)\pi(s), \quad s \in S, \tag{2.23}$$

where $\rho(s) = \lambda \sum_{i=1}^{m} g_{h_i}(s)$ is the *background intensity* of humans visiting s. We model π in (2.23) by a log linear model,

$$\pi(s) = \exp\left(\beta^{\mathsf{T}} d(s) + Y(s)\right), \tag{2.24}$$

where $Y(s)$ is a zero-mean Gaussian process, $\beta = (\beta_0, \ldots, \beta_6)^{\mathsf{T}}$ is a regression parameter, and $d(s) = (1, d_1(s), \ldots, d_6(s))^{\mathsf{T}}$. Here β_0 is an intercept, and $d_1(s), \ldots, d_6(s)$ are six covariates associated with the location $s \in S$, where the index corresponds to the following:

1 ~ forest 10-50 ha, 2 ~ forest 50-150 ha, 3 ~ conifer forest,
4 ~ mixed forest, 5 ~ foliate forest, 6 ~ altitude.

Here $d_1, \ldots, d_5$ are 0-1 functions (equal to 1 in the case of presence of the characteristics). The role of $\exp(Y(s))$ is partly to model deviations of $\rho(s)/\hat{\rho}(s)$ from one, $\hat{\rho}$ being an estimator of unknown ρ. Therefore we do not constrain (2.24) to be less than one, actually, λ is absorbed in $\exp(\beta_0)$. Then $\pi(s)$ is more precisely a *relative risk function.*

The process Y is assumed to be second-order stationary and isotropic with exponential covariance function, i.e.,

$$\operatorname{cov}(Y(s_1), Y(s_2)) = c(\|s_1 - s_2\|; \sigma^2, \alpha) = \sigma^2 \exp(-\|s_1 - s_2\|/\alpha), \tag{2.25}$$

where $\sigma^2 > 0$ is the variance and $\alpha > 0$ is the correlation parameter. A log-Gaussian Cox process is then obtained by assuming that conditionally on $Y = (Y(s))_{s \in S}$ and $\theta = (\beta, \sigma, \alpha)$, the cases Φ form a Poisson process with intensity function $\hat{\rho}(s)\pi(s)$.

A hierarchical Bayesian approach is adapted (cf. [34]). The Gaussian distribution for Y is viewed as a prior and the conditional distribution of Φ given (Y, θ) as the likelihood. Furthermore, a hyper prior density $p(\theta)$ for θ is imposed; specific hyper priors are considered. The likelihood

$$\mathcal{L}(x|Y,\beta) = \exp\left(\nu_2(S) - \int_S \hat{\rho}(s) \exp\left(\beta^{\mathrm{T}} d(s) + Y(s)\right) \mathrm{d}s\right) \times \prod_{\xi \in x} \hat{\rho}(\xi) \exp\left(\beta^{\mathrm{T}} d(\xi) + Y(\xi)\right) \tag{2.26}$$

is derived from the density with respect to the unit rate Poisson process on S, cf. (2.16).

The posterior, that is, the conditional distribution of (Y, θ) given $\Phi = \phi$, can be specified as follows. Suppose that $p(\theta)$ is proper and let E_θ denote expectation conditionally on θ. For $n \geq 1$ and pairwise distinct $s_1, \ldots, s_n \in S$, let $f_{(s_1,\ldots,s_n)}(\cdot \mid \theta)$ denote the conditional density of $(Y(s_1), \ldots, Y(s_n))$ given θ. The posterior density of $(Y(s_1), \ldots, Y(s_n), \theta)$ given $\Phi = \phi$ is defined by

$$f_{(s_1,\ldots,s_n)}(y_1, \ldots, y_n, \theta|x) \propto \tag{2.27}$$
$$E_\theta[\mathcal{L}(x|Y,\beta)|Y(s_1) = y_1, \ldots, Y(s_n) = y_n] f_{(s_1,\ldots,s_n)}(y_1, \ldots, y_n|\theta) p(\theta).$$

The posterior is then given by the consistent set of finite-dimensional posterior distributions with densities of the form (2.27) for $n \geq 1$ and pairwise distinct $s_1, \ldots, s_n \in S$. The integral in (2.26) depends on the continuous random field Y which cannot be represented on a computer. In practice the integral is approximated by a Riemann sum. The aim is an MCMC simulation of the approximate posterior when $\{s_1, \ldots, s_n\}$ agrees with I^M, the set of centres of squares of a lattice covering S with size $M \times M$.

The main obstacle is to handle the high dimensional covariance matrix of $\tilde{Y} = (Y(\eta))_{\eta \in I^M}$. However, the computational cost can be reduced very much by employing the circulant embedding technique described in [26] and [124]; see also [79]. For the MCMC simulations of (Y, θ) given $\Phi = \phi$ a hybrid algorithm as described in [80] was used, where β, σ, and α are updated in turn using so-called truncated Langevin-Hastings updates for β and standard random walk Metropolis updates for σ and α. Geometric ergodicity is thus achieved.

The posterior mean of the relative risk function is plotted as a result of analysis with $M = 64$, see Fig. 2.1. In [7] several choices of background

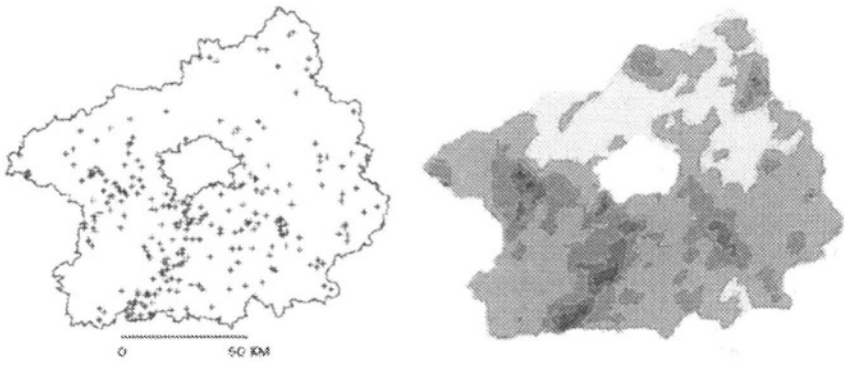

Figure 2.1. Locations of infection by tick-borne encephalitis in Central Bohemia (left). Map of the logarithm of the posterior mean of the relative risk function divided by its maximal value (right). The darker grey-level the larger is the risk of infection.

intensity, which is unknown, are suggested. Model selection is then based on posterior predictive distributions. Among covariates it is shown that the presence of mixed or foliate forest increases the risk of infection.

EXERCISE 2.35 *Prove that the above described model leads to a Poisson process with intensity function* (2.23).

2.7. Weighted random measures, marked point processes

Let Ψ be a random measure in $\mathbb{R}^d$, let C be its Campbell measure (see Definition 2.15) and let W be a locally compact space. Let w be a measurable mapping *(weight function)*

$$w : \operatorname{supp} C \to W$$

(we consider the natural product σ-algebra on $\operatorname{supp} C \subset \mathbb{R}^d \times \mathcal{M}^d$). Then, we call the tuple (Ψ, w) a *weighted random measure* in $\mathbb{R}^d$ with weight space W. Note that a weighted random measure induces a random measure $\tilde{\Psi}$ on the product space $\mathbb{R}^d \times W$:

$$\tilde{\Psi}(B \times D) = \Psi\{x \in B : w(x, \Psi) \in D\},$$

$B \in \mathcal{B}^d$, $D \in \mathcal{B}(W)$. We say that the weighted random measure (Ψ, w) is *stationary* if Ψ is stationary and the weight function is translation covariant, i.e., $w(x, \mu) = w(x + z, t_z\mu)$ for any $(x, \mu) \in \operatorname{supp} C$ and $z \in \mathbb{R}^d$.

If Φ is a point process then the associated weighted random measure is called a *marked point process* with mark space W (this is a special case of the usual notion of a mark process, see e.g. [109, §4.2], where

the marks may be random and not determined by the point process configuration).

EXAMPLE 2.36 *Let Ξ be a random set represented as a locally finite union of C^1-smooth curves in $\mathbb{R}^d$ such that any two curves intersect at most in a finite number of points. Let $\Psi(\cdot) = \mathcal{H}^1(\Xi \cap \cdot)$ be the induced length measure. Clearly $\Xi = \operatorname{supp}\Psi$ and to any $x \in \Xi$ which belongs to one curve only we can assign as weight the tangent direction $w(x, \Psi) \in \mathcal{L}_1$ of the curve at x, obtaining thus a random weighted measure in $\mathbb{R}^d$ with weight space $\mathcal{L}_1$. If Ξ is stationary then the weighted random measure (Ψ, w) is stationary as well.*

Let (Ψ, w) be a stationary weighted random measure in $\mathbb{R}^d$. Due to the stationarity, the intensity measure of the induced random measure $\tilde{\Psi}$ on $\mathbb{R}^d \times W$ can be disintegrated as

$$\mathrm{E}\tilde{\Psi}(B \times D) = \lambda \nu_d(B) \mathcal{W}(D), \quad B \in \mathcal{B}^d, D \in \mathcal{B}(W), \tag{2.28}$$

where $\lambda > 0$ is the intensity of Ψ and $\mathcal{W}$ is a probability measure on W called the *weight distribution.* In case of a marked point process, $\mathcal{W}$ is usually called the mark distribution. A generalization of (2.28) is the Campbell theorem for weighted measures which is represented by the formula

$$\mathrm{E}\int_{\mathbb{R}^d} f(x, w(x, \Psi))\Psi(\mathrm{d}x) = \lambda \int_{\mathbb{R}^d}\int_W f(x, y)\mathcal{W}(\mathrm{d}y)\,\mathrm{d}x \tag{2.29}$$

for any nonnegative measurable function f on $\mathbb{R}^d \times \mathcal{W}$.

For a stationary weighted random measure, the weight distribution can be interpreted as the distribution of the weight at a "typical" point. Let P_0 be the Palm distribution of Ψ at the origin and recall that $\Pr_0$ denotes the corresponding probability distribution. Then we have

$$\mathcal{W}(D) = \Pr_0[w(0, \Psi) \in D] = \int \mathbf{1}_D(w(0, \mu))P_0(\mathrm{d}\mu).$$

The *two-point weight distribution* $\mathcal{W}_h$, $h \in \mathbb{R}^d$, $h \neq 0$, can be introduced by means of the second-order Palm distribution, cf. (2.7), using again the notation $\Pr_{x,y}$ for the second order Palm probability:

$$\begin{aligned} \mathcal{W}_h(D_1 \times D_2) &= \Pr_{0,h}[w(0, \Psi) \in D_1, w(h, \Psi) \in D_2] \\ &= \int \mathbf{1}_{D_1}(w(0, \mu))\mathbf{1}_{D_2}(w(h, \mu))P_{0,h}(\mathrm{d}\mu) \end{aligned} \tag{2.30}$$

for Borel subsets D_1, D_2 of W. Alternatively, we can express $\mathcal{W}_h$ by means of disintegration of the second moment measure of $\tilde{\Psi}$ (in the following we write shortly $w(x) = w(x, .)$ where possible):

THEOREM 2.37 *Let (Ψ, w) be a weighted random measure and f a non-negative measurable function on $(\mathbb{R}^d \times W)^2$. Then*

$$\mathrm{E}\int\int f(x, w(x), y, w(y))\Psi(\mathrm{d}x)\Psi(\mathrm{d}y)$$
$$= \lambda^2 \int_{\mathbb{R}^d}\int_{\mathbb{R}^d}\int_{W^2} f(x, w_1, x+h, w_2)\mathcal{W}_h(\mathrm{d}(w_1, w_2))\mathcal{K}(\mathrm{d}h)\mathrm{d}x.$$

Proof. Using (2.7) and the translation invariance of (Ψ, w) we obtain

$$\mathrm{E}\int\int f(x, w(x), y, w(y))\Psi(\mathrm{d}x)\Psi(\mathrm{d}y)$$
$$= \int_{\mathbb{R}^d\times\mathbb{R}^d} \mathrm{E}_{x,y} f(x, w(x), y, w(y))M_2(\mathrm{d}(x, y))$$
$$= \int_{\mathbb{R}^d\times\mathbb{R}^d} \mathrm{E}_{0,h} f(x, w(0), x+h, w(h))M_2(\mathrm{d}(x, x+h))$$
$$= \int_{\mathbb{R}^d\times\mathbb{R}^d}\int_{W\times W} f(x, w_1, x+h, w_2)\mathcal{W}_h(\mathrm{d}(w_1, w_2))M_2(\mathrm{d}(x, x+h))$$

and the proof is completed by using the disintegration of the second moment measure of Ψ,

$$M_2(\mathrm{d}(x, x+h)) = \lambda^2\mathcal{K}(\mathrm{d}h)\mathrm{d}x.$$

□

EXERCISE 2.38 *Prove formula* (2.29) *using standard measure-theoretic tools.*

2.8. Stationary processes of particles

In general, we consider "particles" to be nonempty compact subsets of $\mathbb{R}^d$. Recall that $\mathcal{K}'$ is the space of all nonempty compact subsets of $\mathbb{R}^d$ equipped with the Hausdorff metric d_H in (1.7). $(\mathcal{K}', d_H)$ is a locally compact Polish space in which each bounded set is compact (see [43, Theorem 9]).

Under a particle process we thus understand a point process Φ on $\mathcal{K}'$. Its intensity measure $\Lambda = \mathrm{E}\Phi$ is a Borel measure on $\mathcal{K}'$. We will assume that it is bounded in the sense

$$\Lambda(\mathcal{K}_B) < \infty \quad \text{for all } B \in \mathcal{K}', \tag{2.31}$$

where $\mathcal{K}_B = \{K \in \mathcal{K}' : K \cap B \neq \emptyset\}$. The set

$$\Xi = \bigcup_{K\in\Phi} K \tag{2.32}$$

is called the *union set* of the process Φ (recall that under $K \in \Phi$ we mean that K is an atom of Φ, see Remark 2.1). Condition (2.31) assures that this union is locally finite. Thus, Ξ is closed and, verifying the necessary measurability properties, one obtains

THEOREM 2.39 *The union set of a point process on $\mathcal{K}'$ satisfying (2.31) is a random closed set in $\mathbb{R}^d$.*

Given $z \in \mathbb{R}^d$, let T_z be the shift operator on $\mathcal{M}(\mathcal{K}')$

$$T_z\mu(\mathcal{U}) = \mu(\{K - z : K \in \mathcal{U}\}), \quad \mathcal{U} \in \mathcal{B}(\mathcal{K}'). \tag{2.33}$$

Further, given a rotation $\rho \in \mathrm{SO}(d)$, we define the corresponding rotation operator R_ρ on $\mathcal{M}(\mathcal{K}')$ by

$$R_\rho\mu(\mathcal{U}) = \mu(\{\rho^{-1}K : K \in \mathcal{U}\}), \quad \mathcal{U} \in \mathcal{B}(\mathcal{K}'). \tag{2.34}$$

DEFINITION 2.40 *A point process on $\mathcal{K}'$ is stationary if its distribution is invariant under T_z for each $z \in \mathbb{R}^d$, and isotropic if its distribution is invariant under R_ρ for any $\rho \in \mathrm{SO}(d)$.*

The intensity measure of a stationary particle process can be disintegrated in the following way. For $K \in \mathcal{K}'$, let $c(K) \in \mathbb{R}^d$ denote a (uniquely defined) *reference point* of a compact set K. We can choose e.g. $c(K)$ as the minimum point in K with respect to the lexicographic order; in fact, the mapping $c : \mathcal{K}' \to \mathbb{R}^d$ can be chosen arbitrarily with the properties of measurability and shift covariance, $c(K+z) = c(K)+z$, $z \in \mathbb{R}^d$. Denote

$$\mathcal{K}'_0 = \{K \in \mathcal{K}' : c(K) = 0\}.$$

The following result can be found e.g. in [120, Theorem 5.5].

THEOREM 2.41 *Let $\Phi \neq 0$ be a stationary point process on $\mathcal{K}'$ with intensity measure Λ satisfying assumption* (2.31). *Then there exists $\alpha \geq 0$ and a probability measure Λ_0 on $\mathcal{K}'_0$ so that for each nonnegative measurable function f on $\mathcal{K}'$ it holds*

$$\int f(K)\Lambda(\mathrm{d}K) = \alpha \int \int f(z + K_0)\Lambda_0(\mathrm{d}K_0)\,\mathrm{d}z. \tag{2.35}$$

REMARK 2.6. We will call α the *intensity* of the process Φ and Λ_0 the distribution of the *typical grain*. Since $\alpha = 0$ corresponds to the trivial process $\Phi = 0$ almost surely, we shall work in the sequel only with particle processes of positive intensity.

DEFINITION 2.42 *The union set Ξ of a Poisson process Φ on $\mathcal{K}'$ is called the Boolean model in $\mathbb{R}^d$ with intensity α and a distribution Λ_0 of typical grain.*

REMARK 2.7. Obviously, if Φ is stationary then the union set Ξ is a stationary random closed set (i.e., $\Xi + z$ has the same distribution as Ξ, $z \in \mathbb{R}^d$).

For a stationary random closed set Ξ in $\mathbb{R}^d$, the volume fraction p and covariance $\mathrm{Cov}(\cdot)$ are defined by

$$p = \Pr[0 \in \Xi], \tag{2.36}$$

$$\mathrm{Cov}(z) = \Pr[0 \in \Xi, z \in \Xi], \quad z \in \mathbb{R}^d. \tag{2.37}$$

EXAMPLE 2.43 *Denote $\mathcal{S} \subset \mathcal{K}'$ the system of all nondegenerate segments in $\mathbb{R}^d$. Each segment $\mathfrak{s} \in \mathcal{S}$ is uniquelly determined by its reference point $z = c(\mathfrak{s})$, length r and direction $\beta \in \mathcal{L}_1$, where $\mathcal{L}_1$ is the space of one-dimensional subspaces in $\mathbb{R}^d$. We can thus endow $\mathcal{S}$ with the euclidean structure by means of the mapping $(z, r, \beta) \mapsto \mathfrak{s}(z, r, \beta)$ from $\mathbb{R}^d \times (0, \infty) \times \mathcal{L}_1$ to calS. A stationary segment process is a stationary process Φ on $\mathcal{K}'$ with values in $\mathcal{S}$. Its primary grain distribution Λ_0 is a probability measure on $\mathcal{S} \subset \mathcal{K}'_0$ which is isomorphic to the space $(0, \infty) \times \mathcal{L}_1$. Factorization (2.35) can be written as*

$$\int_{\mathcal{K}'} f(\mathfrak{s}) \Lambda(\mathrm{d}\mathfrak{s}) = \alpha \int_{\mathbb{R}^d} \int_{(0,\infty)\times\mathcal{L}_1} f(\mathfrak{s}(z, r, \beta)) \Lambda_0(\mathrm{d}(r, \beta))\mathrm{d}z \tag{2.38}$$

(f is an arbitrary nonnegative measurable function on $\mathcal{S}$). Assuming additionally that the segment length and direction are independent, the distribution Λ_0 factorizes into $D \times R$, D being the length distribution and R the direction distribution of a typical segment, and we can write

$$\int_{\mathcal{K}'} f(\mathfrak{s}) \Lambda(\mathrm{d}\mathfrak{s}) = \alpha \int_{\mathbb{R}^d} \int_0^\infty \int_{\mathcal{L}_1} f(\mathfrak{s}(z, r, \beta)) R(\mathrm{d}\beta) D(\mathrm{d}r)\, \mathrm{d}z. \tag{2.39}$$

The length intensity of a stationary segment process Φ is defined by

$$\lambda = \nu_d(B)^{-1} \mathrm{E} \sum_{\mathfrak{s}\in\Phi} \mathcal{H}^1(\mathfrak{s} \cap B), \tag{2.40}$$

where B is any bounded Borel subset of $\mathbb{R}^d$ with positive Lebesgue measure. Using (2.39) one easily obtains

$$\lambda = \alpha \mathrm{E}r, \tag{2.41}$$

where $\mathrm{E}r = \int r\Lambda_0(\mathrm{d}(r,\beta))$ *denotes the mean typical segment length.*

EXERCISE 2.44 *Using the Poisson property and the disintegration of the intensity measure derive the following relations for the Boolean model:*

$$\begin{aligned} 1-p &= \mathrm{e}^{-\alpha\int \nu_d(K_0)\Lambda_0(\mathrm{d}K_0)}, \\ \mathrm{Cov}(z) &= 2p-1+\mathrm{e}^{-\alpha\int \nu_d(K_0\cup(K_0+z))\Lambda_0(\mathrm{d}K_0)}. \end{aligned}$$

2.9. Flat processes

Let $k \in \{0,1,\ldots,d-1\}$ be fixed. A *k-flat process* is a point process on the space $\mathcal{F}_k$ of *k*-dimensional flat subspaces of $\mathbb{R}^d$. A flat $F \in \mathcal{F}_k$ can be parametrized uniquely as $F = L+y$ with a *k*-dimensional linear subspace $L \in \mathcal{L}_k$ and $y \in L^\perp$. Thus, the product topology on $\mathcal{L}_k \times \mathbb{R}^{d-k}$ induces naturally a topology on $\mathcal{F}_k$ (under which, clearly, $\mathcal{F}_k$ is locally compact). There is a natural motion invariant measure on $\mathcal{F}_k$, μ_k, defined by

$$\int f(F)\mu_k(\mathrm{d}F) = \int_{\mathcal{L}_k}\int_{L^\perp} f(L+y)\nu_{d-k}(\mathrm{d}y)U(\mathrm{d}L), \tag{2.42}$$

U being the (unique) rotation invariant distribution on $\mathcal{L}_k$.

We say that a *k*-flat process Φ is *stationary (isotropic)* if its distribution is invariant under the shift mappings T_z (rotations R_ρ) defined on $\mathcal{M}(\mathcal{F}_k)$ as in (2.33) ((2.34), respectively). The intensity measure Λ of a stationary *k*-flat process Φ can be disintegrated in the following way:

$$\int f(F)\Lambda(\mathrm{d}F) = \alpha\int_{\mathcal{L}_k}\int_{L^\perp} f(L+y)\nu_{d-k}(\mathrm{d}y)R(\mathrm{d}L), \tag{2.43}$$

with $\alpha \geq 0$ and a probability measure R on $\mathcal{L}_k$, where f is any nonnegative measurable function on $\mathcal{F}_k$. The number α is called the *intensity* and R the *direction distribution* of the process Φ (for more details, see [103, §4.1]). If Φ is stationary and isotropic then $R = U$, the uniform distribution on $\mathcal{L}_k$, and the intensity measure Λ is a multiple of the motion invariant measure μ_k on $\mathcal{F}_k$. To any flat process Φ we can attach naturally a random measure in $\mathbb{R}^d$

$$\Psi(B) = \mathrm{E}\int \mathcal{H}^k(B\cap F)\Phi(\mathrm{d}F) = \mathrm{E}\sum_{F\in\Phi}\mathcal{H}^k(B\cap F), \tag{2.44}$$

i.e., the *k*-dimensional measure supported by the flats of the process. If Φ is stationary isotropic then clearly Ψ is stationary isotropic as well and

the intensity λ of Ψ can be computed by using the Campbell theorem

$$\begin{aligned}\lambda\nu_d(B) = \mathbb{E}\Psi(B) &= \mathbb{E}\int \mathcal{H}^k(B\cap F)\Phi(\mathrm{d}F)\\ &= \int \mathcal{H}^k(B\cap F)\alpha\mu_k(\mathrm{d}F)\\ &= \alpha\int_{\mathcal{L}_k}\int_{L^\perp}\mathcal{H}^k(B\cap(L+y))\nu_{d-k}(\mathrm{d}y)U(\mathrm{d}L)\\ &= \alpha\nu_d(B),\end{aligned}$$

(we have used (2.42) and the Fubini theorem in the last two steps), hence, $\lambda = \alpha$.

Chapter 3

RANDOM FIBRE AND SURFACE SYSTEMS

Random fibre and surface systems are geometrical formations of great interest in biology, medicine, materials research and other applied sciences. They present models of structures like roots, capillaries, membranes, dislocations, cracks, etc. In stochastic geometry such structures are usually modelled as union sets of processes of particles (in the sense of Subsection 2.8) which may be fibres or (pieces of) surfaces in this case. In literature it is assumed usually that the fibres or surfaces chosen to represent the particles are smooth (at least C^1) which makes it possible to use basic tools of differential geometry to treat at least the lengths (see Stoyan et al., [109]).

We follow here the approach using geometric measure theory and introduced in stochastic geometry by Zähle [125]. Fibres or surfaces are modelled as Hausdorff $(\mathcal{H}^k)$ rectifiable sets of appropriate dimension, $k = 1$ or $d - 1$, in the d-dimensional Euclidean space. The advantage is twofold: first, more general geometric objects are included, and second, the class of Hausdorff rectifiable sets is closed with respect to the usual operations as intersections, planar sections and projections. Although the mathematical background is rather complicated, the applications of the theory can be understood without deep knowledge of geometric measure theory and one can imagine under a Hausdorff rectifiable set a (piecewise) smooth object without risk of confusion (nevertheless, the setting is much more general and a Hausdorff rectifiable set need not be smooth in the classical sense in any point).

A remark should be made about notation. In the literature, the term "fibre (surface) process" is often used in two meanings: it applies to both the process of fibres (surfaces) and to its union set. In order to avoid confusion, we use the notion "process" only for the particle process, and

the union sets, or, more generally, random closed sets which are $\mathcal{H}^1$ $(\mathcal{H}^{d-1})$ -rectifiable, are called "random fibre (surface) systems".

In this chapter only stationary structures are considered. The main object is a random fibre or surface system and the induced random measure (which is the Hausdorff measure of corresponding dimension restricted to the random set). The main characteristic of interest is the intensity λ of the induced random measure (length intensity for random fibre systems and surface area intensity for random surface systems). One of the motivations for the research presented is using anisotropic sampling designs for the intensity estimation and determining the variances of the related intensity estimators. This task needs a thorough investigation of second moment characteristics of the random measures and their relationship to the characteristics of the corresponding random sets or fibre (surface) processes. Of course, the dependence on directions of the random fibre or surface system is crucial.

One class of problems is the study of relations between the process and its transformation by means of a section or projection. This yields a background to stereological methods ([109], [118], [86]). Intersecting a fibre system with a hyperplane or a surface system with a line we obtain a locally finite point set (point process). Intersection of a surface system with a plane yields a fibre system, similarily a projection of spatial fibre system onto a plane. The distribution of the orientation and allocation of section and projection probes is called a "sampling design". Assuming stationarity of the model the shifts of probes do not play any role. The relations between the intensities of the original and the induced systems can be used to estimate the intensity of the induced structure. It is the main aim of Chapter 3 to systemize the basic probes, to study the moment relations up to the second order and apply them to the investigation of statistical properties of intensity estimators. Other tools for the investigation of random sets such as distances and contact distributions (see e.g. Hug et al. [56]) are beyond the scope of the book.

In the last section of this chapter we try to classify unbiased intensity estimators from the point of view of their variances. Asymptotic variances of some estimators are compared.

The basic reference sources for fibre and surface systems are the books of Stoyan et al. [109] and Schneider and Weil [103]. For related stereological methods, see Weibel [118] and Ohser and Mücklich [86]. Variances of intensity estimators were studied among others by Baddeley and Cruz-Orive [10], Schladitz [98] and Mrkvička [82], see also [5] and [14].

3.1. Geometric models

In this section we shall consider a k-dimensional random closed set Ξ in $\mathbb{R}^d$, where $k < d$ (typically, $k = 1$ or $k = d - 1$). To formalize the meaning of a k-dimensional random closed set, we use the general concept due to Zähle [125] who introduced *random $\mathcal{H}^k$-sets* as random closed sets in $\mathbb{R}^d$ which are $\mathcal{H}^k$-rectifiable (see Subsection 1.1.3). It is shown in [125] that the space

$$\mathcal{F}^k := \{F \in \mathcal{F}(\mathbb{R}^d) : F \text{ is } \mathcal{H}^k\text{-rectifiable}\}$$

is an $\mathfrak{F}(\mathbb{R}^d)$-measurable subsystem of $\mathcal{F}(\mathbb{R}^d)$ (see Definition 2.4). Recall that by Theorem 1.5, for a random $\mathcal{H}^k$-set Ξ, the k-dimensional approximative tangent space $\operatorname{Tan}^k(\Xi, x)$ exists for $\mathcal{H}^k$-almost all $x \in \Xi$. As an example of a random $\mathcal{H}^k$-set, consider a locally finite union of $\mathcal{C}^1$-smooth k-dimensional manifolds (fibres if $k = 1$ and surfaces if $k = d - 1$). For particular dimensions, we shall use the following terminology: a random $\mathcal{H}^1$-set will be called a (random) *fibre system* and a random $\mathcal{H}^{d-1}$-set a *(random) surface system.*

A random $\mathcal{H}^k$-set Ξ is often constructed as the union set of a "particle" process, where the particles are again $\mathcal{H}^k$-rectifiable closed sets. Following [125], we call Φ a *$\mathcal{H}^k$-process* if it is a point process on the state space $\mathcal{F}^k$ (of $\mathcal{H}^k$-rectifiable closed sets) with the σ-algebra induced by the σ-algebra $\mathfrak{F}(\mathbb{R}^d)$ on the space of closed sets. In particular, Φ can be a line or fibre process $(k = 1)$, or a hyperplane or surface process $(k = d - 1)$. This approach is slightly more general than that in Subsection 2.8 where only compact particles are allowed. Analogously to condition (2.31), we have to assume that only a finite number of particles hit a bounded region (this condition is necessary in order that the union set be closed). This property will be guaranteed for almost all realizations by the assumption

$$\mathrm{E}\,\mathrm{card}\{K \in \Phi : K \cap W \neq \emptyset\} < \infty \quad \text{for any bounded } W \in \mathcal{B}^d. \tag{3.1}$$

Then, it is not difficult to see that the union set

$$\Xi = \bigcup_{K \in \Phi} K \tag{3.2}$$

is a random $\mathcal{H}^k$-set and if Φ is stationary (in the sense of Definition 2.40) then Ξ is stationary as well.

With a random $\mathcal{H}^k$-set Ξ we can always consider the induced random measure in $\mathbb{R}^d$

$$\mathcal{H}^k \mid \Xi(\cdot) = \mathcal{H}^k(\Xi \cap \cdot)$$

(the restriction of the k-dimensional Hausdorff measure to Ξ). Besides the Hausdorff measure, we shall consider various restrictions of projection measures to Ξ. These are defined in the following subsection.

3.1.1 Projection integral-geometric measures

Let A be a bounded $\mathcal{H}^k$-set in $\mathbb{R}^d$ and let p_L denote the orthogonal projection onto a k-dimensional linear subspace L of $\mathbb{R}^d$. The value

$$\mathrm{TP}_L(A) = \int_L \mathrm{card}\,((A \cap p_L^{-1}\{y\})\nu_k(\mathrm{d}y) \tag{3.3}$$

is called the *total projection of A onto L.* (Note that the total projection may be infinite for some L.) The Crofton formula (Theorem 1.14) with $k = 0$ and $j = 1$ says that, if A is the boundary of a polyconvex set, its mean (w.r.t. rotations) total projection is a multiple of the surface area. This is true even in our general setting and can be stated as follows. Recall that U denotes the uniform (rotationally invariant) probability distribution over the Grassmannian $\mathcal{L}_k$ of k-dimensional subspaces of $\mathbb{R}^d$. The *k-dimensional integral-geometric measure* is defined as

$$\mathcal{I}^k(B) = \frac{1}{\beta_{d,k}} \int_{\mathcal{L}_k} \mathrm{TP}_L(B)U(\mathrm{d}L) \quad B \in \mathcal{B}^d,$$

where

$$\beta_{d,k} = \frac{\Gamma(\frac{k+1}{2})\Gamma(\frac{d-k+1}{2})}{\Gamma(\frac{d+1}{2})\sqrt{\pi}}.$$

The integrability of the function $L \mapsto \mathrm{TP}_L(B)$ and the correctness of the definition follows from [31, §2.10.15].

Since in applications we shall work only with the cases $k = 1$ or $k = d - 1$, we shall denote also

$$\beta_d = \beta_{d,1} = \beta_{d,d-1} = \frac{\Gamma(d/2)}{\Gamma((d+1)/2)\sqrt{\pi}}; \tag{3.4}$$

note that, in particular, $\beta_2 = \frac{2}{\pi}$ and $\beta_3 = \frac{1}{2}$.

THEOREM 3.1 ([31],§3.2.26) *For any bounded Borel $\mathcal{H}^k$-rectifiable set $A \subseteq \mathbb{R}^d$ we have $\mathcal{I}^k(A) = \mathcal{H}^k(A)$.*

It will prove useful in the sequel to use other than the uniform distribution in the definition of the integral-geometric measure.

DEFINITION 3.2 *Given any probability distribution Q on $\mathcal{L}_k$,*

$$\mathcal{I}_Q^k(A) = \frac{1}{\beta_{d,k}} \int_{\mathcal{L}_k} \mathrm{TP}_L(A)Q(\mathrm{d}L), \quad A \in \mathcal{B}^d, \tag{3.5}$$

is the projection (integral-geometric) measure with respect to Q.

In fact, $\mathcal{I}_Q^k(A)$ is the mean total projection of A w.r.t. the distribution Q of the projection space.

Although a relation between $\mathcal{I}_Q^k$ and $\mathcal{I}^k$ can be obtained as a consequence of Theorem 1.12, a detailed proof is presented here for the sake of completeness. Recall that for subspaces $L_1 \in \mathcal{L}_i$ and $L_2 \in \mathcal{L}_{d-i}$, $[L_1, L_2]$ is the volume of the parallelepiped spanned by the vectors of any two orthonormal bases of L_1 and L_2. (If in particular $L_1 \in \mathcal{L}_1$ and $L_2 \in \mathcal{L}_{d-1}$, we have $[L_1, L_2] = |\cos \sphericalangle(L_1, L_2^\perp)|$). Further we define a function on $\mathcal{L}_k$

$$\mathcal{F}_Q(L) = \int_{\mathcal{L}_k} [L, L_1^\perp]\, Q(\mathrm{d}L_1). \tag{3.6}$$

It is always $0 \leq \mathcal{F}_Q(L) \leq 1$, specially $\mathcal{F}_U(L) = \beta_{d,k}$ is constant.

PROPOSITION 3.1 *For any bounded $\mathcal{H}^k$-rectifiable set A and any Borel measurable function $g : A \to [0, \infty)$ we have*

$$\int_A g(x)\mathcal{I}_Q^k(\mathrm{d}x) = \frac{1}{\beta_{d,k}} \int_A g(x)\mathcal{F}_Q\left(\mathrm{Tan}^k(A, x)\right) \mathcal{I}^k(\mathrm{d}x). \tag{3.7}$$

Proof. First, notice that it is sufficient to prove the formula for the case when g is the characteristic function of a measurable set since the general case follows then by usual measure-theoretic arguments. Note further that $\mathcal{I}^k$ may be replaced by $\mathcal{H}^k$ on the right hand side of (3.7) by Theorem 3.1. Recall also that $\mathrm{Tan}^k(A, x)$ is a k-dimensional subspace for $\mathcal{H}^k$-almost all $x \in A$ (see Theorem 1.5), hence $[\mathrm{Tan}^k(A, x), L^\perp]$ is well defined for any $L \in \mathcal{L}_k$ and $\mathcal{H}^k$-almost all $x \in A$. From the coarea theorem (Theorem 1.6) we get

$$\int_{\mathcal{L}_k} \mathrm{TP}_L(A) U(\mathrm{d}L) = \int_A [\mathrm{Tan}^k(A, x), L^\perp]\, \mathcal{H}^k(\mathrm{d}x),$$

since $[\mathrm{Tan}^k(A, x), L^\perp]$ is the $\mathcal{H}^k$-approximate Jacobian of the orthogonal projection of A onto L at x. The result follows then after integration w.r.t. Q. □

Given two probability measures R, Q on $\mathcal{L}_k$, we define the constant

$$\mathcal{F}_{RQ} = \int_{\mathcal{L}_k} \mathcal{F}_Q(L)\, R(\mathrm{d}L). \tag{3.8}$$

The property of symmetry $\mathcal{F}_{RQ} = \mathcal{F}_{QR}$ follows from the Fubini Theorem since $[L_1, L_2^\perp] = [L_2, L_1^\perp]$ for any subspaces $L_1, L_2 \in \mathcal{L}_k$. Note also that $\mathcal{F}_{UQ} = \beta_{d,k} = \beta_{d,d-k}$ for any distribution Q on $\mathcal{L}_k$.

3.1.2 The Campbell measure and first order properties

Let Ξ be a stationary random $\mathcal{H}^k$-set in $\mathbb{R}^d$ and let $\Psi = \mathcal{H}^k \mid \Xi$ denote its induced random measure. We define the intensity λ of Ξ as the intensity of the induced random measure Ψ, i.e.

$$\lambda = \nu_d(B)^{-1}\mathrm{E}\mathcal{H}^k(\Xi \cap B)$$

for any bounded Borel set $B \in \mathcal{B}^d$ of positive Lebesgue measure. We shall always assume that

$$\lambda < \infty. \tag{3.9}$$

DEFINITION 3.3 *Let Q be a probability distribution on $\mathcal{L}_k$. The restriction of $\mathcal{I}_Q^k$ to Ξ is called the (induced) random projection measure and denoted $\Psi_Q = \mathcal{I}_Q^k \mid \Xi$. λ_Q will denote the intensity of Ψ_Q.*

Obviously it holds $\lambda_Q = \mathrm{E}\Psi_Q([0,1]^d)$.

EXAMPLE 3.4 *Let $k = 1$ and let Ξ be the union set of a $\mathcal{H}^1$-process of compact fibres. Then Ψ is the length measure corresponding to Ξ and λ is the mean length of fibres per unit volume. As a probability measure Q on $\mathcal{L}_1$, first consider $Q = \delta_L$, $L \in \mathcal{L}_1$ (one single projection direction). Then for $B \in \mathcal{B}^d$, $\beta_d\Psi_Q(B)$ is equal to the total projected length of fibres in $X \cap B$ onto the line $L \in \mathcal{L}_1$. For a general Q the total projected length is averaged w.r.t. Q. In particular, $\Psi_U = \Psi$.*

EXAMPLE 3.5 *Let $k = d - 1$, Ξ be a stationary $\mathcal{H}^{d-1}$-set and Ψ its surface area measure. Then $\beta_d\Psi_Q(B)$ is an average (w.r.t. Q) total projected area of surfaces in $B \cap \Xi$ projected on hyperplanes with orientation distribution Q.*

Under (3.9), the Campbell measure C of Ψ is defined on $\mathbb{R}^d \times \mathcal{M}^d$ (see Chapter 2); recall that

$$C(B \times \mathcal{U}) = \mathrm{E}(\Psi(B)\mathbf{1}_{\mathcal{U}}(\Psi))$$

and

$$C(B \times \mathcal{U}) = \lambda \int_B P_x(\mathcal{U})\,\mathrm{d}x = \lambda \int_B P_0(t_x\mathcal{U})\,\mathrm{d}x \tag{3.10}$$

for $B \in \mathcal{B}^d$ and $\mathcal{U} \in \mathfrak{M}^d$, where P_x is the Palm distribution of Ψ at $x \in \mathbb{R}^d$ and the shift operator t_x is defined in Section 2.5. The same result can also be stated in the following form

$$\int g(x,\psi)C(\mathrm{d}(x,\psi)) = \lambda \int_{\mathbb{R}^d}\int_{\mathcal{M}^d} g(x, t_x\psi)\,P_0(\mathrm{d}\psi)\,\mathrm{d}x, \tag{3.11}$$

where g is any nonnegative measurable function on $\mathbb{R}^d \times \mathcal{M}^d$.

Analogously, we can define the Campbell measure C_Q and Palm distributions $P_{Q,x}$ related to the stationary random measure Ψ_Q and we have

$$C_Q(B \times \mathcal{U}) = \lambda \int_B P_{Q,x}(\mathcal{U})\,\mathrm{d}x = \lambda \int_B P_{Q,0}(t_x\mathcal{U})\,\mathrm{d}x.$$

Setting $Q = U$ (the uniform distribution), we obtain $C_Q = C$.

We shall equip the random measure Ψ, Ψ_Q with the weight function $w(x, \Psi) = \mathbf{Tan}^k(\Xi, x)$, $x \in \operatorname{supp} \Psi \subset \Xi$, getting thus a stationary weighted random measure (Ψ, w), (Ψ_Q, w), respectively, with the weight space $\mathcal{L}_k$.

DEFINITION 3.6 The *rose of directions* R of the stationary random $\mathcal{H}^k$-set Ξ is the weight distribution of (Ψ, w), i.e.,

$$R(G) = \mathrm{Pr}_0[\mathbf{Tan}^k(\Xi, 0) \in G],$$

where G is a Borel subset of $\mathcal{L}_k$ and Pr_0 denotes the Palm probability at the origin. The *projection rose of directions* R_Q w.r.t. a probability distribution Q on $\mathcal{L}_k$ is defined analogously as the weight distribution of the stationary weighted process (Ψ_Q, w), i.e.

$$R(G) = \mathrm{Pr}_{Q,0}[\mathbf{Tan}^k(\Xi, 0) \in G],$$

where $\mathrm{Pr}_{Q,0}$ is now the probability with respect to the Palm distribution at the origin of the projection measure Ψ_Q.

REMARK 3.1. We shall often write $\mathbf{Tan}^k(\psi, x)$ instead of $\mathbf{Tan}^k(\operatorname{supp}\psi, x)$ if ψ is a realization of the random measure Ψ (Ψ_Q) and $x \in \operatorname{supp}\psi$.

Using (3.11) we obtain the following representation.

LEMMA 3.7 *For any* $B \in \mathcal{B}^d$ *bounded we have*

$$\begin{aligned} \lambda\nu_d(B)R(G) &= \mathrm{E}\int_{B\cap\Xi} \mathbf{1}_G(\mathbf{Tan}^k(\Xi, x))\,\mathcal{H}^k(\mathrm{d}x), \\ \lambda_Q\nu_d(B)R_Q(G) &= \mathrm{E}\int_{B\cap\Xi} \mathbf{1}_G(\mathbf{Tan}^k(\Xi, x))\,\mathcal{I}_Q^k(\mathrm{d}x). \end{aligned}$$

Proof. The equalities are obtained by evaluating the integral of the product $\mathbf{1}_B(x)\mathbf{1}_G(\mathbf{Tan}^k(\psi, x))$ w.r.t. the Campbell measure C, C_Q, respectively. □

The intensities and roses of directions of Ξ and its projection versions are related to each other in the following manner.

PROPOSITION 3.2 *It holds*

1) $\lambda_Q = \beta_{d,k}^{-1} \mathcal{F}_{RQ} \lambda$,

2) $R_Q(G) = \mathcal{F}_{RQ}^{-1} \int_G \mathcal{F}_Q(L)\, R(\mathrm{d}L)$.

Proof. Using the definition and Proposition 3.1 we get

$$\lambda_Q = \mathrm{E}\mathcal{I}_Q^k(\Xi \cap B) = \beta_{d,k}^{-1}\, \mathrm{E} \int_B \mathcal{F}_Q(\mathrm{Tan}^k(\Xi, x))\, \mathcal{H}^k(\mathrm{d}x),$$

where B is any bounded Borel subset of $\mathbb{R}^d$ with unit Lebesgue measure. The last integral can be evaluated by means of the Campbell measure and applying (3.11) we obtain

$$\begin{aligned} \lambda_Q &= \beta_{d,k}^{-1} \int \mathbf{1}_B(x) \mathcal{F}_Q(\mathrm{Tan}^k(\psi, x))\, C(\mathrm{d}(x, \psi)) \\ &= \beta_{d,k}^{-1} \lambda \int_B \int \mathcal{F}_Q(\mathrm{Tan}^k(\psi, 0))\, P_0(\mathrm{d}\psi)\, \mathrm{d}x \\ &= \beta_{d,k}^{-1} \lambda \int \mathcal{F}_Q(L)\, R(\mathrm{d}L) \\ &= \beta_{d,k}^{-1} \lambda \mathcal{F}_{RQ}. \end{aligned}$$

To verify 2), we apply Lemma 3.7 and Proposition 3.1 and we get for B as above

$$\begin{aligned} R_Q(G) &= \lambda_Q^{-1} \mathrm{E} \int_{B \cap \Xi} \mathbf{1}_G(\mathrm{Tan}^k(\Xi, x)) \mathcal{I}_Q^k(\mathrm{d}x) \\ &= \lambda_Q^{-1} \beta_{d,k}^{-1} \mathrm{E} \int_{B \cap \Xi} \mathbf{1}_G(\mathrm{Tan}^k(\Xi, x)) \mathcal{F}_Q(\mathrm{Tan}^k(\Xi, x))\, \mathcal{H}^k(\mathrm{d}x). \end{aligned}$$

The first equality in Lemma 3.7 implies that the last expectation equals

$$\lambda \int_G \mathcal{F}_Q(L)\, R(\mathrm{d}L),$$

and the use of 1) in Proposition 3.2 completes the proof. □

3.1.3 Second-order properties

Let P, P_Q denote the distribution of Ψ, Ψ_Q, respectively. As above, $P_{Q,x}$ will denote the Palm distribution of Ψ_Q at $x \in \mathbb{R}^d$. The variance $\mathrm{var}\, \Psi_Q(B)$ can be expressed using the reduced second moment measure $\mathcal{K}_Q$ of Ψ_Q which is a measure on $\mathcal{B}^d$ defined by means of the Palm distribution

$$\lambda_Q \mathcal{K}_Q(B) = \mathrm{E}_0 \Psi_Q(B),$$

$B \in \mathcal{B}^d$ (cf. (2.19)). The pair-correlation function of Ψ_Q (density of $\mathcal{K}_Q$ with respect to ν_d) will be denoted by p_Q.

Using Theorem 2.31 we obtain for $A, B \in \mathcal{B}^d$

$$\begin{aligned} \mathrm{E}\Psi_Q(A)\Psi_Q(B) &= \int\int \mathbf{1}_A(x)\psi(B)\psi(\mathrm{d}x)P_Q(\mathrm{d}\psi) \\ &= \lambda_Q \int \mathbf{1}_A(x) \int t_x\psi(B)P_{Q,0}(\mathrm{d}\psi)\nu_d(\mathrm{d}x) \\ &= \lambda_Q^2 \int\int \mathbf{1}_A(x)\mathbf{1}_B(x+h)\mathcal{K}_Q(\mathrm{d}h)\nu_d(\mathrm{d}x) \\ &= \lambda_Q^2 \int g_{A,B}(x)\mathcal{K}_Q(\mathrm{d}x), \end{aligned}$$

where $g_{A,B}(x) = \nu_d(A \cap (B - x))$ and $g_B \equiv g_{B,B}$. Thus, we obtain the following general formula for the variance:

THEOREM 3.8 *We have*

$$\operatorname{var}\Psi_Q(B) = \lambda_Q^2 \left(\int g_B(x)\mathcal{K}_Q(\mathrm{d}x) - \nu_d(B)^2 \right).$$

If the pair-correlation function p_Q of Ψ_Q exists, then

$$\operatorname{var}\Psi_Q(B) = \lambda_Q^2 \int g_B(x)(p_Q(x) - 1)\nu_d(\mathrm{d}x). \tag{3.12}$$

REMARK 3.2. Specially for $Q = U$ it holds

$$\operatorname{var}\Psi(B) = \lambda^2 \int g_B(x)(p(x) - 1)\nu_d(\mathrm{d}x)$$

assuming that the pair-correlation function p of Ψ exists.

If the window B has a shape different from a ball then both g_B and the variance $\operatorname{var}\Psi_Q(B)$ in Theorem 3.8 may depend on the orientation of B. Therefore Ψ_Q may be anisotropic even if Ψ is isotropic.

We shall establish now a relation between the measures $\mathcal{K}_Q$ (of Ψ_Q) and $\mathcal{K}$ (of Ψ). Let $\mathcal{W}_h$, $h \in \mathbb{R}^d$, $h \neq 0$, be the two-point weight distribution of Ψ (see (2.30)) defined by

$$\int g(m_1, m_2)\mathcal{W}_h(\mathrm{d}(m_1, m_2)) = \mathrm{E}_{0,h}\, g(\mathrm{Tan}^k(\Psi, 0), \mathrm{Tan}^k(\Psi, h)),$$

where g is any nonnegative measurable function on $\mathcal{L}_k^2$.

PROPOSITION 3.3 *The measures* $\mathcal{K}_Q$ *and* $\mathcal{K}$ *are related by*

$$\mathcal{K}_Q(B) = \frac{1}{\mathcal{F}_{RQ}^2} \int_B I_Q(h)\, \mathcal{K}(\mathrm{d}h), \tag{3.13}$$

where

$$I_Q(h) = \int_{\mathcal{L}_k^2} \mathcal{F}_Q(w_1)\mathcal{F}_Q(w_2)\mathcal{W}_h(\mathrm{d}(w_1, w_2)).$$

If the pair-correlation function p *of* Ψ *exists then*

$$p_Q(h) = \frac{I_Q(h)}{\mathcal{F}_{RQ}^2} p(h) \tag{3.14}$$

is the pair-correlation function of Ψ_Q.

Proof. The second order moment measures of the weighted processes Ψ_Q ,Ψ are related by

$$\begin{aligned} &\mathrm{E} \int \int f(x, w(x), y, w(y)) \Psi_Q(\mathrm{d}x) \Psi_Q(\mathrm{d}y) \\ &\quad = \beta_{d,k}^{-2}\, \mathrm{E} \int \int f(x, w(x), y, w(y)) \mathcal{F}_Q(w(x)) \mathcal{F}_Q(w(y)) \Psi(\mathrm{d}x) \Psi(\mathrm{d}y) \end{aligned}$$

(see Proposition 3.1). Applying Theorem 2.37 to both sides of this equality for the function $f(x, w_1, y, w_2) = \mathbf{1}_A(x)\mathbf{1}_B(y - x)$ we get

$$\lambda_Q^2 \int_A \mathcal{K}_Q(B) \nu_d(\mathrm{d}x) = \beta_{d,k}^{-2} \lambda^2 \int_A \int_B I_Q(h) \mathcal{K}(\mathrm{d}h) \nu_d(\mathrm{d}x).$$

Since this holds for an arbitrary Borel set A, (3.13) follows after using the equality $\beta_{d,k}^{-1}\lambda = \mathcal{F}_{RQ}^{-1}\lambda_Q$ (see Proposition 3.2, assertion 1)). Equation (3.14) is a simple reformulation in terms of densities. □

COROLLARY 3.9

$$\operatorname{var} \Psi_Q(B) = \beta_{d,k}^{-2} \lambda^2 \left(\int g_B(x) I_Q(x) \mathcal{K}(\mathrm{d}x) - \mathcal{F}_{RQ}^2 \nu_d(B)^2 \right).$$

Proof. Follows immediately from Theorem 3.8 and Proposition 3.3. □

EXERCISE 3.10 *Let* Q_1, Q_2 *be two probability measures on* $\mathcal{L}_k$. *Let* p_{12} *be the cross-correlation function of* Ψ_{Q_1} *and* Ψ_{Q_2}, *cf. Section 2.5. Show that if the pair-correlation function* p *of* Ψ *exists, then*

$$p_{12}(x) = \frac{\int_{\mathcal{L}_k^2} \mathcal{F}_{Q_1}(w_1)\mathcal{F}_{Q_2}(w_2)\mathcal{W}_x(\mathrm{d}(w_1, w_2))}{\mathcal{F}_{Q_1 R}\mathcal{F}_{Q_2 R}} p(x)$$

ν_d-*almost surely.*

3.1.4 $\mathcal{H}^k$-processes and Palm distributions

We consider now the case when the random $\mathcal{H}^k$-set Ξ is induced by a $\mathcal{H}^k$-process Φ in the form (3.2). In this subsection, we restrict ourselves to processes with compact particles, i.e., we assume that Φ is a stationary point process on $\mathcal{K}^k = \mathcal{F}^k \cap \mathcal{K}'$, the space of all nonempty compact $\mathcal{H}^k$-rectifiable subsets of $\mathbb{R}^d$, fulfilling (3.1).

Consider the operator T_Q from $\mathcal{N}(\mathcal{K}^k)$ to the space of (nonnegative) measures on $\mathbb{R}^d$ acting as

$$T_Q\phi(\cdot) = \int \mathcal{I}_Q^k(K \cap \cdot)\, \phi(\mathrm{d}K).$$

Due to (3.1), $T_Q\Phi$ is a random measure in $\mathbb{R}^d$. We shall assume in the sequel that

$$\text{a.s. there are no } K \neq L \in \Phi \text{ with } \mathcal{H}^k(K \cap L) > 0. \tag{3.15}$$

Then it is easy to realize that

$$\Psi_Q = T_Q\Phi. \tag{3.16}$$

Let us denote for brevity

$$\chi_Q^K(\cdot) = \mathcal{I}_Q^k(K \cap \cdot)$$

the restriction of the measure $\mathcal{I}_Q^k$ to K. If $Q = U$ we write simply $\chi^K = \chi_U^K$. With this notation we have $T_Q\phi(\cdot) = \int \chi_Q^K(\cdot)\phi(\mathrm{d}K)$. The measurability of T_Q w.r.t. usual σ-algebras follows from [125]. Let $\Lambda = \mathrm{E}\Phi$ be the intensity measure of Φ which can be disintegrated as in Theorem 2.41 into the intensity $\alpha > 0$ and a primary grain distribution Λ_0. We shall use the notation Z_0 for the primary grain, i.e., a random element from $\mathcal{K}^k$ with distribution Λ_0.

The following lemma relates the intensity λ_Q of the induced random measure Ψ_Q to the intensity α of the process Φ:

LEMMA 3.11 *Under the assumptions described above, we have*

$$\lambda_Q = \alpha \int_{\mathcal{K}_0'} \mathcal{I}_Q^k(K_0)\Lambda_0(\mathrm{d}K_0) = \alpha \mathrm{E}\mathcal{I}_Q^k(Z_0).$$

Proof. For any Borel bounded subset $B \subseteq \mathbb{R}^d$ it holds

$$\begin{aligned}
\mathrm{E}\Psi_Q(B) &= \mathrm{E}\int \chi_Q^K(B)\Phi(\mathrm{d}K) \\
&= \int \chi_Q^K(B)\Lambda(\mathrm{d}K) \\
&= \alpha\int\int_{\mathbb{R}^d} \chi_Q^{K_0+x}(B)\nu_d(\mathrm{d}x)\Lambda_0(\mathrm{d}K_0) \\
&= \alpha\int\int_{\mathbb{R}^d} \chi_Q^{K_0}(B-x)\nu_d(\mathrm{d}x)\Lambda_0(\mathrm{d}K_0) \\
&= \alpha\int\int\int \mathbf{1}_{B-y}(x)\nu_d(\mathrm{d}x)\mathbf{1}_{K_0}(y)\mathcal{I}_Q^k(\mathrm{d}y)\Lambda_0(\mathrm{d}K_0) \\
&= \alpha\nu_d(B)\int \mathcal{I}_Q^k(K_0)\Lambda_0(\mathrm{d}K_0).
\end{aligned}$$

□

Let us further introduce the probability distribution Λ_Q on $\mathcal{K}^k$ defined by

$$\int h(K)\Lambda_Q(\mathrm{d}K) = \frac{\int\int_{K_0} h(K_0-y)\mathcal{I}_Q^k(\mathrm{d}y)\Lambda_0(\mathrm{d}K_0)}{\int \mathcal{I}_Q^k(K_0)\Lambda_0(\mathrm{d}K_0)} \tag{3.17}$$

for any nonnegative measurable function h on $\mathcal{K}^k$. (Λ_Q is the distribution of the $\mathcal{I}_Q^k$-weighted typical point K of the process shifted randomly so that its $\mathcal{I}_Q^k$-weighted uniform random point falls into the origin.)

Denote by $\tilde{P}$ the distribution of the point process Φ and by $\tilde{P}_K$ the Palm distribution of Φ at a compact set K. The main theorem of this subsection relates the Palm distribution $P_{Q,0}$ of the projection measure Ψ_Q to the Palm distribution $\tilde{P}_K$.

THEOREM 3.12 *The Palm distribution $P_{Q,0}$ fulfills*

$$P_{Q,0} = \int \left(\tilde{P}_K T_Q^{-1}\right)\Lambda_Q(\mathrm{d}K).$$

REMARK 3.3.In other words, we have

$$P_{Q,0}(\mathcal{U}) = \int \tilde{P}_K(\{\phi : T_Q\phi \in \mathcal{U}\})\Lambda_Q(\mathrm{d}K)$$

for any measurable set $\mathcal{U} \subseteq \mathcal{M}^d$.

Proof.(of Theorem 3.12) Using the Campbell theorem we obtain

$$\begin{aligned}
\mathrm{E}\Psi_Q(B)g(\Psi_Q) &= \int_{\mathcal{M}^d} \psi(B)g(\psi)P_Q(\mathrm{d}\psi) \\
&= \int_{\mathcal{M}(\mathcal{K}^k)} (T_Q\phi)(B)g(T_Q\phi)\tilde{P}(\mathrm{d}\phi) \\
&= \int_{\mathcal{M}(\mathcal{K}^k)} \int_{\mathcal{K}^k} \chi_Q^K(B)g(T_Q\phi)\phi(\mathrm{d}K)\tilde{P}(\mathrm{d}\phi) \\
&= \int_{\mathcal{K}^k} \int_{\mathcal{M}(\mathcal{K}^k)} \chi_Q^K(B)g(T_Q\phi)\tilde{P}_K(\mathrm{d}\phi)\Lambda(\mathrm{d}K).
\end{aligned}$$

Applying the disintegration of the intensity measure Λ, we get

$$\mathrm{E}\Psi_Q(B)g(\Psi_Q) = \alpha \int_{\mathcal{K}_0'} h(B, K_0)\Lambda_0(\mathrm{d}K_0),$$

where

$$h(B, K_0) = \int_{\mathbb{R}^d} \int_{\mathcal{M}(\mathcal{K}^k)} \chi_Q^{K_0+x}(B)g(T_Q\phi)\tilde{P}_{K_0+x}(\mathrm{d}\phi)\nu_d(\mathrm{d}x).$$

Using the Fubini theorem and thereafter the substitution $z = x + y$ we get

$$\begin{aligned}
h(B, K_0) &= \int_{\mathbb{R}^d} \int_{\mathcal{M}(\mathcal{K}^k)} \int_{K_0} \mathbf{1}_{B-x}(y)\mathcal{I}_Q^k(\mathrm{d}y)g(T_Q\phi)\tilde{P}_{K_0+x}(\mathrm{d}\phi)\nu_d(\mathrm{d}x) \\
&= \int_{K_0} \int_{\mathbb{R}^d} \int_{\mathcal{M}(\mathcal{K}^k)} \mathbf{1}_B(x + y)g(T_Q\phi)\tilde{P}_{K_0+x}(\mathrm{d}\phi)\nu_d(\mathrm{d}x)\mathcal{I}_Q^k(\mathrm{d}y) \\
&= \int_{K_0} \int_B \int_{\mathcal{M}(\mathcal{K}^k)} g(T_Q\phi)\tilde{P}_{K_0-y+z}(\mathrm{d}\phi)\nu_d(\mathrm{d}z)\mathcal{I}_Q^k(\mathrm{d}y) \\
&= \int_B \int_{K_0} \int_{\mathcal{M}(\mathcal{K}^k)} g(T_Q\phi)\tilde{P}_{K_0-y+z}(\mathrm{d}\phi)\mathcal{I}_Q^k(\mathrm{d}y)\nu_d(\mathrm{d}z).
\end{aligned}$$

Using now (3.17) and Lemma 3.11, we obtain

$$\mathrm{E}\Psi_Q(B)g(\Psi_Q) = \lambda_Q \int_B \int_{\mathcal{K}^k} \int_{\mathcal{M}(\mathcal{K}^k)} g(T_Q\phi)\tilde{P}_{K+z}(\mathrm{d}\phi)\Lambda_Q(\mathrm{d}K)\nu_d(\mathrm{d}z).$$

¿From the Campbell theorem it follows that

$$\int g(\phi)P_{Q,z}(\mathrm{d}\phi) = \int \int g(T_Q\phi)\tilde{P}_{K+z}(\mathrm{d}\phi)\Lambda_Q(\mathrm{d}K)$$

for ν_d-almost all $z \in \mathbb{R}^d$, and the proof is complete. □

3.1.5 Poisson process

Consider now the case when Φ is a Poisson process. Then Ξ is called a Boolean model and we have by the Slivnyak theorem (Theorem 2.21) $\tilde{P}_K = \delta_{\delta_K} * \tilde{P}$. Hence, for any measurable function h on $\mathcal{M}(\mathcal{K}^k)$ it holds

$$\int h(\phi)\tilde{P}_K(\mathrm{d}\phi) = \int h(\phi)\,(\delta_{\delta_K} * \tilde{P})\,(\mathrm{d}\phi) = \int h(\delta_K + \phi)\tilde{P}(\mathrm{d}\phi).$$

Now from Theorem 3.12 we obtain the following corollary

COROLLARY 3.13 *If Φ is a stationary Poisson process on $\mathcal{K}^k$, then (using the notation introduced above)*

$$P_{Q,0} = \int (\delta_{\chi_Q^K} * P_Q)\Lambda_Q(\mathrm{d}K).$$

Proof. For $M \in \mathcal{M}^d$ measurable it holds

$$\begin{aligned} P_{Q,0}(M) &= \int (\delta_{\delta_K} * \tilde{P})(T_Q^{-1}M)\Lambda_Q(\mathrm{d}K) \\ &= \int \tilde{P}\{\phi \in \mathcal{M}(\mathcal{K}_k) : \delta_K + \phi \in T_Q^{-1}M\}\,\Lambda_Q(\mathrm{d}K) \\ &= \int \tilde{P}T_Q^{-1}\{\phi \in \mathcal{M}(\mathcal{K}_k) : \chi_Q^K + T_Q\phi \in M\}\Lambda_Q(\mathrm{d}K) \\ &= \int P_Q\{\mu \in \mathcal{M}^d : \chi_Q^K + \mu \in M\}\Lambda_Q(\mathrm{d}K) \\ &= \int (\delta_{\chi_Q^K} * P_Q)(M)\Lambda_Q(\mathrm{d}K). \end{aligned}$$

□

REMARK 3.4. The result can be reformulated in the following form: let Z be a random element of $\mathcal{K}^k$ with distribution Λ_Q, defined on the same probability space as Φ_Q and independent of Φ_Q. Then the random measure $\chi_Q^Z + \Phi_Q$ follows the Palm distribution $P_{Q,0}$.

Using Corollary 3.13 we obtain a general formula for the variance of the projection measure of a Boolean model.

THEOREM 3.14 *Let Φ be a stationary Poisson process on $\mathcal{K}^k$ with intensity $\alpha > 0$ and primary grain Z_0. Then for the induced projection measure Ψ_Q and $B \in \mathcal{B}^d$ we have*

$$\begin{aligned} \operatorname{var}\Psi_Q(B) &= \alpha\mathrm{E}\int\int g_B(x-y)\chi_Q^{Z_0}(\mathrm{d}x)\chi_Q^{Z_0}(\mathrm{d}y) \\ &= \alpha\mathrm{E}\int_{Z_0}\int_{Z_0} g_B(x-y)\mathcal{I}_Q^k(\mathrm{d}x)\mathcal{I}_Q^k(\mathrm{d}y). \end{aligned}$$

Proof. We have $\operatorname{var}\Psi_Q(B) = \mathrm{E}\Psi_Q^2(B) - [\mathrm{E}\Psi_Q(B)]^2$ with

$$E\Psi_Q^2(B) = \lambda_Q \int g_B(x)\psi(\mathrm{d}x)P_{Q,0}(\mathrm{d}\psi).$$

Denote $f(\psi) = \int g_B(x)\psi(\mathrm{d}x)$ $(\psi \in \mathcal{M}^d)$, then according to Corollary 3.13

$$\begin{aligned}\int f(\phi)P_{Q,0}(\mathrm{d}\psi) &= \int\int f(\psi)(\delta_{\chi_Q^K} * P_Q)(\mathrm{d}\psi)\Lambda_Q(\mathrm{d}K)\\ &= \int\int f(\chi_Q^K + \psi)P_Q(\mathrm{d}\psi)\Lambda_Q(\mathrm{d}K).\end{aligned}$$

This integral splits in two summands $J_1 + J_2$ due to the linearity of f. The second of them is

$$J_2 = \int\int g_B(x)\psi(\mathrm{d}x)P_Q(\mathrm{d}\psi) = \lambda_Q \int g_B(x)\nu_d(\mathrm{d}x) = \lambda_Q\nu_d(B)^2$$

and thus $\lambda_Q J_2 = [\mathrm{E}\Psi_Q(B)]^2$ cancels out in $\operatorname{var}\Psi_Q(B)$, whereas the first of them yields

$$J_1 = \int\int_K g_B(x)\mathcal{I}_Q^k(\mathrm{d}x)\Lambda_Q(\mathrm{d}K).$$

The theorem follows then immediately by the definition of Λ_Q (3.17). □

Applying now Proposition 3.1 to both integrals, we get

COROLLARY 3.15 *Under the assumptions of Theorem 3.14 we have*

$$\begin{aligned}&\operatorname{var}\Psi_Q(B)\\ &= \beta_{d,k}^{-2}\alpha\mathrm{E}\int_{Z_0}\int_{Z_0} g_B(x-y)\mathcal{F}_Q(\mathrm{Tan}^k(Z_0,x))\mathcal{F}_Q(\mathrm{Tan}^k(Z_0,y))\\ &\qquad\qquad \mathcal{H}^k(\mathrm{d}x)\mathcal{H}^k(\mathrm{d}y).\end{aligned}$$

EXERCISE 3.16 *Let the particles of the* $\mathcal{H}^k$*-process be flat pieces, i.e., the linear hull* span K *is a* k*-flat for any particle* K *from the process* Φ*. In such a case, for any primary grain* K_0, $\mathrm{Tan}^k(K_0,x) = \operatorname{span}K_0 \in \mathcal{L}_k$*. Using Corollary 3.15 and Proposition 3.1, show that*

$$\operatorname{var}\Psi_Q(B) = \beta_{d,k}^{-2}\alpha\mathrm{E}\mathcal{F}_Q(\operatorname{span}Z_0)^2\int_{Z_0}\int_{Z_0} g_B(x-y)\mathcal{H}^k(\mathrm{d}x)\mathcal{H}^k(\mathrm{d}y). \tag{3.18}$$

EXERCISE 3.17 *Let the process* Φ *be as in Exercise 3.16 and assume additionally that* B *is a ball and that the shape and size of the primary*

grain are independent of its direction. Show that then

$$\operatorname{var}\Psi_Q(B) = \beta_{d,k}^{-2}\alpha \int_{\mathcal{L}_k} \mathcal{F}_Q^2(L)R(\mathrm{d}L)\,\mathrm{E}\int_{Z_0}\int_{Z_0} g_B(x-y)\mathcal{H}^k(\mathrm{d}x)\mathcal{H}^k(\mathrm{d}y). \tag{3.19}$$

3.1.6 Flat processes

In this subsection we consider random $\mathcal{H}^k$-sets generated by stationary flat processes. Let Φ be a stationary process of k-dimensional flats in $\mathbb{R}^d$ (see Subsection 2.9) with intensity α and direction distribution R (distribution on $\mathcal{L}_k$). The union set $\Xi = \bigcup_{F\in\Phi} F$ is clearly a stationary random $\mathcal{H}^k$-set with intensity $\lambda = \alpha$ and direction distribution R. Consequently, by Proposition 3.2, the intensity of the projection measure Ψ_Q is

$$\lambda_Q = \alpha\beta_{d,k}^{-1}\mathcal{F}_{RQ}.$$

Let $\mathcal{F}_k$ denote the space of all k-dimensional flats (affine subspaces) in $\mathbb{R}^d$. We shall use the mapping T_Q introduced in Subsection 3.1.4, now interpreted as a mapping on $\mathcal{N}(\mathcal{F}_k)$.

THEOREM 3.18 *The Palm distribution $P_{Q,0}$ of the projection measure induced by a stationary flat process fulfills*

$$P_{Q,0} = \int \left(\tilde{P}_L T_Q^{-1}\right) R(\mathrm{d}L).$$

Proof. Analogously to the proof of Theorem 3.12 we obtain

$$\begin{aligned}&\mathrm{E}\Psi_Q(B)g(\Psi_Q)\\ &\quad= \alpha\int_{\mathcal{L}_k}\int_{L^\perp}\int \chi_Q^{L+x}(B)g(T_Q\phi)\tilde{P}_{L+x}(\mathrm{d}\phi)\nu_{d-k}(\mathrm{d}x)R(\mathrm{d}L).\end{aligned}$$

By Proposition 3.1 we have

$$\chi_Q^{L+x}(B) = \beta_{d,k}^{-1}\mathcal{F}_Q(L)\nu_k(B\cap(L+x))$$

(we can write the Lebesgue measure instead of the Hausdorff one since the measured set belongs to an affine subspace of corresponding dimension). Hence, using Proposition 3.2 and the Fubini theorem, we get

$$\begin{aligned}&\mathrm{E}\Psi_Q(B)g(\Psi_Q)\\ &\quad= \lambda_Q\int_{\mathcal{L}_k}\int_{L^\perp}\int \nu_k(B\cap(L+x))g(T_Q\phi)\tilde{P}_{L+x}(\mathrm{d}\phi)\nu_{d-k}(\mathrm{d}x)R_Q(\mathrm{d}L)\\ &\quad= \lambda_Q\int_B\int_{\mathcal{L}_k}\int g(T_Q\phi)\tilde{P}_{L+x}(\mathrm{d}\phi)R_Q(\mathrm{d}L)\nu_d(\mathrm{d}z)\end{aligned}$$

and the assertion follows again by the Campbell theorem. □

For the Poisson flat process we obtain as a consequence

COROLLARY 3.19 *If Φ is a stationary Poisson process on $\mathcal{F}_k$, then*

$$P_{Q,0} = \int (\delta_{\chi_Q^L} * P_Q) R_Q(\mathrm{d}L).$$

The variance of the projection measure Ψ_Q can be then derived in the same way as in Theorem 3.14 and Corollary 3.15:

THEOREM 3.20 *Let Φ be a stationary Poisson process on $\mathcal{F}_k$. Then the induced projection measure Ψ_Q satisfies for any $B \in \mathcal{B}^d$*

$$\begin{aligned} \operatorname{var} \Psi_Q(B) &= \lambda_Q \int_{\mathcal{L}_k} \int_L g_B(x) \mathcal{I}_Q^k(\mathrm{d}x) R_Q(\mathrm{d}L) \\ &= \lambda \int_{\mathcal{L}_k} \mathcal{F}_Q^2(L) \int_L g_B(x) \nu_k(\mathrm{d}x) R(\mathrm{d}L). \end{aligned}$$

3.2. Intensity estimators

Unbiased estimators of intensity can be naturally formulated by means of projection measures. In this section, formulas including moments of projection measures (mean value and variance) will be applied to obtain statistical estimators of the intensity and their variances. Four sampling schemes will be described according to Table 3.1.

Random fibre and surface systems are considered as particular cases of random $\mathcal{H}^k$-sets ($k = 1$ or $k = d - 1$). The rose of directions R on $\mathcal{L}_1$ will be the tangent distribution for the case of a fibre process (see Definition 3.6) and the distribution of normal direction in the case of a surface process. We shall use the representation of $\mathcal{L}_1$ as the unit sphere $\mathbb{S}^{d-1}$ where unit vectors with opposite orientations are identified. Thus, probability distributions on $\mathcal{L}_1$ can be viewed as even distributions on $\mathbb{S}^{d-1}$ and the function $\mathcal{F}_Q$ in (3.6) takes the form

$$\mathcal{F}_Q(u) = \int_{\mathbb{S}^{d-1}} |\langle u, v \rangle| Q(\mathrm{d}v), \quad u \in \mathbb{S}^{d-1}.$$

Direct probes are based on the total projection, a fibre system is projected onto a line while a surface system is projected onto a hyperplane in $\mathbb{R}^d$. In stereology the total projection is approximated by counting the intersections between the structure and probes, see Fig. 3.1 a,b. In the case of fibre (surface) systems the number of intersections with test hyperplanes (lines) is evaluated, respectively. The organization of these

	fibres	surfaces
direct probes	projection on $\mathbb{R}^1$	projection on $\mathbb{R}^{d-1}$
indirect probes	projection on $\mathbb{R}^{d-1}$	intersection with hyperplane

Table 3.1. Four sampling schemes for the intensity estimation of fibre and surface processes. By projection always the total projection is meant.

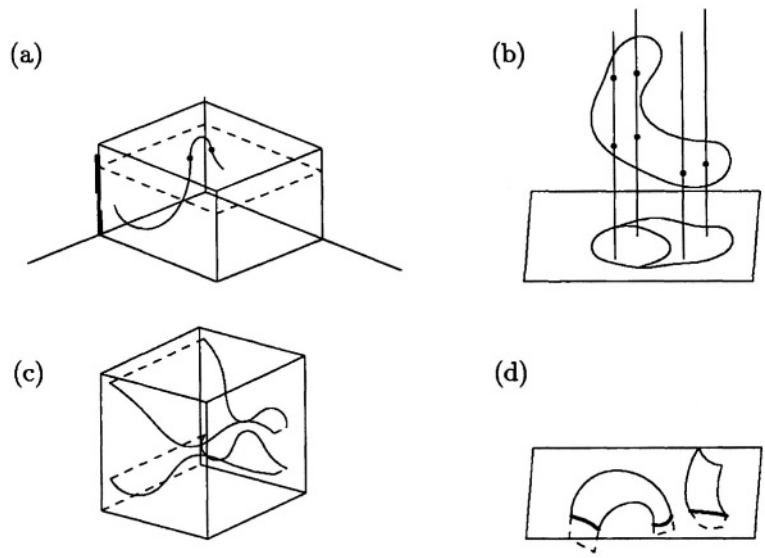

Figure 3.1. Graphs demonstrating the sampling schemes in Table 3.1 for dimension $d = 3$. Direct probes are based on measuring the total projection which can be approximated by counting the intersection number of fibres with planar probes (a) or surfaces with linear probes (b). Indirect probes transform a spatial fibre system to a planar fibre system by projection (c) or a spatial surface system to a planar fibre system using planar intersection (d).

probes, e.g. systematic random, is intensively studied, cf. [20], [63], [64], this topic is beyond the scope of this book.

Indirect probes first transform the random set in a random set in lower dimension and in the second step the induced random set is evaluated, see Fig. 3.1 c), d). In the case of a fibre system, it is projected onto $\mathbb{R}^{d-1}$ which yields an induced fibre system in $\mathbb{R}^{d-1}$. In the case of a surface system, it is intersected with a hyperplane which results also in a fibre system in $\mathbb{R}^{d-1}$. The relation between intensities of both random systems is available and the intensity of the transformed system is estimated using direct probes in lower dimension.

The estimation formulas depend typically on the rose of directions R which is unknown. Two ways how to overcome this difficulty are (i) randomization of probe orientation, (ii) estimation of the rose of directions. They are discussed in Chapters 4, 5, respectively.

3.2.1 Direct probes

Direct probes lead to an unbiased estimator of intensity λ based on the induced projection measure Ψ_Q of the form:

$$\hat{\lambda} = \frac{\beta_d \Psi_Q(B)}{\nu_d(B)\mathcal{F}_{RQ}}, \quad B \in \mathcal{B}^d; \tag{3.20}$$

its unbiasedness follows from Proposition 3.2 for both fibre and surface systems.

The variance of the estimator (3.20) can be expressed by Theorem 3.8 and Proposition 3.2

$$\operatorname{var}\hat{\lambda} = \lambda^2\Big(\frac{1}{\nu_d(B)^2}\int g_B(x)\mathcal{K}_Q(\mathrm{d}x) - 1\Big), \tag{3.21}$$

or, equivalently,

$$\operatorname{var}\hat{\lambda} = \frac{\lambda^2}{\nu_d(B)^2}\int g_B(x)(p_Q(x) - 1)\nu_d(\mathrm{d}x), \tag{3.22}$$

if the pair-correlation function p_Q of Ψ_Q exists.

Explicit formulas for $\operatorname{var}\hat{\lambda}$ stated above can be obtained for Poisson processes, see Theorem 3.14. The important special case $Q = U$, $\Psi_U = \Psi$ is studied in Subsection 4.1.1 as IUR sampling. We present here a few particular cases.

EXAMPLE 3.21 *(Poisson segment process.) Let the random fibre system be the union set of a stationary Poisson segment process Φ in $\mathbb{R}^d$ with intensity α and typical segment distribution Λ_0 (see Example 2.43). Any "centred" segment $s \in \mathcal{K}_0'$ can be parametrized by $s = s(r,u)$ with length $r > 0$ and direction $u \in \mathbb{S}^{d-1}$ (identifying again u with $-u$), thus Λ_0 can be viewed as a distribution on $(0,\infty) \times \mathbb{S}^{d-1}$, even in its second coordinate. We use here the standard notation L_d instead of λ for the length intensity of fibre systems (moreover, we shall write L_A instead of L_2 and L_V instead of L_3, following the usual convention). Using (3.18), we get the expression for the variance of the estimator (3.20)*

$$\operatorname{var}\hat{L}_d = \frac{\alpha}{\nu_d(B)^2\mathcal{F}_{RQ}^2}\int \mathcal{F}_Q^2(u)\int_0^r\int_0^r g_B((s-s')u)\mathrm{d}s\mathrm{d}s'\Lambda_0(\mathrm{d}(r,u))$$

and, after a linear substitution and using the fact that g_B *is an even function, we get*

$$\begin{aligned}\frac{\nu_d(B)^2\mathcal{F}_{RQ}^2}{2\alpha}\operatorname{var}\hat{L}_d &= \int_{(0,\infty)\times\mathbb{S}^{d-1}} \mathcal{F}_Q^2(u)\int_0^r (r-s)g_B(su)\,\mathrm{d}s\,\Lambda_0(\mathrm{d}(r,u)) \\ &= \int_{\mathbb{S}^{d-1}} \mathcal{F}_Q^2(u)\int_0^\infty\int_0^r (r-s)g_B(su)\,\mathrm{d}s\,\Lambda_0(\mathrm{d}r\mid u)R_0(\mathrm{d}u),\end{aligned} \tag{3.23}$$

where we have applied the disintegration

$$\Lambda_0(\mathrm{d}(r,u)) = \Lambda_0(\mathrm{d}r|u)R_0(\mathrm{d}u),$$

$\Lambda_0(\mathrm{d}r|u)$ *being the conditional segment length distribution under given direction* u*, and* R_0 *the direction distribution of the typical segment (note that* R_0 *is not equal to* R *in general but* R *is the length-weighted distribution* R_0*). Summarizing, we obtain the formula*

$$\operatorname{var}\hat{L}_d = \frac{2\alpha}{\nu_d(B)^2\mathcal{F}_{RQ}^2}\int_{\mathbb{S}^{d-1}}\mathcal{F}_Q^2(u)\int_0^\infty g_B(su)\mathrm{E}_u\big((r-s)\mathbf{1}_{[r>s]}\big)\,\mathrm{d}sR_0(\mathrm{d}u) \tag{3.24}$$

where the symbol r *is used to denote the typical segment length and* E_u *stands for the conditional expectation under given segment direction* u*. If the typical segment length and orientation are mutually independent then clearly* $R_0 = R$*, the typical segment length does not depend on* u *and we can write*

$$\operatorname{var}\hat{L}_d = \frac{2\alpha}{\nu_d(B)^2\mathcal{F}_{RQ}^2}\int_{\mathbb{S}^{d-1}}\mathcal{F}_Q^2(u)\int_0^\infty g_B(su)\mathrm{E}\left((r-s)\mathbf{1}_{[r>s]}\right)\mathrm{d}sR(\mathrm{d}u). \tag{3.25}$$

Assume that the direction distribution R_0 *has density* h *with respect to the Hausdorff measure on* $\mathbb{S}^{d-1}$*, and let the pair-correlation function* p_Q *of* Ψ_Q *exist. Comparing* (3.12) *with formula* (3.24)*, we get*

$$\begin{aligned}&\lambda_Q^2\int g_B(x)(p_Q(x)-1)\,\mathrm{d}x \\ &\quad= \frac{2\alpha}{\beta_d^2}\int_{\mathbb{S}^{d-1}}\mathcal{F}_Q(u)^2\int_0^\infty g_B(su)\mathrm{E}_u\left((r-s)\mathbf{1}_{[r>s]}\right)\mathrm{d}s\,h(u)\mathcal{H}^{d-1}(\mathrm{d}u).\end{aligned}$$

Using the relation

$$\lambda_Q = \beta_d^{-1}\mathcal{F}_{RQ}L_d = \beta_d^{-1}\mathcal{F}_{RQ}\alpha\mathrm{E}r$$

from Proposition 3.2 and the substitution to polar coordinates $x = su$ *on the left hand side with*

$$\mathrm{d}x = (d\omega_d)^{-1} s^{d-1} \mathrm{d}s \mathcal{H}^{d-1}(\mathrm{d}u),$$

we get

$$\frac{1}{d\omega_d} \int_{\mathbb{S}^{d-1}} \int_0^\infty s^{d-1} g_B(su)(p_Q(su) - 1) \mathrm{d}s \mathcal{H}^{d-1}(\mathrm{d}u) = \frac{2}{\alpha \mathcal{F}_{RQ}^2 (\mathrm{E}r)^2}$$
$$\times \int_{\mathbb{S}^{d-1}} \mathcal{F}_Q(u)^2 h(u) \int_0^\infty g_B(su) \mathrm{E}_u \left((r-s)\mathbf{1}_{[r>s]}\right) \mathrm{d}s \mathcal{H}^{d-1}(\mathrm{d}u),$$

and the formula for $p_Q(su)$ *follows:*

$$p_Q(su) = 1 + \frac{2d\omega_d}{\alpha s^{d-1}} \frac{\mathcal{F}_Q(u)^2}{(\mathcal{F}_{RQ})^2} \frac{\mathrm{E}_u \left((r-s)\mathbf{1}_{[r>s]}\right)}{(\mathrm{E}r)^2} h(u), \tag{3.26}$$

$u \in \mathbb{S}^{d-1}$, $s > 0$.

REMARK 3.5. Since $\operatorname{var} \hat{L}_d$ in (3.24) depends continuously on Q and since the space of all probability distributions on $\mathbb{S}^{d-1}$ is compact, there surely exists a distribution $Q = Q(B, \Lambda_0)$ for which the variance attains its minimal value. It is, however, difficult to find the solution of this minimization problem in the general case. In the particular case when the segment length and orientation are independent and when B is a ball, then the minimum variance is attained for the uniform distribution U on $\mathbb{S}^{d-1}$, see Exercise 3.25, since

$$\int (\mathcal{F}_Q(u) - \mathcal{F}_{RQ})^2 R(\mathrm{d}u) = \int \mathcal{F}_Q^2(u) R(\mathrm{d}u) - \mathcal{F}_{RQ}^2 \geq 0$$

for any distribution Q and zero is attained when $Q = U$.

EXAMPLE 3.22 *(Poisson hyperplane process.) Consider the random surface system generated by a Poisson hyperplane process* Φ *in* $\mathbb{R}^d$. *The surface area intensity is now denoted by* S_d *and we shall consider its unbiased estimator (3.20) denoted now by* $\hat{S}_d$. *Applying Theorem 3.20 we get*

$$\operatorname{var} \hat{S}_d = \frac{S_d}{\nu_d(B)^2 \mathcal{F}_{RQ}^2} \int_{\mathcal{L}_{d-1}} \mathcal{F}_Q^2(L) I_{d-1}^2(B; L) R(\mathrm{d}L), \tag{3.27}$$

where

$$I_{d-1}^2(B; L) = \int_L g_B(x) \nu_{d-1}(\mathrm{d}x).$$

To continue the example we shall discuss the geometrical interpretation of the integral $I^2_{d-1}(B;L)$. *Using the definition of* g_B *and the Fubini theorem we get*

$$\begin{aligned} I^2_{d-1}(B;L) &= \int_L \int_{\mathbb{R}^d} \mathbf{1}_B(z)\mathbf{1}_B(x+z)\nu_d(\mathrm{d}z)\nu_{d-1}(\mathrm{d}x) \\ &= \int_B \nu_{d-1}(B \cap (L-z))\nu_d(\mathrm{d}z) \\ &= \int_{L^\perp} (\nu_{d-1}(B \cap (L-y)))^2 \,\mathrm{d}y, \end{aligned}$$

which is the translative integral of the square of the intersection area of B *with a translate of* L.

EXERCISE 3.23 *Denote by*

$$\zeta_d(t) = \nu_d(B_1 \cap (B_1 - tu))/\nu_d(B_1), \quad t \geq 0,$$

$(u \in \mathbb{S}^{d-1})$ *the covariance function of the unit ball* B_1 *and verify the following properties of* ζ_d *and its derivative* ζ'_d:

$$\zeta_d(t) = 2\frac{\omega_{d-1}}{\omega_d}\int_{t/2}^1 (1-s^2)^{\frac{d-1}{2}}\,\mathrm{d}s, \quad t \leq 2, \tag{3.28}$$

$$\zeta'_d(t) = -\frac{\omega_{d-1}}{\omega_d}\left(1-\frac{t^2}{4}\right)^{\frac{d-1}{2}}, \quad t \leq 2. \tag{3.29}$$

In particular, in dimensions 2 and 3 we have

$$\zeta_2(t) = \frac{2}{\pi}\arccos\frac{t}{2} - \frac{t}{\pi}\sqrt{1-\frac{t^2}{4}}, \tag{3.30}$$

$$\zeta_3(t) = 1 - \frac{3t}{4} + \frac{t^3}{16}, \quad t \leq 2. \tag{3.31}$$

EXERCISE 3.24 *By using* (3.24), *show that if* Φ *is a Poisson segment process and* $B = B_\rho$ *a ball of radius* ρ, *then the variance of* $\hat{L}_d$ *can be written in the form*

$$\operatorname{var}\hat{L}_d = \frac{2\alpha}{\omega_d \rho^{d-2}\mathcal{F}^2_{RQ}}\int_{(0,\infty)\times\mathbb{S}^{d-1}} \mathcal{F}^2_Q(u)\eta_d(r/2\rho)\Lambda_0(\mathrm{d}(r,u)), \tag{3.32}$$

where

$$\eta_d(t) = 4\int_0^t (t-s)\zeta_d(2s)\,\mathrm{d}s. \tag{3.33}$$

Show that, in particular,

$$\eta_2(t) = \begin{cases} \frac{16}{3\pi}t + 2t^2 - \frac{13+2t^2}{3\pi}t\sqrt{1-t^2} - \frac{1+4t^2}{\pi}\arcsin t, & t \le 1, \\ \frac{16}{3\pi}t - \frac{1}{2}, & t \ge 1; \end{cases} \tag{3.34}$$

$$\eta_3(t) = \begin{cases} 2t^2 - t^3 + \frac{1}{10}t^5, & t \le 1, \\ \frac{3}{2}t - \frac{2}{5}, & t \ge 1. \end{cases} \tag{3.35}$$

EXERCISE 3.25 *Consider the situation from Exercise 3.24 and assume additionally that the segment length and orientation are mutually independent. Show that then the following two formulas for the variance hold:*

$$\operatorname{var}\hat{L}_d = \frac{2\alpha}{\omega_d \rho^{d-2}\mathcal{F}_{RQ}^2}\int \mathcal{F}_Q^2(u)R(\mathrm{d}u)\mathrm{E}\eta_d(r/2\rho), \tag{3.36}$$

$$\operatorname{var}\hat{L}_d = \frac{2\alpha}{\nu_d(B)\mathcal{F}_{RQ}^2}\int \mathcal{F}_Q^2(u)R(\mathrm{d}u)\int_0^\infty \zeta_d(s/\rho)\mathrm{E}\left((r-s)\mathbf{1}_{[r>s]}\right)\mathrm{d}s. \tag{3.37}$$

EXERCISE 3.26 *Let Φ be the Poisson hyperplane process from Example 3.22 and let the set $B = B_\rho$ be a ball of radius ρ. Show that then*

$$I_{d-1}^2(B_\rho; L) = \frac{\beta_{2d}}{\pi\beta_{d+1}^2}\nu_d(B_\rho)^2\rho^{-1} \tag{3.38}$$

and

$$\operatorname{var}\hat{S}_d = \frac{\beta_{2d}}{\pi\beta_{d+1}^2}\frac{S_d}{\rho}(\mathcal{F}_{RQ})^{-2}\int_{\mathcal{L}_{d-1}}\mathcal{F}_Q^2(L)R(\mathrm{d}L). \tag{3.39}$$

EXERCISE 3.27 *Using the Jensen's inequality, show that if Φ is a Poisson hyperplane process and B a ball, then* $\operatorname{var}\hat{S}_d$ *is minimal for the uniform direction distribution $Q = U$.*

3.2.2 Indirect probes

Indirect probes are characterized by the two-stage estimation procedure, cf. Fig. 3.1 c, d. Consider first a stationary random fibre system Ξ in $\mathbb{R}^d$ (which may be generated by a fibre process Φ) and let a thin slab $v^\perp \times [0,t]$ of normal orientation $v \in \mathbb{S}^{d-1}$ and thickness $t > 0$ be given. The intersection of Ξ with the slab $v^\perp \times [0,t]$ is then projected orthogonally on the hyperplane $v^\perp$ and the resulting stationary random fibre system in $v^\perp$ is denoted by $\Xi^{v,t}$, the corresponding fibre process in $v^\perp$ (if it exists) by $\Phi^{v,t}$ and the induced projection measure by $\Psi_Q^{v,t}$, Q being an even probability distribution on $\mathbb{S}^{d-2}(v^\perp) = \mathbb{S}^{d-1} \cap v^\perp$.

The following result is well known at least under some additional regularity assumptions, see e.g. [89], [83]. Let

$$\mathcal{G}_Q(v) = \int_{\mathbb{S}^{d-1}} |\sin \sphericalangle(u,v)|\, Q(\mathrm{d}u), \quad v \in \mathbb{S}^{d-1}, \tag{3.40}$$

denote the sine transform of an even probability distribution Q on $\mathbb{S}^{d-1}$. We shall use the spherical projection

$$\pi_{v^\perp} : u \mapsto \frac{p_{v^\perp} u}{\|p_{v^\perp} u\|}$$

from $\mathbb{S}^{d-1} \setminus \{-v, v\}$ to $\mathbb{S}^{d-2} \subset v^\perp$. (Recall that $p_{v^\perp}$ is the orthogonal projection onto $v^\perp$.)

LEMMA 3.28 *The length intensities L_d of the original random measure Ψ induced by Ξ and $L_{d-1}^{v,t}$ of the random measure $\Psi^{v,t}$ in $v^\perp$ are related by*

$$L_{d-1}^{v,t} = tL_d \mathcal{G}_R(v), \tag{3.41}$$

where R is the direction distribution of Ψ. Assume further that

$$R(\{-v, v\}) = 0. \tag{3.42}$$

Then the direction distribution R^v of $\Xi^{v,t}$ (considered as an even probability measure on $\mathbb{S}^{d-2} \subset v^\perp$) does not depend on $t > 0$ and is related to the direction distribution R (an even measure on $\mathbb{S}^{d-1}$) by

$$\mathcal{G}_R(v) \int_{S^{d-2}} h(w) R^v(\mathrm{d}w) = \int_{\mathbb{S}^{d-1}} h(\pi_{v^\perp} u) |\sin \sphericalangle(u, v)| R(\mathrm{d}u), \tag{3.43}$$

where h is any even nonnegative measurable function on $\mathbb{S}^{d-2}$.

Proof. We shall represent the approximate tangent spaces $\mathrm{Tan}^1(\Xi, x) \in \mathcal{L}_1$ as unit vectors, without taking care about their orientation. Note that if $x \in v^\perp \times [0, t]$ and $\mathrm{Tan}^1(\Xi, x)$ is not equal to $\pm v$ then

$$\mathrm{Tan}^1(\Xi^{v,t}, p_{v^\perp} x) = \pi_{v^\perp}(\mathrm{Tan}^1(\Xi, x)).$$

Let B be a bounded Borel subset of $v^\perp$ with $\nu_{d-1}(B) > 0$ and let $W = B \times [0, t]$. The projection $p_{v^\perp}$ restricted to $\Xi \cap W$ is Lipschitz and its one-dimensional approximate Jacobian at $x \in \Xi \cap W$ equals

$$|\sin \sphericalangle(\mathrm{Tan}^1(\Xi, x), v)|$$

$\mathcal{H}^1$-almost everywhere. Thus, applying the area formula (Theorem 1.6) we get

$$\int_{W \cap \Xi} h(\pi_{v^\perp} \mathrm{Tan}^1(\Xi, x)) |\sin \sphericalangle(\mathrm{Tan}^1(\Xi, x), v)| \mathcal{H}^1(\mathrm{d}x)$$
$$= \int_{B \cap \Xi^{v,t}} h(\mathrm{Tan}^1(\Xi^{v,t}, y)) \mathcal{H}^1(\mathrm{d}y).$$

By Lemma 3.7, the expectation of the left hand side is equal to

$$tL_d\nu_{d-1}(B)\int_{\mathbb{S}^{d-1}} h(\pi_{v^\perp}u)|\sin\sphericalangle(u,v)|R(\mathrm{d}u),$$

whereas the expectation of the right hand side is

$$L_{d-1}^{v,t}\nu_{d-1}(B)\int_{\mathbb{S}^{d-2}} h(w)R^v(\mathrm{d}w).$$

The choice of the function $h\equiv 1$ gives (3.41). On the other hand, if h is arbitrary and (3.42) holds then we get (3.43) after applying (3.41). □

Let now Ξ be a stationary random surface system in $\mathbb{R}^d$ (which may be generated as the union set of a stationary surface or hyperplane process Φ). Given $v\in\mathbb{S}^{d-1}$, let $\Xi^v=\Xi\cap v^\perp$ be the intersection of the random set with the hyperplane perpendicular to v (corresponding to the union set of the intersection surface or hyperplane process Φ^v in $v^\perp$); note that Ξ^v is a stationary random surface system in $v^\perp$ (cf. [125]). Further, let Ψ^v, Ψ_Q^v denote again the induced projection measures. Analogously as in Lemma 3.28 one can show that the surface intensity S_{d-1}^v of Ξ^v is related to the surface intensity S_d of Ξ by

$$S_{d-1}^v = S_d\mathcal{G}_R(v), \tag{3.44}$$

R being the normal direction distribution of Ξ, and that, provided that (3.42) holds, the normal direction distribution R^v of Ξ^v fulfills (3.43).

PROPOSITION 3.4 *Let Q be an even probability measure on $\mathbb{S}^{d-1}$ concentrated on $\mathbb{S}^{d-2}\subset v^\perp$, $v\in\mathbb{S}^{d-1}$ fixed, and let B be a bounded Borel subset of $v^\perp$ with $\nu_{d-1}(B)>0$. Then*

$$\beta_{d-1}\mathrm{E}\Psi_Q^v(B)=\nu_{d-1}(B)\mathcal{F}_{RQ}S_d$$

in the case of a stationary random surface system, and

$$\beta_{d-1}\mathrm{E}\Psi_Q^{v,t}(B)=t\nu_{d-1}(B)\mathcal{F}_{RQ}L_d$$

in the case of a stationary random fibre system. Consequently,

$$\hat{S}_d^*=\frac{\beta_{d-1}\Psi_Q^v(B)}{\nu_{d-1}(B)\mathcal{F}_{RQ}} \quad\text{and}\quad \hat{L}_d^*=\frac{\beta_{d-1}\Psi_Q^{v,t}(B)}{t\nu_{d-1}(B)\mathcal{F}_{RQ}} \tag{3.45}$$

are unbiased estimators for S_d, L_d, respectively.

Proof. Follows immediately from (3.43), (3.41) and (3.44) observing that

$$\begin{aligned}
\mathcal{G}_R(v)\mathcal{F}_{R^vQ} &= \mathcal{G}_R(v)\int_{\mathbb{S}^{d-1}}\int_{\mathbb{S}^{d-2}} |\cos \sphericalangle(u,w)| R^v(\mathrm{d}u)Q(\mathrm{d}w) \\
&= \int_{\mathbb{S}^{d-1}}\int_{\mathbb{S}^{d-1}} \sin \sphericalangle(u,w)|\cos \sphericalangle(p_{v^\perp}u,w)| R(\mathrm{d}u)Q(\mathrm{d}w) \\
&= \int_{\mathbb{S}^{d-1}}\int_{\mathbb{S}^{d-1}} |\cos \sphericalangle(u,w)| R(\mathrm{d}u)Q(\mathrm{d}w) \\
&= \mathcal{F}_{RQ}.
\end{aligned}$$

□

REMARK 3.6. Formulas (3.20) (for direct probes) and (3.45) (for indirect probes) have the same structure, but the quantities in (3.45) correspond to a smaller dimension $d-1$.

Under the assumption of Proposition 3.4, we denote by Q both the measure on $\mathcal{L}_1(v^\perp)$ in the numerator of (3.45) (or in $\mathcal{F}_{R^vQ}$) and the measure on $\mathcal{L}_1$ in the quantity $\mathcal{F}_{RQ}$ in the denominator of (3.45).

The variances of the estimators (3.45) are obtained using the tools in Subsection 3.1.3 for stationary processes and especially by Theorem 3.14 for Poisson processes. We intend to get some more explicit results here in some particular cases.

EXAMPLE 3.29 *(Poisson line process.) Let Φ be a stationary (anisotropic) Poisson line process in $\mathbb{R}^d$ with intensity α and union set Ξ (cf. Subsection 2.9). The direction distribution R coincides with the direction distribution of a typical line. (As above, we consider R as an even distribution on $\mathbb{S}^{d-1}$.) We assume that*

$$R(\{u \in \mathbb{S}^{d-1} : u \perp v\}) = 0, \tag{3.46}$$

i.e., that there are almost surely no lines perpendicular to v. Then the induced process $\Phi^{v,t}$ (given the projection onto $v^\perp$ of the intersection of Φ with the slab $v^\perp \times [0,t]$) is a stationary segment process with intensity $\alpha^{v,t}$ and primary segment distribution $\Lambda_0^{v,t}$ (joint distribution of segment length and orientation). It is clear that a line of orientation $u \in \mathbb{S}^{d-1}$ of the original process generates a segment of length $t\tan \sphericalangle(u,v)$ and orientation $\pi_{v^\perp}(u)$ in the projected process and that a typical line contributes to the typical segment distribution of the projection with the weight of the cosine of its angle with v. Thus we get the following relation (valid

for arbitrary line processes, even without the Poisson assumption):

$$\int_{(0,\infty)\times\mathbb{S}^{d-2}} h(r,w)\,\Lambda_0^{v,t}(\mathrm{d}(r,w)) \tag{3.47}$$
$$= \mathcal{F}_R(v)^{-1}\int h(t|\tan\sphericalangle(u,v)|,\pi_{v^\perp}u)|\cos\sphericalangle(u,v)|\,R(\mathrm{d}u)$$

where h *is any nonnegative measurable function on* $(0,\infty)\times\mathbb{S}^{d-1}$.

Clearly, the length intensity $L_{d-1}^{v,t}$ *of the segment process is equal to the product of the intensity* $\alpha^{v,t}$ *with the mean segment length* $\mathrm{E}r$. *It follows from* (3.47) *that*

$$\mathrm{E}r = \frac{\mathcal{G}_R(v)}{\mathcal{F}_R(v)}t,$$

and, applying (3.41), *we get the relation*

$$\alpha^{v,t} = (\mathrm{E}r)^{-1}tL_d\mathcal{G}_R(v) = L_d\mathcal{F}_R(v).$$

The variance of $\hat{L}_d^*$ *can now be expressed by applying* (3.24) *to the fibre process* $\Phi^{v,t}$. *We get*

$$\operatorname{var}\hat{L}_d^* = \frac{2L_d\mathcal{F}_R(v)}{t^2\nu_{d-1}(B)^2\mathcal{F}_{RQ}^2}\int_{\mathbb{S}^{d-2}}\mathcal{F}_Q(w)^2\int_0^\infty g_B(sw)f^{v,t}(s\mid w)\,\mathrm{d}s\,R_0^v(\mathrm{d}w), \tag{3.48}$$

where

$$f^{v,t}(s\mid w) = \int_s^\infty (r-s)\Lambda_0^{v,t}(\mathrm{d}r\mid w) \tag{3.49}$$

and R_0^v *is the direction distribution of a typical segment of* $\Phi^{v,t}$ *which is, by Lemma 3.47, the spherical projection of the* $|\cos\sphericalangle(u,v)|$*-weighted distribution* R.

EXAMPLE 3.30 *(Poisson hyperplane process.) Let* Φ *be a stationary Poisson hyperplane process with intensity* S_d *and normal direction distribution* R *on* $\mathbb{S}^{d-1}$. *Due to (3.27), we have*

$$\operatorname{var}\hat{S}_d^* = \frac{S_{d-1}^v}{(\nu_{d-1}(B)\mathcal{F}_{RQ})^2}\int_{\mathbb{S}^{d-2}}\mathcal{F}_Q(w)^2I_{d-2}^2(B,w^\perp)\,R^v(\mathrm{d}w)$$

(recall that $I_{d-2}^2(B,w^\perp) = \int\nu_{d-2}(B\cap(w^\perp+t))^2\,dt$.*) Since*

$$\mathcal{F}_Q(\pi_{v^\perp}u) = |\sin\sphericalangle(u,v)|^{-1}\mathcal{F}_Q(u),$$

we get by using (3.43) and (3.44)

$$\operatorname{var}\hat{S}_d^* = \frac{S_d}{(\nu_{d-1}(B)\mathcal{F}_{RQ})^2}\int_{\mathbb{S}^{d-1}}\frac{\mathcal{F}_Q(u)^2}{|\sin\sphericalangle(u,v)|}I_{d-2}^2(B,u^\perp\cap v^\perp)\,R(\mathrm{d}u). \tag{3.50}$$

EXERCISE 3.31 *Show that*

$$\mathcal{F}_Q(u) = |\sin \sphericalangle(u,v)|\mathcal{F}_Q(\pi_{v^\perp} u)$$

for $u \in \mathbb{S}^{d-1} \setminus \{-v, v\}$ *and, using* (3.32) *and* (3.48), *verify the following formula for a Poisson line process* Φ *and ball* $B = B_\rho$*:*

$$\begin{aligned} \operatorname{var} \hat{L}_d^* &= \frac{2L_d \mathcal{F}_R(v) t^{-2}}{\omega_{d-1}\rho^{d-3}\mathcal{F}_{RQ}^2} \int_{(0,\infty)\times\mathbb{S}^{d-2}} \mathcal{F}_Q(w)^2 \eta_{d-1}(r/2\rho)\Lambda_0^{v,t}(\mathrm{d}(r,w)) \\ &= \frac{2L_d t^{-2}}{\omega_{d-1}\rho^{d-3}\mathcal{F}_{RQ}^2} \int_{\mathbb{S}^{d-1}} \mathcal{F}_Q(u)^2 \frac{\eta_{d-1}\left(\frac{t|\tan\sphericalangle(u,v)|}{2\rho}\right)|\langle u,v\rangle|}{|\sin\sphericalangle(u,v)|^2} R(\mathrm{d}u) \end{aligned} \tag{3.51}$$

(the function η_{d-1} *is given in* (3.33)*).*

EXERCISE 3.32 *Let* Φ*,* B *be as in Exercise 3.31 and assume moreover that* R *is rotationally symmetric around* v*. Show that in this case*

$$\operatorname{var} \hat{L}_d^* = \frac{2L_d}{\omega_{d-1}\rho^{d-3}t^2} \frac{\int \frac{\mathcal{F}_Q^2(u)|\langle u,v\rangle|}{|\sin\sphericalangle(u,v)|^2} R(\mathrm{d}u)}{\mathcal{F}_{RQ}^2} \int_0^\infty \eta_{d-1}(r/2\rho) D^{v,t}(\mathrm{d}r), \tag{3.52}$$

where the segment length distribution $D^{v,t}$ *of the induced process* $\Phi^{v,t}$ *is the first marginal distribution of* $\Lambda_0^{v,t}$*. (Hint: Note that by the rotational symmetry of* R*, the typical segment length and orientation of the induced segment process are mutually independent, and apply* (3.36) or (3.37)*.)*

EXERCISE 3.33 *Let* Φ *be a Poisson hyperplane process as in Example 3.30 and let* $B = B_\rho$ *be a* $(\mathrm{d}-1)$*-dimensional ball of radius* ρ*. Show that then*

$$\operatorname{var} \hat{S}_d^* = \frac{\beta_{2d-2}}{\pi\beta_d^2} S_d \rho^{-1} (\mathcal{F}_{RQ})^{-2} \int_{\mathbb{S}^{d-1}} \frac{\mathcal{F}_Q(u)^2}{|\sin\sphericalangle(u,v)|} R(\mathrm{d}u), \tag{3.53}$$

(cf. (3.39)*).*

3.2.3 Application - fibre systems in soil

A useful model of a probability distribution R on the sphere $\mathbb{S}^2$ for applications is a parametric family of Dimroth-Watson distributions, see [21]. It has the probability density w.r.t. uniform distribution U

$$h(u) = \text{const} \ \exp\left(2\kappa\langle u, u_0\rangle^2\right), \quad u \in \mathbb{S}^2, \tag{3.54}$$

where $\kappa \in [-\infty, \infty]$ is a parameter and $u_0 \in \mathbb{S}^2$ determines the axis of rotational symmetry. The directions are clustering around this axis as

$\kappa \to +\infty$. For $\kappa = 0$ we have a uniform distribution and for $\kappa < 0$ the girdle distribution is obtained with limiting uniform distribution in the equator (perpendicular to u_0) plane for $\kappa \to -\infty$. Choose the spherical coordinates $u = (\theta, \varphi)$ so that u_0 determines the vertical (z) axis. Here $\theta \in (0, \pi)$ is the latitude and $\varphi \in [0, 2\pi)$ the longitude. Then we can write the density of Dimroth-Watson distributions with respect to the Hausdorff measure $\mathcal{H}^2$ on $\mathbb{S}^2$ as

$$h(\theta, \varphi) = \frac{1}{4\pi U_0(\kappa)} \exp(2\kappa \cos^2 \theta) \tag{3.55}$$

(independent of φ because of rotational symmetry), here

$$U_0(\kappa) = \int_0^1 e^{2\kappa x^2} \mathrm{d}x.$$

A practical application of the theory of fibre processes comes from the soil science (cooperation with Biometrie, INRA Montfavet, France) where earthworms burrows form a natural fibre system in a three-dimesional soil specimen.

The earthworm burrow system in a soil can be described as a highly non-isotropic fibre system in $\mathbb{R}^3$ composed of roughly straight segments (galleries) of small thickness when compared to their length. This system forms an organized porosity which can influence properties of the soil as gas transfer or colonization by roots. Therefore, scientists are interested in modelling such systems and describing them by means of their first-order properties like the length intensity and the rose of directions.

Galleries' characteristics (length and orientation) depend on the earthworm species. In the region we are interested in, the earthworm population is mainly due to Aporrectodea longa and Aporrectodea nocturna which can be regarded as the main burrowing species whose galleries are mainly vertically oriented. Such an earthworm burrow system is modelled as the realization of a Poisson segment process ([81]) whose length and orientation are independent and admit the following densities:

(i) α is the intensity of the Poisson point process of segment centres,

(ii) the segment length is exponentially distributed with density $h(r) = (1/\mathrm{E}r)\exp(-r/\mathrm{E}r)$,

(iii) the directional distribution R is Dimroth-Watson with density (3.55) and a parameter κ.

The intensity α represents the mean number of burrows per unit volume, $\mathrm{E}r$ the mean segment length and κ the concentration parameter. The higher κ the more vertical are the galleries. The parameter $L_V = \alpha \mathrm{E}r$ is the mean length of galleries per unit volume.

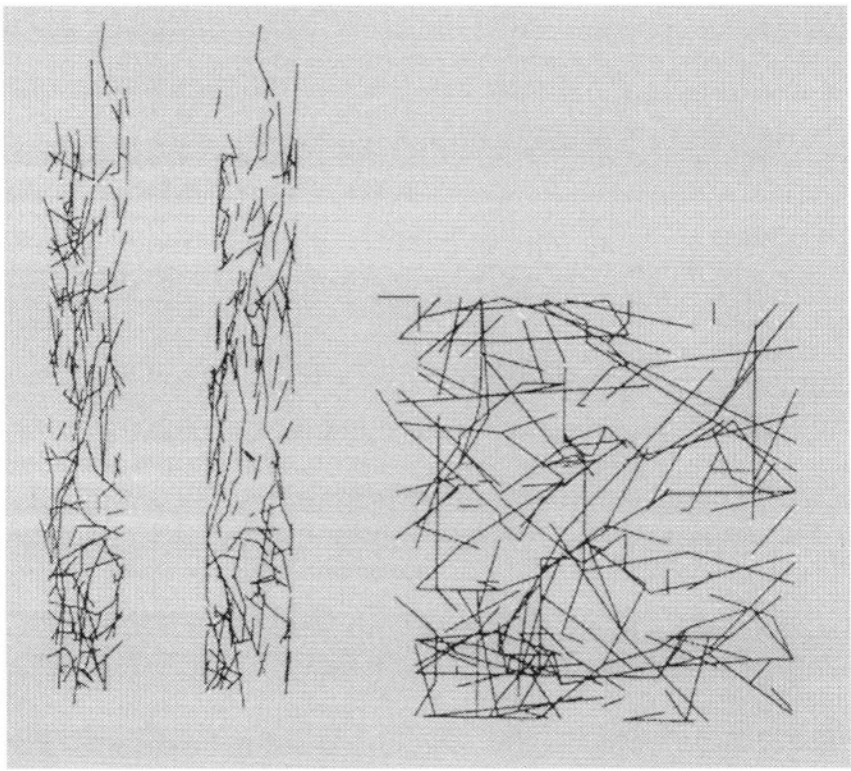

Figure 3.2. The data set of the soil specimen. Projections on the xz (left), yz (middle) and xy (right) planes of the observed earthworm galleries are presented. The scale is multiplied by 5 on the last projection. The observed parallelepiped is 1dm×1dm×9dm.

For the study, a full description of a natural burrow system is available to enumerate various sampling characteristics. It was obtained in situ using the following method. A face, from a large pit, was rendered as flat as possible. A column of soil ($1 \times 1 \times 9$ dm) was described by destroying it little by little and every burrow segment was characterized by the three-dimensional coordinates of its extremities, see Fig. 3.2.

Globally, the structure is non-stationary with gradient in vertical direction. In order to avoid this problem, cubic subsamples B of $1 \times 1 \times 1$ dm were used assuming local stationarity (i.e. in each subsample). The length intensity L_V may then be estimated using (3.20) with uniform direction distribution $Q = U$, i.e. as $\hat{L}_V^{\ell} = \Psi(B)/\nu_3(B)$, where Ψ is the length measure. An unbiased estimator of α is $\hat{\alpha} = N/\nu_3(B)$, where N

is the number of upper segment points (reference points) observed in B. Segments which hit the boundary of the observed column of soil are only partially observed. This edge effect causes problems when estimating the mean segment length $\mathrm{E}r$. Larger segments have greater probability to hit the column than smaller ones, therefore the standard expectation estimator (sample mean) fails. We can estimate $\mathrm{E}r$ as $\Psi(B)/N$ which is a ratio of unbiased estimators. The parameter κ of the directional distribution was estimated using standard maximum likelihood method.

Numerical results are presented (cf. [9]) for the lower cubic subsample B ($\nu_3(B) = 1$). It is $\hat{L}_V^{\ell} = \Psi(B) = 15.5\,\mathrm{dm}^{-2}$, $\hat{\alpha} = N = 17\,\mathrm{dm}^{-3}$. The estimated parameters are $\mathrm{E}r = 0.91\,\mathrm{dm}$ and $\kappa = 1.13$. The pair-correlation function of the segment process is expressed by (3.26) as

$$p(s,\theta,\varphi) = 1 + \frac{\exp(2\kappa\cos^2\theta)\exp(-s/\mathrm{E}r)}{2\pi L_V s^2 U_o(\kappa)}.$$

Plugging in the estimated parameter values, we obtain the approximation

$$1 + \frac{\exp(2.26\cos^2\theta)\exp(-s/0.91)}{266.78s^2}.$$

Similarly, assuming a projection of the segment system onto a vertical line, we can estimate L_V by (3.20) with distribution $Q = \delta_{\mathbf{v}}$, where $\mathbf{v}$ denotes the vertical direction in $\mathbb{R}^3$. The pair-correlation function of the corresponding induced measure is

$$p_Q(s,\theta,\varphi) = 1 + \frac{0.008}{s^2}\cos^2\theta\exp(2.26\cos^2\theta)\exp(-s/0.91).$$

A discussion of the variances of estimators in this application is left to the end of Chapter 3 (Example 3.53).

3.3. Projection measure estimation

The random projection measure was defined (see Definition 3.3) by means of the integral-geometric measure which is based on the number of intersections between a structure and a probe, see (3.5). The variance of the projection measure was used to describe the properties of the estimators of length (surface) intensity in Section 3.2.

Consider a surface process Φ in $\mathbb{R}^3$ (the case of a fibre process is analogous). Its projection measure Ψ_Q, even in the most simple case $Q = \delta_u$ (projection in a single direction $u \in \mathbb{S}^2$), cannot be measured directly. It is usually estimated by using a grid of parallel lines, counting the total number of intersection points of the structure with the grid inside an observation window and multiplying by the grid element (here the area of

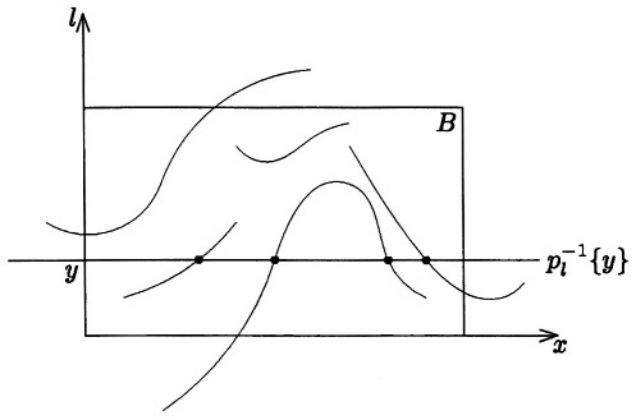

Figure 3.3. Intersection of a fibre system by a test line

a square). Given Φ, this estimator tends almost surely to the projection measure of the window if the distance of parallel lines (subspaces) tends to 0. Often, however, stronger convergence properties are required, e.g. convergence in L^2, which need not be satisfied in general, as illustrated by Example 3.34.

3.3.1 Convergence in quadratic mean

We shall limit ourselves to fibre systems in $\mathbb{R}^2$, nevertheless, the reader will realize that most of our results can be easily extended to higher dimensions. Let $u \in \mathbb{S}^1$ be fixed; we may assume without loss of generality that the coordinate system is chosen so that u lies on the vertical axis in Fig. 3.3 and let $l = \operatorname{span}\{u\}$ denote this axis. Let Φ be a stationary fibre process in $\mathbb{R}^2$ with length intensity L_A. We shall denote for brevity $\Psi_u \equiv \Psi_{\delta_u}$ the projection measure of Φ onto l and, given $y \in l$ and a bounded Borel set $B \subset \mathbb{R}^2$, we denote by

$$N_y(B) = \mathcal{H}^0(p_l^{-1}\{y\} \cap B \cap \Phi)$$

the number of intersection points of Φ with the line $p_l^{-1}\{y\}$ inside B (see Fig. 3.3).

Let $\mathbb{Z}$ denote the set of integers and $a > 0$. For a bounded set $B \in \mathcal{B}^2$ let

$$\hat{\Psi}_u^a(B) = \frac{a\pi}{2} \sum_{i \in \mathbb{Z}} N_{ia}(B), \tag{3.56}$$

denote the total number of intersection points of Φ in B with a grid of equidistant lines parallel to the x-axis, multiplied by the line distance a and the constant factor $\beta_2^{-1} = \pi/2$. Obviously, $\hat{\Psi}_u^a$ is an approximation

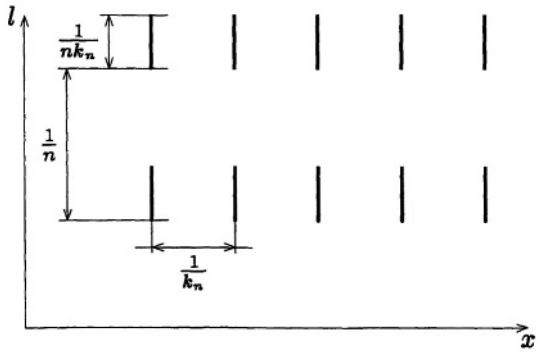

Figure 3.4. The segment process Φ_n in Example 3.34

of the projection measure Ψ_u based on the number of intersections. The quality of this approximation is investigated in this Section.

EXAMPLE 3.34 *Let* (k_n) *be a sequence of natural numbers and* (p_n) *a sequence of real numbers from* (0,1) *such that* $\sum_n p_n = 1$ *and* $p_n k_n \to \infty$, $n \to \infty$. *Given* $n \in \mathbb{N}$, *let* Φ_n *be a stationary segment process in the plane with segments parallel to the vertical axis, of constant length* $(nk_n)^{-1}$, *arranged in a regular rectangular lattice with vertical edge length* n^{-1} *and horizontal edge length* k_n^{-1} *(see Fig. 3.4). Let* Φ *be the stationary segment process with* $\Pr[\Phi = \Phi_n] = p_n$. *The length intensities of all processes* Φ_n *and, hence, also of* Φ, *are equal to* 1. *Clearly, the projection measures* $(\Psi_n)_u$ *and* Ψ_u *have intensities equal to* $\pi/2$ *since all segments are parallel to the vertical axis. The grid estimator of* Ψ_u *satisfies, by its construction*

$$\frac{2}{\pi}(\hat{\Psi}_n)_u^{1/n}(W) = \begin{cases} k_n & \textit{with probability } k_n^{-1}, \\ 0 & \textit{with probability } 1 - k_n^{-1}, \end{cases}$$

where W is a unit square with edges parallel to the axes. Thus we have

$$\begin{aligned} \frac{4}{\pi^2} \int_{[\Phi=\Phi_n]} \left|\hat{\Psi}_u^{1/n}(W) - \Psi_u(W)\right|^2 d\Pr &= p_n\left(k_n^{-1}(k_n-1)^2 + (1-k_n^{-1})\right) \\ &= p_n\left(k_n + o(n)\right), \quad n \to \infty. \end{aligned}$$

Consequently, $\hat{\Psi}_u^a(W)$ *does not converge to* $\Psi_u(W)$ *in* L^2 *as* $a \to 0_+$.

It is clear that

$$\lim_{a \to 0_+} \hat{\Psi}_u^a(B) = \Psi_u(B) \quad a.s.$$

for any Borel bounded subset $B \subset \mathbb{R}^2$. Hence, due to a well known measure-theoretic result, the convergence in L^2 is equivalent to the uniform integrability of $|\hat{\Psi}_u^a(B)|^2$, see Proposition 1.2 (analogously for the

L^p convergence). We present a sufficient condition for the uniform integrability. Recall that, given a Borel set $B \subset \mathbb{R}^2$, the symbol $\mathcal{K}_B$ denotes the family of all compact sets in $\mathbb{R}^2$ hitting B.

THEOREM 3.35 *Let Φ be a stationary fibre process in $\mathbb{R}^2$ with primary grain (fibre, $(\mathcal{H}^1, 1)$ rectifiable set) Z_0 satisfying*

$$\mathcal{H}^0(Z_0 \cap p_l^{-1}\{y\}) \le K \text{ for all } y \in \mathbb{R} \text{ a.s.} \tag{3.57}$$

for some constant $K > 0$, and let further

$$\mathrm{E}\,(\Phi(\mathcal{K}_B))^p < \infty \tag{3.58}$$

for some $p \ge 1$ and Borel bounded set $B \subset \mathbb{R}^2$. Then the random variables $|\hat{\Psi}_u^a(B)|^p$, $a > 0$, are uniformly integrable and, consequently,

$$\mathrm{E}|\hat{\Psi}_u^a(B) - \Psi_u(B)|^p \to 0, \quad a \to 0_+.$$

REMARK 3.7. Note that a stationary Poisson fibre process Φ satisfies (3.58) with any $1 \le p < \infty$.

Proof. The key observation is that if $\hat{\Psi}_u^a(B) > c$, then $\Phi(\mathcal{K}_B) \ge [c/K]$ due to (3.57) (here $[\cdot]$ denotes the integer part). Thus we have

$$\begin{aligned}
&\int_{[\hat{\Psi}_u^a(B)>c]} \left(\hat{\Psi}_u^a(B)\right)^p d\Pr \\
&\quad = \sum_{n=[c/K]}^{\infty} \int_{[\hat{\Psi}_u^a(B)>c, \Phi(\mathcal{K}_B)=n]} \left(\hat{\Psi}_u^a(B)\right)^p d\Pr \\
&\quad \le \frac{2}{\pi} \sum_{n=[c/K]}^{\infty} (nK)^p \Pr[\Phi(\mathcal{K}_B) = n] \\
&\quad = \frac{2}{\pi} \mathrm{E}\left(\Phi(\mathcal{K}_B)^p \mathbf{1}_{[\Phi(\mathcal{K}_B)\ge c/K]}\right)
\end{aligned}$$

and the last expression tends to 0 with $c \to \infty$ due to (3.58). □

Finally, we present a result from [17] giving the exact rate of convergence in L^2 of $\hat{\Psi}_u^a$, under assumptions on the pair-correlation function. As above, Φ is a stationary fibre process in $\mathbb{R}^2$ with length intensity L_A and rose of directions R.

LEMMA 3.36 *Suppose that $B = [0, A] \times [0, Y]$ is a rectangle in $\mathbb{R}^2$ with edge of length Y parallel to u. Suppose furthermore that the pair correlation function of Φ_u has the form (in polar coordinates)*

$$p_u(s, \theta) = 1 + \frac{c(\theta)}{s} + g(\theta), \tag{3.59}$$

where c, g *are continuous functions on* $[-\pi, \pi)$ *satisfying asymptotic equalities*

$$\begin{aligned} c(\theta) &\sim K_+(\pi/2-\theta)^{\alpha_+} \text{ when } \theta \to \pi/2, \\ c(\theta) &\sim K_-(\theta+\pi/2)^{\alpha_-} \text{ when } \theta \to -\pi/2 \end{aligned}$$

for some real constants $K_-, \alpha_-, K_+, \alpha_+;\ \alpha_-, \alpha_+ > 0$, *and*

$$\begin{aligned} g(\theta) &\sim D_+(\pi/2-\theta)^{\beta_+} \text{ when } \theta \to \pi/2, \\ g(\theta) &\sim D_-(\theta+\pi/2)^{\beta_-} \text{ when } \theta \to -\pi/2 \end{aligned}$$

for some real constants $D_+, D_-, \beta_+, \beta_-;\ \beta_+, \beta_- > 0$.

Then the covariance $\operatorname{cov}(N_y, N_{y+z})$ *is continuous at* $z = 0$ *for any* y.

If $\alpha_+ > 1$, $\alpha_- > 1$, $\beta_+ > 1$, $\beta_- > 1$, *then the derivative* $\frac{\partial \operatorname{cov}(N_y, N_{y+z})}{\partial z}$ *exists at* $z = 0$ *for any* y *and is equal to*

$$L_A^2 \mathcal{F}_R^2(u) \left(A \int_{-\pi/2}^{\pi/2} \frac{g(\theta)}{\cos^2(\theta)} \mathrm{d}\theta - \int_{-\pi/2}^{\pi/2} \frac{|\sin(\theta)|\, c(\theta)}{\cos^2(\theta)} \mathrm{d}\theta \right). \tag{3.60}$$

The proof of the following theorem from [17] is based on the Matheron's formula for the variance of the estimator under systematic sampling on the line (see [68]).

THEOREM 3.37 *Under the assumptions of Lemma 3.36, if* $\alpha_+ > 1$, $\alpha_- > 1$, $\beta_+ > 1$, $\beta_- > 1$ *then the speed of convergence*

$$\hat{\Psi}_u^a(B) \xrightarrow{a \to 0} \Psi_u(B)$$

in L^2 *is given by:*

$$\begin{aligned} &\mathrm{E}\left(\hat{\Psi}_u^a(B) - \Psi_u(B)\right)^2 \\ &= -\frac{2Ya^2}{3\pi^2} L_A^2 \mathcal{F}_R^2(u) \left(A \int_{-\pi/2}^{\pi/2} \frac{g(\theta)}{\cos^2\theta} \mathrm{d}\theta - \int_{-\pi/2}^{\pi/2} \frac{|\sin\theta| c(\theta)}{\cos^2(\theta)} \mathrm{d}\theta \right) + o(a^2). \end{aligned}$$

Proof. For $a > 0$ let K_a be the set of integers in the convex hull of the projection of B onto the y-axis and $|K_a| = \operatorname{card} K_a$. ¿From [68], the variance of the estimator fulfills

$$\sigma_a^2 := \operatorname{var}\left(\frac{1}{Y} \int_Y N_y(B) \mathrm{d}y - \frac{1}{|K_a|} \sum_{k \in K_a} N_{ka}(B) \right) = \frac{1}{6} \gamma'(0) \frac{a}{|K_a|} + o(a^2)$$

since the covariogram of $N_y(B)$ defined as

$$\gamma(z) = \operatorname{var} N_0(B) - \operatorname{cov}(N_0(B), N_z(B))$$

is differentiable at 0 by Lemma 3.36. Thus

$$\mathrm{E}\left(\hat{\Psi}_u^a(B) - \Psi_u(B)\right)^2 = \frac{4}{\pi^2} Y^2 \sigma_n^2 = \frac{2}{3\pi^2} Y^2 \frac{a}{|K_a|} \gamma'(0).$$

Now we apply (3.60) to $\gamma'(0) = -\frac{\partial \mathrm{cov}\,(N_0(B), N_z(B))}{\partial z}$ to obtain the assertion. □

3.3.2 Examples

In the following two examples an application of Theorem 3.37 will be presented. Let $B \subset \mathbb{R}^2, A, Y, u$ be as in Lemma 3.36. If necessary, we extend the function p_u to the domain $[-\pi, \pi)$ by setting $p_u(s, -\theta) = p_u(s, \theta)$, $\theta \in [0, \pi)$.

EXAMPLE 3.38 *(Poisson line process). For a stationary isotropic Poisson line process in the plane it holds*

$$p(s, \theta) = 1 + \frac{1}{\pi s L_A} \quad \textit{and} \quad p_u(s, \theta) = 1 + \frac{\pi \cos^2 \theta}{4 s L_A}.$$

In (3.59) we have $c(\theta) = \frac{\pi \cos^2 \theta}{4 L_A}$ *and* $g(\theta) = 0$. *Since* $\alpha_+ = \alpha_- = 2$, $\hat{\Psi}_u^a(B)$ *converges in* L^2 *to* $\Psi_u(B)$ *with*

$$\mathrm{E}(\hat{\Psi}_u^a(B) - \Psi_u(B))^2 = \frac{4 Y a^2 L_A}{3\pi^3} + o(a^2),$$

see Theorem 3.37, where a is the distance between two section lines.

For a stationary Poisson line process with probability density h *of the rose of directions R we have similarly*

$$p_u(s, \theta) = 1 + \frac{2h(\theta) \cos^2 \theta}{s L_A \mathcal{F}_R^2(u)}, \quad \textit{i.e.} \quad c(\theta) = \frac{2h(\theta) \cos^2 \theta}{L_A \mathcal{F}_R^2(u)}.$$

EXAMPLE 3.39 *(Poisson segment process). Let* Φ *be a stationary Poisson segment process, cf. Example 3.21, in* $\mathbb{R}^2$ *with intensity* α *and suppose that the typical segment length (with distribution D) and segment direction (with distribution R) are mutually independent. Let R admit a density* h *with respect to the Hausdorff measure on* $\mathbb{S}^{d-1}$. *Using formula* (3.26), *we can express the pair-correlation function* p_u *of the projection measure* Ψ_u *of* Φ *in polar coordinates* $(s, \theta) \in (0, \infty) \times [-\pi, \pi)$ *as*

$$p_u(s, \theta) = 1 + \frac{4\pi h(\theta) \cos^2(\theta) f(s)}{\alpha s (\mathrm{E}r)^2 \mathcal{F}_R^2(u)},$$

where $f(s) = \int_s^\infty (t - s) D(\mathrm{d}t)$.

Finally, assume that the length of segments is fixed and equal to $q = \mathrm{E}r$ *and that the process is isotropic (i.e.,* $h(\theta) = \frac{1}{2\pi}$, $\theta \in [-\pi, \pi)$*). Then* $f(s) = q - s$ *if* $s < q$ *and* $f(s) = 0$ *if* $s > q$*. Thus we obtain* ($L_A = \alpha \mathrm{E}r$)

$$p_u(s,\theta) = \begin{cases} 1 + \frac{\pi^2 \cos^2\theta}{2L_A s} - \frac{\pi^2 \cos^2\theta}{2L_A q} & \text{for } s < q, \\ 1 & \text{for } s > q, \end{cases}$$

i.e. $c(\theta) = \frac{\pi^2 \cos^2\theta}{2L_A}$ *and* $g(\theta) = -\frac{\pi^2 \cos^2\theta}{2L_A q}$ *for* $s < q$ *and* $\alpha_+ = \alpha_- = \beta_+ = \beta_- = 2$ *in the notation of Lemma 3.36. Theorem 3.37 yields*

$$\mathrm{E}(\hat{\Psi}_u^a(B) - \Psi_u(B))^2 = \frac{4Ya^2 L_A}{3\pi^2}\left(\frac{A\pi}{q} + 2\right) + o(a^2)$$

when $a \to 0_+$*. Strictly speaking, the assumptions of Lemma 3.36 are not satisfied since the pair-correlation function* $p_u(s,\theta)$ *has the required form only for* $s < q$*. Nevertheless, an analysis of the proof of Lemma 3.36 in [17] shows that it is enough to require that* $p_u(s,\theta)$ *has the required form for sufficiently small* $s > 0$*; in fact, it suffices to assume that*

$$p_u(s,\theta) = 1 + \frac{c(\theta)}{s} + g(\theta) + o(1), \quad s \to 0_+, \ \theta \in [-\pi, \pi).$$

This extension covers e.g. the anisotropic case with exponentially distributed segment lengths ($D(r) = 1 - e^{-r/q}\, r, q > 0$)*, where*

$$p_u(s,\theta) = 1 + \frac{4\pi h(\theta)\cos^2(\theta) e^{-s/q}}{sL_A \mathcal{F}_R(u)^2}.$$

Putting now $e^{-s/q} = 1 - \frac{s}{q} + o(s)$ *the model function* p_u *is obtained.*

3.4. Best unbiased estimators of intensity

In this Section, we shall overview some results about the best unbiased estimators of the intensity of stationary processes. These results are limited to Poisson processes since very little is known so far about the comparison of estimators in the non-Poissonian case. The notions of sufficient and complete statistics introduced in Subsection 1.2.3 will be used.

We start with an easy result. Let $\widetilde{\Phi}$ be a Poisson process on a Polish space X with *finite* intensity measure $\alpha\overline{\Lambda}$, $\overline{\Lambda}$ being a known finite Borel measure on X and $\alpha > 0$ an unknown parameter. Note that the Poisson process is clearly finite almost surely if its intensity measure is finite, cf. Subsection 2.4. Then the total number of points of $\widetilde{\Phi}$ divided by $\overline{\Lambda}(X)$,

$$T(\widetilde{\Phi}) = \overline{\Lambda}(X)^{-1}\widetilde{\Phi}(X),$$

is a sufficient statistic for α (indeed, the conditional distribution of $\widetilde{\Phi}$ under $\widetilde{\Phi}(X) = n$ is that of a binomial process of n independent identically distributed points on X with distribution proportional to $\overline{\Lambda}$, see Exercise 2.29). Further, let h be a measurable function on $\{0,1,...\}$ such that $\mathrm{E}_\alpha h(\widetilde{\Phi}(X)) = 0$ for any $\alpha > 0$. Then

$$e^{-\alpha\overline{\Lambda}(X)} \sum_{n=0}^{\infty} \frac{\overline{\Lambda}(X)^n}{n!} h(n)\alpha^n = 0, \quad \alpha > 0,$$

hence $h(n) = 0$ for any $n = 0, 1, \ldots$. Thus the statistics $\widetilde{\Phi}(X)$ and, consequently, also $T(\widetilde{\Phi})$ are complete. Applying Theorem 1.23 we thus obtain the following

THEOREM 3.40 *The estimator*

$$e(\widetilde{\Phi}) = \overline{\Lambda}(X)^{-1}\widetilde{\Phi}(X)$$

is the uniformly best unbiased estimator of the parameter α if $\widetilde{\Phi}$ is a finite Poisson process on X with intensity measure $\alpha\overline{\Lambda}$, $\overline{\Lambda}$ being a known finite measure on X. Further, if $\bar{e}(\widetilde{\Phi})$ is any unbiased estimator of a parameter function $\tau(\alpha)$ then

$$e_\tau(\widetilde{\Phi}) = \mathrm{E}_\alpha[\bar{e}(\widetilde{\Phi}) \mid \widetilde{\Phi}(X)]$$

is the UBUE of the parameter function $\tau(\alpha)$.

Consider the particular case when $X = W$ is a bounded subset of $\mathbb{R}^d$ and $\overline{\Lambda}$ is the restriction of ν_d to W (thus, $\widetilde{\Phi}$ can be viewed as a restriction to W of a stationary Poisson process in $\mathbb{R}^d$ with intensity α). Then, Theorem 3.40 says that the number of points observed in W divided by $\nu_d(B)$ is the best unbiased estimator of the intensity α, which is in no way surprising.

3.4.1 Poisson line processes

Consider now another application. Let X be the set of all lines in $\mathbb{R}^2$ intersecting a bounded window $W \subset \mathbb{R}^2$ with $\nu_2(W) > 0$, and let $\overline{\Lambda} = \mu_2 \mid X$ be the restriction of the motion invariant measure μ_2 (see (2.42)) from the space of all lines to X. Let $\widetilde{\Phi}$ be the restriction to X of a stationary isotropic Poisson line process Φ in $\mathbb{R}^2$ with intensity measure $\alpha\overline{\Lambda}$. Theorem 3.40 says that the total number of lines intersecting W divided by $\mu_2(X)$ is the UBUE of the intensity α. We recall that $\mu_2(X)$ equals the mean width of W if W is convex.

Note that the intensity α may also be viewed as the length intensity λ of the measure Ψ induced by the line process Φ by means of (2.44). The considerations mentioned above can be summarized as

COROLLARY 3.41 *The total number of lines of a stationary isotropic planar Poisson line process hitting a bounded window W divided by the constant* $\mu_2(X)$

$$e(\Phi) = \mu_2(X)^{-1}\Phi(X)$$

is the best unbiased estimator of the length intensity of the induced random measure.

It was observed already by Ohser [84] and Baddeley and Cruz-Orive [3] that this estimator, $e(\Phi)$, has lower variance than the natural "length-measuring" unbiased estimator

$$e_\ell(\tilde{\Phi}) = \nu_2(W)^{-1} \sum_{L\in\Phi} \nu_1(L \cap W)$$

though $e(\Phi)$ uses only "0-dimensional" information about the process. If the isotropy assumption is dropped but the direction distribution R of the process Φ is known, we have to divide the number of lines by another constant,

$$\int \nu_1\{y \in L^\perp : (L+y) \cap W \neq \emptyset\}\, R(\mathrm{d}L).$$

The situation becomes much more complicated if the direction distribution is unknown. Then we have to consider the "large" parameter space of pairs (α, R), where $\alpha > 0$ and R is a probability distribution on $\mathcal{L}_1$. This was considered in detail by Schladitz [98] who obtained the following results (these were formulated more generally for Poisson k-flats in $\mathbb{R}^d$, the basic idea can, however, be seen in our setting). First, note that

$$e(\tilde{\Phi}) = \sum_{F\in\tilde{\Phi}} \frac{1}{\nu_1(p_{F^\perp}W)} \tag{3.61}$$

is an unbiased estimator of λ ($p_{F^\perp}W$ denotes the orthogonal projection of W into the orthogonal complement of F), cf. [32]. Here $e(\tilde{\Phi})$ is a weighted estimator where the weights are inversely proportional to the probability of a line to be included in the sample.

Thus, due to Theorem 1.23, it is enough to find a sufficient statistic for (α, R) in order to get a UBUE for α (and R). Consider now the experiment $(\mathcal{L}_1, \mathcal{B}(\mathcal{L}_1), (R : R \in \mathcal{R}))$, where $\mathcal{R}$ is a subset of Borel probability measures on $\mathcal{L}_1$. Suppose that there is a statistic T on $\mathcal{L}_1$

sufficient for $R \in \mathcal{R}$. T is called *power sufficient* if for any $n \in \mathbb{N}$, the n-th tensor power of T,

$$T^{\otimes n}(L_1, \ldots, L_n) = T(L_1) \cdots T(L_n),$$

is sufficient for the n-th power R^n (i.e., w.r.t. the experiment $(\mathcal{L}_1^n, \mathcal{B}(\mathcal{L}_1^n), (R^n : R \in \mathcal{R}))$. (Note that the power sufficiency is implied by the sufficiency if the distributions $R \in \mathcal{R}$ are dominated by a σ-finite measure.)

LEMMA 3.42 *If T is a power sufficient statistic for $R \in \mathcal{R}$ then the statistic*

$$S : \tilde{\Phi} \mapsto (\tilde{\Phi}(X), T(L_1) \cdots T(L_{\tilde{\Phi}(X)}))$$

is sufficient for (λ, R) (we denote here by $L_1, \ldots, L_{\tilde{\Phi}(X)}$ the lines of the process $\tilde{\Phi}$ shifted to the origin).

Proof. We have to show that the conditional distribution of $\widetilde{\Phi}$ given $S(\widetilde{\Phi})$ is independent of (α, R). We can condition first by $\widetilde{\Phi}(X) = n$, getting a distribution on $(\mathcal{F}_1)^n$ given by

$$\begin{aligned} &\mathrm{E}_{\alpha,R}[f(\widetilde{\Phi}) \mid \widetilde{\Phi}(X) = n] \\ &= c \int_{\mathcal{L}_1} \cdots \int_{\mathcal{L}_1} \int_{p_{L_1^\perp} W} \cdots \int_{p_{L_n^\perp} W} f(L_1 + y_1, \ldots, L_n + y_n) \\ &\qquad \nu_1(\mathrm{d}y_n) \cdots \nu_1(\mathrm{d}y_1) R(\mathrm{d}L_n) \cdots R(\mathrm{d}L_1) \end{aligned}$$

with a constant c depending on the window W. Since T is power sufficient for $R \in \mathcal{R}$, the subsequent conditioning by $T = t$ will yield a distribution independent of $R \in \mathcal{R}$. □

Note that the completeness of the statistic T (for $R \in \mathcal{R}$) implies the completeness of the statistic $S(\widetilde{\Phi})$ for (α, R), $\alpha > 0$, $R \in \mathcal{R}$.

Conditioning the estimator (3.61) by S, we get

THEOREM 3.43 ([98, THEOREM 1]) *Let T be a statistic on $\mathcal{L}_1$ which is complete and power sufficient for $R \in \mathcal{R}$. Then*

$$e(\widetilde{\Phi}) = \sum_{F \in \widetilde{\Phi}} \mathrm{E}\left[\frac{1}{\nu_1(p_{L^\perp} W)} \,\middle|\, T(L) \right]$$

is the UBUE for the length intensity λ of a stationary line process observed in a bounded window W with unknown direction distribution $R \in \mathcal{R}$.

Another possible application of Theorem 3.40 concerns Poisson particle processes (cf. [82]).

3.4.2 Poisson particle processes

Let Φ be a stationary Poisson process on $\mathcal{K}'$ with intensity measure Λ satisfying (2.31). Due to (2.35), Λ disintegrates into the intensity $\alpha > 0$ (unknown parameter) and the primary grain distribution Λ_0 which is assumed to be known.

Further, let $X \subset \mathcal{K}'$ be a measurable subset with $0 < \Lambda(X) < \infty$.

Denote $\widetilde{\Phi} = \Phi \mid X$ the restriction of Φ; $\widetilde{\Phi}$ is a finite Poisson process on X with intensity measure $\widetilde{\Lambda} = \Lambda \mid X$. Applying (2.35) to the function $\mathbf{1}_X f$, we get the following factorization of $\widetilde{\Lambda}$:

$$\int_X f(K)\widetilde{\Lambda}(\mathrm{d}K) = \alpha \int_{\mathcal{K}_0'} \int_{W(K_0)} f(z + K_0)\mathrm{d}z\Lambda_0(\mathrm{d}K_0), \qquad (3.62)$$

where $W(K_0) = \{z : z+K_0 \in X\} \subset \mathbb{R}^d$ and f is an arbitrary nonnegative measurable function on X. Due to (3.62) we can write

$$\widetilde{\Lambda} = \alpha\overline{\Lambda}$$

with a finite known measure $\overline{\Lambda}$ on X. Thus, we get as a consequence of Theorem 3.40

COROLLARY 3.44 *The estimator*

$$e(\widetilde{\Phi}) = \widetilde{\Lambda}(X)^{-1}\widetilde{\Phi}(X)$$

is the UBUE for the intensity α of a stationary Poisson particle process among all estimators using the information on particles from X. Further, if $\bar{e}(\widetilde{\Phi})$ is an unbiased estimator of a function of intensity $\tau(\alpha)$, then

$$e_\tau(\widetilde{\Phi}) = \mathrm{E}_\alpha[\bar{e}(\widetilde{\Phi} \mid \Phi(X)]$$

is the UBUE of $\tau(\alpha)$ among all estimators using the information on particles from X.

Consider the following particular examples for the choice of the set X. Let $W \subset \mathbb{R}^d$ be a bounded set (observation window) of positive Lebesgue measure.

1) Denote

$$X_1 = \{K \in \mathcal{K}' : c(K) \in W\} = \{c + K_0 : c \in W, K_0 \in \mathcal{K}_0'\}, \quad (3.63)$$

i.e. the set of all particles with reference points in W. We have $W(K_0) = W$ for any K_0 and, from (3.62),

$$\widetilde{\Lambda}(X_1) = \alpha\overline{\Lambda}(X_1) = \alpha\nu_d(W).$$

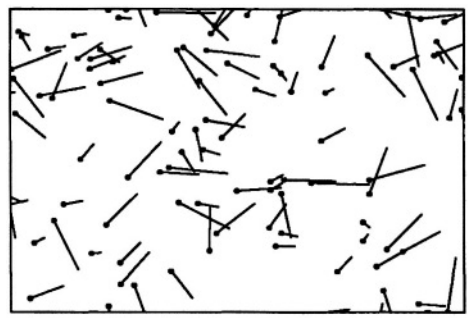

Figure 3.5. An example of a realization of a stationary Poisson segment process in a planar window W with distinguished reference points.

2) Denote

$$X_2 = \{K \in \mathcal{K}' : K \cap W \neq \emptyset\} \tag{3.64}$$

(the set of all particles hitting W). We have $W(K_0) = W \oplus \check{K}_0$ (the dilation of W by K_0) and, again from (3.62),

$$\tilde{\Lambda}(X_2) = \alpha\bar{\Lambda}(X_2) = \alpha \mathrm{E}\nu_d(W \oplus \check{Z}_0),$$

Z_0 being the (random) primary grain.

3.4.3 Comparison of estimators of length intensity of Poisson segment processes

In this subsection we consider the particular case of a stationary Poisson segment process in $\mathbb{R}^d$. Segments are denoted by s and each segment is determined by its reference point $c(s)$ (e.g. the lexicographic minimum), length $r > 0$ and orientation $L \in \mathcal{L}_1$ (see Subsection 2.8). A simulated realization of a segment process in the plane is shown in Fig. 3.4.3.

The length intensity λ of the stationary segment process Φ (2.40) is a simple function of the intensity α, $\lambda = \alpha \mathrm{E}r$ and, consequently, we can apply Corollary 3.44 to find the following uniformly best unbiased estimators of λ:

1) Considering the set X_1 in (3.63) of all segments with reference point in the observing window W, we get the estimator

$$\hat{\lambda}_1 = \frac{\Phi(X_1)\mathrm{E}r}{\nu_d(W)}$$

which is UBUE among all estimators based on the data from X_1.

2) Considering the set $\boldsymbol{X_2}$ in (3.64) of all segments hitting W, we get the estimator

$$\hat{\lambda}_2 = \frac{\Phi(X_2)\mathrm{E}r}{\mathrm{E}\nu_d(W \oplus \check{Z}_0)}$$

which is UBUE among all estimators based on the data from $\boldsymbol{X_2}$.

Of course, $\mathbf{var}\,\hat{\lambda}_2 \leq \mathbf{var}\,\hat{\lambda}_1$ since $X_1 \subset X_2$.

We consider also a natural length intensity estimator

$$\hat{\lambda}_\ell = \frac{1}{\nu_d(W)} \sum_{s \in \Phi} \nu_1(s \cap W) \tag{3.65}$$

which is based on measuring the segment lengths in W. Since $\hat{\lambda}_\ell$ belongs to the family of estimators based on information from $\boldsymbol{X_2}$ we have $\mathrm{var}\,\hat{\lambda}_2 \leq \mathbf{var}\,\hat{\lambda}_\ell$. It is, however, not possible to compare in general the estimator $\hat{\lambda}_\ell$ with $\hat{\lambda}_1$ since these estimators are based on different data. The variances of these two estimators can be computed explicitely by means of Lemma 2.20; for a comparison in some particular cases, see [82].

LEMMA 3.45 *We have, for* $i = 1, 2$,

$$\mathbf{var}\,\hat{\lambda}_i = \frac{\alpha(\mathrm{E}r)^2}{\overline{\Lambda}(X_i)}.$$

Proof. Using Lemma 2.20 and (2.38) we get for $i = 1, 2$

$$\begin{aligned} \mathbf{var}\,\hat{\lambda}_i &= \int \left(\frac{\mathrm{E}r}{\overline{\Lambda}(X_i)} 1_{X_i}(s) \right)^2 \Lambda(\mathrm{d}s) \\ &= \left(\frac{\mathrm{E}r}{\overline{\Lambda}(X_i)} \right)^2 \alpha \int_{\mathcal{L}_1 \times (0,\infty)} \int_{W_i(r,\beta)} \mathrm{d}z \Lambda_0(\mathrm{d}(r,\beta)) \\ &= \frac{\alpha(\mathrm{E}r)^2}{\overline{\Lambda}(X_i)}, \end{aligned}$$

where $W_i(r,\beta) = \{z : s(z,r,\beta) \in X_i\}$. □

LEMMA 3.46 *For the estimator* (3.65) *it holds*

$$\mathbf{var}\,\hat{\lambda}_\ell = \frac{1}{(\nu_d(W))^2} \int \nu_1(s \cap W)^2 \Lambda(\mathrm{d}s). \tag{3.66}$$

EXAMPLE 3.47 *The formula for the variance in Lemma 3.46 was calculated explicitely in the case of a planar stationary Poisson segment*

process with mutually independent typical segment length r and orientation β (we represent here one-dimensional subspaces β by angles from an interval $[0, \pi)$). Assume that the fourth moment of the segment length is finite and consider a square window W of edge length a. In such a case

$$\operatorname{var} \hat{\lambda}_\ell = \frac{\alpha}{a^4}\left(a^2\mathrm{E}r^2 - \frac{1}{3}a\mathrm{E}r^3\mathrm{E}(\sin|\beta| + \cos|\beta|) + \frac{1}{3}\mathrm{E}r^4\mathrm{E}(\sin|\beta|\cos|\beta|)\right).$$

As a consequence we get

THEOREM 3.48 *Let Φ be a stationary Poisson segment process in $\mathbb{R}^2$ with independent typical segment length and orientation and let the typical segment length r have a finite fourth moment. Let W be the observation window from Example 3.47. Then there exists an $a_0 > 0$ such that*

$$\operatorname{var} \hat{\lambda}_1 \leq \operatorname{var} \hat{\lambda}_\ell \quad \text{for any } a > a_0.$$

Moreover, the limit

$$\lim_{a\to\infty} \frac{\operatorname{var} \hat{\lambda}_1}{\operatorname{var} \hat{\lambda}_\ell} = \frac{(\mathrm{E}r)^2}{\mathrm{E}r^2}$$

is less than 1 *unless the segment length r is constant almost surely.*

It follows that in this particular case, the estimator $\hat{\lambda}_1$ is asymptotically better than $\hat{\lambda}_\ell$. The value of the bound a_0 for the window side length was computed explicitely for some particular length and direction distributions in [82].

EXERCISE 3.49 *Prove Lemma 3.46. Hint: Use Lemma 2.20.*

3.4.4 Asymptotic normality

Consider a $\mathcal{H}^k$-process Φ satisfying (3.1) and (3.15) which induces a random measure $\Psi_Q = T_Q\Phi$ for a given probability distribution Q on $\mathcal{L}_k$, see Subsection 3.1.4. Recall that

$$\lambda_Q = \alpha\mathrm{E}\mathcal{I}_Q^k(Z_0) \tag{3.67}$$

is the intensity of Ψ_Q, where α is the intensity and Z_0 the primary grain of Φ.

We are interested in asymptotic properties of intensity estimators discussed in Subsection 3.4.2, especially in conditions under which asymptotic normality holds. Let a nondecreasing sequence (W_n) of convex bodies be given with inradii growing to infinity. In the case of a Poisson point

process Φ it is not difficult to verify that the central limit theorem for the ratio $\Psi_Q(W_n)/\nu_d(W_n)$ is valid under mild assumptions.

THEOREM 3.50 *If*

$$\tau = \mathrm{E}\mathcal{I}_Q^k(Z_0)^2 < \infty \tag{3.68}$$

then the convergence

$$\sqrt{\nu_d(W_n)}\left(\frac{\Psi_Q(W_n)}{\nu_d(W_n)} - \lambda_Q\right) \xrightarrow{d} N(0, \sigma_Q^2), \quad n \to \infty,$$

holds with $\sigma_Q^2 = \alpha\tau$.

Proof. We present a sketch of the proof, details are left to exercises, see also [88]. Denote

$$S_n = \sqrt{\nu_d(W_n)}\left(\frac{\Psi_Q(W_n)}{\nu_d(W_n)} - \lambda_Q\right) = \frac{\Psi_Q(W_n) - \mathrm{E}\Psi_Q(W_n)}{\sqrt{\nu_d(W_n)}}.$$

Combining the factorization (3.62) with (2.14), the characteristic function of the random variable S_n can be expressed as

$$\mathrm{E}e^{itS_n} = \exp\left(\alpha\mathrm{E}\int \left(e^{itY_n(z)} - 1 - itY_n(z)\right)\mathrm{d}z\right), \quad t \in \mathbb{R},$$

where

$$Y_n(z) = \frac{\mathcal{I}_Q^k((Z_0 + z) \cap W_n)}{\sqrt{\nu_d(W_n)}}.$$

It can be shown (cf. Exercise 3.54) that

$$\alpha \int \mathrm{E}Y_n(z)^2 \,\mathrm{d}z \to \sigma_Q^2, \quad n \to \infty. \tag{3.69}$$

To obtain the desired convergence of the characteristic function of S_n, it remains to show that

$$\mathrm{E}e^{itS_n} = \mathrm{E}\int \left(e^{itY_n(z)} - 1 - itY_n(z) + \frac{t^2 Y_n(z)^2}{2}\right)\mathrm{d}z \to 0, \quad n \to \infty \tag{3.70}$$

(cf. Exercise 3.55). □

The ratio

$$\hat{\lambda}_{\ell,n} = \frac{\Psi_Q(W_n)}{\nu_d(W_n)} \tag{3.71}$$

is, according to Theorem 3.50, a natural unbiased estimator of the intensity λ_Q. Therefore if $\mathrm{E}\mathcal{I}_Q^k(Z_0)^2 < \infty$ then for $n \to \infty$

$$\sqrt{\nu_d(W_n)}(\hat{\lambda}_{\ell,n} - \lambda_Q) \xrightarrow{d} N(0, \sigma_Q^2). \tag{3.72}$$

Another unbiased estimator of λ arises from the results of Subsection s:ppp. It requires $\mathrm{E}\mathcal{I}_Q^k(Z_0)$ to be known. Then it suffices to estimate α:

$$\hat{\alpha}_{1,n} = \sum_{K \in \Phi} \frac{\mathbf{1}_{[c(K) \in W_n]}}{\nu_d(W_n)} = \frac{\Phi(\{K \in \mathcal{K}' : c(K) \in W_n\})}{\nu_d(W_n)},$$

where $c(K)$ is the reference point of K (see Subsection 2.8). ¿From Corollary 3.44 it follows that for any fixed n and for known $\mathrm{E}\mathcal{I}_Q^k(Z_0)$,

$$\hat{\lambda}_{1,n} = \hat{\alpha}_{1,n}\mathrm{E}\mathcal{I}_Q^k(Z_0)$$

is the uniformly best unbiased estimator of λ among all estimators based on the information on $K \in \mathcal{K}'$ with $c(K) \in W_n$.

Theorem 3.50 yields the following special result for the estimator $\hat{\lambda}_{1,n}$:

COROLLARY 3.51 *Under the assumptions of Theorem 3.50,*

$$\sqrt{\nu_d(W_n)}\left(\hat{\lambda}_{1,n} - \lambda\right) \xrightarrow{d} N(0, \sigma_1^2), \tag{3.73}$$

where $\sigma_1^2 = \alpha[\mathrm{E}\mathcal{I}_Q^k(Z_0)]^2$.

Choosing $Q = U$ (uniform distribution over $\mathcal{L}_k$), central limit theorems are obtained for Hausdorff measures over the Boolean models formed by Poisson $\mathcal{H}^k$-processes.

Consider a stationary Poisson segment process Φ with intensity α and let Ψ be again the induced random measure with length intensity $\lambda = \alpha \mathrm{E}r$ with $r = \mathcal{H}^1(\mathfrak{s}_0)$ where $\mathfrak{s}_0$ is a typical segment. Assume that $\mathrm{E}r^2 < \infty$. We get from (3.72) that for $n \to \infty$

$$\sqrt{\nu_d(W_n)}\left(\hat{\lambda}_{\ell,n} - \lambda\right) \xrightarrow{d} N(0, \alpha \mathrm{E}r^2),$$

where

$$\hat{\lambda}_{\ell,n} = \frac{\Psi(W_n)}{\nu_d(W_n)} = \sum_{\mathfrak{s} \in \Phi} \frac{\mathcal{H}^1(\mathfrak{s} \cap W_n)}{\nu_d(W_n)}$$

is the natural length intensity estimator considered in (3.71). We can apply Corollary 3.51 also to get the asymptotic variance of the UBUE estimator of λ,

$$\hat{\lambda}_{1,n} = \sum_{\mathfrak{s} \in \Phi} \frac{\mathbf{1}_{[c(\mathfrak{s}) \in W_n]}}{\nu_d(W_n)} \mathrm{E}r$$

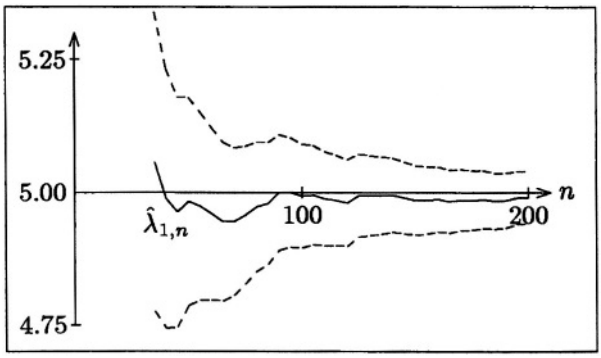

Figure 3.6. **The estimators $\hat{\lambda}_{1,n}$ (solid line) and their 95% approximate confidence intervals (dashed lines) as functions of n.**

assuming the mean length to be known: we have

$$\sqrt{\nu_d(W_n)}\left(\hat{\lambda}_{1,n} - \lambda\right) \xrightarrow{d} N(0, \alpha(\mathrm{E}r)^2).$$

These formulas tell again (even more generally than in Theorem 3.48) that the estimator $\hat{\lambda}_{1,n}$ is asymptotically better than $\hat{\lambda}_{\ell,n}$, unless r is constant almost surely.

EXAMPLE 3.52 *The asymptotic normality is used in statistics for the construction of approximate confidence intervals for estimated parameters. A single realization of a stationary Poisson segment process in $\mathbb{R}^2$ was evaluated in windows of increasing size $W_n = [-n, n]^2$. The length and orientation of segments was independent with marginal uniform distribution R and uniform length on $[0, a]$. For $a = 10$, $\alpha = 1$ the behavior of the estimators $\hat{\lambda}_{1,n}$ and $\hat{\lambda}_{\ell,n}$ is drawn in Figures 3.6 and 3.7. Formulas for confidence intervals are derived in [88]. Observe that confidence intervals are broader for $\hat{\lambda}_{\ell,n}$.*

EXAMPLE 3.53 *This example is a continuation of Subsection 3.2.3, where a pattern of an earthworm burrow system in a soil was studied. Under the assumption that the model of Poisson segment process is valid we can apply the theory of UBUE from this section. Recall the natural estimator* (3.65) *of length intensity presented in Subsection 3.2.3 ($\hat{L}_V^{\ell} = \hat{\lambda}_{\ell} = 15.50$). In Subsection 3.4.3, we learned that the counting estimator $\hat{L}_V = \hat{\lambda}_1$ is UBUE among the estimators based on segments with reference points within the window (here cubic subregion) observed, provided that the mean segment length $\mathrm{E}r$ is known. This estimator is asymptotically better than $\hat{L}_V^{\ell}$ with increasing window size.*

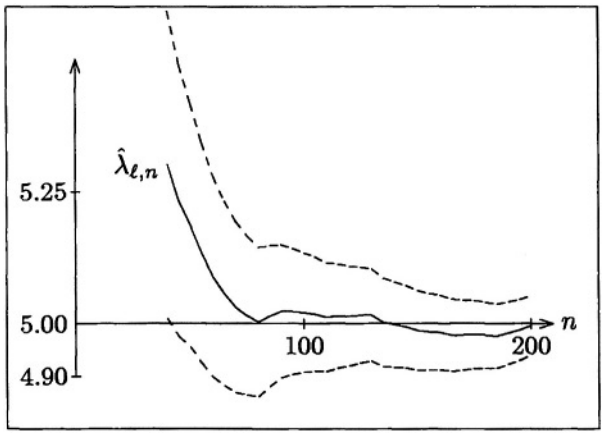

Figure 3.7. The estimators $\hat{\lambda}_{\ell,n}$ (solid line) and their 95% approximate confidence intervals (dashed lines) as a function of n.

Under the assumption of exponentially distributed segment length it holds $\mathrm{E}r^2 = 2(\mathrm{E}r)^2$ *so the asymptotic variance of* $\hat{L}_V^\ell$ *is twice larger than that of* $\hat{L}_V$.

We are not able to evaluate $\operatorname{var} \hat{L}_V$ *since* $\mathrm{E}r$ *is unknown. Using the estimator of* $\mathrm{E}r$ *in place of the true value is not allowed here since it leads to coincidence of both estimators. ¿From formula* (3.66) *we obtain (after numerical integration)* $\operatorname{var} \hat{L}_V^\ell = 18.7$.

EXERCISE 3.54 *Derive the convergence* (3.69) *in the proof of Theorem 3.50.*
Hint: apply Lemma 2.20 to the functions $f(K) = g(K) = \mathcal{I}_Q^k((K+z) \cap W_n)$, $K \in \mathcal{K}^k$, *use assumption (3.68), the fact that*

$$\frac{\nu_d((W_n - x) \cap (W_n - y))}{\nu_d(W_n)} \to 1, \quad n \to \infty, \quad \textit{for every } x, y \in \mathbb{R}^d$$

and the Lebesgue dominated convergence theorem.

EXERCISE 3.55 *Prove formula* (3.70) *in the proof of Theorem 3.50.*
Hint: Apply the inequality

$$\left| \mathrm{e}^{itx} - 1 - itx + \frac{t^2x^2}{2} \right| \le t^2x^2 1_{\{|x|>\varepsilon\}} + \frac{\varepsilon x^2 |t|^3}{6}$$

valid for $\varepsilon > 0$ *and* $t, x \in \mathbb{R}$.

Chapter 4

VERTICAL SAMPLING SCHEMES

The stereological concept of measurements in a sample of IUR sections is often hardly applicable in practice, especially in metallography. Therefore, another method was developed which consists in choosing a fixed direction called vertical and carrying out the measurements in a sample of planes containing the vertical axis (vertical planes). This idea goes back to Baddeley, Gundersen and Cruz-Orive, see e.g. [1], [4], and was later developed by Gokhale [36], [38], [39].

In this chapter, we focus mainly on random fibre- and surface systems again, nevertheless, particle processes are considered as well. The properties of various estimators of geometrical characteristics obtained from the vertical sampling design are studied. Further applications are presented in Chapter 6.

Both the model-based and design-based approaches are considered, since our aim here is to explain their relation. The model-based approach is based on stochastic models of objects as described in Chapter 2. In the design-based approach deterministic systems of geometrical objects are studied and randomness enters through probes.

Throughout this chapter we shall consider a random fibre or surface system Ξ in $\mathbb{R}^d$ which is a special case of the random $\mathcal{H}^k$-set introduced in Chapter 3. In fact, most results can easily be extended to a general $0 \leq k \leq d$, nevertheless, with respect to its better illustrativity, we shall limit ourselves to the cases $k = 1, d - 1$.

In the model-based approach, recall first Section 3.2. In formula (3.20) and further in Proposition 3.4, estimators of intensity are suggested which depend on the unknown rose of directions. As already mentioned, there are two ways how to overcome this problem:

a) to randomize the sampling orientations,

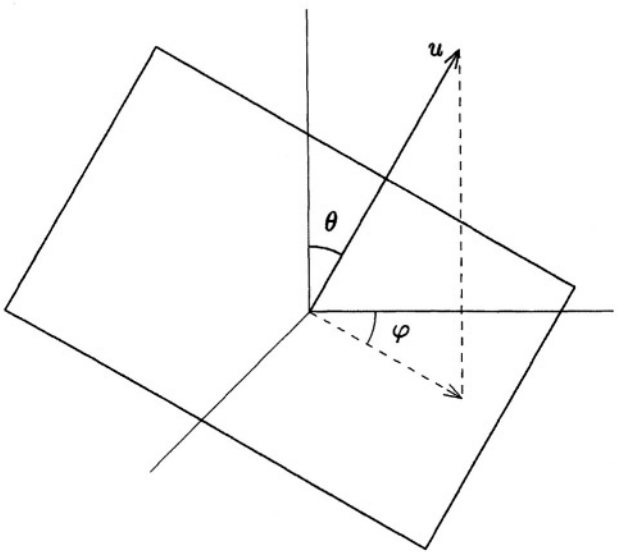

Figure 4.1. IUR plane in $\mathbb{R}^3$ with normal direction $u = (\theta, \varphi)$.

b) to estimate the rose of directions using methods of Chapter 5.

The strategy a) commonly used will be discussed in this chapter. Classical global stereological formulas (e.g. $V_V = A_A$ for volume and area fraction, $S_V = 2P_L$ for surface intensity, etc.) based on Crofton and Cauchy formula, cf. Subsection 1.1.4, make use of isotropic uniform random (IUR) probes. In the design-based approach they are described in [118]. In the model-based approach under the assumption of stationarity, IUR means the uniform distribution of orientations of probes. In the following we shall distinguish between the isotropy of a random probe and the isotropy of a random set or a random process as defined in Chapter 2.

To realize IUR sampling in practice means to cut the specimen in isotropic orientations, i.e., the section plane is chosen with a uniform random normal direction u, see Fig. 4.1. In practice, this may be a difficult task, sometimes even technically impossible (for hard materials). The difficulties persist in spite of the existence of the theory of systematic sampling on the sphere that has been developed recently, see [44]. They can be overcome, however, at least in some practically important cases, e.g. when fibre and surface processes are investigated. A test system achieving this goal is the so called vertical uniform random (VUR) sampling. This consists of probes chosen uniformly randomly parallel to the given vertical direction.

Consider the particular case $d = 3$ and recall Table 3.2. For an unknown rose of directions, an unbiased estimate of intensity using VUR direct probes is impossible. In the case of indirect probes the situation is different, since then, in fact, two-stage sampling is involved. As will be shown in this chapter, using VUR probes in the first stage and a suitable sampling Q in the second stage, unbiased estimators of intensity are available, cf. [4], [36].

4.1. Randomized sampling

First it should be specified what is meant by the *randomization.* In general, an arbitrary probability distribution of the positions of test probes is called randomization. When stationarity of the random (fibre or surface) system is assumed, it is sufficient to consider rotations (and reflections) of test probes only. In this sense, a distribution Q in the definition of a projection measure Ψ_Q (Definition 3.3) is a randomization (of projection directions). In the following, however, a more special notion of randomization is considered. The intensity estimators defined in Chapter 3 depend on an unknown rose of directions R. By the randomization we shall mean a distribution of test probes which leads to an estimator independent of R. While in the case of direct probes this concerns Q in (3.20) only, in a two-stage sampling a special combination of Q and a distribution of v in (3.45) is needed.

4.1.1 IUR sampling

The randomization by means of IUR probes in the case of direct probes is simple: taking $Q = U$ uniform in (3.20) we obtain the intensity estimator

$$\hat{\lambda} = \frac{\Psi(B)}{\nu_d(B)} \tag{4.1}$$

with variance

$$\operatorname{var} \hat{\lambda} = \lambda^2 \left(\frac{1}{\nu_d(B)^2} \int g_B(x) \mathcal{K}(\mathrm{d}x) - 1 \right). \tag{4.2}$$

Both formulas are independent of R while formula (3.22) is not since p_Q depends on R. Thus, IUR direct probes are theoretically equivalent to the direct measurement of the fibre length (surface area) in the original space. This is frequently impossible in applications and stereological methods are used. The value $\Psi(B)$ in (4.1) is approximated by intersection counting, cf. Fig. 3.1 (a), (b). If λ_N denotes the intensity of the number of intersections of the stationary fibre (surface) system with a uniformly randomly rotated test hyperplane (line, respectively), we get

by means of (3.3) and Theorem 3.1

$$\lambda = \frac{1}{\beta_d}\lambda_N.$$

In $\mathbb{R}^3$, since $\beta_3 = \frac{1}{2}$, this leads to the well-known formulas

$$S_V = 2P_L, \quad L_V = 2P_A, \tag{4.3}$$

P_L, P_A being the mean number of intersections per unit length of IUR test line (intersecting surfaces), per unit area of IUR test plane (intersecting fibres), respectively. In practice a single IUR test probe leads to an unbiased estimator.

Now consider indirect probes. While in Proposition 3.4 the orientation v of the probe is fixed, here it is random with a uniform probability distribution on $\mathbb{S}^{d-1}$. This together with Q uniform is called again the isotropic uniform random (IUR) sampling. In the following, we shall write $\mathcal{V} = v^{\perp}$ (the subspace perpendicular to v) and $B_{\mathcal{V}}$ will be a Borel subset of $\mathcal{V}$ of positive finite Lebesgue measure independent of $\mathcal{V}$ (for example, we can choose $B_{\mathcal{V}} = B_\rho \cap \mathcal{V}$, where B_ρ is the ball in $\mathbb{R}^d$ with centre in origin and radius $\rho > 0$). The IUR intensity estimators based on indirect probes are

$$\hat{S}_d^{\mathrm{IUR}} = \frac{\Psi^v(B_{\mathcal{V}})}{\mu_d \nu_{d-1}(B_{\mathcal{V}})}, \quad \hat{L}_d^{\mathrm{IUR}} = \frac{\Psi^{v,t}(B_{\mathcal{V}})}{t\mu_d \nu_{d-1}(B_{\mathcal{V}})}, \tag{4.4}$$

where

$$\mu_d = \frac{\beta_d}{\beta_{d-1}} = \frac{\Gamma(d/2)^2}{\Gamma((d-1)/2)\Gamma((d+1)/2)},$$

in particular, $\mu_3 = \frac{\pi}{4}$.

PROPOSITION 4.1 *The estimators* (4.4) *are unbiased.*

Proof. Let the projection measure Ψ be induced by a stationary random surface system. Then we have for a fixed direction $v \in \mathbb{S}^{d-1}$ by (3.44)

$$\mathrm{E}\Psi^v(B_{\mathcal{V}}) = S_d \mathcal{G}_R(v)\nu_{d-1}(B_{\mathcal{V}}),$$

so that

$$\mathrm{E}\hat{S}_d^{\mathrm{IUR}} = \frac{\mathrm{E}(\mathrm{E}\Psi^v(B_{\mathcal{V}}) \mid v)}{\mu_d \nu_{d-1}(B_{\mathcal{V}})} = \frac{S_d}{\mu_d}\mathrm{E}\mathcal{G}_R(v) = S_d.$$

Analogously for $\hat{L}_d^{\mathrm{IUR}}$, using (3.41). □

REMARK 4.1. Note that assumptions (3.42) and (3.46) are clearly satisfied for almost all directions $v \in \mathbb{S}^{d-1}$.

REMARK 4.2. For $d = 3$ it is $\mu_3 = \frac{\pi}{4}$ and the estimators in (4.4) correspond to the stereological formulas

$$S_V = \frac{4}{\pi} L_A, \quad L_V = \frac{4}{\pi t} L_A. \tag{4.5}$$

EXERCISE 4.1 *Show that* $\mathcal{G}_U(v) = \mu_d$ *for all* $v \in \mathbb{S}^{d-1}$.

4.1.2 Application - effect of steel radiation

To demonstrate IUR intensity estimation together with an application of the cross-correlation function, see Subsection 2.5, a real data analysis follows. Microstructural defects in materials are usually modelled in terms of point, fibre or surface systems. Dislocations are geometrically fibres in 3D space and when observed on a projected slab they form fibres in 2D space. In addition to the dislocations length intensity (called dislocation density by engineers), the arrangement of dislocations, described by the pair-correlation function, is an important characteristics of the dislocation substructure which reflects the prior treatment of the material.

In a ferritic reactor pressure steel, in addition the relation of a dislocation substructure to both homogeneously distributed precipitate particles and heterogeneously formed radiation-induced defects can be studied by means of a cross-correlation function defined in (2.22).

In Fig. 4.2 the weld metal microstructures are presented as obtained by the transmission electron microscope (TEM) projection of a thin slab (foil). The difference between the two micrographs of CrMoV steel is that the middle microstructure comes from a metal irradiated by fast neutrons in a nuclear reactor. This leads to a formation of extended defects which concentrate to dislocation substructure. Simultaneously, the recovery of a dislocation substructure can occur; the dislocations move and become pinned to existing particles. The conjecture is that in this state the correlation between two substructures is stronger than in the non-irradiated case. In addition, another specimen was selected (Fig. 4.2 right) as an example of a microstructure where dislocations are the dominant nucleae centres for precipitated particles. Here the strongest correlation is expected.

In our example, dislocations are modelled by a stationary fibre process with the corresponding length measure Ψ. The length intensity L_V of Ψ is estimated by (4.4) based on indirect probes where t is the slab thickness. In fact, formula (4.5) is applied and the estimate of L_A is obtained by measuring the length of observed fibres using an image analyser.

Consider the point process of particle projection centroids and the fibre system of dislocation projections, and let Ψ_1, Ψ_2 denote the cor-

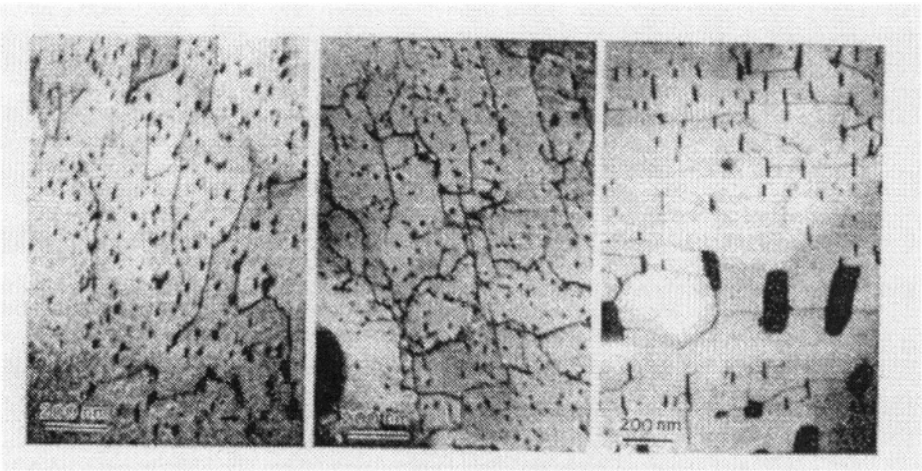

Figure 4.2. Micrographs of CrMoV ferritic steel, non-irradiated (left), CrMoV ferritic steel, irradiated (middle), Zr-1Nb weld alloy (right).

material	*estimated* L_V $[\mu m^{-2}]$	*slope Sl*
CrMoV steel, non-irradiated	74	0.0015
CrMoV steel, irradiated	160	-0.0595
Zr-1Nb, non-irradiated	40	-0.1595

Table 4.1. Results of the study of correlation between two substructures of steels under different conditions

responding induced random measures. The cross-correlation function is used in the form derived from the K-function

$$p_{1,2}(r) = \frac{1}{2\pi r} \frac{\mathrm{d}K_{1,2}(r)}{\mathrm{d}r},$$

where from (2.22)

$$K_{1,2}(r) = \mathcal{K}_{1,2}(B_r(0)).$$

The estimation procedure was based on these formulas, cf. [86].

The quantitative criterion is based on the estimated slope Sl of $p_{1,2}$ at the origin: the more negative slope, the larger correlation between substructures. Results in Table 4.2 involve estimated intensities and slopes. They confirm that the cross-correlation function is a useful tool for a basic description of relations in a mixed population of objects.

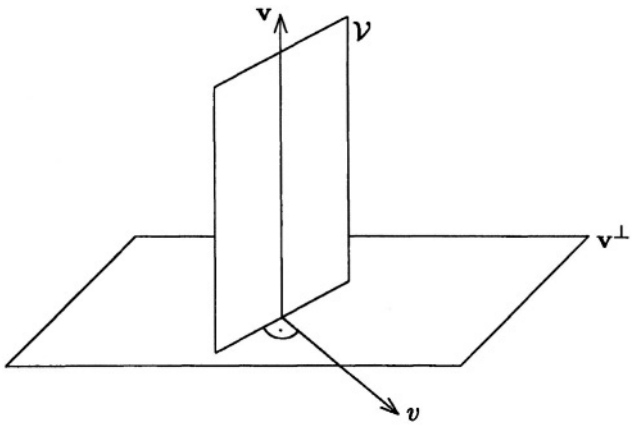

Figure 4.3. VUR plane $\mathcal{V}$ in $\mathbb{R}^3$ with normal direction v.

4.1.3 VUR sampling

An ingenious randomization for indirect probes is represented by a vertical uniform random (VUR) sampling design. Consider a fixed direction $\mathbf{v} \in \mathbb{S}^{d-1}$, called vertical, and define the class $\mathfrak{V} \subset \mathcal{L}_{d-1}$ of hyperplanes containing the given direction $\mathbf{v}$. Elements $\mathcal{V} \in \mathfrak{V}$ are determined by their normal directions $v \in \mathbb{S}^{d-2} \subset \mathbf{v}^\perp$, $\mathcal{V} = v^\perp$.

Thus, the distribution on the vertical plane $\mathcal{V} = v^\perp \in \mathfrak{V}$ is determined by means of the distribution of its normal direction $v \in \mathbb{S}^{d-2} \subset \mathbf{v}^\perp$, see Fig. 4.3. (As in Subsection 3.2.2, all distributions on the unit spheres are even since they represent distributions on the corresponding spaces of one-dimensional linear subspaces.) Correspondingly, the *uniform vertical plane distribution* is the distribution of $\mathcal{V} = v^\perp$ with uniform distribution of $v \in \mathbb{S}^{d-2} \subset \mathbf{v}^\perp$. We shall use the notation $U_{\mathbf{v}}$ for both the uniform vertical plane distribution and for the uniform distribution over the sphere $\mathbb{S}^{d-2} \subset \mathbf{v}^\perp$.

In the first stage, consider (i) in the case of a surface system Ξ a uniform random element $\mathcal{V} \in \mathfrak{V}$, (ii) in the case of a fibre system Ξ a thin slab of thickness t parallel to a uniform random vertical plane $\mathcal{V}$. Then, Ψ^v ($\Psi^{v,t}$, respectively) is the induced process in $\mathbb{R}^{d-1}$ according to Subsection 3.2.2. The special case of Q in the second stage which, together with VUR probes, yields the desired randomization is described in the following theorem.

THEOREM 4.2 *Let Ξ be a stationary random fibre (surface) system in $\mathbb{R}^d$ and assume that a bounded measurable window $B_{\mathcal{V}}$ is given in any vertical plane $\mathcal{V} \in \mathfrak{V}$ so that $\nu_{d-1}(B_{\mathcal{V}}) > 0$ independent of $\mathcal{V}$ and the mapping $\mathcal{V} \mapsto B_{\mathcal{V}}$ is measurable. Let $Q^*_{\mathcal{V}}$ be the probability distribution*

on $\mathbb{S}^{d-2} \subset \mathcal{V}$ *given by*

$$Q^*_{\mathcal{V}}(\mathrm{d}w) = \frac{d-1}{d-2}\mu_d |\sin \sphericalangle(w, \mathbf{v})| U_{\mathcal{V}}(\mathrm{d}w), \tag{4.6}$$

where $U_{\mathcal{V}}$ *is the uniform distribution over* $\mathbb{S}^{d-2} \subset \mathcal{V}$. *If* $\mathcal{V}$ *is a uniform random vertical plane, then*

$$L_d = \frac{\mathrm{E}(\mathrm{E}\Psi^{v,t}_{Q^*_{\mathcal{V}}}(B_{\mathcal{V}}) \mid \mathcal{V})}{t\mu_d \nu_{d-1}(B_{\mathcal{V}})}, \tag{4.7}$$

$$S_d = \frac{\mathrm{E}(\mathrm{E}\Psi^{v}_{Q^*_{\mathcal{V}}}(B_{\mathcal{V}}) \mid \mathcal{V})}{\mu_d \nu_{d-1}(B_{\mathcal{V}})}, \tag{4.8}$$

respectively.

Note that $Q^*_{\mathcal{V}}$ is indeed a probability distribution. The proof of Theorem 4.2 is based on the following integral-geometric formula:

LEMMA 4.3 *For any nonnegative measurable function* h *on* $\mathbb{S}^{d-1}$ *we have*

$$\int_{\mathbb{S}^{d-1}} h(u)U(\mathrm{d}u) = \int_{\mathfrak{V}} \int_{\mathbb{S}^{d-2}(\mathcal{V})} h(u)Q^*_{\mathcal{V}}(\mathrm{d}u)U_{\mathbf{v}}(\mathrm{d}\mathcal{V}),$$

where U *denotes the uniform distribution over* $\mathbb{S}^{d-1}$.

Proof. In the proof of the lemma, c will denote a constant depending on the dimension d only and it may differ from one expression to the other. Using the coarea theorem (Theorem 1.6) for the spherical projection

$$\phi : u \mapsto \frac{p_{\mathbf{v}^\perp} u}{\|p_{\mathbf{v}^\perp} u\|}, \quad u \in \mathbb{S}^{d-2}(\mathcal{V}) \setminus \{-\mathbf{v}, \mathbf{v}\},$$

with Jacobian $J_{d-3}\phi(u) = |\sin \sphericalangle(u, \mathbf{v})|^{d-3}$ (see Exercise 4.5), we get

$$\begin{aligned}\int_{\mathbb{S}^{d-2}(\mathcal{V})} h(u)Q^*_{\mathcal{V}}(\mathrm{d}u) &= c \int_{\mathbb{S}^{d-2}(\mathcal{V})} h(u) |\sin \sphericalangle(u, \mathbf{v})| \mathcal{H}^{d-2}(\mathrm{d}u) \\ &= c \int_{\mathbb{S}^{d-3}(\mathcal{V} \cap \mathbf{v}^\perp)} \int_{\mathbb{S}^1(\mathrm{span}\{\mathbf{v}, l\})} h(u) |\sin \sphericalangle(u, \mathbf{v})|^{d-2} \mathcal{H}^1(\mathrm{d}u) \mathcal{H}^{d-3}(\mathrm{d}l).\end{aligned}$$

The measure

$$G \mapsto \int \mathcal{H}^{d-3}(G \cap \mathbb{S}^{d-3}(\mathcal{V} \cap \mathbf{v}^\perp)) U_{\mathbf{v}}(\mathrm{d}\mathcal{V})$$

is rotationally invariant on $\mathbb{S}^{d-2}(\mathbf{v}^\perp)$, thus it is a multiple of the uniform distribution $U_\mathbf{v}$ on $\mathbb{S}^{d-2}(\mathbf{v}^\perp)$. Consequently, the right hand side of the equality to be proved is

$$c\int_{\mathbb{S}^{d-2}(\mathbf{v}^\perp)}\int_{\mathbb{S}^1(\mathrm{span}\,\{l,\mathbf{v}\})} h(u)|\sin \sphericalangle(u,v)|^{d-2}\mathcal{H}^1(\mathrm{d}u)\mathcal{H}^{d-2}(\mathrm{d}l).$$

Applying again the coarea formula to the spherical projection ψ defined as ϕ above but on the whole $\mathbb{S}^{d-1}\setminus\{-\mathbf{v},\mathbf{v}\}$, with Jacobian $J_{d-2}\psi(u) = |\sin \sphericalangle(u,\mathbf{v})|^{d-2}$, we get that the last expression is equal to

$$c\int_{\mathbb{S}^{d-1}} h(u)\mathcal{H}^{d-1}(\mathrm{d}u).$$

Thus, we have proved the desired formula up to a constant. But the total measure on both sides is clearly one, hence the proof is finished. □

We proceed now to the proof of Theorem 4.2.

Proof. First, note that (3.42) is satisfied for almost all horizontal directions $v \in \mathbb{S}^{d-2} \subset \mathbf{v}^\perp$. Due to the first two formulas in Proposition 3.4 and the relation $\frac{\beta_d}{\beta_{d-1}} = \mu_d$ it suffices to prove that $\mathrm{E}\mathcal{F}_{RQ_\mathbf{v}^*} = \beta_d$. Using Lemma 4.3 we get

$$\mathrm{E}\mathcal{F}_{RQ_\mathbf{v}^*} = \int_{\mathfrak{V}} \mathcal{F}_{RQ_\mathbf{v}^*} U_\mathbf{v}(\mathrm{d}V) = \int_{\mathbb{S}^{d-1}}\int_{\mathbb{S}^{d-1}} |\cos \sphericalangle(u,w)| U(\mathrm{d}u)R(\mathrm{d}w)$$

and since the inner integral on the right equals β_d for any w, the whole expression equals β_d. □

The measure $\Psi^v_{Q_\mathbf{v}^*}$ ($\Psi^{v,t}_{Q_\mathbf{v}^*}$) involves both sampling stages: Ξ^v ($\Xi^{v,t}$) is the induced random set after the first stage, then the induced structure is projected with respect to projection orientation distribution. We shall see later that in $\mathbb{R}^3$ the projection measure $\Psi^v_{Q_\mathbf{v}^*}$ ($\Psi^{v,t}_{Q_\mathbf{v}^*}$) can be approximated by means of the number of intersections of the induced fibre process (in both cases) with appropriate cycloidal test lines.

COROLLARY 4.4 *Unbiased intensity estimators for S_d and L_d using VUR probes are*

$$\hat{L}_d^{\mathrm{VUR}} = \frac{\Psi^{v,t}_{Q_\mathbf{v}^*}(B_\mathbf{v})}{t\mu_d\nu_{d-1}(B_\mathbf{v})}, \qquad \hat{S}_d^{\mathrm{VUR}} = \frac{\Psi^{v}_{Q_\mathbf{v}^*}(B_\mathbf{v})}{\mu_d\nu_{d-1}(B_\mathbf{v})}, \tag{4.9}$$

respectively, using the notation from Theorem 4.2.

Practical use of the suggested estimators will be described in the design-based approach in Subsection 4.2.

EXERCISE 4.5 *Derive the formula*

$$J_{d-2}\pi_L(v) = |\sin \sphericalangle(v,u)|^{d-2},$$

for $u = L^\perp$, $L \in \mathcal{L}_{d-1}$, *for the spherical projection*

$$\pi_L : \mathbb{S}^{d-1} \setminus \{-u, u\} \to L \cap \mathbb{S}^{d-1} = \mathbb{S}^{d-2}(L).$$

4.1.4 Variances of estimation of length

The variances of intensity estimators under randomized sampling have a general form

$$\operatorname{var} \hat{\lambda}_d = \operatorname{var} \mathrm{E}(\hat{\lambda}_d \mid v) + \mathrm{E}\operatorname{var}(\hat{\lambda}_d \mid v). \tag{4.10}$$

In (4.10) the first term on the right hand side is the variance of conditional expectation of $\hat{\lambda}$ given the probe orientation v. The second term is the expectation of the variance of $\hat{\lambda}$ conditioned by a fixed probe v. Note that in the VUR sampling for R rotationally symmetric around the vertical axis the first variance term is zero for the estimator (4.9).

Consider the length intensity estimators $\hat{L}_d^{\mathrm{IUR}}$ (4.4) and $\hat{L}_d^{\mathrm{VUR}}$ (4.9) for a stationary random fibre system Ξ observed in a (projected) slab of thickness t, with direction distribution R. The first term in (4.10) can be easily expressed as a function of the direction distribution R of Ξ:

PROPOSITION 4.2 *For a stationary random fibre system* Ξ *in* $\mathbb{R}^d$ *satisfying*

$$R(\{-\mathbf{v}, \mathbf{v}\}) = 0 \tag{4.11}$$

we have

$$\begin{aligned} \operatorname{var} \mathrm{E}(\hat{L}_d^{\mathrm{IUR}} \mid v) &= L_d^2 \beta_d^{-2} \operatorname{var} \mathcal{G}_R(v), \\ \operatorname{var} \mathrm{E}(\hat{L}_d^{\mathrm{VUR}} \mid v) &= L_d^2 \beta_d^{-2} \operatorname{var} \mathcal{F}_{RQ_v^*}, \end{aligned}$$

where the variance is understood with respect to an isotropic uniform random vector $v \in \mathbb{S}^{d-1}$ *in the first equation and with respect to the horizontal uniform random direction* $v \in \mathbb{S}^{d-2} \subset \mathbf{v}^\perp$ *in the second equation.*

Proof. The formulas are based on Proposition 3.4. Assumption (3.46) is always satisfied for almost all IUR directions v and using (4.11) we get easily that (3.46) is fulfilled also for almost all horizontal directions $v \perp \mathbf{v}$. The formulas from Proposition 3.4 yield

$$\begin{aligned} \beta_{d-1} \mathrm{E}\Psi^{v,t}(B_V) &= t\nu_{d-1}(B_V)\mathcal{F}_{RU_V} L_d, \\ \beta_{d-1} \mathrm{E}\Psi^{v,t}_{Q_V^*}(B_V) &= t\nu_{d-1}(B_V)\mathcal{F}_{RQ_V^*} L_d. \end{aligned}$$

Note that $\mathcal{F}_{RU_\nu} = \mathcal{G}_R(v)$. □

The second variance term, $\mathbf{Evar}\,\hat{L}_V^{\mathrm{IUR}}$ ($\mathbf{Evar}\,\hat{L}_d^{\mathrm{VUR}}$) depends in a more complicated way on the second order distribution of the induced random measures $\Psi^{v,t}$ ($\Psi_{Q_\nu^*}^{v,t}$, respectively), see Proposition 3.8.

EXAMPLE 4.6 *We shall present some particular results for the case when* Φ *is a Poisson line process and the probe* B_ν *a ball in* $\mathcal{V} = v^\perp$ *of radius* ρ. *Applying the results from Subsection 3.29, especially Equation* (3.51), *we can write*

$$\mathbf{var}\,(\hat{L}_d^{\mathrm{IUR}} \mid v) = \frac{2L_d\beta_{d-1}^2}{\beta_d^2\omega_{d-1}\rho^{d-3}t^2}\int_{\mathbb{S}^{d-1}} \eta_{d-1}\left(\frac{t|\tan \sphericalangle(u,v)|}{2\rho}\right)|\langle u,v\rangle| R(\mathrm{d}u), \tag{4.12}$$

since $\mathcal{F}_{U_\nu}(w) = \beta_{d-1}$ *for any* $w \in \mathbb{S}^{d-2} \subset v^\perp$ *(the function* η_{d-1} *is defined in* (3.33)). *Similarly, for the VUR estimator we get*

$$\mathbf{var}\,(\hat{L}_d^{\mathrm{VUR}} \mid v) = \frac{2L_d}{\beta_d^2\omega_{d-1}\rho^{d-3}t^2} \int_{\mathbb{S}^{d-1}} \mathcal{F}_{Q_\nu^*}(\pi_\nu u)^2\,\eta_{d-1}\left(\frac{t|\tan \sphericalangle(u,v)|}{2\rho}\right)|\langle u,v\rangle| R(\mathrm{d}u), \tag{4.13}$$

under assumption (4.11) *(almost surely no line is parallel to the vertical axis). Applying the expectations to the equations* (4.12) and (4.13), *we get the following formulas for the second terms in* (4.10):

$$\mathbf{Evar}\,(\hat{L}_d^{\mathrm{IUR}} \mid v) = \frac{2L_d}{\mu_d^2\omega_{d-1}\rho^{d-3}t^2} C_d(t/\rho) \tag{4.14}$$

with

$$C_d(t/\rho) = \int_{\mathbb{S}^{d-1}} \eta_{d-1}\left(\frac{t|\tan \sphericalangle(u,v)|}{2\rho}\right)|\langle u,v\rangle| U(\mathrm{d}v)$$

(independent of $u \in \mathbb{S}^{d-1}$*), and*

$$\mathbf{Evar}\,(\hat{L}_d^{\mathrm{VUR}} \mid v) = \frac{2L_d}{\beta_d^2\omega_{d-1}\rho^{d-3}t^2} \tag{4.15}$$

$$\int_{\mathbb{S}^{d-1}}\int_{\mathbb{S}^{d-1}} \mathcal{F}_{Q_\nu^*}(\pi_\nu u)^2\eta_{d-1}\left(\frac{t|\tan \sphericalangle(u,v)|}{2\rho}\right)|\langle u,v\rangle| U_\nu(\mathrm{d}v) R(\mathrm{d}u).$$

REMARK 4.3. It was observed in [5] that while the expectation $\mathbf{Evar}\,(\hat{L}_d^{\mathrm{IUR}} \mid v)$ is a consistent part of the variance of the estimator (in the sense that it tends to zero when the radius of the window tends to infinity), $\mathbf{var}\,\mathbf{E}(\hat{L}_d^{\mathrm{IUR}} \mid v)$ is an inconsistent part. This drawback disappears, when we consider a number (growing to infinity) of IUR probes instead of a single one.

4.1.5 Variances of estimation of surface area

For the intensity estimators (4.4) and (4.9) of a stationary random surface system Ξ in $\mathbb{R}^d$ we apply again (4.10)

$$\begin{aligned} \operatorname{var} \hat{S}_d^{\mathrm{IUR}} &= \operatorname{var} \mathrm{E}(\hat{S}_d^{\mathrm{IUR}} \mid v) + \operatorname{Evar}(\hat{S}_d^{\mathrm{IUR}} \mid v), \\ \operatorname{var} \hat{S}_d^{\mathrm{VUR}} &= \operatorname{var} \mathrm{E}(\hat{S}_d^{\mathrm{VUR}} \mid v) + \operatorname{Evar}(\hat{S}_d^{\mathrm{VUR}} \mid v), \end{aligned}$$

where, again, the expectation and variance is taken with respect to the IUR vector $v \in \mathbb{S}^{d-1}$ in the first case and with respect to the uniform horizontal random vector $v \in \mathbb{S}^{d-2} \subset \mathbf{v}^{\perp}$ in the second case. The variances of the conditional mean values can again be easily expressed by using Proposition 3.4:

PROPOSITION 4.3 *For a stationary random surface system Ξ in $\mathbb{R}^d$ we have*

$$\begin{aligned} \operatorname{var} \mathrm{E}(\hat{S}_d^{\mathrm{IUR}} \mid v) &= S_d^2 \beta_d^{-2} \operatorname{var} \mathcal{G}_R(v), \\ \operatorname{var} \mathrm{E}(\hat{S}_d^{\mathrm{VUR}} \mid v) &= S_d^2 \beta_d^{-2} \operatorname{var} \mathcal{F}_{RQ_v^*}. \end{aligned}$$

The conditional variances can again be expressed by means of the reduced second moment measure of the section random measures. In particular, we get by applying Theorem 3.8

$$\operatorname{var}(\hat{S}_d^{\mathrm{IUR}} \mid v) = \left(\frac{S_d \mathcal{G}_R(v)}{\mu_d \nu_{d-1}(B_v)} \right)^2 \int g_{B_v}(x)(p^v(x) - 1)\mathrm{d}x, \tag{4.16}$$

$$\operatorname{var}(\hat{S}_d^{\mathrm{VUR}} \mid v) = \left(\frac{S_d \mathcal{F}_{RQ_v^*}}{\beta_d \nu_{d-1}(B_v)} \right)^2 \int g_{B_v}(x)(p^v_{Q_v^*}(x) - 1)\mathrm{d}x, \tag{4.17}$$

provided that the pair-correlation functions p^v of Ψ^v and $p^v_{Q_v^*}$ of $\Psi^v_{Q_v^*}$ exist. Again, more specific results can be obtained for a Poisson hyperplane process.

EXAMPLE 4.7 *Let Φ be a stationary Poisson hyperplane process with normal direction distribution R and $B_v = B_\rho$ a ball of radius ρ. Then, applying* (3.53), *we obtain*

$$\operatorname{Evar}(\hat{S}_d^{\mathrm{IUR}} \mid v) = \frac{\beta_{2d-2}}{\pi \mu_d \beta_d^2} \frac{S_d}{\rho}, \tag{4.18}$$

$$\operatorname{Evar}(\hat{S}_d^{\mathrm{VUR}} \mid v) = \frac{\beta_{2d-2}}{\pi \beta_d^4} \frac{S_d}{\rho} \mathrm{E} \int \frac{\mathcal{F}_{Q_v^*}(u)^2}{|\sin \sphericalangle(u, v)|} R(\mathrm{d}u). \tag{4.19}$$

REMARK 4.4. Note that the part $\operatorname{Evar}(\hat{S}_d^{\cdot} \mid v)$ of the variance of $\hat{S}_d^{\cdot}$ is a multiple of the ratio S_d/ρ for both (IUR and VUR) estimators,

whereas the part $\mathbf{var}\,\mathrm{E}\hat{S}_d^{\cdot}$ is a multiple of S_d^2 and does not depend on the probe size. The bounds for $\mathbf{var}\,\mathcal{G}_R(v)$ ($v \in \mathbb{S}^{d-1}$ isotropic random) are as follows: It is $\mathbf{var}\,\mathcal{G}_R(v) = 0$ for $R = U$ and $\max_R \mathbf{var}\,\mathcal{G}_R(v) = \frac{d-1}{d} - \mu_d^2$ for $R = \delta_{u_0}$, $u_0 \in \mathbb{S}^{d-1}$ arbitrary; in particular, $\max_R \mathbf{var}\,\mathcal{G}_R(v) = \frac{2}{3} - \frac{\pi^2}{16} = 0.0498$ in dimension $d = 3$.

Further explicit and numerical results are obtained for the most important special case $d = 3$. Consider a stationary random surface system Ξ in $\mathbb{R}^3$ with intensity $S_d = S_V$. Let the z-axis be the vertical axis, i.e., $\mathbf{v} = (0, 0, 1)$ in the coordinates, and let horizontal directions $v \in \mathbf{v}^\perp$ be parametrized by

$$v = (\cos\xi, \sin\xi, 0), \quad \xi \in (0, \pi).$$

For fixed ξ, a halfcircle of $\mathbb{S}^1 \subset \mathcal{V} = v^\perp$ can be parametrized as

$$(-\sin\xi\sin\alpha, \cos\xi\sin\alpha, \cos\alpha), \quad \alpha \in (0, \pi),$$

where α is the angle between ξ and the vertical axis, and the distribution $Q_{\mathcal{V}}^*$ is then described as

$$Q_{\mathcal{V}}^*(\mathrm{d}\alpha) = \frac{1}{2}\sin\alpha\mathrm{d}\alpha. \tag{4.20}$$

In view of this representation, we shall write often Ψ^ξ, Q_ξ^* instead of $\Psi^v, Q_{\mathcal{V}}^*$, respectively.

We shall represent unit vectors $u \in \mathbb{S}^2$ in spherical coordinates

$$u = (\cos\varphi\sin\theta, \sin\varphi\sin\theta, \cos\theta),$$

$\varphi \in [0, 2\pi)$ being the longitude and $\theta \in (0, \pi)$ the latitude. Correspondingly, the distribution R will be considered as distribution $R(\mathrm{d}(\theta, \varphi))$ on $(0, \pi/2] \times [0, 2\pi)$ (remind that R was even on the sphere).

If $u \in \mathcal{V}$, (i.e., $\varphi = \xi \pm \pi/2$), then the value $\mathcal{F}_{Q_\xi^*}(u)$ depends on the latitude of u only and equals

$$\mathcal{F}_{Q_\xi^*}(\theta, \xi + \frac{\pi}{2}) = \begin{cases} \frac{\cos\alpha + \alpha\sin\alpha}{2}, & \alpha \in (0, \pi/2], \\ \frac{-\cos\alpha + (\pi - \alpha)\sin\alpha}{2}, & \alpha \in [\pi/2, \pi). \end{cases}$$

For a general $u = (\theta, \varphi) \in \mathbb{S}^2$ we have $\mathcal{F}_{Q_\xi^*}(u) = |p_{\mathcal{V}}u|\mathcal{F}_{Q_\xi^*}(\pi_{\mathcal{V}}u)$ (remind that $\pi_{\mathcal{V}}$ denotes the spherical projection onto $\mathbb{S}^1(\mathcal{V})$). For $\xi = 0$ we have $p_{\mathcal{V}}u = (0, \sin\varphi\sin\theta, \cos\theta)$, $|p_{\mathcal{V}}u| = \sqrt{1 - \cos^2\varphi\sin^2\theta}$. Thus,

$$\mathcal{F}_{Q_0^*}(\theta, \varphi) = \frac{1}{2}\left(\cos\theta + |\sin\varphi|\sin\theta\arctan|\tan\theta\sin\varphi|\right), \tag{4.21}$$

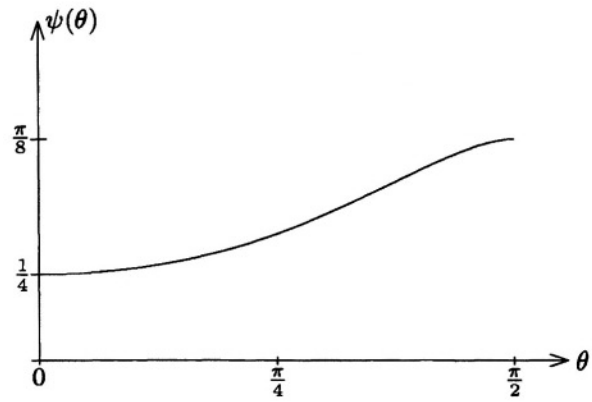

Figure 4.4. The function ψ from (4.24).

$\varphi \in [0, 2\pi), \theta \in (0, \pi/2]$ (cf. [51]). We can now express the mean conditional variances from (4.18) and (4.19). We have

$$\mathrm{Evar}\,(\hat{S}_V^{\mathrm{IUR}} \mid v) = \frac{64}{3\pi^3}\frac{S_V}{\rho} \tag{4.22}$$

and

$$\mathrm{Evar}\,(\hat{S}_V^{\mathrm{VUR}} \mid \xi) = \frac{64}{3\pi^2}\frac{S_V}{\rho}\mathcal{J}_R(\mathbf{v}), \tag{4.23}$$

where

$$\begin{aligned}\mathcal{J}_R(\mathbf{v}) &= \mathrm{E}\int_{S^2}\frac{(\mathcal{F}_{Q_\xi^*}(u))^2}{|\sin \sphericalangle(u,v)|}R(\mathrm{d}u)\\ &= \frac{2}{\pi}\int_0^{2\pi}\int_0^{\pi/2}\frac{\mathcal{F}_{Q_0^*}(\theta,\varphi)^2}{\sqrt{1-\cos^2\varphi\sin^2\theta}}\bar{R}(\mathrm{d}\theta)\mathrm{d}\varphi\\ &= \int_0^{\pi/2}\psi(\theta)\,\bar{R}(\mathrm{d}\theta),\end{aligned}$$

denoting by $\bar{R}$ the marginal distribution of R of the latitude $\theta \in (0, \pi/2]$, and with the function

$$\psi(\theta) = \frac{1}{2\pi}\int_0^{\pi/2}\frac{(\cos\theta + \sin\varphi\sin\theta\arctan(\tan\theta\sin\varphi))^2}{\sqrt{1-\cos^2\varphi\sin^2\theta}}\mathrm{d}\varphi, \tag{4.24}$$

see Fig. 4.4. Note that always

$$0.25 \le \mathcal{J}_R(\mathbf{v}) \le \pi/8 < 0.4.$$

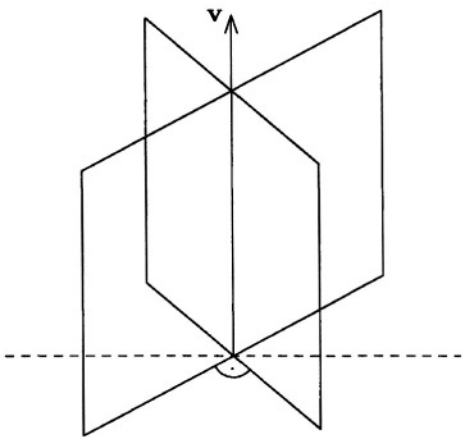

Figure 4.5. **Two perpendicular vertical planes**

Another surface intensity estimator considered in this subsection is the *vertical spatial grid estimator,* see [22], which is based on two perpendicular vertical sections with randomized longitude orientation, see Fig. 4.5.

The vertical spatial grid estimator $\hat{S}_V^{\mathrm{VSG}}$ of S_V is defined as

$$\hat{S}_V^{\mathrm{VSG}} = \frac{2}{\pi \nu_2(B_\xi)} \left(\Psi_{Q_\xi^*}^{\xi}(B_\xi) + \Psi_{Q_{\xi+\pi/2}^*}^{\xi+\pi/2}(B_{\xi+\pi/2}) \right), \tag{4.25}$$

where $\xi \in [0, \pi)$ represents the vertical plane $\mathcal{V} = v^\perp \in \mathfrak{V}$ as described above, B_ξ is a Borel subset of $\mathcal{V}$ of finite positive measure independent of ξ and ξ is random with uniform distribution in $(0, \pi)$.

PROPOSITION 4.4 *The estimator* $\hat{S}_V^{\mathrm{VSG}}$ (4.25) *is unbiased.*

Proof. In fact, the estimator $\hat{S}_V^{\mathrm{VSG}}$ is defined as the mean of two (dependent) VUR estimators, hence, its unbiasedness follows from the unbiasedness of the VUR estimator. □

The variance of the vertical spatial grid estimator again satisfies

$$\operatorname{var} \hat{S}_V^{\mathrm{VSG}} = \mathrm{E} \operatorname{var} (\hat{S}_V^{\mathrm{VSG}} \mid \xi) + \operatorname{var} \mathrm{E}(\hat{S}_V^{\mathrm{VSG}} \mid \xi). \tag{4.26}$$

It is clear that the variance of conditional mean value of the VSG estimator is lower or equal to that of the VUR estimator (cf. Exercise 4.10). On the other hand, the evaluation of $\hat{S}_V^{\mathrm{VSG}}$ is more difficult since it is based on information from two vertical sections whereas $\hat{S}_V^{\mathrm{VUR}}$ depends on a single vertical section only. A method of practical implementation of $\hat{S}_V^{\mathrm{VSG}}$ using confocal microscopy is described in [22].

EXAMPLE 4.8 *Consider now a Poisson process of compact discs in* $\mathbb{R}^3$ *with random radii independent of orientations. Let* R *denote the distribution of unit normals to the discs (an even distribution on* $\mathbb{S}^2$*) and* D *the distribution of the random disc radius* r*. Note that a (vertical) plane* $\mathcal{V} = v^\perp$ *hits a disc of radius* r *and normal direction* u *with probability proportional to* $r|\sin \sphericalangle(u,v)|$*. The section* $\Phi \cap \mathcal{V}$ *is a segment process in* $\mathcal{V}$ *where the typical segment radius and orientation are again independent random variables. The typical segment length has density*

$$l(s) = \frac{1}{4\mathrm{E}r} \int_{s/2}^{\infty} s(r^2 - s^2/4)^{-1/2} D(\mathrm{d}r), \quad s > 0, \tag{4.27}$$

with mean $\mathrm{E}s = \mathrm{E}r^2/\mathrm{E}r$*, and the typical segment normal direction has distribution* R^v *which is related to* R *by* (3.43)*. Using the results from Chapter 3, we can express the variance of the VUR estimator as follows (cf. [65]). Using* (3.37)*, we get*

$$\begin{aligned} &\operatorname{var}(\hat{S}_V^{\mathrm{VUR}} \mid \xi) \\ &\quad = \frac{2\alpha^v}{(\beta_3^2 \nu_2(B_\rho)} \int (\mathcal{F}_{Q_\mathcal{V}^*}(w))^2 R^v(\mathrm{d}w) \int_0^\infty \zeta_2(t/\rho) \mathrm{E}\left((s-t)\mathbf{1}_{[s>t]}\right) \mathrm{d}t \end{aligned}$$

with function ζ_2 *from Exercise 3.23. The intensity* α^v *of the segment process* $\Phi \cap \mathcal{V}$ *fulfills* $\alpha^v \mathrm{E}s = L_A^v = \mathcal{G}_R(v) S_V$ *(cf.* (3.44)*) and*

$$\mathcal{G}_R(v) \int (\mathcal{F}_{Q_\mathcal{V}^*}(w))^2 R^v(\mathrm{d}w) = \int \frac{\mathcal{F}_{Q_\mathcal{V}^*}(u)^2}{|\sin \sphericalangle(u,v)|} R(\mathrm{d}u)$$

by Lemma 3.28. The mean w.r.t. vertical planes of the last expression is equal to $\mathcal{J}_R(\mathbf{v})$*. Further computations lead to*

$$\begin{aligned} \mathrm{E}\left((s-t)\mathbf{1}_{[s>t]}\right) &= \int_t^\infty (s-t) l(s) \mathrm{d}s \\ &= \frac{1}{4\mathrm{E}r} \int_{t/2}^\infty \int_t^{2r} (s-t) s (r^2 - s^2/4)^{-1/2} \,\mathrm{d}s \, D(\mathrm{d}r) \\ &= \frac{1}{\mathrm{E}r} \int_{t/2}^\infty \left(r^2 \arccos \frac{t}{2r} - \frac{t}{2} \sqrt{r^2 - \frac{t^2}{4}} \right) D(\mathrm{d}r) \\ &= \frac{1}{\mathrm{E}r} \mathrm{E}\left(r^2 \zeta_2(t/r)\right). \end{aligned}$$

This yields the final result

$$\mathrm{E}\operatorname{var}(\hat{S}_V^{\mathrm{VUR}} \mid \xi) = \frac{8 S_V}{\pi \rho^2} \mathcal{J}_R(\mathbf{v}) \int_0^\infty \zeta_2(t/\rho) \frac{\mathrm{E}(r^2 \zeta_2(t/r))}{\mathrm{E}r^2} \mathrm{d}t. \tag{4.28}$$

Note that if the disc radius r tends to infinity almost surely then the mean variance of the VUR estimator tends to

$$\frac{4S_V}{\pi^2\rho^2}\mathcal{J}_R(\mathbf{v})\int_0^\infty \zeta_2(t/\rho)\,\mathrm{d}t = \frac{64}{3\pi^2}\frac{S_V}{\rho}\mathcal{J}_R(\mathbf{v}),$$

(cf. Exercise 4.14), which agrees with formula (4.23) *for Poisson planes.*

EXAMPLE 4.9 *In the following example we consider a Poisson plane process Φ in $\mathbb{R}^3$ with the rose of directions R from the parametric family of Dimroth-Watson distribution on $\mathbb{S}^2$ with density* (3.55). *Under the above assumptions, consider four estimators of S_V which are applicable for R unknown. Their theoretical variances are obtained for the Dimroth-Watson distribution with vertical axis of anisotropy:*

a) estimator $\hat{S}_V$ (3.20) based on direct probes with $Q = U$ (IUR projections - equivalently measuring of surface areas);

b) $\hat{S}_V^{\mathrm{VUR}}$ - the vertical section estimator (4.9) with z axis as vertical axis;

c) $\hat{S}_V^{\mathrm{VSG}}$ - the vertical spatial grid estimator (4.25) with z axis as vertical axis;

d) $\hat{S}_V^{\mathrm{IUR}}$ - the IUR section estimator (4.4) with $Q = U$ in the section plane.

All estimators are applied with a ball $B = B_\rho$ as probe. Using (3.39) we get $\operatorname{var}\hat{S}_V = \frac{3}{5}\frac{S_V}{\rho}$ independently of R. Due to the rotation symmetry of R around the vertical axis, we have $\operatorname{var}\mathrm{E}\hat{S}_V^{\mathrm{VUR}} = \operatorname{var}\mathrm{E}\hat{S}_V^{\mathrm{VSG}} = 0$. Thus, using (4.23), *we get*

$$\operatorname{var}\hat{S}_V^{\mathrm{VUR}} = \frac{64}{3\pi^2}\frac{S_V}{\rho}\mathcal{J}_R(\mathbf{v}),$$

where

$$\mathcal{J}_R(\mathbf{v}) = \frac{1}{4\pi U_0(\kappa)}\int_0^{\pi/2}\psi(\theta)\exp(2\kappa\cos^2\theta)\sin\theta\mathrm{d}\theta.$$

The function $\mathcal{J}_R$ was evaluated by numerical integration. The variance of the VSG estimator was obtained by numerical integration as well, using the formula from Exercise 4.10.

The variance of $\hat{S}_V^{\mathrm{IUR}}$ consists of two summands, $\mathbf{E}\operatorname{var}\hat{S}_V^{\mathrm{IUR}} = \frac{64}{3\pi^3}\frac{S_V}{\rho}$ (see (4.22)) and $\operatorname{var}\mathrm{E}\hat{S}_V^{\mathrm{IUR}} = 4S_V^2\operatorname{var}\mathcal{G}_R(v)$ *by Proposition 4.3, where $\mathcal{G}_R(v) = \mathcal{G}_R(\theta_0)$ depends on the latitude θ_0 of v only and equals*

$$\mathcal{G}_R(\theta_0) = \frac{1}{\pi U_0(\kappa)}\int_0^{\pi/2}F(\theta,\theta_0)\exp\left(2\kappa\cos^2\theta\right)\sin\theta\mathrm{d}\theta$$

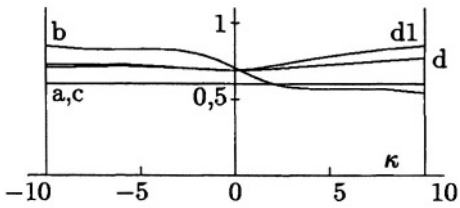

Figure 4.6. Graphs of the multiple of $\frac{S_V}{\rho}$ in variances of estimators a), b), c), d) of S_V in Example 4.9. In d), d1) the special cases $S_V\rho = 1$, $S_V\rho = 2$ are drawn, respectively.

Estimator	$\kappa = -\infty$	$\kappa = 0$	$\kappa = +\infty$
a)	0.6	0.6	0.6
b)	0.849	0.705	0.54
c)	0.606	0.602	0.6
d)	0.708	0.688	0.769
d1)	0.728	0.688	0.850

Table 4.2. Limit values of estimation variances in Example 4.9.

with

$$F(\theta, \theta_0) = \int_0^\pi \sqrt{1 - (\cos\varphi \sin\theta \sin\theta_0 + \cos\theta \cos\theta_0)^2}\, \mathrm{d}\varphi,$$

and

$$\operatorname{var} \mathcal{G}_R(\theta_0) = \frac{2}{\pi} \int_0^{\pi/2} (\mathcal{G}_R(\theta_0))^2 \sin\theta_0 \mathrm{d}\theta_0 - \frac{\pi}{4}.$$

The graphs of variances as a function of κ *are plotted in Fig. 4.6*

In Table 4.2, the limit values of the estimator variances for the cases a)-d1) shown in Fig. 4.6 for $\kappa = -\infty, 0, +\infty$ *are presented.*

It is not surprising that for $\kappa = +\infty$, $\hat{S}_V$ *has a smaller variance than* $\hat{S}_V^{\mathrm{VUR}}$, *cf. Exercises 4.15, 4.16. For roses R where nearly horizontal surfaces do not prevail the vertical spatial grid yields a substantial improvement in efficiency against a single vertical uniform random section and is almost as good as the complete information in a).*

EXERCISE 4.10 *Show that the difference between the variances of the VUR and VSG estimators is*

$$\operatorname{var} \mathrm{E}(\hat{S}_V^{\mathrm{VUR}} \mid \xi) - \operatorname{var} \mathrm{E}(\hat{S}_V^{\mathrm{VSG}} \mid \xi) = S_V^2 \mathrm{E}\left(\mathcal{F}_{RQ_\xi^*} - \mathcal{F}_{RQ_{\xi+\pi/2}^*}\right)^2$$

and *that the mean conditional variance of the VSG estimator fulfills*

$$\mathrm{E}\,\mathrm{var}\,(\hat{S}_V^{\mathrm{VSG}} \mid \xi) = \frac{1}{2}\mathrm{E}\,\mathrm{var}\,(\hat{S}_V^{\mathrm{VUR}} \mid \xi) + \frac{8}{\pi^2|B_\xi|^2}\mathrm{E}\,\mathrm{cov}\left(\Psi^{\xi}_{Q^*_\xi}(B_\xi), \Psi^{\xi+\pi/2}_{Q^*_{\xi+\pi/2}}(B_{\xi+\pi/2})\right).$$

EXERCISE 4.11 *Show that for a vertical plane* $\mathcal{V} = v^\perp$,

$$\mathcal{F}_{U_\mathcal{V}}(u) = |p_\mathcal{V} u|\mathcal{F}_{U_\mathcal{V}}(\pi_\mathcal{V} u) = |\sin \sphericalangle(u, v)|\beta_{d-1}$$

($p_\mathcal{V}$ denotes the orthogonal and $\pi_\mathcal{V}$ the spherical projections onto $\mathcal{V}$).

EXERCISE 4.12 *Using Exercises 3.33 and* (4.11), *prove formulas* (4.18) *and* (4.19).

EXERCISE 4.13 *Verify formula* (4.27) *for the typical segment length density of the planar section of a Poisson process of compact discs from Example 4.8. Hint: Express first the segment length conditional density under condition that the segment comes from a disc of given radius* r, *and then make the expectation over* r.

EXERCISE 4.14 *Using* (3.28), *show that*

$$\int_0^\infty \zeta_2(t)dt = \frac{8}{3\pi}.$$

EXERCISE 4.15 *In the situation of Example 4.9 show that for* $\kappa = +\infty$ *a single vertical test segment* p *of length* 2ρ *yields the estimator* $\hat{S}_V^{\mathrm{VL}} := P/2\rho$, *P being the number of intersections of* p *with* Φ, *with variance* $\mathrm{var}\,\hat{S}_V^{\mathrm{VL}} = S_V/2\rho$.

EXERCISE 4.16 *Using Corollary 3.41, show that the estimator* $\hat{S}_V^{\mathrm{VL}}$ *from Exercise 4.15 is UBUE.*

4.1.6 Cycloidal probes

The basic idea of VUR sampling design is that the projection measure with $Q = Q^*_\mathcal{V}$ (cf. (4.20)) is applied in the vertical sections ($\mathcal{V}$ denotes a vertical plane). It is well known [1] that, instead of intersecting the specimen with line grids of different orientations and mixing with respect to the distribution $Q^*_\mathcal{V}$, intersections with cycloidal systems can be applied. This follows formally from the following lemma.

LEMMA 4.17 *The measure* $Q^*_\mathcal{V}$ *is the tangent orientation distribution of a cycloid in the plane* $\mathcal{V}$ *given by parametic equations*

$$x = a(t - \sin t), \quad y = a(1 - \cos t), \quad t \in [0, 2\pi], \tag{4.29}$$

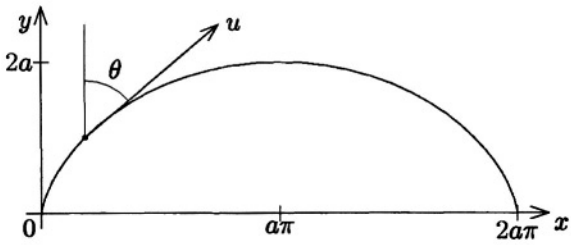

Figure 4.7. A MAJPV cycloid in the plane and its tangent angle θ.

$a > 0$.

Proof. The angle θ of the tangent to the cycloid (4.29) at t fulfills

$$\sin\theta = \sqrt{\frac{1-\cos t}{2}}, \quad \cos\theta = \cos\frac{t}{2}.$$

Since the length element is $\mathrm{d}s = a\sqrt{2(1-\cos t)}\mathrm{d}t$ we obtain $\sin\theta\mathrm{d}\theta \approx \mathrm{d}s$ as desired. □

REMARK 4.5. The cycloid in (4.29) has major axis perpendicular to the vertical axis; it will be denoted MAJPV. The MINPV cycloid will be the cycloid obtained from (4.29) using rotation by $\pi/2$ and its tangent direction distribution is $Q_{\mathcal{V}}(\mathrm{d}\theta) = \frac{1}{2}\cos\theta\mathrm{d}\theta$, θ being again the angle with the vertical axis.

We shall use the spherical coordinates on $\mathbb{S}^2$ as in the previous section. A vertical plane $\mathcal{V} = \mathcal{V}_\xi$ is parametrized by the longitude $\xi \in [-\pi, \pi)$ so that $\mathcal{V} = v^\perp$ and $v = (\pi/2, \xi)$ in spherical coordinates. We shall often write Q^*_ξ instead of $Q^*_{\mathcal{V}}$.

Let Ξ be a stationary random fibre system in $\mathbb{R}^3$ with length intensity L_V and a rose of directions R. The projection measure $\Psi^{\xi,t}_{Q^*_\xi}$ can alternatively be represented as the mean number of intersections of $\Xi^{v,t}$ with a MINPV cycloid. This follows from the following lemma.

LEMMA 4.18 *Let Z be a Borel $(\mathcal{H}^1, 1)$-rectifiable set in a vertical plane $\mathcal{V} = \mathcal{V}_\xi$ and let C denote the MINPV cycloid in $\mathcal{V}$. Then*

$$\mathcal{I}^1_{Q^*_\xi}(Z) = \frac{\pi}{2}\mathcal{H}^1(C)^{-1}\int_{\mathcal{V}} \mathcal{H}^0(Z \cap (C+z))\nu_2(\mathrm{d}z).$$

Proof. Applying Theorem 1.12, we get

$$\int_{\mathcal{V}} \mathcal{H}^0(Z\cap(C+z))\nu_2(\mathrm{d}z) = \int_Z\int_C [\mathrm{Tan}^1(Z,a), \mathrm{Tan}^1(C,b)]\mathcal{H}^1(\mathrm{d}b)\mathcal{H}^1(\mathrm{d}a).$$

We have

$$[\mathrm{Tan}^1(Z,a),\mathrm{Tan}^1(C,b)] = \sin \sphericalangle(\mathrm{Tan}^1(Z,a),\mathrm{Tan}^1(C,b))$$

and, hence, using the MAJPV cycloid $C^\perp$ (cycloid C rotated by $\pi/2$ in the vertical plane), we have

$$\begin{aligned}\int_C [\mathrm{Tan}^1(Z,a),\mathrm{Tan}^1(C,b)]\mathcal{H}^1(\mathrm{d}b) &= \int_{C^\perp} \cos \sphericalangle(\mathrm{Tan}^1(Z,a),\mathrm{Tan}^1(C^\perp,b))\mathcal{H}^1(\mathrm{d}b)\\ &= \mathcal{H}^1(C)\mathcal{F}_{Q^*_\xi}(\mathrm{Tan}^1(Z,a))\end{aligned}$$

by Lemma 4.17. But Proposition 3.1 yields

$$\int_Z \mathcal{F}_{Q^*_\xi}(\mathrm{Tan}^1(Z,a))\mathcal{H}^1(\mathrm{d}a) = \frac{2}{\pi}\mathcal{I}^1_{Q^*_\xi}(Z),$$

which completes the proof. □

COROLLARY 4.19 *For a stationary random fibre system* Ξ *in* $\mathbb{R}^3$, $\xi \in [-\pi,\pi)$, $t>0$ *and bounded Borel set* $B \subset \mathcal{V}_\xi$ *we have*

$$\Psi^{\xi,t}_{Q^*_\xi}(B) = \frac{\pi}{2}\mathcal{H}^1(C)\int_{\mathcal{V}_\xi} \mathcal{H}^0(\Xi^{\xi,t}\cap B\cap(C+z))\,\mathrm{d}z,$$

where $C \subset \mathcal{V}_\xi$ *is the MINPV cycloid.*

Proof. Apply Lemma 4.18 with $Z = \Xi^{\xi,t}\cap B$. □

If Ξ is a stationary random surface system in $\mathbb{R}^3$ the situation is analogous but attention must be paid to one difference. Here, in the general setting of a surface system in $\mathbb{R}^3$, the section $\Xi^\xi = \Xi\cap\mathcal{V}_\xi$ is considered as a *surface* system in the 2-dimensional space $\mathcal{V}_\xi$, i.e. again a random $\mathcal{H}^1$-set as in the fibre system case, but the rose of directions R^ξ is now the distribution of *normal* directions to Ξ^ξ and the projection measure $\Psi^\xi_{Q^*_\xi}$ must be considered with respect to this normal direction distribution. It follows that $\Psi^\xi_{Q^*_\xi}$ can now be expressed by means of intersections with a MAJPV cycloid, in contrast to the fibre system case.

COROLLARY 4.20 *For a stationary random surface system* Ξ *in* $\mathbb{R}^3$, $\xi \in [-\pi,\pi)$, $t>0$ *and bounded Borel set* $B \subset \mathcal{V}_\xi$ *we have*

$$\Psi^\xi_{Q^*_\xi}(B) = \frac{\pi}{2}\mathcal{H}^1(C)\int_{\mathcal{V}_\xi} \mathcal{H}^0(\Xi^{\xi,t}\cap B\cap(C+z))\,\mathrm{d}z,$$

where $C \subset \mathcal{V}_\xi$ *is the MAJPV cycloid* (4.29).

The formulas from Corollaries 4.19 and 4.20 are plugged in (4.9) to obtain unbiased intensity estimators. Further step is to approximate the integrals by sums so that unbiasedness remains valid. This will be proved in a self-contained design-based approach below to remind original papers on this topic.

4.2. Design-based approach

In this section the explanation is switched to the *design-based approach* to show examples how stereological estimators are designed for practice, see [118], [54], [29], [30]. In this approach, the structure (fibres, surfaces, volumes) is studied within a reference volume (material specimen, block of tissue, etc.), typically three-dimensional. The structure is considered fixed and the intensity (L_V, S_V, V_V) is defined as a ratio of the total quantity (length, surface area, volume) within the reference volume to its volume. The randomness enters in the problem of estimation by means of probes. The common point with the model-based approach is the choice of probe orientation. Stereological formulas (e.g. (4.3), (4.5)) obtained in both approaches are the same. The model-based approach is more restrictive because of the stationarity assumption. In Subsection 3.3, the relation between the total projection in a single direction and the number of intersections was explained. This principle (i.e. substitution of the total projection by the number of intersections) can be used for any distribution Q of projection orientations.

The observed structure ϕ will now be considered as a (deterministic) fibre or surface system, formally a $(\mathcal{H}^1, 1)$ or $(\mathcal{H}^2, 2)$-rectifiable set (cf. Subsection 3.1) contained in a bounded reference set $W \subset \mathbb{R}^3$ of positive volume. The length (surface) intensity is defined as $L_V = \mathcal{H}^1(\phi)/\nu_3(W)$ ($S_V = \mathcal{H}^2(\phi)/\nu_3(W)$, respectively) and the rose of directions R is the distribution of tangent directions of ϕ if ϕ is a fibre system and the distribution of normal directions if ϕ is a surface system.

The following construction shows the connection with the model-based approach. Assume that ϕ is a fibre system (the surface system case is analogous) and let T be a regular point lattice in $\mathbb{R}^3$ with fundamental region Δ of volume $\nu_3(\Delta) = \nu_3(W)$. Let Ξ be the stationary random $\mathcal{H}^1$-set $\bigcup_{z \in T}(\phi + z)$ translated by a uniform random shift from Δ. The length intensities L_V and rose of directions R of Ξ and ϕ are the same.

4.2.1 VUR sampling design

We restrict the explanation of the design-based stereology to an important special class of methods based on vertical uniform random sam-

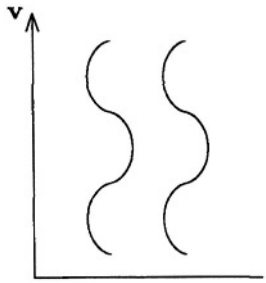

Figure 4.8. An example of a system of MINPV cycloids.

pling design. The idea of VUR sections was described by Baddeley [1], [4] for the intensity (S_V) estimation of surface systems in $\mathbb{R}^3$. Later, a method was described in [36] for the estimation of the length intensity of a fibre system in $\mathbb{R}^3$ from VUR projections. The properties of these design-based estimators were further investigated in [40] and [51]. We describe in the following the length intensity estimator in detail.

Let ϕ be a fibre system in W. It is usual to use regular cycloidal grids (see Fig. 4.8), i.e. sets $T_C = \bigcup_{z \in T}(C + z)$, where T is a regular point lattice in $\mathcal{V}$ of planar fundamental region Δ. The length density of the test system is $l = \frac{\mathcal{H}^1(C)}{\nu_2(\Delta)}$. In the following, saying "superimpose a cycloidal grid on $\mathcal{V}$" always means that the grid must have a uniform random position with respect to translations in the vertical plane. The VUR length intensity estimator can then be constructed as follows.

(i) Given the vertical direction $\mathbf{v} \in \mathbb{S}^2$ choose a horizontal direction $\xi \in \mathbb{S}^1(\mathbf{v}^\perp)$ uniformly randomly, consider the vertical plane $\mathcal{V}_\xi$.

(ii) Take a systematic random series of vertical slabs of thickness t parallel to $\mathcal{V}_\xi$ with a position of a slab front plane uniform random on an interval $[0, \tau]$ in $\mathcal{V}_\xi^\perp$ and $\tau > t > 0$ being the distance (shift) between front planes of neighbouring slabs.

(iii) Project the content of any of the vertical slabs within W on $\mathcal{V}_\xi$ and superimpose a cycloidal grid T_C of MINPV cycloids with length density l.

(iv) Count the total number I^c of intersections between projections of ϕ and test lines and put

$$\hat{L}_V^{\mathrm{VUR}} = \frac{2\tau}{tl\nu_3(W)} I^c. \tag{4.30}$$

PROPOSITION 4.5 (GOKHALE [36]) *Formula* (4.30) *presents an unbiased estimator of the length intensity* L_V. *For a fixed vertical plane we have*

$$\mathrm{E}(\hat{L}_V^{\mathrm{VUR}} \mid \xi) = 2L_V \mathcal{F}_{RQ_\xi^*}. \tag{4.31}$$

Proof. The proof is based on the translative formula in Theorem 1.12. Since the structure is deterministic, it must be assumed that the probes are shifted uniformly randomly. Let $\tilde{C}$ be the cycloidal cylinder $C \oplus [0, tv]$, see Fig. 4.9 (here v is, as usually, the horizontal unit vector with longitude ξ), let $\tilde{T}$ be the spatial point lattice $T \oplus \{i\tau : i \in \mathbb{Z}\}$ and, finally, let $\tilde{T}_{\tilde{C}}$ be the spatial grid of cycloidal cylinders $\bigcup_{z\in\tilde{T}}(z + \tilde{C})$. The number I^c corresponds then to the number of intersections of the structure with $\tilde{T}_{\tilde{C}}$, i.e.,

$$I^c = \mathcal{H}^0(\phi \cap \tilde{T}_{\tilde{C}}).$$

Since the grid is shifted randomly we can write for a fixed ξ

$$\mathrm{E}(I^c \mid \xi) = \frac{1}{\tau\nu_2(\Delta)} \int_{\mathbb{R}^3} \mathcal{H}^0(\phi \cap (\tilde{C} + z))\, \mathrm{d}z$$

and the last integral equals by Theorem 1.12

$$\int_\phi \int_{\tilde{C}} [\mathrm{Tan}^1(\phi, a), \mathrm{Tan}^2(\tilde{C}, b)] \mathcal{H}^2(\mathrm{d}b) \mathcal{H}^1(\mathrm{d}a).$$

Clearly $\mathrm{Tan}^2(\tilde{C}, b) = \mathrm{span}\{\mathrm{Tan}^1(C, b), v\}$ and, therefore,

$$[\mathrm{Tan}^1(\phi, a), \mathrm{Tan}^2(\tilde{C}, b)] = \sin \sphericalangle(\mathrm{Tan}^1(\phi, a), \mathrm{Tan}^1(C, b)).$$

As in the proof of Lemma 4.18, it follows from Lemma 4.17 that

$$\int_C \sin \sphericalangle(\mathrm{Tan}^1(\phi, a), \mathrm{Tan}^1(C, b)) \mathcal{H}^1(\mathrm{d}b) = \mathcal{H}^1(C) \mathcal{F}_{Q_\xi^*}(\mathrm{Tan}^1(\phi, a)).$$

Thus, we get

$$\mathrm{E}(I^c \mid \xi) = \frac{t}{\tau\nu_2(\Delta)} \mathcal{H}^1(C) \mathcal{H}^1(\phi) \mathcal{F}_{RQ_\xi^*}.$$

Since $\mathcal{H}^1(C) = \nu_2(\Delta)l$, (4.31) follows. The unbiasedness of $\hat{L}_d^{\mathrm{VUR}}$ is obtained as a consequence since $\mathrm{E}\mathcal{F}_{RQ_\xi^*} = \frac{1}{2}$ (see the proof of Theorem 4.2). □

REMARK 4.6. Note that the estimator (4.30) is based, in fact, on a version of the formula $L_V = 2P_A$ (see (4.3)). If we consider a section

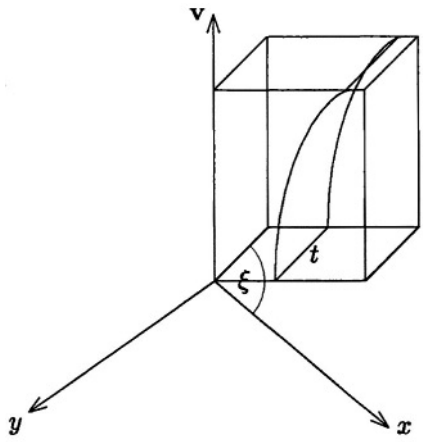

Figure 4.9. Projection of a MINPV cycloidal test cylinder

with the cycloidal cylinder system instead, we have $\hat{L}_V^{\mathrm{VUR}} = 2\frac{I^c}{A}$, where $A = \frac{tl\nu_3(W)}{\tau}$ is the mean intersection area of the testing surface with W.

If ϕ is a surface system in W, the procedure of surface intensity estimation is even a bit simpler. We choose again uniformly randomly a horizontal direction ξ, take a series of parallel sections of ϕ parallel with $\mathcal{V}_\xi$ and with distance τ, superimpose the MAJPV cycloidal grid in each section and count the total number of intersections I^c. Then, cf. [4],

$$\hat{S}_V^{\mathrm{VUR}} = \frac{2\tau}{l\nu_3(W)} I^c \tag{4.32}$$

is an unbiased estimator of the surface intensity S_V and the conditional mean for fixed ξ is given as in (4.31).

4.2.2 Further properties of intensity estimators

Besides estimation variances studied in Section 4.1 by means of projection measures, other simple properties of intensity estimators can be quantified. When using the estimator (4.30) in practice several orientations ξ of vertical slabs are used. It is of interest to know how many such orientations are necessary to obtain a reliable estimate. The following derivation enables us to make some conclusions in this direction. It is not important whether the model or design-based approach is used. We restrict ourselves to fibre systems but the corresponding results are true for surface systems as well, cf. [40].

The estimator $\hat{L}_V^{\mathrm{VUR}}$ in (4.30) is unbiased when a VUR probe is used. To describe the quality of the estimator from another standpoint than its

variance, we may consider the analogous estimator based on a sample of fixed vertical planes only. Given $\xi \in [-\pi, \pi)$, let $\hat{L}_V^{\xi}$ denote the estimator of type (4.30) based on the vertical plane $\mathcal{V}_\xi$ only (that means, instead of a VUR plane, a fixed vertical plane $\mathcal{V}_\xi$ is used). We have from (4.31)

$$\mathrm{E}\hat{L}_V^{\xi} = 2L_V \mathcal{F}_{RQ_\xi^*},$$

hence, the relative bias is

$$\frac{\mathrm{E}\hat{L}_V^{\xi} - L_V}{L_V} = 2\mathcal{F}_{RQ_\xi^*} - 1.$$

Remind that

$$\mathcal{F}_{RQ_\xi^*} = \int \mathcal{F}_{Q_\xi^*}(\theta, \varphi) R(\mathrm{d}(\theta, \varphi))$$

and the function

$$\mathcal{F}_{Q_\xi^*}(\theta, \varphi) = \mathcal{F}_{Q_0^*}(\theta, \varphi - \xi)$$

is given in (4.21).

Consider now m fixed horizontal directions $\xi_1, \ldots, \xi_m$. Then the estimator

$$\hat{L}_V^m = \frac{1}{m} \sum_{i=1}^{m} \hat{L}_V^{\xi_i}$$

is based on measurements in m given vertical planes. Its *relative bias* is

$$\frac{\mathrm{E}\hat{L}_V^m - L_V}{L_V} = \int g_m(\xi_1, \ldots, \xi_m; \theta, \varphi)\, R(\mathrm{d}(\theta, \varphi)),$$

where $g_m = 2f_m - 1$ and

$$f_m(\xi_1, \ldots, \xi_m; \theta, \varphi) = \frac{1}{m} \sum_{i=1}^{m} \mathcal{F}_{Q_{\xi_i}^*}(\theta, \varphi).$$

The worst bias will appear if the direction distribution R will be extremal, i.e., if the fibres are lines (segments) of a fixed orientation (θ_0, φ_0). Then

$$\frac{\mathrm{E}\hat{L}_V^m - L_V}{L_V} = g_m(\xi_1, \ldots, \xi_m; \theta_0, \varphi_0). \tag{4.33}$$

EXAMPLE 4.21 *Bounds for values of* $g_m(\{\xi_1, \ldots, \xi_m; \theta_0, \varphi_0)$ *were evaluated theoretically in the particular case when the* ξ_i*'s are taken systematically, i.e.*

$$\xi_i = \frac{2\pi}{m}(i-1),\ i = 1, 2, \ldots, m,$$

and in *the worst case* (4.33). *It holds*

$$x\frac{\cos x}{\sin x} - 1 \leq g_m \leq x \sin x - 1, \tag{4.34}$$

$x = \frac{\pi}{2m}$, m *odd. For* $m = 5$ *specially*

$$-0.03 \leq g_5(\xi_1, \ldots, \xi_5; \theta_0, \varphi_0) \leq 0.02$$

is valid for any direction of the line element (θ_0, φ_0). *For* $m = 3$ *the values of* g_3 *are scattered between*

$$-0.09 \leq g_3(\xi_1, \xi_2, \xi_3; \theta_0, \varphi_0) \leq 0.05.$$

We conclude that it is enough to use five systematic directions of vertical slabs to obtain an estimator with relative bias less than 3% in the worst case. Of course, if the fibre system is isotropic then a single direction of vertical slab may be enough to obtain reliable results and the same holds if it is anisotropic but has an axis of symmetry which should be chosen as the vertical axis.

EXERCISE 4.22 *An upper bound for the relative bias of* $\hat{L}_V^m$ *can be found as follows. From the definition of* $\mathcal{F}_Q$, *for any vertical plane* $\mathcal{V}$ *and unit vectors* $u, u' \in \mathbb{S}^2$ *we have*

$$|\mathcal{F}_{Q_\mathcal{V}^*}(u) - \mathcal{F}_{Q_\mathcal{V}^*}(u')| \leq \|p_\mathcal{V}(u - u')\|$$

(recall that $p_\mathcal{V}$ *is the orthogonal projection to* $\mathcal{V}$*). Hence, in spherical coordinates,*

$$|\mathcal{F}_{Q_\xi^*}(\theta, \varphi) - \mathcal{F}_{Q_{\xi'}^*}(\theta, \varphi)| \leq 2\left|\sin\frac{\xi - \xi'}{2}\right| \sin\theta$$

and, consequently,

$$\frac{1}{m}\left|\sum_{i=1}^{m} \mathcal{F}_{Q_{\xi_i}^*}(\theta, \varphi) - \sum_{i=1}^{m} \mathcal{F}_{Q_{\xi_i+\xi}^*}(\theta, \varphi)\right| \leq |\xi| \sin\theta.$$

Taking the mean value w.r.t. $\xi \in (0, \pi/m)$, *we obtain finally*

$$|g_m(\xi_1, \ldots, \xi_m; \theta, \varphi)| \leq \frac{\pi}{m} \sin\theta.$$

The constant factor can be decreased by taking finer estimates.

EXERCISE 4.23 *Using bounds* (4.34) *show that the convergence rate* m^{-2} *can be achieved for the relative bias* (4.33).

4.2.3 Estimation of average particle size

The particle size in $\mathbb{R}^3$ is an important parameter, which can be expressed in various ways, cf. Chapter 6. In stereology different size parameters and averaging procedures lead to different descriptors of average size of particle systems such as average mean width [25], volume-weighted mean volume [45], etc. In this subsection the review of VUR sampling designs is continued by showing that the average size of a finite system of convex particles can be estimated using VUR projections.

The *mean width* $\bar{b}(K) = \int_{\mathcal{L}_1} \text{length}(p_\ell K) U(\mathrm{d}\ell)$ of a convex particle K was mentioned already in formula (1.20), it holds $M(K) = \pi \bar{b}(K)$. For a fixed collection of particles we denote by $\bar{\bar{b}}$ the average mean width. In the following, a method based on vertical projections suggested in [39] is discussed. A practical procedure for estimating the average width of a finite collection of convex particles from the measurements performed on the projected images follows:

(i) Select the vertical axis given by the vertical direction $\mathbf{v}$ in $\mathbb{S}^2$. Choose a VUR plane $\mathcal{V}_\xi$. Enclose the specimen containing the collection of particles in a vertical slab of thickness t with faces parallel to $\mathcal{V}_\xi$.

(ii) Observe the total projection of the reference space onto the vertical plane $\mathcal{V}_\xi$. It is assumed that the projected images of all particles are observed in the total vertical projection.

(iii) Superimpose a grid containing uniformly spaced MINPV cycloids on the projected image, see Fig. 4.10. Let l denote the length density of the cycloidal grid.

(iv) Count the number of intersections I^c between the cycloids and the boundaries of the projected images of the convex particles. Repeat this step for several systematic random projection directions ξ all of which are perpendicular to the vertical axis. From these observations, evaluate the average value $\bar{I}^c$.

(v) Use the total vertical projections to determine the total number N_0 of particles in the projected image. Estimate $\bar{\bar{b}}$ by

$$\hat{\bar{b}} = \frac{\bar{I}^c}{2lN_0}. \tag{4.35}$$

THEOREM 4.24 *Formula* (4.35) *presents an unbiased estimator of average mean particle width* $\bar{\bar{b}}$.

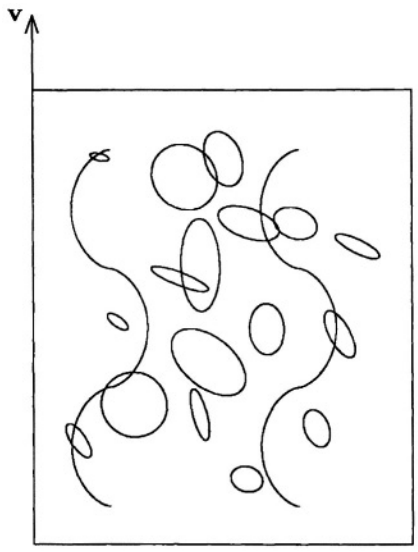

Figure 4.10. **A total vertical projection with superimposed cycloidal grid.**

Proof. Let a finite set of bounded convex particles be given. Since it is assumed that for each vertical plane the projections of all particles are completely accessible, the total number of particles is known and it is sufficient to consider the problem for a single convex particle K. For the mean width it holds

$$\bar{b}(K) = \int_{\mathbb{S}^2} b(K,u)\, U(\mathrm{d}u),$$

where $b(K,u)$ is the width of K in direction u (i.e., the length of the projection $p_u K$ of K onto a line of direction u). Using the decomposition of the uniform distribution U from Lemma 4.3, we get

$$\bar{b}(K) = \int_{\mathfrak{V}} \int_{\mathbb{S}^1(\mathcal{V})} b(K,u)\, Q^*_{\mathcal{V}}(\mathrm{d}u) U_{\mathbf{v}}(\mathrm{d}\mathcal{V})$$

(recall that $U_{\mathbf{v}}$ is the uniform distribution over the space $\mathfrak{V}$ of vertical planes). Further, note that for $u \in \mathbb{S}^1(\mathcal{V})$, the width of K in direction u is the same as the width of the projection $p_{\mathcal{V}}K$ of K on $\mathcal{V}$ in direction u, and this equals one half of the total projection of the boundary

$$b(K,u) = b(p_{\mathcal{V}}K, u) = \frac{1}{2}\mathrm{TP}_u(p_{\mathcal{V}}K).$$

Hence, referring to the definition of the integral-geometric measure (Subsection 3.1.1),

$$\int_{\mathbb{S}^1(\nu)} b(K,u)\, Q^*_\nu(\mathrm{d}u) = \frac{1}{\pi}\mathcal{I}^1_{Q^*_\nu}(\partial p_\nu K).$$

Applying now Lemma 4.18, we get

$$\begin{aligned}\int_{\mathbb{S}^1(\nu)} b(K,u)\, Q^*_\nu(\mathrm{d}u) &= \frac{1}{2}\mathcal{H}^1(C)\int_\nu \mathcal{H}^0(\partial p_\nu K \cap (C+z))\mathrm{d}z \\ &= \frac{1}{2}l\mathrm{E}\mathcal{H}^0(\partial p_\nu K \cap T_C) \\ &= \frac{l}{2}\mathrm{E}I^c,\end{aligned}$$

where T_C is the cycloidal grid of length intensity l and the mean value is understood w.r.t. random uniform grid translations. Now summing over the N_0 convex particles one obtains $\mathrm{E}I^c/l = 2\sum \bar{b}_1(K)$ and averaging over vertical planes $\mathcal{V}$ finally $\bar{\bar{b}} = \mathrm{E}I^c/2lN_0$. □

EXAMPLE 4.25 *Consider a single particle ϕ obtained by rotating a square around its diagonal of length s. Its mean width can be obtained as*

$$\bar{\bar{b}} = \frac{1}{2\pi}M(\phi), \quad M(\phi) = \lim_{\varepsilon\to 0} M(\phi_\varepsilon),$$

where $M(\cdot)$ is the integral mean curvature and $\phi_\varepsilon = \phi \oplus B_\varepsilon$ the dilation of ϕ by a ball of radius ε. After an easy calculation one obtains

$$\bar{\bar{b}} = s\left(\frac{1}{2} + \frac{\pi}{8}\right). \tag{4.36}$$

We study the properties of the above estimator in this simple case for a special choice of a cycloidal test system, see Fig. 4.11. To express the expectation and variance of I^c in (4.35), the function $P(y,z)$ was introduced in [50] as the number of intersections of the projected particle $\tilde{\phi}$ with the single cycloid

$$(y + 1 + \cos t, z + t - \sin t),\ t \in (0, 2\pi).$$

The graph of the function $P(y,z)$ is plotted in Fig. 4.12.

It holds $I^c = \int\int P(y,z)\,\mathrm{d}z\,\mathrm{d}y$. More difficult is the evaluation of the variance of the estimator which depends on the geometry of the sampling design. To get this one should evaluate for each pair $(i,j) \in \mathbb{Z}^2$ the function

$$M_{i,j}(y,z) = P(y,z)P\left(y + i\frac{s}{4},\, z + j\frac{s}{2}\right).$$

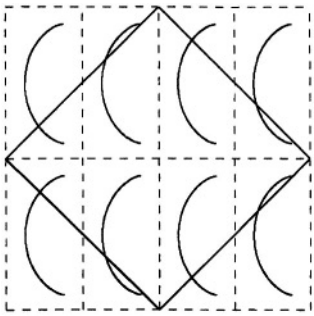

Figure 4.11. Projection $\tilde{\phi}$ of a particle ϕ from Example 4.25, embedded in a square. The square is divided into cells each of which contains one cycloid. The cycloidal test system is randomly shifted.

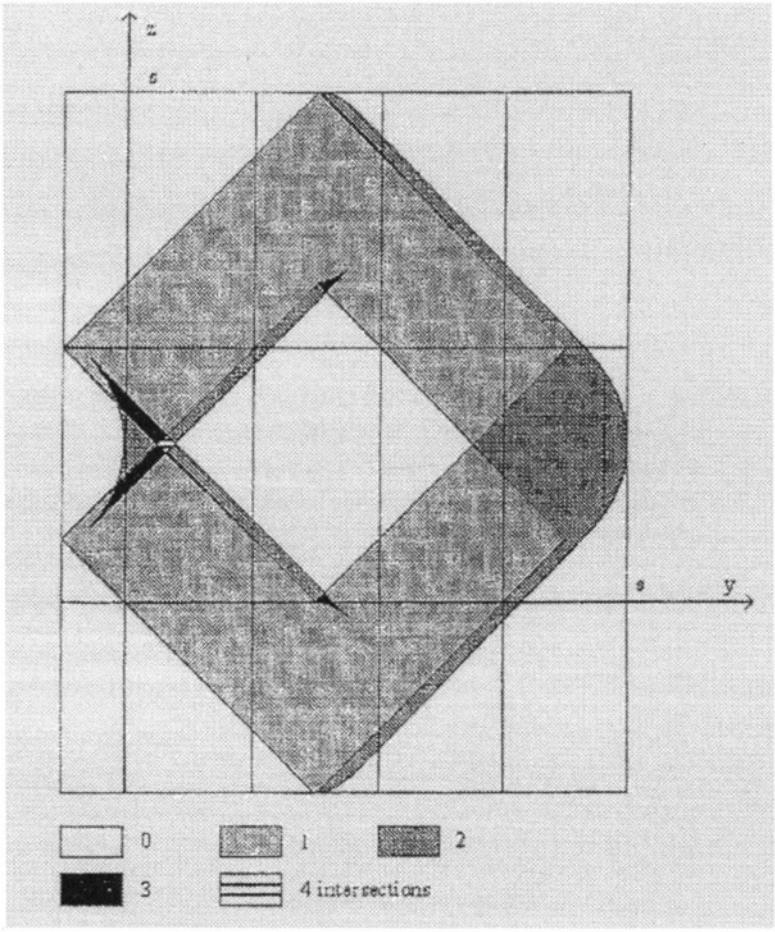

Figure 4.12. The function $P(y,z)$ of the number of intersections between the projection $\tilde{\phi}$ of the particle and a test cycloid.

Then (see [50])

$$EI_c^2 = \frac{8}{s^2}\sum_{i,j} S(i,j), \quad S(i,j) = \int\int M_{i,j}(y,z)\mathrm{d}y\mathrm{d}z.$$

Generally, if the particles are such that any projection may not have an infinite number of intersections with the test cycloid, then the estimator (4.35) has a finite variance.

EXERCISE 4.26 *Verify formula* $\bar{\bar{b}} = \frac{\bar{N}_A}{\bar{N}_V}$, *where* $\nu_3(W)\bar{N}_A$ *is the mean number of particles hit by an IUR grid of unit distance parallel planes. Hint: In the design-based setting, note that*

$$\nu_3(W)\bar{N}_A = \sum_i \int V_0(K_i \cap F)\,\mu_2(\mathrm{d}F),$$

where (K_i) *is the collection of particles, and apply the Crofton formula (Theorem 1.14).*

EXERCISE 4.27 *Verify formula* (4.36).

4.2.4 Estimation of integral mixed surface curvature

Since $\mathcal{H}^2$-rectifiability does not guarantee the existence of curvatures at almost all points of a surface in $\mathbb{R}^3$, we shall consider a more special model in this subsection. Consider a system $\phi = \phi_1 \cup \cdots \cup \phi_n$ of C^2-smooth surfaces $\phi_1, \ldots, \phi_n$ in a bounded reference volume $W \subset \mathbb{R}^3$, and assume that the intersection $\phi_i \cap \phi_j$ has $\mathcal{H}^2$-measure zero for any $i \neq j$. Then, $\mathcal{H}^2$-almost all points of ϕ belong to exactly one smooth surface ϕ_i, and the principal normal curvatures k_1 and k_2 are defined at this point, as well as the mean and Gauss curvatures $H = \frac{k_1+k_2}{2}$, $K = k_1k_2$, respectively (see (1.15)). In the present study, another characteristic MC called mixed curvature and defined by

$$\mathrm{MC} = \frac{1}{4}(3k_1^2 + 2k_1k_2 + 3k_2^2) \tag{4.37}$$

is of interest.

Integrating the Gauss or mean curvatures over the whole surface system one obtains integral characteristics which are multiples of certain intrinsic volumes (Minkowski quermassintegrals) in the case of boundaries of convex bodies (see [97] or cf. Section 1.1.4). The integral mixed curvature MC_V of ϕ per unit volume of the reference space W is defined as follows:

$$\mathrm{MC}_V = \frac{1}{4\nu_3(W)}\int_\phi \mathrm{MC}(x)\mathcal{H}^2(\mathrm{d}x). \tag{4.38}$$

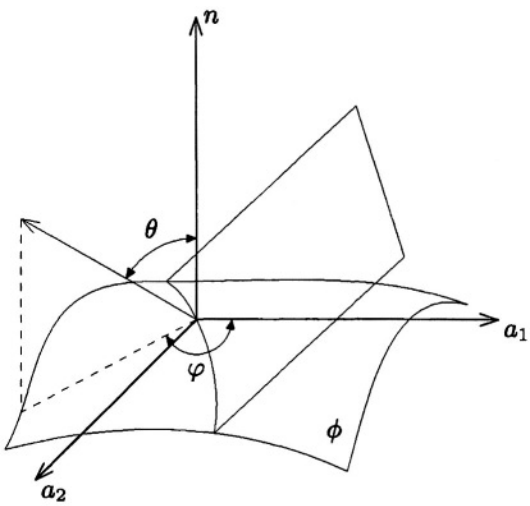

Figure 4.13. Intersection of a surface ϕ with the plane. The orthonormal frame $\{a_1, a_2, n\}$ is chosen so that a_1, a_2 is the principal direction corresponding to k_1, k_2, respectively, and n is the normal direction to the surface. The curvature k of the section curve in ϕ at the origin is given by formula (4.39).

The integral mixed curvature MC_V is an integral characteristic of global curvature, it is always nonnegative.

The problem of stereological estimation of global curvature characteristics has been studied since the eighties. It appeared that stereological formulas are available for MC_V rather than for other characteristics.

Intersection of a smooth surface with a plane is a smooth curve provided that the tangent plane at any intersection point is not parallel with the sectioning plane (it is a well-known fact that this property is satisfied for almost all planes w.r.t. the integral-geometric measure on the space of all planes). The curvature k of this curve at a point $x \in \phi$ (defined as the reciprocal of the curvature radius) is related to the principal curvatures k_1, k_2 by means of the Euler-Meusnier formula in differential geometry [97]:

$$k = \frac{k_1 \sin^2 \varphi + k_2 \cos^2 \varphi}{\sin \theta}, \tag{4.39}$$

where θ is the angle formed by the normals to the section plane and to the surface ϕ at x, and φ is the angle formed by the tangent to the section curve at x and the principal direction of ϕ at x corresponding to the second principal curvature k_2, see Fig. 4.13.

This equation plays the main role in the derivation of stereological formulas for MC_V.

Given a plane L in $\mathbb{R}^3$, let T_L denote a uniformly randomly shifted grid of equidistant planes parallel to L, with distance $s > 0$ of neighbour planes. The next result was proved in [77] (i) and in [38] (ii).

THEOREM 4.28 *(i) For an IUR plane L it holds*

$$\mathrm{MC}_V = \frac{4s}{\pi\nu_3(W)}\mathrm{E}\int_{\phi\cap T_L} k^2(x)\,\mathcal{H}^1(\mathrm{d}x). \tag{4.40}$$

(ii) If V is a VUR plane then

$$\mathrm{MC}_V = \frac{2s}{\nu_3(W)}\mathrm{E}\int_{\phi\cap T_\mathcal{V}} k^2(x)\sin\gamma(x)\,\mathcal{H}^1(\mathrm{d}x), \tag{4.41}$$

where $\gamma(x)$ is the angle of the tangent to $\phi\cap\mathcal{V}$ at x with the vertical axis $\mathbf{v}$. If T_ℓ is a regular grid of vertical lines in $T_\mathcal{V}$, with distance t of neighbour lines in one vertical plane, then

$$\mathrm{MC}_V = \frac{2st}{\nu_3(W)}\mathrm{E}\sum_{x\in T_\ell\cap\phi} k^2(x). \tag{4.42}$$

Proof. Note that ϕ is obviously a $(\mathcal{H}^2, 2)$-rectifiable set. Let L be a fixed 2-dimensional plane in $\mathbb{R}^3$ with unit normal vector $u \perp L$. Applying the coarea formula (Theorem 1.6) for the mapping $g : x \mapsto \langle x, u\rangle, x \in \phi$, we obtain

$$\int_{L^\perp}\int_{\phi\cap(L+y)} k^2(x)\,\mathcal{H}^1(\mathrm{d}x)\,\mathrm{d}y = \int_\phi \sin\theta(x)k^2(x)\,\mathcal{H}^2(\mathrm{d}x),$$

since $\sin\theta(x)$ is the one-dimensional Jacobian of g at x. Using (4.39), the last integral is equal to

$$\int_\phi \frac{k_1^2\sin^4\varphi + 2k_1k_2\sin^2\varphi\cos^2\varphi + k_2^2\cos^4\varphi}{\sin\theta}\mathrm{d}\mathcal{H}^2.$$

Note that φ is the longitude and θ the latitude of the unit normal to L in the orthonormal frame $\{a_1, a_2, n\}$ formed by the principal direction a_1, a_2 and normal direction n of ϕ at x. Thus, after averaging w.r.t. IUR

planes L, we get

$$\begin{aligned}
&\mathrm{E}\int_{\phi\cap T_L} k^2\,\mathrm{d}\mathcal{H}^1\\
&\quad= s^{-1}\mathrm{E}\int_{L^\perp}\int_{\phi\cap(L+y)} k^2(x)\,\mathcal{H}^1(\mathrm{d}x)\,\mathrm{d}y\\
&\quad= \frac{1}{4s}\int_0^{2\pi}\int_\phi \left(k_1^2\sin^4\varphi + 2k_1k_2\sin^2\varphi\cos^2\varphi + k_2^2\cos^4\varphi\right)\mathrm{d}\mathcal{H}^2\,\mathrm{d}\varphi\\
&\quad= \frac{\pi}{16s}\int_\phi \left(3k_1^2 + 2k_1k_2 + 3k_2^2\right)\mathrm{d}\mathcal{H}^2\\
&\quad= \frac{\pi\nu_3(W)}{4s}\mathrm{MC}_V,
\end{aligned}$$

which proves (4.40). For a fixed vertical plane $\mathcal{V}$, we obtain analogously

$$\begin{aligned}
&\int_{\mathcal{V}^\perp}\int_{\phi\cap(\mathcal{V}+y)} k^2(x)\sin\gamma(x)\,\mathcal{H}^1(\mathrm{d}x)\,\mathrm{d}y\\
&\quad= \int_\phi \sin\theta(x)\sin\gamma(x)k^2(x)\,\mathcal{H}^2(\mathrm{d}x)\\
&\quad= \int_\phi \frac{k_1^2\sin^4\varphi + 2k_1k_2\sin^2\varphi\cos^2\varphi + k_2^2\cos^4\varphi}{\sin\theta}\sin\gamma\,\mathrm{d}\mathcal{H}^2.
\end{aligned}$$

The averaging should be maintained now over vertical planes only. Let $0 \le \xi < 2\pi$ be the angle formed by $\mathcal{V}$ and a fixed horizontal direction. Writing down the relation between ξ and φ, one gets the transformation

$$\mathrm{d}\xi = \frac{\sin\theta}{\sin\gamma}\mathrm{d}\varphi,$$

hence

$$\begin{aligned}
&\mathrm{E}\int_{\phi\cap T_\mathcal{V}} k^2\sin\gamma\,\mathrm{d}\mathcal{H}^1\\
&\quad= s^{-1}\mathrm{E}\int_{\mathcal{V}^\perp}\int_{\phi\cap(\mathcal{V}+y)} k^2(x)\,\mathcal{H}^1(\mathrm{d}x)\,\mathrm{d}y\\
&\quad= \frac{1}{2\pi s}\int_0^{2\pi}\int_\phi \left(k_1^2\sin^4\varphi + 2k_1k_2\sin^2\varphi\cos^2\varphi + k_2^2\cos^4\varphi\right)\mathrm{d}\mathcal{H}^2\,\mathrm{d}\varphi\\
&\quad= \frac{1}{8s}\int_\phi \left(3k_1^2 + 2k_1k_2 + 3k_2^2\right)\mathrm{d}\mathcal{H}^2\\
&\quad= \frac{\nu_3(W)}{2s}\mathrm{MC}_V,
\end{aligned}$$

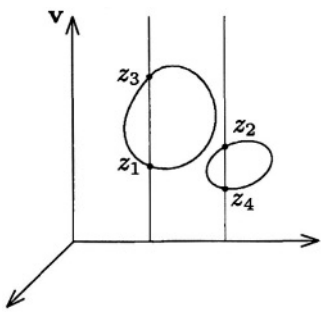

Figure 4.14. Sections of two particle surfaces by a vertical test plane. A test system of parallel vertical test lines is superimposed in the vertical plane and intersections between test lines and particle section boundaries are registered. Planar curvatures $k(i)$ at the registered points t_i are measured and involved in formula (4.43).

which verifies (4.41). Equation (4.42) follows from (4.41), see Exercise 4.31. □

Formula (4.41), and especially (4.42), is more straightforward for practical use. All what is needed is to choose a VUR plane $\mathcal{V}$, put a systematic random grid of vertical lines on it and measure curvatures $k(i)$ at intersection points z_i, see Fig. 4.14. The procedure can be repeated for a series of shifts of the vertical plane. Then

$$\widehat{\mathrm{MC}}_V = \frac{2}{\mathrm{E}l} \sum_i k(i)^2 \tag{4.43}$$

is an unbiased estimator of MC_V, where $\mathrm{E}l$ is the mean (w.r.t. shifts) total length l of all test lines in W. Note that if t is the spacing of the test lines in a vertical plane and s the spacing of the vertical planes then $\mathrm{E}l = \nu_3(W)/st$, hence (4.43) agrees with (4.42). The properties of the estimator (4.43) will further be investigated.

Since arbitrarily large curvatures may appear in the planar section the present stereological relation is ill-posed and the estimator (4.43) may have poor statistical properties. To make the point whether the variance $\mathrm{var}\,\widehat{\mathrm{MC}}_V$ is finite or infinite, the following general principle can be used.

THEOREM 4.29 *Let f be an integrable non-negative function on $\mathbb{R}^2$ with bounded support* $\mathrm{supp}\, f$ *and* $\|f\|_2 = \sqrt{\int f^2(z)\mathrm{d}z}$ *its L^2-norm. Let T be a rectangular lattice of points with uniform random location in $\mathbb{R}^2$ with horizontal, vertical spacings being s, t, respectively. Consider an*

unbiased estimator of the integral $I = \int f(x)\mathrm{d}x$:

$$\hat{I} = st \sum_{z \in T} f(z).$$

Then $\mathbf{var}\, \hat{I} < \infty$ *if and only if* $\|f\|_2 < \infty$.

Proof. The supremum of the covariogram $g(h) = \int f(z)f(z+h)\,\mathrm{d}z$ lies at the origin, $g(0) = \|f\|_2$ and g is nonnegative with bounded support. It holds

$$E\hat{I}^2 = st \sum_{k,l \in \mathbb{Z}^2} g(ks, lt)$$

(see [68]). Thus, the mean square of $\hat{I}$ can be sandwiched as follows:

$$stg(0) \leq E\hat{I}^2 \leq stCg(0),$$

where C is the finite number of lattice points hitting the bounded support $\operatorname{supp} g$, and the result follows. □

EXAMPLE 4.30 *Let* ϕ *be a sphere with radius R. At each point of the sphere, the principal curvatures are* $k_1 = k_2 = R^{-1}$ *and* $3k_1^2 + 2k_1k_2 + 3k_2^2 = 8R^{-2}$. *Therefore*

$$\mathrm{MC} = \frac{1}{4}\int_{\phi} \frac{8}{R^2}\mathrm{d}\mathcal{H}^2 = \frac{1}{4}\frac{8}{R^2}4\pi R^2 = 8\pi.$$

Using Theorem 4.29 it is easily shown that the variance of the estimator (4.43) is infinite in this case. The function f *is specially the squared linear curvature*

$$k^2(x,y) = \frac{2}{R^2 - y^2}, \quad x^2 + y^2 < R^2,$$

$k^2(x,y) = 0$ *otherwise. Then the relevant integral for* $\|f\|_2$ *is*

$$\int_0^R \int_0^{\sqrt{R^2-x^2}} \frac{\mathrm{d}y}{(R^2 - y^2)^2}\,\mathrm{d}x = \infty$$

and by Theorem 4.29 it follows that $\mathbf{var}\,\widehat{\mathrm{MC}}$ *is infinite.*

In the application below (Subsection 4.2.6), a natural modification of the estimator is considered for the case of MC_V estimation of a surface system of convex particles. It consists in omitting the particle sections (caps) with diameter less than $\varepsilon > 0$. Formula (4.43) is used for a sample of remaining larger caps. This naturally arises when using an image

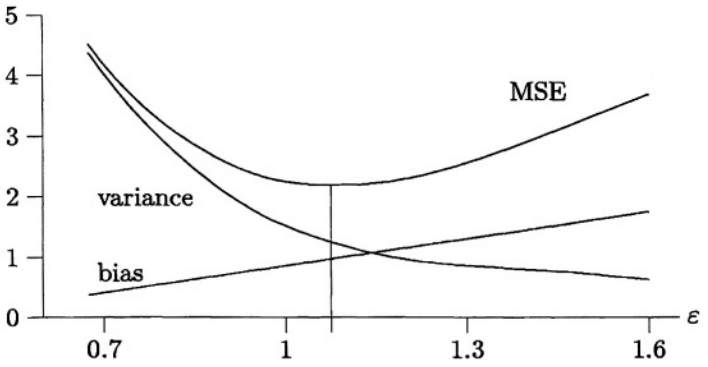

Figure 4.15. The analysis of the modified estimator of MC_V for the sphere with radius $R = 1$ embedded in a cube with edge length 2. The bias, variance and mean square error $\text{MSE} = \text{var}\,\widehat{\text{MC}} + (\text{bias}\,\widehat{\text{MC}})^2$ are plotted on a limited range of ε.

analyser for measurement, but problems with discrete curvature measurement are even more delicate. The modified estimator is biased but it has a finite variance. If ϕ is as in Example 4.30 the relevant integral for $\|f\|_2$ when using Theorem 4.29 is

$$\int_0^R \int_0^{\min(\sqrt{R^2-x^2},\, R-\delta)} \frac{\mathrm{d}y}{(R^2-y^2)^2}\mathrm{d}x < \infty,$$

where $\delta = R - \frac{1}{2}\sqrt{4R^2-\varepsilon^2}$. In Fig. 4.15 it is demonstrated how with increasing ε the variance decreases while the bias increases.

EXERCISE 4.31 *Using the coarea formula, show that for a* $(\mathcal{H}^1, 1)$*-rectifiable set* A *and line* ℓ *in the plane, and for any Lipschitz function* g *defined on* A,

$$\int_A g(a)\sin\sphericalangle(\mathrm{Tan}^1(A,a),\ell)\,\mathcal{H}^1(\mathrm{d}a) = \int_{\ell^\perp} \sum_{a\in A\cap(\ell+y)} g(a)\mathrm{d}y.$$

4.2.5 Gradient structures

In materials science engineers frequently deal with *gradient structures* which appear as a result of operations like rolling etc. The resulting structure is inhomogeneous in a single direction and homogeneous in the remaining two coordinates. In fact the pattern from soil science studied in Subsection 3.2.3 belongs to the class of gradient structures, too. In stereology of gradient structures the use of vertical probes naturally leads to choosing the vertical axis as the direction of inhomogeneity.

In the model-based approach, consider a non-stationary surface system Ξ in $\mathbb{R}^3$ with intensity $S_V(z)$ depending on the last coordinate z of

(x, y, z). This means rigorously that the intensity of the induced random measure has density $S_V(z)$ which depends on the last coordinate only, i.e.,

$$\mathrm{E}\mathcal{H}^2(\Xi \cap B) = \int_B S_V(z)\,\mathrm{d}x\,\mathrm{d}y\,\mathrm{d}z$$

for any Borel set $B \subset \mathbb{R}^3$. The rose of normal directions $R(z;\cdot)$ is then defined for any height z (it is the distribution of the normal to the surface at a typical point of the surface with last coordinate equal to z). We shall assume additionally that the process is rotationally symmetric around the vertical axis z. Hahn and Stoyan [46] suggested an intensity estimator using only horizontal test lines in vertical planes. Let $\mathcal{V}$ be a vertical plane, ℓ a horizontal line segment in $\mathcal{V}$ of length l and height $z-z_0$, and $\alpha_1, \ldots, \alpha_n$ the angles formed by the test segment ℓ and section fibres $\mathcal{V} \cap \Xi$. If the roses of directions satisfy $R(z_0; \{\mathbf{v}\}) = 0$ for all z_0 ($\mathbf{v}$ is the vertical direction) then

$$\hat{S}_V(z_0) = \frac{1}{l} \sum_{i=1}^{n} (\alpha_i + \cot \alpha_i)$$

is an unbiased estimator of $S_V(z_0)$. Due to the cotangens in the formula, the estimator variance is infinite and a possible modification of the estimation is discussed in [46].

As another example (in the design-based approach) let us consider the integral mixed curvature MC_V for a smooth surface system ϕ in $\mathbb{R}^3$ as in Subsection 4.2.4. Its gradient version is the function

$$\mathrm{MC}_V(z) = \frac{1}{4\nu_2(W \cap H_z)} \int_{\phi \cap H_z} (3k_1^2 + 2k_1k_2 + 3k_2^2)\,\mathrm{d}\mathcal{H}^1,$$

where z belongs to the projection of W to the vertical axis and H_z is a plane perpendicular to vertical axis on level z. Estimator (4.43) of the global characteristic MC_V cannot be used to estimate $\mathrm{MC}_V(z)$ for one particular value of z since there a vertical test line need not (and typically does not) intersect the structure in H_z. Nevertheless, a kernel estimator may be used:

$$\widehat{\mathrm{MC}}_V(z) = \frac{2}{mh} \sum_{i=1}^{n} k^2(z_i) \mathrm{Ke}\left(\frac{z - z_i}{h}\right), \tag{4.44}$$

where m is the number of vertical test lines in VUR planes hitting W, Ke is a unimodal kernel function satisfying $\int \mathrm{Ke}(z)\mathrm{d}z = 1$, and h is a bandwidth; its choice is recommended in the statistical literature [105].

Formula (4.44) can be justified in the following way. Let the range of variable z be an interval $[a, b]$ and suppose that W is a (generalized) cylinder along the vertical axis (so that the intersection of W with a vertical line is either empty or a horizontal translate of the projection of W on the vertical axis). Then integrating (4.44) over this range we obtain

$$\lim_{h\to 0_+} \frac{1}{b-a} \int_a^b \widehat{\mathrm{MC}}_V(z)\mathrm{d}z = \frac{2}{(b-a)m} \sum_i k^2(z_i) \qquad (4.45)$$

and since $l = (b-a)m$ is the (constant) total length of test lines between H_a and H_b, the right hand side of (4.45) coincides with estimator (4.43) of the global integral mixed curvature of Φ intersected with the horizontal slab $a \le z \le b$ and, hence its expectation is $\int_a^b \mathrm{MC}_V(z)\mathrm{d}z$.

The implementation of formula (4.44) is as follows. For a VUR section, the test system from Fig. 4.13 is used and the z coordinate z_i of each intersection point is registered together with the planar curvature $k_i = k(z_i)$. For any coordinate z, formula (4.44) can then be used for the evaluation of $\widehat{\mathrm{MC}}_V(z)$.

4.2.6 Microstructure of enamel coatings

A simple but instructive example of the microstructural evaluation of $\widehat{\mathrm{MC}}_V(z)$ in a gradient structure presents the bubble structure of enamel coatings.

Enamel coatings are widely used for the corrosion protection of metals. An important property of an enamel coating is their bubble structure, which develops as a result of gas evolution during firing. The bubble structure affects the corrosion properties of the coating in two ways: first the presence of large bubbles, the diameter of which is comparable to the coating thickness, deteriorates the coating since thin bubble walls are broken easily; secondly uniformly distributed small bubbles are desirable since they reduce the tendency towards fishscaling and support elasticity.

Stereological methods can be used to describe the parameters of bubbles. In [8] the longitudinal sections were used to estimate the number and size distribution of bubbles for various enamel coatings. In [12] the transverse sections of enamels to study the gradient character of the enamel microstructure are used. The parameter MC_V itself is important even if it cummulates the properties of number and size (since bubbles are almost spherical). In practice this parameter is combined with detection of large bubbles which can be done using the X-ray defectoscopy. Conditionally that big bubbles are not present, large values of MC_V are desirable corresponding to sufficiently rich amount of small bubbles. Small MC_V values generally imply bad enamel properties, ei-

ther corresponding to lack of bubbles or to the presence of large bubbles. Interesting may be also the shape of function $\mathbf{MC}_V(z)$ as the following practical example demonstrates.

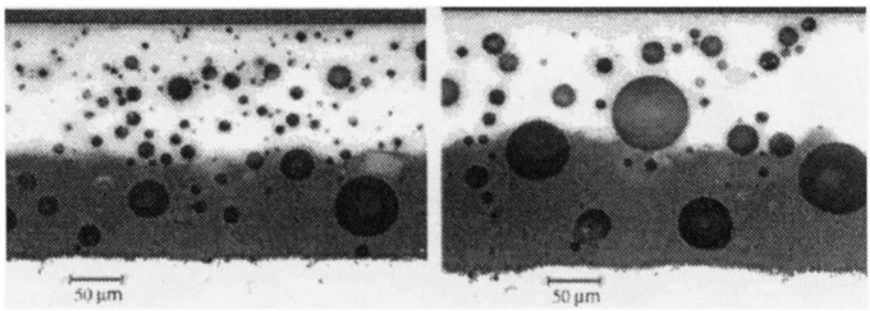

Figure 4.16. Transverse sections of enamel coatings A (left) and B (right), magnification 200×. The grey layer corresponds to the ground-coat enamel, it was separated from the steel sheet. The thickness of this layer is about 0.11 mm (specimen A) and 0.13 mm (specimen B). The top white layer corresponds to the titanium enamel, its thickness is 0.16 mm in both cases. In the expression $\mathrm{MC}_V(d)$, the value $d = 0$ corresponds to the enamel surface and $d = 0.16$ to the boundary between both layers. That means vertical axis of the sampling method coincides with vertical direction (in opposite orientation) in the figure.

To illustrate the use of the procedure suggested in Subsection 4.2.5, two specimens of a two-layer enamel were chosen, see [8], for the material specification and production. In Fig. 4.16 samples from transverse sections are presented.

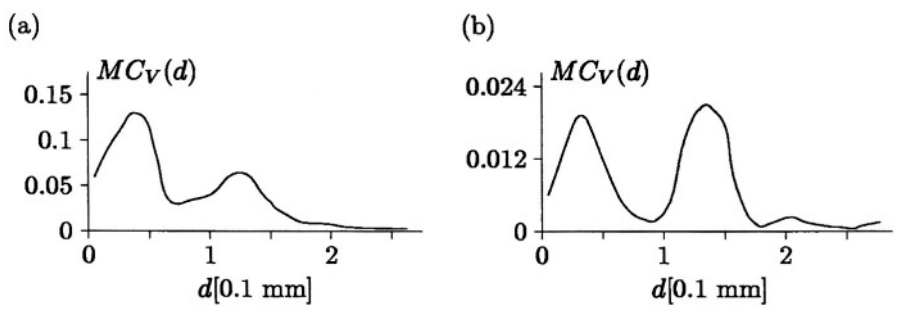

Figure 4.17. Graphs of $\mathrm{MC}_V(d)$ (a), (b) estimated by (4.44) for microstructure in Fig. 4.16 A, B, respectively.

Numerical results are presented in Fig. 4.17 for specimens A, B corresponding to microstructures in Fig. 4.16. Samples which present VUR sections were covered by a systematic random grid of test lines and the intersections with bubble section profiles registered. The problem of es-

timation of linear curvature k is discussed in [18], here we simply put $k = 1/r$, where r is the radius of circular profile. In the evaluation of (4.44) the kernel function

$$\mathrm{Ke}(z) = \begin{cases} 3(1 - z^2)/4, & z \in [-1, 1], \\ 0 & \text{elsewhere,} \end{cases}$$

was used. In the resulting graphs of estimated $\mathrm{MC}_V(d)$ (Fig. 4.17), d corresponds to the depth from enamel surface. The reliability of the results depends on the number of samples measured but still the following conclusions are evident: The magnitude of $\mathrm{MC}_V(d)$ differs: for specimen A it is about six times greater than for specimen B, that means enamel A has better physical properties. The ground-coat layer (range $d > 0.16$ mm) has worse properties (especially for specimen A) than the top layer (range $z \in [0, 0.16]$). A bimodal character of the curve is apparent for both specimens A and B.

Chapter 5

FIBRE AND SURFACE ANISOTROPY

5.1. Introduction

Consider a stationary random set Ξ in $\mathbb{R}^d$. We say that Ξ is *isotropic* if its distribution is invariant under rotations in $\mathbb{R}^d$. Note that an isotropic particle process in the sense of Definition 2.40 induces as union set an isotropic random set.

Any stationary random set that differs from isotropic is called *anisotropic*. Anisotropy is thus a rather broad notion. We shall consider in this chapter mainly random fibre and surface systems. Their rose of tangent (normal) direction, see Definition 3.6, is an anisotropy measure; if the model is isotropic, then clearly R equals the uniform distribution U.

On the other hand, the uniformness of the rose of tangent (normal) directions does not imply "complete" isotropy of the random fibre or surface system; consider as example a union of small circles in the plane arranged in horizontal rows. Such an anisotropy is due to the spatial displacement of particles. It was formalized and studied e.g. in [108].

A well-known stereological inverse problem (formulated in [49]) relates the rose of directions to the rose of intersections between the process and a test system. In its simplest form it goes back to the Buffon needle problem published in 1777. The *rose of intersections* $P_L(u)$ of a random fibre (surface) system is defined as the intensity of intersections of the random structure with a hyperplane of normal direction u (line of direction u, respectively). Of course, grids of parallel hyperplanes (lines) are used in practice.

Given the observed numbers of intersections (in the individual directions), the aim is to estimate the rose of directions. There are several approaches to the solution of the corresponding theoretical integral equa-

tion. Analytical solutions are usually very unstable and lead to various difficulties. The most promising seems to be the approach which makes use of an analogy from convex geometry relating the support function of a zonoid to its generating measure. We review *estimators of the rose of directions* separately in the planar and spatial case, since the background is qualitatively different. The main aim is to describe chosen statistical properties of the estimators and to compare different methods and models. Various test systems are investigated and demonstrating examples added.

Besides of random fibre and surface systems, we shall consider in the last section also full-dimensional random sets of certain types for which the distribution of outer normal direction over the boundary can be introduced. This distribution will be called *orientation-dependent rose of directions* and some estimation approaches will be outlined.

5.2. Analytical approach

As a basic model in the planar case, consider a stationary fibre system Ξ in $\mathbb{R}^2$ (i.e., a random $\mathcal{H}^1$-set, see Subsection 3.1) with induced random measure

$$\Psi(\cdot) = \mathcal{H}^1(\Xi \cap \cdot).$$

The random set Ξ is often realized as a union set of a stationary planar fibre process Φ (as in Chapter 3, under a fibre process we understand an $\mathcal{H}^1$-process). A realization of Ξ is an $\mathcal{H}^1$-rectifiable set by definition. For any realization ϕ of Ξ, the tangent direction $\mathbf{Tan}^1(\phi, x)$ is well defined at $\mathcal{H}^1$ -almost all $x \in \phi$. We shall denote $\mathbf{Tan}^1(\phi, x)$ for brevity by $w_\phi(x)$ or only $w(x)$.

As in the previous chapters, L_A will denote the length intensity (mean length per unit area) of Ξ and R the rose of directions (distribution of $w(x)$ at a typical point of Ξ). Recall that in the planar case, R is an even distribution on the unit circle $\mathbb{S}^1$. It is often more convenient to work with angles than with unit vectors. Consider the mapping assigning to each $u \in \mathbb{S}^1$ the angle $\alpha \in (0, \pi]$ such that $u = \pm e^{i\alpha}$, and let $\bar{R}$ denote the image of R under this mapping. Then, $\bar{R}$ is the rose of directions represented on the interval $(0, \pi]$.

5.2.1 Intersection with x_1-axis in $\mathbb{R}^2$

First a general stereological relation in $\mathbb{R}^2$ is derived, cf. [73]. From the Campbell theorem (2.29) for weighted measures, it follows for an arbitrary nonnegative measurable function f on $\mathbb{R}^2 \times (0, \pi]$ that

$$\mathrm{E} \int_{\mathbb{R}^2} f(x, w(x)) \Psi(\mathrm{d}x) = L_A \int_{\mathbb{R}^2} \int_{(0,\pi]} f(x, \alpha) \bar{R}(\mathrm{d}\alpha) \mathrm{d}x. \qquad (5.1)$$

LEMMA 5.1 *Let ϕ be an $\mathcal{H}^1$-rectifiable set in $\mathbb{R}^2$ and $g : \mathbb{R}^2 \to \mathbb{R}$ a nonnegative measurable function. Then*

$$\int \sum_{x_1:(x_1,x_2)\in\phi} g(x_1,x_2)\nu_1(\mathrm{d}x_2) = \int_\phi g(x)\sin w(x)\mathcal{H}^1(\mathrm{d}x), \tag{5.2}$$

where $x = (x_1, x_2) \in \mathbb{R}^2$.

For the proof, see Exercise 5.1.

THEOREM 5.2 *Let Ξ be a stationary random $\mathcal{H}^1$-set in $\mathbb{R}^2$ and $f : \mathbb{R} \times (0,\pi] \to \mathbb{R}$ a nonnegative measurable function. Then, for the intersection of Ξ with the x_1-axis it holds*

$$\mathrm{E}\sum_{x_1:(x_1,0)\in\Xi} f(x_1, w(x_1,0)) = L_A \int\int f(x_1,\alpha)\sin\alpha\bar{R}(\mathrm{d}\alpha)\mathrm{d}x_1. \tag{5.3}$$

Proof. Let $g : \mathbb{R} \to \mathbb{R}_+$ be a nonnegative measurable function with $\int g(t)\mathrm{d}t = 1$. Using (5.1), (5.2) and the stationarity we obtain

$$\begin{aligned} L_A \int\int\int g(x_2) f(x_1,\alpha)\sin\alpha\bar{R}(\mathrm{d}\alpha)\nu_2(\mathrm{d}x) &= \mathrm{E}\int\int g(x_2) f(x_1, w(x))\sin w(x)\Psi(\mathrm{d}x) \\ &= \mathrm{E}\int \sum_{x_1:(x_1,x_2)\in\Xi} g(x_2) f(x_1, w(x_1,x_2))\nu_1(\mathrm{d}x_2) \\ &= \mathrm{E}\int g(x_2)\mathrm{d}x_2 \sum_{x_1:(x_1,0)\in\Xi} f(x_1, w(x_1,0)). \end{aligned}$$

□

The intersection of Ξ with x_1-axis forms a stationary point process, we shall denote its intensity by P_L. Let $\bar{R}_1$ denote the distribution of the fibre tangent direction $w(x)$ at a typical intersection point (considered again as a probability distribution on $(0,\pi]$). Using special forms of f in Theorem 5.2, relations are obtained between the fibre process and the induced structure on the test line (here the x_1-axis).

COROLLARY 5.3 *For any $\beta \in (0,\pi]$ we have*

$$P_L\,\bar{R}_1((0,\beta]) = L_A \int_{(0,\beta]} \sin\alpha\bar{R}(\mathrm{d}\alpha); \tag{5.4}$$

consequently

$$\bar{R}_1((0,\beta]) = \frac{\int_{(0,\beta]} \sin\alpha \bar{R}(\mathrm{d}\alpha)}{\int_{(0,\pi]} \sin\alpha \bar{R}(\mathrm{d}\alpha)}, \tag{5.5}$$

if $\bar{R}(\{0\}) < 1$.

Proof. Setting $f(x_1,\alpha) = \mathbf{1}_{[0,l]}(x_1)\mathbf{1}_{(0,\beta]}(\alpha)$ in (5.3) one obtains (5.4). Using (5.4) twice for the values β and the limit value $\beta = \pi$, (5.5) is concluded. □

EXAMPLE 5.4 *If* $\bar{R}(\{0\}) = 0$ *one can get* L_A *and* $\bar{R}$ *from* P_L *and* $\bar{R}_1$ *(the latter pair of quantities can be estimated from the observation in the neighbourhood of a linear section). From (5.4) it follows*

$$\bar{R}([0,\beta)) = \frac{P_L}{L_A} \int_{(0,\beta]} (\sin\alpha)^{-1} \bar{R}_1(\mathrm{d}\alpha)$$

and for $\beta = \pi$ *in particular*

$$L_A = P_L \int_{(0,\pi]} (\sin\alpha)^{-1} \bar{R}_1(\mathrm{d}\alpha).$$

REMARK 5.1. Note that the limit value of (5.4) for $\beta = \pi$ yields the well-known formula

$$P_L = L_A \int \sin\alpha \bar{R}(\mathrm{d}\alpha) \tag{5.6}$$

which corresponds to the frequent case that the information on intersection angles is not available.

EXERCISE 5.5 *Prove Lemma 5.1. Hint: Apply the coarea formula (Theorem 1.6) for the second coordinate projection restricted to X, with Jacobian* $x \mapsto \sin w(x)$.

5.2.2 Relating roses of directions and intersections

Let Ξ be a stationary random $\mathcal{H}^1$-set in $\mathbb{R}^2$ as in the previous subsection. Let $P_L(\beta)$, $\beta \in (0,\pi]$, be the rose of intersections, i.e. the mean number of points of $\Xi \cap l(\beta)$ per unit length with a test straight line $l(\beta)$ with normal direction $(\cos\beta, \sin\beta)$. The basic integral equation relating the rose of directions of Ξ to its rose of intersections is obtained by a simple generalization of (5.6). Consider $(0,\pi]$ with addition modulo π. The addition may be interpreted as rotation of straight lines around origin in the plane.

Considering a rotation by β, we get from (5.6)

$$P_L(\beta) = L_A \mathcal{F}_R(\beta), \tag{5.7}$$

where

$$\mathcal{F}_R(\beta) = \int_{[0,\pi)} |\cos(\beta - \alpha)| \, \bar{R}(\mathrm{d}\alpha)$$

is the cosine transform (cf. (3.6)). Equivalently, we can write

$$P_L(u) = L_A \mathcal{F}_R(u), \tag{5.8}$$

where the cosine transform is

$$\mathcal{F}_R(u) = \int_{\mathbb{S}^1} |\langle u, v \rangle| R(\mathrm{d}v), \tag{5.9}$$

if we consider R as distribution on $\mathbb{S}^1$ and the test line is parametrized by its unit normal vector u.

Relations analogous to (5.8) hold in $\mathbb{R}^3$ as well. Let Ξ be a stationary random $\mathcal{H}^1$-set in $\mathbb{R}^3$ with length intensity L_V and rose of directions R (distribution of the tangent direction at a typical point, considered as an even distribution on the unit sphere $\mathbb{S}^2$). Let the test system be a plane or its subset and let $P_A(u)$ be the intensity of the stationary point process obtained by intersecting Ξ with a test plane of normal direction $u \in \mathbb{S}^2$. Then we have

$$P_A(u) = L_V \int_{\mathbb{S}^2} |\langle u, v \rangle| R(\mathrm{d}v) = L_V \mathcal{F}_R(u). \tag{5.10}$$

By the obvious duality between fibres and surfaces, a stationary random $\mathcal{H}^2$-set (induced usually by a stationary random surface system) in $\mathbb{R}^3$ of intensity S_V (mean surface area per unit volume) and rose of (normal) directions R (distribution of the normal direction at a typical point) induces on a test line of direction $u \in \mathbb{S}^2$ a stationary point process with intensity $P_L(u)$ and again,

$$P_L(u) = S_V \int_{\mathbb{S}^2} |\langle u, v \rangle| R(\mathrm{d}v) = S_V \mathcal{F}_R(u). \tag{5.11}$$

In fact, equations (5.10) and (5.11) hold for fibre and surface systems in any dimension d, if the integration domain is changed to $\mathbb{S}^{d-1}$.

Let λ stand for the length or surface intensity. Integrating (5.10) or (5.11) with respect to the uniform distribution U over $\mathbb{S}^{d-1}$, we obtain

$$P_L := \int P_L(u) U(\mathrm{d}u) = \lambda \mathcal{F}_{RU} = \lambda \beta_d$$

(see (3.4) for the constant β_d). Thus, even for an unknown rose of directions R it is possible to estimate the intensity λ, e.g. by considering an average of observations $P_L(u_j)$ with unit vectors u_j spread over $\mathbb{S}^{d-1}$. We shall not deal with the intensity estimation which was the main scope of the previous chapters. Therefore, in the following, the problem of estimating R can be considered to be equivalent to the problem of estimating λR.

EXERCISE 5.6 *Verify* (5.10) *and* (5.11) *by using the coarea formula (Theorem 1.6) lor the projection onto the line spanned by* u *or hyperplane perpendicular to* u, *respectively.*

EXERCISE 5.7 *Show the following generalization of* (5.8)*: The mean number of intersections of a stationary planar fibre system* Ξ *with a curve of length* ℓ *and normal direction distribution* Q *is* $L_A \ell \mathcal{F}_{RQ}$.

5.2.3 Estimation of the rose of directions

Several methods based on formula (5.8) in the plane have been suggested for the estimation of the rose of directions of a planar fibre system, cf. [49], [27], [71], [59], [94], [11]. The aim is to estimate R given estimates η_j of $P_L(\beta_j)$, $\beta_j \in (0, \pi]$, $j = 1, \dots, n$, where η_j is the observed number of intersections per unit length of the test probe of orientation β_j. This was done basically in three ways.

First, if a continuous probability density ρ of $\bar{R}$ exists we can differentiate (5.7) to obtain

$$P_L''(\beta + \frac{\pi}{2}) + P_L(\beta + \frac{\pi}{2}) = 2L_A \rho(\beta) \tag{5.12}$$

(see [109, §9.3.2]), which yields an explicit solution. This is in practice hardly tractable since the second derivative P_L'' has to be evaluated from discrete data. However, the formula is useful when a parametric model for R is available, cf. [27].

Another natural approach to the solution of (5.7) is the *Fourier analysis.* Hilliard [49] showed that for the Fourier images

$$\mathfrak{F}R(k) = \int_0^\pi \mathrm{e}^{2ik\alpha} R(\mathrm{d}\alpha), \quad k = \dots, -1, 0, 1, \dots, \tag{5.13}$$

and $\mathfrak{F}P_L(k) = \int_0^\pi P_L(\alpha)\mathrm{e}^{2ik\alpha}\mathrm{d}\alpha$, it holds

$$\mathfrak{F}R(k) = \frac{1}{2L_A}(-1)^{k-1}(4k^2 - 1)\mathfrak{F}P_L(k), \quad k = \dots, -1, 0, 1, \dots. \tag{5.14}$$

However, when estimating $\mathfrak{F}P_L(k)$ from the data and using (5.14) for the estimation of $\mathfrak{F}R$, the variances of $\mathfrak{F}R(k)$ may tend to infinity.

Another approach is based on convex geometry and will be described in a separate section.

EXAMPLE 5.8 *Consider the fibre system with four test lines of equal length 1 and normal orientations* $\beta_i = (2i+1)\pi/4$, $i = 0,1,2,3$, *respectively (Fig. 5.1). The intersection counts measured are* $\eta_i = 6,3,7,7$ *for* $i = 0,1,2,3$, *respectively. First, a parametric approach is used for the estimation of the rose of directions. Using a cardioidal model [95] for* ρ*:*

$$\rho(\alpha) = \frac{1}{\pi}(1 - k\cos 2(\alpha - \alpha_0)), \tag{5.15}$$

we obtain from (5.12)

$$P_L(\beta) = \frac{2L_A}{\pi}\left(1 - \frac{k}{3}\cos 2(\beta - \alpha_0)\right), 0 \le \beta < \pi. \tag{5.16}$$

Using the least squares method, a fitted curve is obtained for $P_L(\beta)$, *see Fig. 5.2 (a), with estimated parameters* $k = 1.08$, $\alpha_0 = 38^o$, $L_A = 9.03$. *Since* $k > 1$ *the model is in fact unsatisfactory (the density* ρ *of the rose of directions should be nonnegative). Still this estimator is plotted in Fig. 5.2 (b), negative loops along the orientation* $\frac{3\pi}{4}$ *are not observed because they are very small. The presence of negative values is a common problem of analytical estimators (also those based on Fourier expansions).*

Consider further the three-dimensional situation. Because of similarity of integral equations (5.10), (5.11) for fibre and surface systems in $\mathbb{R}^3$, we restrict ourselves to the case of a stationary fibre system Ξ. The problem is again to estimate the rose of directions R given a sample of test directions $u_1, \ldots, u_k \in \mathbb{S}^2$ and estimates $\eta_i = n_i/A$, where n_i is the number of intersections of Ξ with a planar test probe of area A and normal orientation u_i. Similarly to the planar case and leaving aside the procedure based on convex geometry, there are basically two other approaches to the solution.

First, a parametric approach means that a parametric type of the distribution on the sphere is suggested and the parameters estimated from the data on intersection counts. In [21], the axial *Dimroth- Watson* distribution (3.54) was used and the parameter $\kappa \in \mathbb{R}$ is estimated using maximum likelihood techniques.

Secondly, an inversion formula to (5.10) is available ([49], [72]) using *spherical harmonics.* It is based on the fact that spherical harmonics are eigenfunctions of the cosine transform. Kanatani [59] approximates η_i by a finite series of even spherical harmonics and the inverse is then

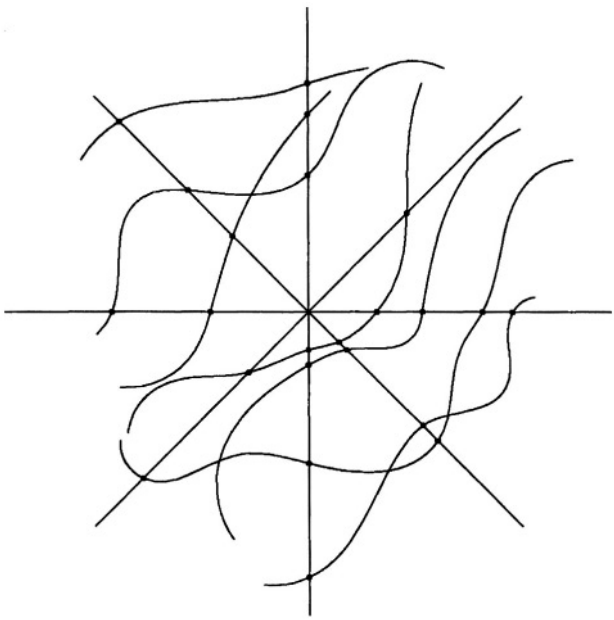

Figure 5.1. A fibre system intersected by a system of test lines of unit lengths.

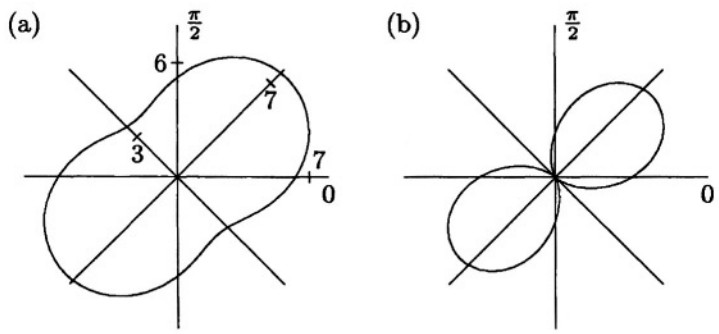

Figure 5.2. (a) Polar plot of intersection counts η_i from Fig. 5.1 and the rose of intersections fitted by means of the cardioidal model. (b) Polar plot of the rose of directions evaluated from (a) using the cardioidal model.

evaluated directly. An explicit inverse formula from [72] says

$$\rho(v) = \frac{1}{L_V} \sum_{n=0}^{\infty} \frac{4n+1}{c_n} \int_{\mathbb{S}^2} P_A(u) Q_{2n}(\langle u, v \rangle) U(\mathrm{d}u), \tag{5.17}$$

where Q_m is the *Legendre polynomial* of order m and ρ the probability density of R (with respect to U). The constants c_n are

$$c_n = \frac{(-1)^{n+1}}{4n^2-1} \frac{1 \cdot 3 \cdot 5 \cdot \ldots \cdot (2n-1)}{2 \cdot 4 \cdot 6 \cdot \ldots \cdot (2n-2)}, \quad n = 0, 1, \ldots.$$

To conclude, analytical solutions of the inverse problem (5.8) in both two and three dimensions may lead to estimators of the rose of directions which are not nonnegative densities. Typically these methods are not useful for sharp or multimodal anisotropies.

EXERCISE 5.9 *Differentiating* (5.7), *derive formula* (5.12).

EXERCISE 5.10 *Derive formula* (5.14). *Hint: Write down the definition of* $\mathfrak{F}P_L(k)$, *insert* (5.7) *and use Fubini theorem.*

5.3. Convex geometry approach

In this section, the notions of convex geometry introduced in Subsection 1.1.2 will be used, namely the support function, zonoid and zonotope. Recall (1.8) that a zonoid is a (centrally symmetric) convex body Z in $\mathbb{R}^d$ with support function

$$h(Z, u) = \int_{\mathbb{S}^{d-1}} |\langle u, v \rangle| \mu(\mathrm{d}v), \tag{5.18}$$

where μ is its generating measure (an even measure on $\mathbb{S}^{d-1}$).

Consider now a stationary fibre (surface) system Ξ in $\mathbb{R}^d$. Due to formula (5.10), the rose of intersections $P_A(u)$ $(P_L(u))$ is the support function of the zonoid with generation measure λR, where λ is the length (surface) intensity and R the rose of directions of Ξ, respectively. This idea was observed by Matheron [69] and the corresponding zonoid Z associated with R was called *Steiner compact.* Because of the uniqueness of the generating measure of zonoids, the association is unique. The problem is, as before, to estimate (in atomic form) the generating measure μ or its normalized version R (rose of directions) from discrete data η_i, $i = 1, \ldots, n$, interpreted as the support function values $h(Z_n, u_i)$ of a zonotope Z_n estimating Z in (1.8).

Let η_i be estimations of the rose of intersection $P_L(u_i)$ at given directions $u_1, \ldots, u_n \in \mathbb{S}^1$. The construction of the zonotope from the measurement data (η_i) is simple in $\mathbb{R}^2$. It is sufficient to set

$$\hat{Z} = \bigcap_{i=1}^{n} \{x \in \mathbb{R}^2;\ \langle x, u \rangle \leq \eta_i\}; \tag{5.19}$$

this is clearly a zonotope (as every centred polygon in $\mathbb{R}^2$), and it fulfills $h(\hat{Z}, u_i) = \eta_i$, $i = 1, \dots k$. The situation is more complicated in $\mathbb{R}^3$, where the centrally symmetric convex body (5.19) need not be a zonotope. Here the method is based on the following existence result due to Campi, Goodey and Weil:

THEOREM 5.11 ([16]) *For a zonoid $Z \subset \mathbb{R}^d$ and unit vectors $u_1, \dots, u_k$ there always exists a zonotope Z_k which is the Minkowski sum of at most k segments and fulfills*

$$h(Z, \pm u_1) = h(Z_k, \pm u_1), \dots, h(Z, \pm u_k) = h(Z_k, \pm u_k). \tag{5.20}$$

To find a zonotope in $\mathbb{R}^3$ fitting the given measurement data, an optimization procedure based on the constructive proof of Theorem 5.11 was suggested in [16]. A further substantial step forwards in this direction was made by Kiderlen [61].

If a zonotope Z_k satisfying (5.20) is found, its generating measure of the type (1.9) yields after normalization to a probability measure the desired estimator R_k of the rose of directions R. Let $\mathcal{M}$ denote the cone of all (nonnegative) Borel finite measures on $\mathbb{S}^{d-1}$. The d_H-convergence on $\mathcal{K}'$ is equivalent to the weak convergence on $\mathcal{M}$ with respect to the transformation (1.8) (cf. [61]). Since the weak convergence on $\mathcal{M}$ is metrized by the Prohorov metric, a natural way to describe theoretically the quality of the estimator is by means of the Prohorov distance between R_k and R.

DEFINITION 5.12 *Let R,T be two finite Borel measures on a Polish space X. The Prohorov distance of R and T is defined as*

$$r(T, R) = \inf\{\varepsilon > 0 : R(C) \le T(C^\varepsilon) + \varepsilon,\ T(C) \le R(C^\varepsilon) + \varepsilon \text{ for all closed } C \subset X\}, \tag{5.21}$$

where $C^\varepsilon = C \oplus B_\varepsilon$.

If both R and T are probability measures, we can write equivalently

$$r(T, R) = \inf\{\varepsilon > 0 : T(C) \le R(C^\varepsilon) + \varepsilon \text{ for all closed } C \subset X\}. \tag{5.22}$$

Under a further restriction that the probability measure T is discrete with a finite support, the following reduction to finitely many conditions is possible. It holds

$$r(T, R) = \inf\{\varepsilon > 0 : T(C) \le R(C^\varepsilon) + \varepsilon \text{ for all } C \subset \operatorname{supp} T\}. \tag{5.23}$$

This enables to compute the Prohorov distance approximately with an arbitrary precision using discrete steps of ε, cf. [11].

The estimation of R by means of the Steiner compact will be treated separately for the planar and spatial cases in the following subsections.

EXERCISE 5.13 *Verify the equivalence of* (5.21) *and* (5.23) *for probability measures R, T.*

5.3.1 Steiner compact in $\mathbb{R}^2$

The relation (5.18) between an even finite measure μ on $\mathbb{S}^1$ and its associated zonoid Z has a direct consequence of geometrical nature. Given $u \in \mathbb{S}^1$, let $p_Z(u)$ denote the support line of Z of normal direction u,

$$p_Z(u) = \{x \in \mathbb{R}^2 : \langle x, u\rangle = \max_{y \in Z} \langle y, u\rangle\},$$

and let $T_Z(u)$ be the intersection point of $p_Z(u)$ with Z if it is unique; if $Z \cap p_Z(u)$ is a line segment we let $T_Z(u)$ be its endpoint with respect to the anti-clockwise orientation of the boundary ∂Z of Z. If x, y are two points of ∂Z, the length of the arc of ∂Z from x to y in the anti-clockwise direction will be denoted by $l_Z(x, y)$. The following result is a consequence of the unique correspondence between zonoids and their generating measures, see [69].

THEOREM 5.14 *An even finite Borel measure μ on $\mathbb{S}^1$ and its associated zonoid Z determined by* (5.18) *fulfill*

$$\mu((u, v]) = \frac{1}{4} l_Z(T_Z(u*), T_Z(v*)), \quad u, v \in \mathbb{S}^1,$$

where $(u, v]$ denotes the half-closed arc on $\mathbb{S}^1$ passing from u to v in the anti-clockwise direction, and $u*$ denotes the unit vector obtained by rotating $u \in \mathbb{S}^1$ by the angle $\frac{\pi}{2}$ in the anti-clockwise direction.

For the proof, see Exercise 5.19

Consequently, the proportional length (per unit area) of fibres with tangents within an interval of directions is the same as the proportional length of the boundary ∂Z bounded by the pair of equally oriented tangents.

For a stationary fibre system Ξ and the zonoid (Steiner compact) Z associated with the rose of directions R of Ξ, it holds by (5.18)

$$h(Z, u) = L_A \mathcal{F}_R(u), \quad u \in \mathbb{S}^1,$$

i.e. comparing with (5.8),

$$h(Z, u) = P_L(u), \quad u \in \mathbb{S}^1. \tag{5.24}$$

A graphical method of estimation of the rose of directions by means of its related Steiner compact set was suggested in [94]. Let

$$p_i = \eta_i = \frac{N_i}{l} \tag{5.25}$$

be the estimators of the support function values at directions (axial) $u_i \in \mathbb{S}^1$, $i = 1, \ldots, n$, where N_i is the number of intersections of the studied fibre system with a test segment of length l and normal direction u_i. Set $u_{i+n} = -u_i$, $i = 1, \ldots, n$, and extend the p_i's n-periodically to be defined for all $i \in \mathbb{Z}$. Then by (5.19), the convex polygon ($2n$-gon)

$$Z_n = \{x : \langle x, u_i \rangle \leq p_i,\ i = 1, \ldots, 2n\} \tag{5.26}$$

provides a basis to the estimation of the Steiner compact Z related to R. The measure μ_n corresponding to Z_n according to Theorem 5.14 is

$$\mu_n = \sum_{i=1}^{2n} h_i \delta_{u_i}, \tag{5.27}$$

where h_i are the lengths of edges of the polygon Z_n. More precisely, the edge of outer normal direction u_i has length h_i. In fact Z_n may have less edges than $2n$ if $h_i = 0$ for some i.

The edge lengths h_i can be computed from the p_i's as follows. Let β_i be the angle corresponding to p_i, i.e., $u_i = (\cos\beta_i, \sin\beta_i)$, and assume that the directions are ordered so that $0 < \beta_1 < \cdots < \beta_n \leq \pi$ and $\beta_{i+kn} = \beta_i + k\pi$ for $1 \leq i \leq n$ and $k \in \mathbb{Z}$. Then we have (cf. [11])

$$h_i = \left(\min_{j<i} \frac{p_i \cos(\beta_j - \beta_i) - p_j}{\sin(\beta_j - \beta_i)} - \max_{j>i} \frac{p_i \cos(\beta_j - \beta_i) - p_j}{\sin(\beta_j - \beta_i)} \right)_+, \tag{5.28}$$

$i = 1, \ldots, n$, where $a_+ = \max\{a, 0\}$ is the positive part of the number a. Finally, after normalization

$$h_i' = \frac{h_i}{\sum_{i=1}^{2n} h_i}, \tag{5.29}$$

we obtain the desired estimator R_n of the rose of directions R:

$$R_n = \sum_{i=1}^{2n} h_i' \delta_{u_i}. \tag{5.30}$$

The d_H-convergence of Z_n is investigated in [94]. It appears that the estimator (5.30) itself need not be consistent due to the fact that one

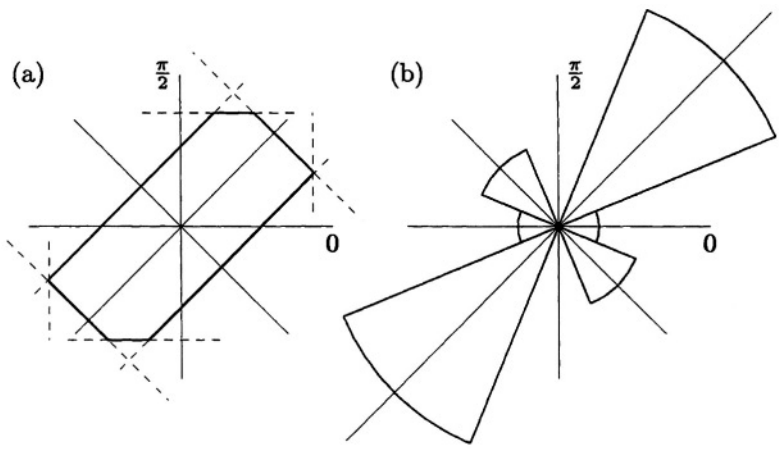

Figure 5.3. A Steiner compact Z_n (a) and the estimated rose of directions (b) for data from Example 5.8. In (b) a circular plot is used where h_i' in (5.30) correspond to the radii of classes.

single underestimated observation N_i may cause a substantial decrease of the estimated zonotope, see the following example.

EXAMPLE 5.15 *We continue in Example 5.8. This time the data from Fig. 5.1 are evaluated by means of the described graphical method. Using formula (5.26), the zonotope in Fig. 5.3 (left) is constructed (recall that the test lines are characterized by its unit normal vectors) and from (5.28), the estimator (5.27) is obtained and plotted in Fig. 5.3 (right). The dominant direction is recognized, however, the second largest atom at* $\frac{3\pi}{4}$ *is unrealistic. It arises as a consequence of the sparse test system.*

A modification of the Steiner compact estimator by means of *smoothing* was developed in [94]. For an integer n, the data p_i are smoothened using moving averages:

$$\bar{p}_i = \sum_{j=-r}^{r} c_j p_{i+j}, \; i = 1, \ldots, n, \tag{5.31}$$

where r is a natural number and $c_{-r}, \ldots, c_r$ are smoothing constants with $c_{-r} + \cdots + c_r = 1$. Of course, choice of the smoothing constants c_i and size of smoothened data r depend on the sample size n. Instead of Z_n, we consider then the zonotope

$$\bar{Z}_n = \{x : \langle x, u_i \rangle \leq \bar{p}_i, \; i = 1, \ldots, 2n\}.$$

The rose of directions is then estimated again by (5.30), where the edge lengths h_i and their normalizations h_i' are taken from the zonotope $\bar{Z}_n$.

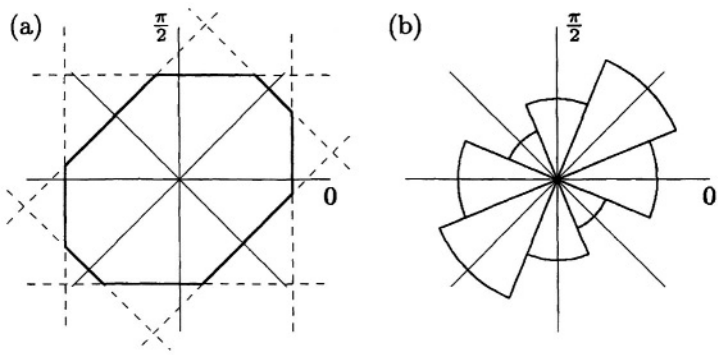

Figure 5.4. A Steiner compact (a) and the estimated rose of directions (b) for data from Example 5.8 using the modified method with smoothing described in Example 5.17.

The following result implies in fact a strong consistency of the estimation procedure.

THEOREM 5.16 ([94]) *Let* $\varepsilon > 0$ *and* $\alpha \in (0,1)$. *Then there exist natural numbers* n, r, *unit vectors* $u_1, \dots u_n \in \mathbb{S}^1$ *and smoothing constants* $c_{-r}, \dots, c_r$ *such that for any planar fibre system* Ξ, *if* $p_1, \dots, p_n$ *are i.i.d. Gaussian variables with means* $P_L(u_1), \dots, P_L(u_k)$, *then*

$$\Pr(d_H(\tilde{Z}_n, Z) \leq \varepsilon L_A) \geq \alpha.$$

REMARK 5.2. a) In the proof presented in [94], the following parameters are used: r sufficiently large, $n = r^2$, $u_i = i\pi/n$, $c_j = (2r+1)^{-1}$, $j = -r, \dots, r$. Of course, other smoothing constants may be used as well.
b) The normality assumption seems to be quite appropriate when using independent test lines, which can be achieved when independent realizations of a random fibre system are available.

EXAMPLE 5.17 *Again for the data from Example 5.8 we use the modified Steiner compact estimator with* $r = 1$ *and* $(c_{-1}, c_0, c_1) = (\frac{1}{4}, \frac{1}{2}, \frac{1}{4})$. *In Fig. 5.4 (a) the Steiner compact estimated from the smoothed rose of intersections is drawn, the estimator of the rose of directions in Fig. 5.4 (b) corresponds better to the data.*

EXAMPLE 5.18 *In the end of this section, an example of evaluation of a real specimen from metallography, see Fig. 5.5, is presented. In a two-phase structure we consider the planar fibre system of boundaries between black and white phases in a specimen section. The intersection counting was carried out at 12 equidistant orientations. The results of*

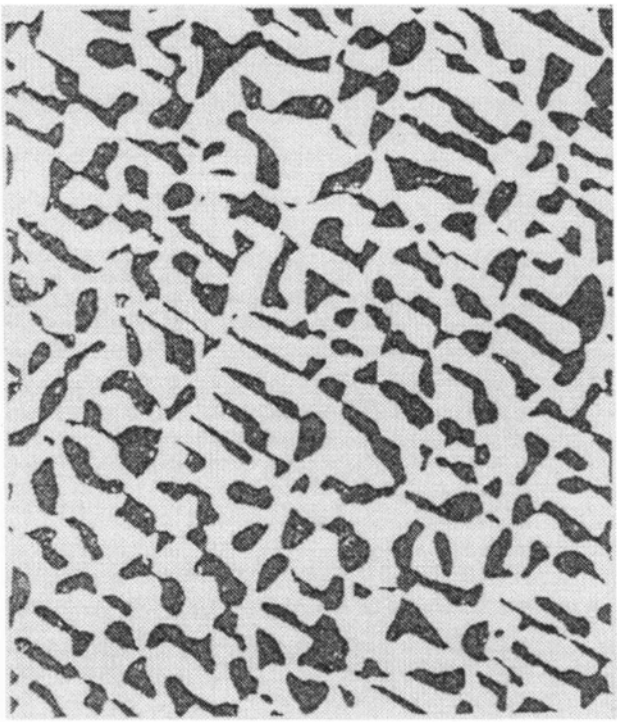

Figure 5.5. **The metallographic sample of an AlMgCuZn alloy, magnification 100×.**

estimation of the rose of directions are plotted in Fig. 5.6: (i) the cardioidal model R_{12}^*, *(ii) the Steiner compact* K_{12} *and the corresponding estimator* R_{12}. *The advantages of the Steiner compact are apparent, because the cardioidal model suppresses the evident multimodality of the rose of directions.*

EXERCISE 5.19 *Prove Theorem 5.14, using the following construction: given a finite even Borel measure* μ on $(0, 2\pi]$, *let* $F(\varphi) = \mu((0, \varphi])$ *be its distribution function and* F^{-1} *its generalized inverse given by* $F^{-1}(t) = \varphi$ *iff* $F(\varphi) \geq t$ *and* $F(\varphi_-) < t$. *Consider the closed convex curve*

$$c : t \mapsto \int_0^\beta (\cos F^{-1}(t), \sin F^{-1}(t))\, \mathrm{d}t, \quad t \in [0, F(2\pi)],$$

and let Z be the convex body surrounded by c. *Show that Z is centrally symmetric with width* $b_u(Z) = \frac{1}{2}\mathcal{F}_\mu(u)$, $u \in \mathbb{S}^1$, *hence 4Z is (up to a shift) the zonoid associated with* μ. *Further, it follows from the construc-*

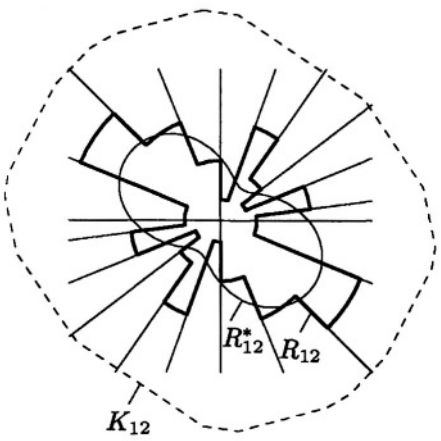

Figure 5.6. Two methods of the rose of directions estimation: the cardioidal model R^*_{12}, the Steiner compact K_{12} and the corresponding estimate R_{12}.

tion that $T_Z((\sin F^{-1}(t), -\cos F^{-1}(t))) = c(t)$ *and that* $l_Z(c(t), c(t')) = \mu([F^{-1}(t), F^{-1}(t')])$.

EXERCISE 5.20 *Derive formula* (5.28) *using analytical geometry.*

EXERCISE 5.21 *Verify that the Prohorov distance between the uniform distribution* U *over* $\mathbb{S}^1$ *and the uniform distribution* U_n *over the* $2n$ *directions* $\frac{i\pi}{n}$, $i = 1, \ldots, 2n$, *is*

$$r(U, U_n) = \frac{\pi}{2n + \pi}.$$

EXERCISE 5.22 *Let* U_n *be the discrete uniform distribution from Example 5.21 and let* V_n *be the uniform distribution over the* $2n$ *directions* $\frac{(2i-1)\pi}{2n}$, $i = 1, \ldots, 2n$. *Show that their Prohorov distance is*

$$r(\mu_n, \nu_n) = \frac{\pi}{2n},$$

whereas the Hausdorff distance of the associated Steiner compact sets is

$$d_H(K_n, L_n) = \frac{1}{4n} \arctan \frac{\pi}{n}.$$

This example shows that the Prohorov distance and Hausdorff metric are not equivalent metrics, though they define the same convergence.

5.3.2 Poisson line process.

A *line process* is a particular case of a flat process, see Subsection 2.9. In particular, any line ℓ in $\mathbb{R}^2$ can be uniquely represented by parameters

$(\alpha, y) \in \mathcal{C}_1 = [0, \pi) \times \mathbb{R}$ so that

$$\ell = \{(x_1, x_2) : x_1 \sin\alpha + x_2 \cos\alpha = y\}.$$

Here α determines the direction of the line and y its signed distance from the origin. We have y positive, negative for lines intersecting the positive, negative horizontal semiaxis in $\mathbb{R}^2$, respectively. A stationary line process Φ can thus be represented by means of a point process $\tilde{\Phi}$ on $\mathcal{C}_1$ and the intensity measure Λ of Φ is (see [109])

$$\Lambda(\mathrm{d}(\alpha, y)) = L_A \mathrm{d}y\, R(\mathrm{d}\alpha). \tag{5.32}$$

By definition, the line process Φ is Poisson whenever the corresponding point process in $\mathcal{C}_1$ is Poisson. The stationarity of Φ implies the translation invariance of $\tilde{\Phi}$ in the second coordinate y, the vice versa is, however, not true.

In Theorem 5.16 the independence of intersection numbers measured on different test lines is assumed. In practice often a single realization (observed in a window) is available and all test lines placed in it, which results in dependent samples. In this section attention is paid to such a case.

We will investigate the intersections of a line process with test segments of constant length l and of varying directions. Consider the unit semicircle $x = \cos\beta$, $y = \sin\beta$, $\beta \in [-\frac{\pi}{2}, \frac{\pi}{2}]$. Denote $\alpha_n = \frac{\pi}{2n}$ and define the test system $\mathcal{T}$ of n segments s_i inscribed in the semicircle, see Fig. 5.7 (a). The segments have centres (x_j, y_j), $x_j = \cos\beta_j \cos\alpha_n$, $y_j = \sin\beta_j \cos\alpha_n$, normal directions $\beta_j = (2j - n - 1)\alpha_n$, $j = 1, \ldots, n$. The segments have equal lengths $l = 2\sin\alpha_n$. The total length of $\mathcal{T}$ converges to π with $n \to \infty$. Any straight line in the plane has at most two intersections with the test system $\mathcal{T}$. Denote by A_i, A_{ij} the subsets of $\mathcal{C}_1$ corresponding to lines which intersect exactly one, two segments, respectively. In Fig. 5.7 (b), these subsets are drawn in the case of $n = 3$. Consider a stationary Poisson line process Φ with intensity L_A and a rose of directions R. Denote by N_i, N_{ij} the independent Poisson distributed random variables with parameters λ_i, λ_{ij}, respectively, corresponding to numbers of intersections of Φ with given i–th, i–th and j–th segment, respectively. It holds

$$\lambda_{ij} = L_A \int_{A_{ij}} \mathrm{d}y\, R(\mathrm{d}\alpha), \quad \lambda_i = L_A \int_{A_i} \mathrm{d}y\, R(\mathrm{d}\alpha).$$

From a realization of the process Φ we get estimators of the support function values of the associated zonoid at β_j

$$p_j = \frac{1}{l}(N_j + \sum_i N_{ij}), \quad j = 1, \ldots, n \tag{5.33}$$

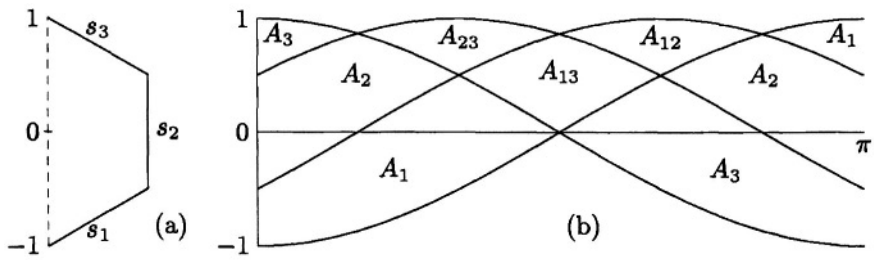

Figure 5.7. The test system $\mathcal{T}$ for $n = 3$ (a), the corresponding subsets A_i, A_{ij}, $i, j = 1, \ldots, n$, $i < j$ (b).

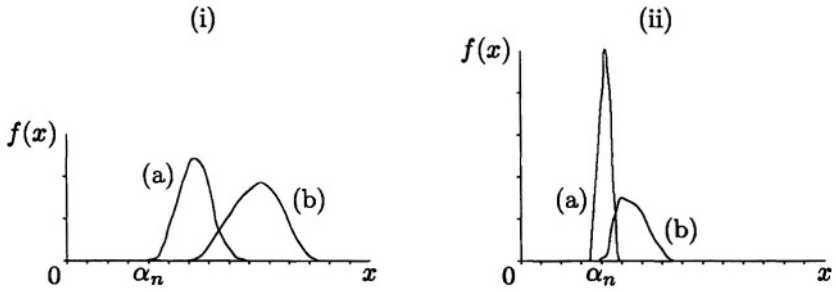

Figure 5.8. (i) Estimated probability density functions of the Prohorov distance $r(R_n, U)$, $n = 8$, $\alpha_n = 0.19$, for $L_A = 50$ (a), $L_A = 1000$ (b). (ii) The same case as in (i) after smoothing with $r = 2$, $c_j = \frac{1}{5}$, $j = -2, \ldots, 2$.

(cf. (5.25)).

The aim is to obtain the probability distribution of the Prohorov distance between the estimator R_n in (5.30) and the true rose of directions R. For a stationary Poisson line process and a special test system in Fig. 5.7, this can be achieved by just simulating the data N_i, N_{ij} from the Poisson distribution, evaluating the estimators and finally the Prohorov distance. The results from 1000 independent simulations for $R = U$ uniform yield approximations of the probability density of the Prohorov distance $r(R_n, R)$; these are shown in Fig. 5.8 (i) (without smoothing), (ii) (with smoothing), respectively.

EXERCISE 5.23 *Show that the support function values* p_j *in* (5.33) *satisfy*

$$\operatorname{cov}(p_i, p_j) = \frac{1}{l^2} \operatorname{var} N_{ij}, \quad i \neq j.$$

5.3.3 Curved test systems

In Chapter 4 the use of cycloidal test lines in stereology was studied. Here we shall investigate the role of general curved test systems

in the estimation of the rose of directions of a planar fibre process following [11]. Consider a test system $\mathcal{T}'$ of arcs with finite total length l and $\mathcal{T}'(B)$, $B \in \mathcal{B}^2$, the corresponding length measure of $\mathcal{T}'$ in B. Assume that $\mathcal{T}'$ is $(\mathcal{H}^1, 1)$-**rectifiable**, hence the tangent (normal) direction $w_{\mathcal{T}'}(x)$ $(n_{\mathcal{T}'}(x))$ of $\mathcal{T}'$ at x is defined for $\mathcal{H}^1$-**almost** all $x \in \mathcal{T}'$. The normal direction distribution Q of $\mathcal{T}'$ is given by

$$\int_{(0,\pi]} f(\alpha)Q(\mathrm{d}\alpha) = \int f(n_{\mathcal{T}'}(x))\mathcal{T}'(\mathrm{d}x),$$

where f is any nonnegative measurable function on $(0, \pi]$. It will be convenient to assume Q to be extended π-**periodically** over the whole real line.

Denote by $\mathcal{T}'(\beta)$ the rotation of $\mathcal{T}' = \mathcal{T}'(0)$ by an angle of $\beta \in (0, \pi]$ in the anti-clockwise direction. The direction distribution Q_β of $\mathcal{T}'(\beta)$ is related to Q by

$$\int f(\alpha)Q_\beta(\mathrm{d}\alpha) = \int f(\alpha + \beta)Q(\mathrm{d}\alpha).$$

Let Ξ be a stationary fibre system in $\mathbb{R}^2$ with length intensity L_A and rose of directions R. In this subsection, we shall use its version $\bar{R}$ normalized to a probability measure on $(0, \pi]$. Due to Theorem 1.12, Ξ intersects $\mathcal{T}'(\beta)$ in a finite number of points almost surely, and let

$$P_L^Q(\beta) = l^{-1}\mathrm{E}\mathcal{H}^0(\Xi \cap \mathcal{T}'(\beta)), \quad \beta \in (0, \pi],$$

denote the related rose of intersections. The following result is due to Mecke [71].

PROPOSITION 5.1 *Let Ξ, $\mathcal{T}'$ be as above. Then*

$$P_L^Q(\beta) = L_A \mathcal{F}_{R*Q_-}(\beta), \quad \beta \in (0, \pi], \tag{5.34}$$

where Q_- is the reflection of Q (i.e., $Q_-(B) = Q(-B)$ for any Borel set B) and $R * Q_-$ is the convolution of measures (see Subsection 1.1.1).

REMARK 5.3. In particular, for $Q = U$ uniform it follows that $P_L^U(\beta) = \frac{2}{\pi}L_A = P_L$ does not depend on β.

Proof. Let C denote a unit square in $\mathbb{R}^2$. Due to the stationarity of Ξ we have

$$\begin{aligned}\mathrm{E}\mathcal{H}^0(\Xi \cap \mathcal{T}'(\beta)) &= \mathrm{E}\int_C \mathcal{H}^0((\Xi + z) \cap \mathcal{T}'(\beta))\mathrm{d}z \\ &= \mathrm{E}\int_{\mathbb{R}^2} \mathcal{H}^0\Big(((\Xi \cap C) + z) \cap \mathcal{T}'(\beta)\Big)\mathrm{d}z.\end{aligned}$$

Applying Theorem 1.12, we get further

$$\begin{aligned}
\mathrm{E}\mathcal{H}^0(\Xi \cap \mathcal{T}'(\beta)) &= \int_{\Xi\cap C}\int_{\mathcal{T}'} |\sin \sphericalangle(w_\Xi(x), w_{\mathcal{T}'}(y))|\mathcal{H}^1(\mathrm{d}y)\mathcal{H}^1(\mathrm{d}x) \\
&= L_A l \int_{[0,\pi)}\int_{[0,\pi)} |\cos(\alpha_1 - \alpha_2)| Q_\beta(\mathrm{d}\alpha_2) R(\mathrm{d}\alpha_1) \\
&= L_A l \int_{[0,\pi)}\int_{[0,\pi)} |\cos(\alpha_1 - \alpha_2 - \beta)| Q(\mathrm{d}\alpha_2) R(\mathrm{d}\alpha_1) \\
&= L_A l \int_{[0,\pi)} |\cos(\alpha - \beta)| (R * Q_-)(\mathrm{d}\alpha) \\
&= L_A l \mathcal{F}_{R*Q_-}(\beta).
\end{aligned}$$

□

Generally, comparing (5.7) and (5.34) we see that if there is a statistical method for estimating R from (5.7), the same method estimates $R * Q_-$ from (5.34) when using a curved test system. Unfortunately, the system of probability measures with convolution operation does not possess a natural inverse element to solve equation $R * Q_- = Q_1$ for an unknown R, cf. [48].

The Dirac measure δ_γ, $\gamma \in (0, \pi]$, provides the rotation $Q_\gamma = Q * \delta_\gamma$ of a given distribution Q by γ. The effect of the convolution operation of measures on Steiner compact sets may be observed most easily when both measures are discrete: if $R = \sum_{i=1}^n a_i \delta_{\alpha_i}$, $Q = \sum_{j=1}^m b_j \delta_{\gamma_j}$, $\sum a_i = \sum b_j = 1$, $a_i, b_j > 0$, $\alpha_i, \gamma_j \in (0, \pi]$, then the convolution $R * Q$ is again a measure with finite support, namely

$$R * Q = \sum_{i=1}^n \sum_{j=1}^m a_i b_j \delta_{\alpha_i + \gamma_j}.$$

The Steiner compact set (zonotope) associated with the discrete measure $R * Q$ has form $Z = \sum_{i=1}^k [-c_{ij}, c_{ij}]$, cf. (1.5), where $c_{ij} = a_i b_j (\cos(\alpha_i + \gamma_j), \sin(\alpha_i + \gamma_j))$ in coordinates.

The following result comes from [49], [71].

PROPOSITION 5.2 *For the Fourier images* $\mathfrak{F}R(k)$, $\mathfrak{F}Q(k)$ *defined by (5.13) and for* $\mathfrak{F}P_L^Q(k) = \int_0^\pi P_L^Q(\beta)\mathrm{e}^{2ik\beta}d\beta$ *it holds*

$$\mathfrak{F}R(k)\mathfrak{F}Q(-k) = \frac{1}{2L_A}\frac{(-1)^{k-1}}{4k^2-1}\mathfrak{F}P_L^Q(k), \quad k = \ldots, -1, 0, 1, \ldots. \tag{5.35}$$

Proof. The formula follows from (5.14) and from the fact that $\mathfrak{F}(R * Q_-)(k) = \mathfrak{F}R(k)\mathfrak{F}Q(-k)$. □

Further we observe that the local smoothing in (5.31) can be expressed in terms of the convolution with a discrete measure Q representing the orientation distribution of a test system.

PROPOSITION 5.3 *Let Q be the π-periodic extension of the discrete measure $Q = \sum_{j=-r}^{r} c_j \delta_{\gamma_j}$, $c_j > 0$, $\sum_{j=-r}^{r} c_j = 1$, $\gamma_j \in (0, \pi]$, $j = -r, \ldots, r$. Then*

$$P_L^Q(\beta) = \sum_{j=-r}^{r} c_j P_L(\beta - \pi + \gamma_j), \quad \beta \in (0, \pi].$$

Naturally, it is not necessary to restrict oneself to atomic measures Q for local smoothing; diffuse measures correspond to curved test systems.

EXAMPLE 5.24 *Let $R = \delta_0$ and let Q_- be the uniform distribution on $(0, \alpha_0)$ for some $0 < \alpha_0 < \pi/2$ small. Then $\mathcal{F}_R(\alpha) = |\cos\alpha|$ and $\mathcal{F}_{R*Q_-}(\alpha) = \alpha_0^{-1}|\sin(\alpha + \alpha_0) - \sin\alpha|$ if $\pi/2 < \alpha < \alpha + \alpha_+ < \pi/2$, with an apparent smoothing effect for $\alpha_0 > 0$ small.*

It is concluded that curved test systems present an alternative to local smoothing in (5.31) when estimating the Steiner compact. It should be kept in mind that using the rose of intersections $P_L^Q(\beta)$ (i.e. using local smoothing) we get estimators of $R * Q_-$ instead of R. In $\mathbb{R}^3$, the convolution operation for measures on $\mathbb{S}^2$ does not exist in a simple form because of the complexity of the space of rotations in $\mathbb{R}^3$.

EXERCISE 5.25 *Prove Proposition 5.3. Hint: Evaluate $\mathcal{F}_{R*Q}(\beta)$ and use* (5.34).

5.3.4 Steiner compact in $\mathbb{R}^d$, $d \geq 3$

The complications in approximating the zonoid associated with the rose of directions R in $\mathbb{R}^d$, $d \geq 3$, are due to the special nature of zonotopes and zonoids. The intersection of supporting halfspaces determined by the estimated rose of intersections (5.19) produces a centrally symmetric polytope but it is not a zonotope in general because its lower dimensional (two-dimensional) faces need not be centrally symmetric. Also the interpolation and smoothing procedures do not produce zonoids but only generalized zonoids. They are centrally symmetric but their even generating measures determined by (1.8) are not nonnegative as required but only signed ones [99]. Consequently, the inversion of the integral equation (5.10) proposed in [49], [59] need not give a nonnegative estimator of the rose of directions R as pointed out in [41].

More correct solutions based on Theorem 5.11 were suggested by Kider- len [61]. The basic idea is an approximation of the generating measure $\mu = L_d R$ by a measure with finite support

$$T_m = \{v_1, \dots, v_m, -v_1, \dots, -v_m\} \subset \mathbb{S}^{d-1}, \tag{5.36}$$

such that $Z_m = \bigoplus_{i=1}^{m} \alpha_i [v_i, -v_i]$ is a zonotope estimating a zonoid Z corresponding to μ. The problem is a suitable choice of T_m and of the weights α_i such that $Z_m \to Z$ in the Hausdorff metric if $m \to \infty$.

Let Ξ be a stationary random fibre system in $\mathbb{R}^d$ with intensity L_d and a rose of directions R. Consider n fixed test hyperplanes $u_i^\perp$ with normals $u_i \in \mathbb{S}^{d-1}$, $i = 1, \dots, n$, such that they do not contain a common line. Denote $\eta_i = \mathcal{H}^0(\Xi \cap W_i)$ the number of intersection points counted in $\Xi \cap W_i$, where $W_i \subset u_i^\perp$ are the observation windows of unit areas $\nu_{d-1}(W_i) = 1$ in the test hyperplanes. All the η_i's then constitute a random vector $\eta(\mu) = (\eta_1, \dots, \eta_n)$ with mean value $\mathrm{E}\eta(\mu) = (\mathrm{E}\eta_1, \dots, \mathrm{E}\eta_n)$, where in $\mathbb{R}^3$ we have, cf. (5.10)

$$\mathrm{E}\eta_i = P_A(u_i) = L_V \mathcal{F}_R(u_i), \quad i = 1, \dots, n.$$

In contrast to the test system $\mathcal{T}'$ in the planar case, we assume here that $\eta_1, \dots, \eta_n$ are independent, which can be ensured by examining independent realizations of Ξ for different planes $u_i^\perp$.

The idea of a maximum likelihood (ML) estimator of the measure μ was formulated in [67] and is further developed in [61]. Assume that Ξ is the union set of a stationary Poisson line process, hence the η_i's are Poisson distributed random variables. Further, assume that the observed realization $\hat{\eta} = (\hat{\eta}_1, \dots, \hat{\eta}_n)$ of $\eta(\mu)$ is a non-zero vector. The ML estimator $\hat{\mu}$ maximizes the log-likelihood function $\mathfrak{L}(\mu) : \mu \mapsto \log \Pr(\eta(\mu) = \hat{\eta})$, i.e. (cf. (2.16))

$$\mathfrak{L}(\mu) = \sum_{i=1}^{n} \left(\hat{\eta}_i \log(L_d \mathcal{F}_R(u_i)) - L_d \mathcal{F}_R(u_i) \right). \tag{5.37}$$

The convex optimization problem

(i) minimize $-\mathfrak{L}(\mu)$ with respect to $\mu \in \mathcal{M}$

has always a solution, see [67] (recall that $\mathcal{M}$ denotes the cone of all finite Borel (nonnegative) even measures on $\mathbb{S}^{d-1}$). It is not unique but any two solutions μ_1, μ_2 are *tomographically equivalent,* i.e. they satisfy

$$\mathrm{E}\eta_i(\mu_1) = \mathrm{E}\eta_i(\mu_2)$$

for all $i = 1, \dots, n$. For large n and regularly distributed u_i on $\mathbb{S}^{d-1}$, the Prohorov distance of tomographically equivalent measures is small.

It was shown in [61] that it is sufficient to solve a discretized version of (i), namely

(ii) minimize $-\mathfrak{L}(\mu)$ with respect to $\mu \in \mathcal{M}(T_m)$,

where $\mathcal{M}(T_m)$ is the cone of all finite even measures with support contained in the finite set T_m. Numerical methods must be used in order to find a solution to (ii) in the finite-dimensional cone $\mathcal{M}(T_m)$. There is a choice of T_m which is optimal in the sense of the following theorem. We will specify this just for $d = 3$, for general formulation see [61], where the theorem is proved under assumption that Ξ is the union set Poisson line process and, consequently, $\eta(\mu)$ is multivariate Poisson distributed.

THEOREM 5.26 ([61]) *Under the above assumptions concerning the choice of test planes and* $\hat{\eta}$, *the problem* (ii) *has a solution. If* T_m *is the set of all unit vectors orthogonal to linearly independent pairs in* $\{u_1, \dots, u_n\}$ *then any solution of* (ii) *is a solution of* (i).

Clearly $m \leq n(n-1)/2$ for $d = 3$. Denote $R_{m,n}$ the ML estimator of the rose of directions based on n test orientations and T_m as introduced in Theorem 5.26; hence $\hat{\mu} = L_d R_{m,k}$ if $\hat{\mu}$ is the solution of (ii). It can be shown that Theorem 5.26 holds for general stationary fibre systems, too. It need not be a maximum likelihood estimator then (the Poisson property of η_i may fail), but it is consistent in the following sense [61]. An asymptotically smooth sequence $\{u_1, u_2, \dots\} \in \mathbb{S}^{d-1}$ is a sequence in $\mathbb{R}^d$ such that the sequence of measures $\tau_k = \frac{1}{k} \sum_{i=1}^{k} \delta_{u_i}$ converges weakly in $\mathcal{M}$ and the limit has a positive density.

THEOREM 5.27 ([61]) *Let* Ξ *be the union set of a stationary fibre system in* $\mathbb{R}^d$ *with generating measure* $\mu = L_d R$ *which is not supported by any great circle in* $\mathbb{S}^{d-1}$, *and let* $\{u_1, u_2, \dots\}$ *be an asymptotically smooth sequence in* $\mathbb{S}^{d-1}$. *Let* $\eta_1, \dots, \eta_k$ *be independent intersection counts in unit windows in* $\{u_1^{\perp}, \dots, u_k^{\perp}\}$, *respectively, and let there exist a constant* $c \in \mathbb{R}$ *such that* $\mathbb{E}(\mathcal{H}^0(\Xi \cap B^{d-1})^2) \leq c$ *for all unit* $(d-1)$*-dimensional balls* B^{d-1}. *Then R is estimated consistently by the ML estimator in the strong sense, i.e. we have*

$$\lim_{k \to \infty} d_H(R_{m,k}, R) = 0$$

almost surely.

To obtain a numerical solution $\hat{\mu}$ of problem (ii) the EM algorithm is proposed in [61]. The principle of EM algorithm is described in detail in Chapter 6 where it is used for solving another problem.

The second approach to the estimation of R in [61] is based on an idea of [16] and it generalizes the 2D approach based on (5.19). Theorem 5.11 implies the possibility of approximating zonoids by zonotopes in fixed directions $u_1, \ldots, u_n$. Next we are looking for a zonotope Z which is contained in a polytope

$$Q_n = \bigcap_{i=1}^{n} \{x \in \mathbb{R}^d;\ \langle x, u\rangle \leq h(Z, u_i)\}. \tag{5.38}$$

In contrast to the planar case, Q_n need not be a zonotope in dimension $d \geq 3$. Theorem 5.26 suggests the choice of T_m which should contain the set of orientations of line segments forming the zonotope Z. Then only the lengths of its line segments have to be determined. Using $Z_m = \bigoplus_{i=1}^{m} \alpha_j[-v_j, v_j]$ we get a *linear program*

$$\begin{aligned} &\text{minimize:} && \textstyle\sum_{i=1}^{n}(h(Z,u_i) - \sum_{j=1}^{m} \alpha_j |\langle v_j, u_i\rangle|), \\ &\text{subject to:} && \textstyle\sum_{j=1}^{m} \alpha_j |\langle v_j, u_i\rangle| \leq h(Z,u_i),\ i = 1,\ldots,k, \\ & && \alpha_j \geq 0, \quad j = 1,\ldots,m. \end{aligned}$$

It can be derived from Theorem 5.26 that there exists a solution of this linear program with objective function value 0, which yields the desired zonotope and, by optimization theory, at most k of the α_j's are nonzero. However, the substitution of estimators $\hat{\eta}_i$ for $h(Z, u_i)$ is dangerous in this case because the values of $\hat{\eta}_i$ substantially lower then $\mathcal{F}_{\mathcal{R}}(u_i)$ (their presence cannot be excluded) can produce an estimate $R_m = 0$ with a positive probability. Consequently, it is recommended to replace $\hat{\eta}_i$ by their arithmetic averages obtained by independent replicated sampling. Using a numerical optimization procedure to the solution of linear program (LP) the estimator of the rose of directions is obtained and a consistency theorem analogous to Theorem 5.27 can be formulated, see [61], where also both estimators (EM and LP) are compared. It is concluded that for a smaller sample size the maximum likelihood estimator (using EM) is slightly better while for larger sample sizes the linear programming should be preferred because the slightly worse performance of the LP estimator is well compensated by its being less time consuming.

EXERCISE 5.28 *Derive formula* (5.37) *in detail.*

EXERCISE 5.29 *Show the tomographical equivalence of any two solutions of optimization problem (i).*

5.3.5 Anisotropy estimation using MCMC

In this section it is shown that besides methods suggested by [61] (refered in Subsection 5.3.4), a Bayesian approach is applicable for the estimation of the rose of directions and the Markov chain Monte Carlo (cf. Subsection 1.2.2) technique is useful. The presented method was developed in [90] and denoted MH. Assume that Ξ is the union set of a stationary Poisson line process with intensity L_V and a rose of directions R. Let all assumptions from the previous subsection between (5.36) and (5.37) be fulfilled.

The log-likelihood function $\mathfrak{L}$ is then, cf. (5.37)

$$\mathfrak{L}(L_V, R) = \sum_{i=1}^{n} \left(\hat{\eta}_i \log(L_V \mathcal{F}_R(u_i)) - L_V \mathcal{F}_R(u_i) \right). \tag{5.39}$$

A parametric model for the rose of directions is used, namely

$$R = \sum_{j=1}^{m} a_j \delta_{t_j}, \tag{5.40}$$

where $a_j \geq 0$, $\sum_{j=1}^{m} a_j = 1$ and $t_j \in T_m$ in (5.36). Hence, all feasible vectors $a = (a_1, \ldots, a_m)$ form a *simplex* $\mathcal{S}$ in $\mathbb{R}^m$. In this model it is

$$\mathcal{F}_R(u_i) = \sum_{j=1}^{m} a_j |\langle u_i, t_j \rangle|.$$

In the Bayesian approach we put prior on a, L_V. An indeterminate prior is a reasonable choice, i.e. a is uniform random on $\mathcal{S}$ and L_V uniform random on an interval $B = [0, L_V^{\max}]$, where $L_V^{\max}$ is an upper bound for possible values of L_V (which is justified in practice and in theory $L_V^{\max}$ vanishes).

The posterior distribution Π of (L_V, a) given $\hat{\eta}_i$, $i = 1, \ldots, n$ in this model has a density π proportional to the product of prior and likelihood (using (5.39))

$$\pi(L_V, a_1, \ldots, a_m) \propto \tag{5.41}$$

$$L_V^{\sum_{i=1}^{n} \hat{\eta}_i} \exp\{-L_V \sum_{i=1}^{n} \sum_{j=1}^{m} a_j \mid \langle u_i, t_j \rangle \mid\} \prod_{i=1}^{n} \left(\sum_{j=1}^{m} a_j \mid \langle u_i, t_j \rangle \mid \right)^{\hat{\eta}_i}$$

on $M = B \times \mathcal{S}$ with respect to the restricted Lebesgue measure. The density π vanishes outside M. Denoting by $\bar{L}_V, \bar{a}_1, \ldots, \bar{a}_m$ the marginal posterior means, $\bar{L}_V$ is a Bayes estimator of L_V and the desired Bayes

estimator of the rose of directions R of Ξ is

$$\hat{R} = \sum_{j=1}^{m} \bar{a}_j \delta_{t_j}. \tag{5.42}$$

From the consistency of the maximum likelihood estimator in Theorem 5.27, using the compactness of the parametric space M and Lemmas 1.25, 1.24 it follows that the Bayes estimator (5.42) is consistent as well.

Since the complicated form of the density π does not allow to evaluate the estimator (5.42) analytically simulation techniques are used for this purpose. The Metropolis algorithm, see Subsection 1.2.2, can be used for the simulation of the posterior distribution. The state space for the Markov chain Y is M i.e. a compact subset of $\mathbb{R}^{m+1}$ with positive $\mathcal{H}^m$ measure. The random walk Metropolis algorithm with proposal density $q(x, y) = f(y - x)$, cf. Example 1.20, is applied where f is the density of the product of centered normal distributions $\mathcal{N}(0, \sigma_L^2) \times \mathcal{N}(0, \sigma_a^2 I)$ corresponding to L_V (one-dimensional) and a ($(m-1)$-dimensional because of the condition $\sum_{i=1}^{m} a_i = 1$). Here I is the unit matrix of order $m - 1$ and $\sigma_L > 0$, $\sigma_a > 0$. For more details see [90].

Let (L_V, a) be a state of the chain and (L_V', a') a proposal. The acceptance probability in (1.26) is

$$\alpha((L_V, a), (L_V', a')) = \begin{cases} 1 & \text{if} \quad (L_V, a) \in M^c, \\ 0 & \text{if} \quad (L_V, a) \in M \text{ and } (L_V', a') \in M^c \end{cases}$$

and

$$\alpha((L_V, a), (L_V', a')) = \min\left\{1, \left(\frac{L_V'}{L_V}\right)^{\sum \hat{\eta}_i} \exp\left(L_V \sum_{i=1}^{n} w_i - L_V' \sum_{i=1}^{n} w_i'\right) \prod_{i=1}^{n} \left(\frac{w_i'}{w_i}\right)^{\hat{\eta}_i}\right\}$$

for both (L_V, a), $(L_V', a') \in M$. Here the expression $w = Ca$ is used, $w = (w_1, \ldots, w_n)$, where $C = \{C_{ij}\}$ is a matrix with elements $C_{ij} = |\langle h_i, t_j \rangle|$, $i = 1, \ldots n$, $j = 1, \ldots m$.

Let P be the resulting probability kernel (cf. (1.27)) restricted to $M \times \mathcal{B}(M)$. The Markov chain with kernel P is aperiodic, ψ-irreducible and uniformly ergodic. From the uniform ergodicity of P the central limit theorem holds (1.25) for ergodic averages $\frac{1}{k}\sum_{i=1}^{k} f(Y_i)$ of any square integrable function f of the limiting distribution Π and any starting value of the chain realization.

EXAMPLE 5.30 *Simulations were performed in order to study the proposed MH estimator. Consider a stationary Poisson line process* Φ *in*

$\mathbb{R}^3$ *with the rose of directions* R_1 *of Fisher type with density*

$$f(x) = \frac{e^{\kappa|\langle x,u_0\rangle|}}{\int_{\mathbb{S}^2} e^{\kappa|\langle x,u\rangle|}\mathcal{H}^2(du)}, \quad x \in \mathbb{S}^2 \tag{5.43}$$

and concrete values $u_0 = (0.572, 0.572, 0.588)$, $\kappa = 10$. *Let the number of test directions be* $n = 10$ *and let* u_i, $i = 1, \ldots, 10$, *be outer normal directions to the faces of a regular icosahedron in standard position (i.e., with a face in* xy*-plane and an edge in* x*-axis) and unit face area contents. Ten independent realizations of* Φ *with* $L_V = 100$ *are simulated and the realizations* $\hat{\eta}_i$, $i = 1, \ldots, 10$, *of the intersection process are obtained. The set* T_m (5.36) *supporting the estimating rose* (5.40) *consists of* $m = 45$ *(pairs of) vectors. Parameters* $\bar{L}_V, \bar{a}_1, \ldots, \bar{a}_m$ *are estimated as posterior means using the MCMC algorithm. The starting iteration is*

$$L_V^{(0)} = 2\frac{\sum \hat{\eta}_i}{n}, \qquad a_i^{(0)} = \frac{1}{m}, \qquad i \in \{1, \ldots, m\}. \tag{5.44}$$

Note that $L_V^{(0)}$ *is an unbiased estimator for the length intensity in the isotropic case, see* (4.3). *The variances of the proposal distributions were chosen* $\sigma^2_{L_V} = 1$ *and* $\sigma_a^2 = 0.001$. *From the simulated Markov chain* $(L_V^{(j)}, a^{(j)})$, $a^{(j)} = (a_1^{(j)}, \ldots, a_m^{(j)})$, *the ergodic averages*

$$\bar{a}_i = \frac{1}{10000}\sum_{t=1}^{10000} a_i^{(100t+5000)}, \qquad i = 1, \ldots, m, \tag{5.45}$$

are evaluated. Figure 5.9 shows the resulting MH estimator (5.42). *We can see that the estimator detects both the anisotropy of* R_1 *and the symmetry of* R_1 *well.*

In [90] three estimators (MH, EM and LP) were compared in simulations w.r.t. both bias (Prohorov distance) and variability (characteristics of empirical covariance of vector a). It was shown that MH estimator may have a smaller variability than EM and LP.

EXERCISE 5.31 *Write down a computer code for the MH algorithm of the presented rose of directions estimation.*

EXERCISE 5.32 *Run the algorithm from Exercise 5.31 for data simulated from the uniform rose of directions. Use faces of a regular octahedron as test probes.*

5.4. Orientation-dependent direction distribution

The rose of directions R of a stationary fibre or surface system in $\mathbb{R}^d$ considered so far was an even (centrally symmetric) probability measure on $\mathbb{S}^{d-1}$. Consider now, roughly speaking, a full (d)-dimensional

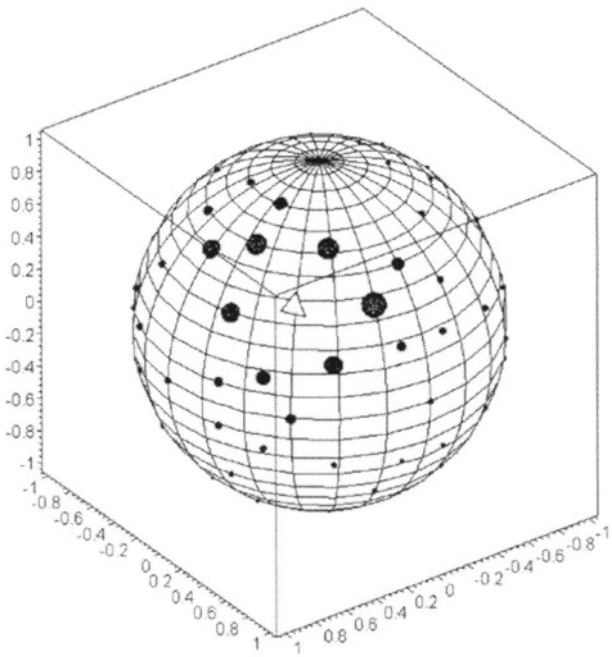

Figure 5.9. MH estimator of the rose of directions in the simulation study. In each point $\pm t_j$, $t_j \in T_m \subseteq \mathbb{S}^2$ a small sphere is drawn with radius proportional to $\bar{a}_j$. The axis of the Fisher distribution is denoted by a triangle.

stationary random closed set Ξ with (piecewise) smooth boundary and let $n(x) \in \mathbb{S}^{d-1}$ be the unit *outer* normal vector to $x \in \Xi$ (defined at almost all boundary points x of Ξ). The distribution R_o of $n(x)$ at a typical point x (with respect to the Palm distribution of the random measure $\mathcal{H}^{d-1} \mid \partial\Xi$) is called the *orientation dependent rose of normal directions* of Ξ. Note that R_o need not be an even measure, consider e.g. a random set Ξ formed by translation equivalent triangles. Note also that the symmetrized version

$$R(B) = \frac{1}{2}(R_o(B) + R_o(-B)), \quad B \subset \mathbb{S}^{d-1} \text{ Borel},$$

is the usual rose of (normal) directions of the stationary surface system $\partial\Xi$. For some applications, estimations of the oriented version R_o of the rose of directions might be demanded.

For a rigorous description of the model Ξ we need the rectifiability of the boundary $\partial\Xi$ and the existence of an oriented normal vector field de-

fined a.e. on $\partial\Xi$ which could be interpreted as outer normal vector field. It seems that no approach encompassing such general sets as those with Hausdorff rectifiable boundaries has been established so far. Usually, one can find in the literature the oriented (normal) direction distribution in connection with curvature measures (in fact, R_o is a multiple of the mean curvature measure of Ξ of order $d-1$) which require much stronger assumptions, e.g. (poly)convexity, smoothness or positive reach. We shall limit ourselves in this section to random sets with realizations in the family $\mathcal{R}$ of locally finite unions of convex bodies with nonempty interiors (sets from $\mathcal{R}$ belong to the extended convex ring and the additional assumption of nonempty interiors guarantees the full-dimensionality). A stationary random set Ξ with values in $\mathcal{R}$ can be realized as union set of a stationary process of convex or polyconvex (finite unions of convex) bodies with nonempty interiors. Most of the results are valid also for certain finite unions of sets with positive reach (see [96]).

Given a set $A \subseteq \mathbb{R}^d$ and $a \in A$, the *normal cone* of A at a is defined as

$$\mathrm{Nor}\,(A,a) = \{n \in \mathbb{R}^d : \langle n,u\rangle \le 0 \text{ for any } u \in \mathrm{Tan}\,(A,a)\},$$

where $\mathrm{Tan}\,(A,a)$ is the (usual) tangent cone defined in Subsection 1.1.3.

LEMMA 5.33 *If $X \in \mathcal{R}$ then ∂X is $\mathcal{H}^{d-1}$-rectifiable and at $\mathcal{H}^{d-1}$-almost all $x \in \partial X$, the outer normal direction $n(x) \in \mathrm{Nor}\,(X,x) \cap \mathbb{S}^{d-1}$ to X is uniquely determined.*

Proof. Let $X = \bigcup_{i=1}^{\infty} K_i$ with convex bodies K_i of nonempty interiors. The boundary of each K_i is $(d-1)$-rectifiable (cf. Exercise 1.9). Hence, the union $\bigcup_i \partial K_i$ is locally $(d-1)$-rectifiable and the boundary ∂X is $\mathcal{H}^{d-1}$-rectifiable as a measurable subset of $\bigcup_i \partial K_i$. It follows from Theorem 1.5 that the approximate tangent space $\mathrm{Tan}^{d-1}(\partial X, x)$ is a $(d-1)$-dimensional subspace. Due to the relatively simple structure of convex bodies, it is clear that the approximate tangent cone agrees with the usual one, $\mathrm{Tan}\,(\partial X, x)$. By the full-dimensionality assumption we have that the tangent cone $\mathrm{Tan}\,(X,x)$ must be a halfspace at such a point x and, therefore, the unit outer normal vector is uniquely determined. □

Lemma 5.33 enables us to define the orientation dependent rose of normal directions R_o of Ξ as the distribution of Ξ at a typical point x of $\partial\Xi$:

$$R_o(\cdot) = \mathrm{Pr}_0[n(0) \in \cdot],$$

where Pr_0 is the Palm probability under condition $0 \in \partial\Xi$. Using the stationarity of Ξ (and, hence, of $\partial\Xi$), we can write equivalently by The-

orem 2.31

$$R_o(\cdot) = (S_d \nu_d(B))^{-1} \mathrm{E}\mathcal{H}^{d-1}(\{x \in B \cap \partial\Xi : n(x) \in \cdot\}),$$

where S_d is the surface intensity of Ξ and B is any Borel subset of $\mathbb{R}^d$ with finite positive volume.

REMARK 5.4. The product $S_d R_o$ is called the *mean normal measure* of Ξ by Weil [119] and it coincides with the density of the second projection of the $(d-1)$-st generalized curvature measure (support measure) of Ξ. This follows e.g. from the integral representation of curvature measure [96, Theorem 4.1].

REMARK 5.5. The notion mean normal measure is often used also in connection with a stationary particle process. If Φ is a stationary process of convex particles in $\mathbb{R}^d$ (cf. Subsection 2.8) with intensity α and primary grain Z_0, its mean normal measure is defined as

$$S(\Phi, \cdot) = \alpha \mathrm{E} S(Z_0, \cdot),$$

where $S(Z_0, \cdot) = \mathcal{H}^{d-1}(\{x \in \partial Z_0 : n(x) \in \cdot\})$ is the normal measure of the convex body Z_0. If Φ is Poisson then the mean normal measure of the union set $\Xi = \bigcup_{K \in \Phi} K$ equals $1 - V_V$ times the mean normal measure of Φ, where V_V denotes the volume fraction of the union set Ξ (see e.g. [103, Satz 5.4.2]).

The estimation of R_o is much more difficult than that of the unoriented version R. Note that the rose of intersections $P_L(u)$, $u \in \mathbb{S}^{d-1}$, determines only R but not R_o (consider a union set of a process of translation equivalent triangles; the rose of intersections remains unchanged if we replace the triangles by its symmetric images, but the oriented rose of directions will change). In fact, linear probes do not provide sufficient information for the estimation of R_o.

The following estimation procedure was suggested by Schneider [100]. The integral formula

$$\begin{aligned} &\mathrm{E}\mathcal{H}^{d-2}(\{x \in \partial\Xi \cap u^\perp : \langle n(x), u\rangle > 0\}) \qquad (5.46) \\ &\quad = S_d \int_{\mathbb{S}^{d-1}} \sqrt{1 - \langle u, v\rangle^2}\, \mathbf{1}_{\{\langle u,v\rangle > 0\}}\, R_o(\mathrm{d}v), \quad u \in \mathbb{S}^{d-1}, \end{aligned}$$

holds and is invertible in the sense that the values in (5.46) at each $u \in \mathbb{S}^{d-1}$ determine the mean normal measure $S_V R_o$ of Ξ uniquely. The values on the left hand side of (5.46) can be estimated from flat sections, nevertheless, two close parallel sections are needed in order to determine

which points $x \in \partial\Xi$ in the section have the unit outer normal $n(x)$ directed into the halfspace given by the vector u.

Another method based on measuring dilation volumes was proposed in [92] for $d = 2$ and [93] in general dimension. This is based on the following two results which are formulated in the design-based setting (with a deterministic bounded set) in [93] but can be easily transformed to the case of a stationary random set as follows, see also [55].

Given a polyconvex set X in $\mathbb{R}^d$, its *normal measure* is defined as

$$S(X;\cdot) = \mathcal{H}^{d-1}(\{x \in \partial X : n(x) \in \cdot\})$$

(note that this is the twofolf of the $(d-1)$st area measure of X, see [93]). If K is a convex body we define

$$V_{d-1,1}(X,K) = \int_{\mathbb{S}^{d-1}} h(K,-u)\, \sigma_{d-1}(X;\mathrm{d}u).$$

Note that $V_{d-1,1}(X,K)$ may be interpreted as generalized mixed volume since it equals a multiple of the mixed volume, $dV(X,\dots,X,-K)$, if X is convex as well (cf. [99]).

THEOREM 5.34 ([93, THEOREM 3.1]) *Let X be as above and let K be a convex body such that the orthogonal projection of its support function onto the subspace of spherical harmonics on $\mathbb{S}^{d-1}$ of degree n is nonzero for any integer $n \geq 0$, $n \neq 1$. Then the normal measure $S(X;\cdot)$ is uniquely determined by the values of $V_{d-1,1}(X,\rho K)$, $\rho \in \mathrm{SO}(d)$.*

The proof is based on a uniqueness result for spherical harmonic expansions due to Schneider [99]. In dimension $d = 2$ the argument is rather easy since then the n-th Fourier coefficient of the function $\varphi \mapsto V_{1,1}(X,\rho_\varphi K)$, where ρ_φ is the rotation by $\varphi \in [0,2\pi)$, equals the product of the nth Fourier coefficients of $S(X;\cdot\,)$ and of $h(-K,\cdot)$. But the assumption says that all Fourier coefficients of $h(K,\cdot)$ are nonzero except of that of order one. The Fourier coefficient of order one of $S(X;\cdot)$ is always zero due to a symmetry property of the area measures.

REMARK 5.6. An example of a convex body fulfilling the assumption of Theorem 5.34 is a triangle having at least one angle which is not a rational multiple of π (for any dimension $d \geq 2$).

For a stationary random set Ξ from $\mathcal{R}$ with finite surface intensity S_d and oriented normal direction distribution R_o, we define the corresponding densities

$$\bar{V}_{d-1,1}(\Xi,K) = \lim_{r\to\infty} \frac{1}{\nu_d(rB)} \mathrm{E} V_{d-1,1}(\Xi \cap rB, K),$$

where B is any convex body containing the origin in its interior; see [103] for the correctness. Since also

$$S_d R_o = \lim_{r\to\infty} \frac{1}{\nu_d(rB)} \mathrm{E}\sigma_{d-1}(\Xi \cap rB)$$

in the weak sense (see [103]), we have

COROLLARY 5.35 *The mean normal measure $S_d R_o$ of a stationary random set Ξ from $\mathcal{R}$ is uniquely determined by the values of $\bar{V}_{d-1,1}(\Xi, \rho K)$, $\rho \in \mathrm{SO}(d)$, if K is a convex body fulfilling the assumption of Theorem 5.34.*

Theorem 5.34 and Corollary 5.35 suggest to estimate the functional $\bar{V}_{d-1,1}(\Xi, \rho K)$ for rotations of a suitably chosen convex test set K. Of course, the determination of the mean normal measure from these values is a difficult problem, some suggestions for the planar case can be found in [92].

For the estimation of $\bar{V}_{d-1,1}(\Xi, K)$, we may use the volume fractions of dilations of Ξ with infinitesimal multiples of K. This is based on the following result.

THEOREM 5.36 *Let X be a polyconvex set in $\mathbb{R}^d$ and K a convex body. Then*

$$V_{d-1,1}(X, K) = \lim_{\varepsilon\to 0_+} \frac{\nu_d\big((X \oplus \varepsilon(-K)) \setminus X\big)}{\varepsilon}.$$

For the proof see [55]; another proof can be found in [93] for more general sets X but with additional assumptions concerning the relation of X and K.

For a stationary random set Ξ, we may approximate $\bar{V}_{d-1,1}(\Xi, K)$ by $(\nu_d(rB))^{-1}\mathrm{E}V_{d-1,1}(\Xi \cap rB, K)$ which, by Theorem 5.36, tends as $r \to \infty$ to the limit as $\varepsilon \to 0$ of the volume fraction of the collar set $(\Xi \oplus \varepsilon(-K)) \setminus \Xi$ through ε. Thus, we have

COROLLARY 5.37 *Let Ξ be a stationary random set with values in $\mathcal{R}$ with volume fraction V_V and K a convex body. Then*

$$\bar{V}_{d-1,1}(\Xi, K) = \lim_{\varepsilon\to 0_+} \frac{V_V(\Xi \oplus \varepsilon(-K)) - V_V(\Xi)}{\varepsilon}.$$

Instead of convex sets, finite sets may be taken for test sets. It was shown by Kiderlen and Jensen [62] that for a polyconvex set X which is topologically regular (i.e., it equals the closure of its interior) and for a finite set $M = \{m_1, \ldots, m_k\}$ containing the origin,

$$V_{d-1,1}(X, \operatorname{conv} M) = \phi'_M(0_+), \tag{5.47}$$

where $\phi'_M(0_+)$ is the derivative of

$$\phi_M(t) = \nu_d(X \oplus \varepsilon(-M)) = \nu_d\left(\bigcup_{m\in M}^{k} (X + tm)\right),$$

see also [91] for the case $m = 3$ (which is sufficient to determine the normal measure) and more general sets X. Note that we can use alternatively the volumes of intersections,

$$\psi_N(t) = \nu_d\left(\bigcap_{m\in N}^{k} (X + tm)\right)$$

for subsets $N \subseteq M$ and derive $\phi_M(t)$ by using the inclusion-exclusion formula. Consequently, the mean normal measure of a topologically regular stationary random set Ξ from $\mathcal{R}$ is uniquely determined by the values $\overline{\psi}'_M(0_+)$ for finite test sets M with at most three elements, where $\overline{\psi}_M(t)$ is the volume fraction of

$$\bigcap_{m\in M} (\Xi + tm).$$

A practical method using digitized images is suggested in [62].

Chapter 6

PARTICLE SYSTEMS

In this chapter, a special problem for particle systems is studied which is called the *stereological unfolding*. It consists in the estimation of particle parameters characterizing size, shape, orientation, etc. from the information obtained on a planar section.

In the first part of the chapter, stereological unfolding problems for the joint distribution of particle parameters are discussed. We focus on problems including particle directions (called orientations); this part of development is not presented in a review Chapter 6 on unfolding problems in Ohser and Mücklich [86]. Further, the EM-algorithm and its use for the solution of unfolding integral equations is explained. Finally, numerical results are presented using real data from metallography.

In the second part of the chapter, a stereological problem of prediction of extremal particle parameters is investigated using the statistical extreme value theory of de Haan [24]. This is still an unsolved problem of considerable importance since in many applications extremal properties are more critical than e.g. mean values.

6.1. Stereological unfolding

The history of unfolding problems started by the Wicksell's paper [122] on spherical and ellipsoidal particles. There is a vast literature on the estimation of a distribution of sphere radii from the observed distribution of radii of circular particle sections, for a review see [109]. The problem of spheroids (i.e. rotational ellipsoids) was shown in [19] to be undetermined if both prolate and oblate spheroids are included in the particle system. Consequently, the cases when all particles are either oblate or prolate are considered separately. Modern numerical methods of the solution of various unfolding problems were presented

in [86]. We start with a general background. Throughout the whole chapter, considerations are restricted to particles and particle systems in $\mathbb{R}^3$, though, of course, some results might be formulated in a more general d-dimensional setting.

6.1.1 Planar sections of a single particle

In this chapter, a particle is always a convex particle, typically of a given shape. We consider first a fixed single particle K and a fixed 2-dimensional subspace $L \in \mathcal{L}_2$. If z is taken uniformly randomly from the projection $p_{L^\perp}K$, then

$$(K - z) \cap L$$

is a random convex body in the plane L.

We shall be mostly interested in planar sections with section planes which are random not only in translation but also in direction. Let Q be a probability distribution on $\mathcal{L}_2$ (or, equivalently, an even distribution on $\mathbb{S}^2$) and consider the measure μ_Q on the space $\mathcal{F}_2$ of planes in $\mathbb{R}^3$ defined by

$$\mu_Q(\mathrm{d}F) = \nu_2(\mathrm{d}z)\, Q(\mathrm{d}L),$$

where $F = L + z$ and $z \in L^\perp$ (note that if $Q = U$ is the uniform distribution then $\mu_U = \mu_2$ is the integral-geometric measure of 2-dimensional flats in $\mathbb{R}^3$ introduced in (2.42)). Let further $\mu_Q^{K\uparrow}$ be the restriction of μ_Q to the flats hitting K, normalized to a probability measure (of course, we have to assume that K is full-dimensional, or that Q is not concentrated in those subspaces L which contain a translate of K). If F is a random plane with distribution $\mu_Q^{K\uparrow}$ then $K \cap F$ is a random section body of K. Note that in this case, the section body, though being two-dimensional, is not contained in a fixed two-dimensional subspace of $\mathbb{R}^3$. The distribution of the random section body can be described in the following way. If f is a nonnegative measurable function on the space of convex bodies, then

$$\mathrm{E}f(K \cap F) = \Big(\int b_L K Q(\mathrm{d}L) \Big)^{-1} \int_{\mathcal{L}_2} \int_{p_{L^\perp}K} f(K \cap (L + z))\mathrm{d}z Q(\mathrm{d}L), \tag{6.1}$$

where $b_L K = \nu_1(p_{L^\perp}K)$ is the width of K in direction $L^\perp$. We shall be interested in the distribution of some multidimensional parameter $\mathbf{y}$ of $K \cap F$ which is translation invariant.

6.1.2 Planar sections of stationary particle processes

Let Φ be a stationary particle process in $\mathbb{R}^3$, i.e., a stationary point process on the space $\mathcal{C}'$ of nonempty compact convex subsets of $\mathbb{R}^3$ (see Subsection 2.8). Let N_V denote its intensity and Λ_0 the distribution of primary grain Z_0 (distribution on $\mathcal{C}'$). We shall start with a fixed section plane L.

LEMMA 6.1 *If Φ is as above and $L \in \mathcal{L}_2$, then*

$$\Phi \cap L := \{K \cap L : K \in \Phi\}$$

is a stationary particle process in the two-dimensional space L with intensity

$$N_A = N_V \int b_L(K)\Lambda_0(\mathrm{d}K)$$

and primary grain distribution $\Lambda_0^{(L)}$ given by

$$\int f(K')\Lambda_0^{(L)}(\mathrm{d}K') = \Big(\int\int b_L(K)\Lambda_0(\mathrm{d}K)\Big)^{-1} \int_{p_{L^\perp}K} f((K-z)\cap L)\mathrm{d}z\Lambda_0(\mathrm{d}K),$$

where f is any translation invariant nonnegative measurable function on the space of convex bodies in L.

REMARK 6.1. Both equations from Lemma 6.1 can be written as one equation:

$$N_A \int f(K')\Lambda_0^{(L)}(\mathrm{d}K') = N_V \int\int_{p_{L^\perp}K} f((K-z)\cap L)\mathrm{d}z\Lambda_0(\mathrm{d}K). \quad (6.2)$$

Proof. Consider the mapping

$$\tau : K \mapsto K \cap L$$

from $\mathcal{C}'$ to the space $\mathcal{C}'(L)$ of convex bodies in L. τ is measurable with respect to the Hausdorff metric in both spaces (see [69]) and τ commutes with shifts in L. In the setting of random measures, the point process $\Phi \cap L$ is the image measure $\Phi \circ \tau^{-1}$ of the random measure Φ and, therefore, also its intensity measure fulfills $\Lambda^{(L)} = \Lambda \circ \tau^{-1}$ with $\Lambda = \mathrm{E}\Phi$.

Thus, we have for any integrable function f on $\mathcal{C}'$, using Theorem 2.41,

$$\begin{aligned}\int f(K)\Lambda^{(L)}(\mathrm{d}K) &= \int f(K\cap L)\Lambda(\mathrm{d}K)\\ &= N_V\int\int f((K_0+x)\cap L)\nu_3(\mathrm{d}x)\Lambda_0(\mathrm{d}K_0)\\ &= N_V\int\int_{p_L\perp K}\int_L f(((K_0-z)\cap L)+y)\nu_2(\mathrm{d}y)\mathrm{d}z\Lambda_0(\mathrm{d}K_0),\end{aligned}$$

from which the desired relations follow. □

Consider further a randomization of the section plane (subspace) L with respect to a distribution Q. The section process $\Phi\cap L$ must be considered now as a particle process in the whole $\mathbb{R}^3$ whose particles are, however, two-dimensional convex bodies. Of course, $\Phi\cap L$ is not a stationary particle process in $\mathbb{R}^3$, but it is a mixture of stationary planar particle processes. Using Lemma 6.1, we can write down its intensity measure. We shall use the notation Φ^Q for the section process $\Phi\cap L$ and $\Lambda^Q=\mathrm{E}\Phi^Q$ for its intensity measure.

PROPOSITION 6.1 *Under the notation introduced above, we have for any stationary process Φ of convex particles in $\mathbb{R}^3$ and probability distribution Q on $\mathcal{L}_2$*

$$\begin{aligned}&\int f(K)\Lambda^Q(\mathrm{d}K)\\ &= N_V\int\int\int_{p_L\perp K}\int_L f(((K_0-z)\cap L)+y)\nu_2(\mathrm{d}y)\mathrm{d}z\Lambda_0(\mathrm{d}K_0)Q(\mathrm{d}L)\\ &= N_V\bar{b}(Z_0)\int\int\int_{F_0} f((K_0\cap F)+y)\nu_2(\mathrm{d}y)\mu_Q^{K_0\uparrow}(\mathrm{d}F)\Lambda_0(\mathrm{d}K_0),\end{aligned}$$

where F_0 denotes the plane F shifted to the origin and $\mu_Q^{K_0\uparrow}$ is the distribution of a Q-weighted random section plane of K_0 introduced above, and

$$\bar{b}(Z_0)=\int b_L(Z_0)Q(\mathrm{d}L)$$

is the mean width of Z_0 w.r.t. the distribution Q.

REMARK 6.2. In view of Proposition 6.1, we can interpret

$$N_A = N_V\bar{b}(K_0) \tag{6.3}$$

as the intensity and the random convex body

$$\int (Z_0 \cap F)\mu_Q^{Z_0\uparrow}(\mathrm{d}F)$$

(up to a shift) as the primary grain of the section process $\Phi \cap L$, if Z_0 is the primary grain of Φ.

EXERCISE 6.2 *Prove Proposition 6.1. Hint: Use Lemma 6.1 and the definition of* $\mu_Q^{K_0\uparrow}$.

6.1.3 Unfolding of particle parameters

Assume that the primary grain distribution Λ_0 of Φ is parametric, i.e., that the primary grain $K_0 = K_0(\mathbf{x})$ is determined by a multidimensional parameter $\mathbf{x} \in \mathbb{R}^n$ with distribution function $H(\mathrm{x})$. Let further $\mathbf{y} \in \mathbb{R}^m$ be a multidimensional characteristic of the section body $K_0 \cap F$. We denote by $\mathrm{P}(\mathrm{d}\mathbf{y} \mid \mathbf{x})$ the conditional distribution function of $K_0 \cap F$ provided that K_0 is described by the parameter $\mathbf{x}$. Of course, the parameters $\mathbf{x}$, $\mathbf{y}$ are supposed to be translation invariant as characteristics of primary grains.

Applying Proposition 6.1, we get the relation for the distribution function G of $\mathbf{y}$ as a Stieltjes integral

$$N_A G(\mathbf{y}) = N_V \int \bar{b}(K_0(\mathbf{x}))P(\mathbf{y} \mid \mathbf{x})\mathrm{d}H(\mathbf{x}). \tag{6.4}$$

If probability densities $\mathrm{d}H(\mathbf{x}) = h(\mathbf{x})\mathrm{d}\mathbf{x}$ and $P(\mathrm{d}\mathbf{y} \mid \mathbf{x}) = p(\mathbf{y} \mid \mathbf{x})\mathrm{d}\mathbf{x}$ exist, then the density g of G exists as well and satisfies

$$N_A g(\mathbf{y}) = N_V \int \bar{b}(K_0(\mathbf{x}))p(\mathbf{y} \mid \mathbf{x})h(\mathbf{x})\mathrm{d}\mathbf{x}. \tag{6.5}$$

The stereological unfolding problem consists of the evaluation of unknown particle characteristics h, N_V from the particle section distribution g and N_A which can be estimated from sections by planes with a given distribution Q. Formula (6.5) presents an inverse problem since the aim is to obtain the probability density h. For special kernel functions

$$k(\mathbf{x}, \mathbf{y}) = \bar{b}(K_0(\mathbf{x}))p(\mathbf{y} \mid \mathbf{x})h(\mathbf{x}),$$

an analytical inversion is available. A numerical solution frequently starts from the formulation (6.4) in terms of distribution functions.

EXAMPLE 6.3 *(Wicksell's corpuscule problem, [122]) Consider a system of spherical particles with random radius of distribution function* $H(x)$.

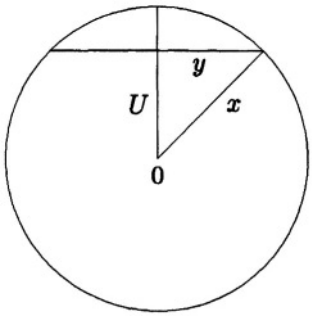

Figure 6.1. **Wicksell corpuscule problem: a particle and its section (thick line).**

The intersection with an IUR section yields a system of circular particle sections with random radius Y and a distribution function $G(y)$. *Then (6.4) takes the form*

$$N_A G(y) = 2N_V \int_y^\infty (x - \sqrt{x^2 - y^2}) \mathrm{d}H(x), \quad y \geq 0, \tag{6.6}$$

since

$$P(y \mid x) = \Pr(U \geq \sqrt{x^2 - y^2}) = 1 - \sqrt{1 - \frac{y^2}{x^2}},$$

where U is a uniform location of a section plane on $[0, x]$, *see Fig. 6.1, and the width of any particle is constant and equals* $2x$. *The moments* $\alpha_k = \int x^k \mathrm{d}H(x)$ *and* $\chi_k = \int y^k \mathrm{d}G(y)$ *are related by*

$$\chi_k = \frac{\Gamma(\frac{1}{2})\Gamma(\frac{k+2}{2})}{2\Gamma(\frac{k+3}{2})} \frac{\alpha_{k+1}}{\alpha_1}, \tag{6.7}$$

for $k = -1, 0, 1, \ldots$. *For* $k = -1$ *a formula for the mean size* $\alpha_1 = \frac{\pi}{2\chi_{-1}}$ *is obtained from (6.7), however when using empirical mean* $\hat{\chi}_{-1} = \frac{1}{n}\sum_i y_i^{-1}$, y_i *being realizations of Y, in this formula we obtain an estimator with infinite variance, see [117]. This is typical for ill-posed inverse problems. Ill-posedness in practice means that small errors in the estimation of the quantity on the left hand side in (6.6) may lead to large errors in the estimation of* $H(x)$.

Further, attention is paid to unfolding problems with more than one particle parameters. The setting presented here is, in fact, equivalent to that used by Cruz-Orive [19] for the size-shape unfolding problem of spheroids (either all oblate or all prolate). Formulas (1),(5) in that paper, p.237-8, say that under the IUR sampling design

$$g(y_1, y_2) = \int\int p(y_1, y_2 \mid x_1, x_2) h(x_1, x_2 \mid \uparrow) \mathrm{d}x_1 \mathrm{d}x_2, \tag{6.8}$$

where $(x_1, x_2), (y_1, y_2)$ is the size and shape factor of a particle, particle section, respectively, and $h(x_1, x_2 \mid \uparrow)$ denotes the probability density of (x_1, x_2) given that the particle is hit by the IUR random plane. Note that $h(x_1, x_2 \mid \uparrow)$ is obtained from the unconditional probability density $h(x_1, x_2)$ using weighting by the particle mean width, i.e.

$$h(x_1, x_2 \mid \uparrow) = \frac{\bar{b}(K_0(x_1, x_2))}{\int \bar{b}(K_0(w_1, w_2))h(w_1, w_2)\mathrm{d}w_1\mathrm{d}w_2} h(x_1, x_2); \qquad (6.9)$$

hence, (6.8) is equivalent to (6.5).

In stereological literature at most two parameters (size-shape factor, size-orientation) have been typically investigated. Theoretically the problems lead to Abel type integral equations which can occasionally be solved analytically, cf. [19] for size-shape distribution of spheroids or [37] for size-orientation distribution of circular plates. For these and also for more difficult problems (e.g. size-number of vertices for polyhedra, size-shape of prisms) numerical methods are developed, cf. [85]. Moreover, if the function $\boldsymbol{p}$ in (6.5) is hard to be derived analytically, its discrete version is recommended to be obtained by means of simulations.

For the purpose of a numerical solution of unfolding problems, data are grouped into classes (naturally obtained when using an image analyser for the measurement of planar sections). The integral equation (6.4) is transformed to a system of linear equations which are solved by means of an iterative EM-algorithm. This well-known method in statistics was first used in stereology by Silverman et al. [106], later systemically by [86]. EM-algorithm has the following advantages:

(i) it converges quickly to a nonnegative solution (estimator of the desired distribution);

(ii) the method is nonparametric histogram-based.

On the other hand, the solution may not be unique, it depends on an initial iteration. However, the common use of a given planar histogram as an initial iteration is unifying and verified in practice.

Further important issues concerning unfolding methods may be found in the literature: quantification of ill-posedness by the magnitude of condition numbers of the matrix of corresponding linear equations (Gerlach & Ohser [35]), variances of the estimates under the Poisson assumption (Ohser & Sandau [87]). The latter paper yields the most thorough analysis of these aspects for the Wicksell corpuscule problem and its variants, including thin sections and linear probes. It shows that condition numbers are reasonably small and that the relative error of estimation can be split into two parts. One part consists of the relative discretization

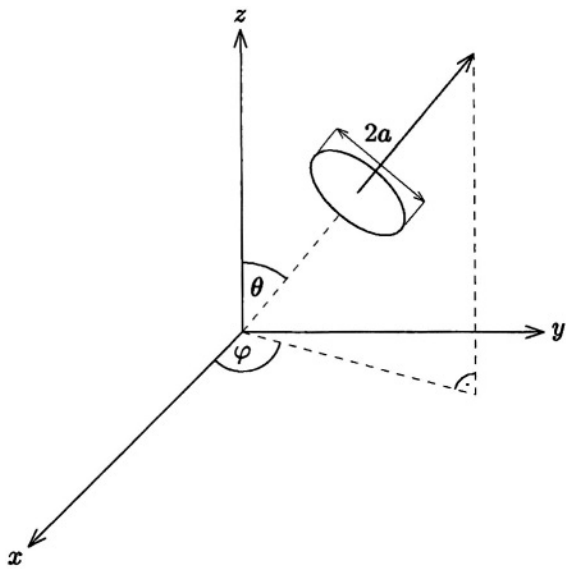

Figure 6.2. A circular plate oriented in spherical coordinates.

error that increases with increasing class size and the second part is the relative statistical error which decreases with increasing class size.

EXERCISE 6.4 *Derive formula* (6.4). *Hint: Use Proposition 6.1.*

EXERCISE 6.5 *Derive formula* (6.7).

6.2. Bivariate unfolding

To demonstrate the approach from Section 6.1, a bivariate problem is solved. While the size-shape problems are reviewed in [86], a solution of a size-orientation problem is presented in detail here. For this purpose vertical sections, cf. Chapter 4, are applied. The IUR sampling design can be used only for inferring rotation invariant particle characteristics (size, shape), whereas the VUR sampling design makes it possible to obtain information on the direction (orientation) as well.

6.2.1 Platelike particles

Let Φ be a stationary particle process in $\mathbb{R}^3$ with intensity N_V and primary grain being a *circular plate* of zero thickness, random radius $a > 0$ and normal direction (θ, ϕ), see Fig. 6.2. Here $\theta \in [0, \frac{\pi}{2}]$ is the latitude (angle between the plate normal and a fixed vertical axis) and $\phi \in [0, 2\pi)$ the longitude. Assume that there exists a joint probability density function h_1 of a, θ, ϕ, with respect to the measure $\sin\theta \mathrm{d}\theta \mathrm{d}\phi \mathrm{d}a$,

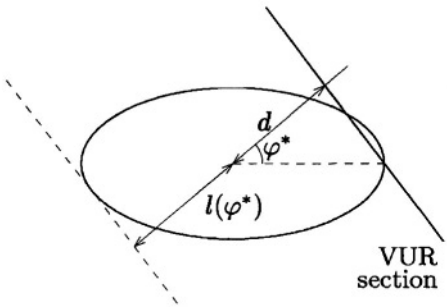

Figure 6.3. Projected platelike particle and its VUR section (thick line).

and denote

$$h(a,\theta) = \frac{1}{2\pi}\int_0^{2\pi} h_1(a,\theta,\phi)\,\mathrm{d}\phi$$

the joint probability density function of the radius a and angle θ. Note that h is nonnegative with

$$\int\int h(a,\theta)\sin\theta \mathrm{d}\theta \mathrm{d}a = 1.$$

In a vertical uniform random section plane, particle sections are observed as segments of length $2A > 0$ and forming an angle $\alpha \in [0, \frac{\pi}{2}]$ with the vertical axis.

Let N_A be the intensity (mean number of particle sections per unit area) and $g(A,\alpha)$ the density of joint distribution of A and α of the section process in the sense of Proposition 6.1 and Remark 6.2. Gokhale [37] derived an integral equation connecting h and g. First, a short proof of this result is presented.

THEOREM 6.6 *Under the notation given above, we have*

$$N_A g(A,\alpha) = N_V \frac{4}{\pi}\int_A^\infty \int_{\pi/2-\alpha}^{\pi/2} \frac{A\cos^2\theta \sin\theta h(a,\theta)\,\mathrm{d}\theta\,\mathrm{d}a}{\sin^2\alpha\sqrt{(a^2-A^2)(\sin^2\alpha-\cos^2\theta)}}, \tag{6.10}$$

for any $A > 0$ *and* $\alpha \geq \frac{\pi}{2} - \theta$.

Proof. Let a plate K_0 with parameters a, θ, ϕ be centred at the origin. A vertical uniform random section plane F is described by its distance d from the origin and longitude of its normal ϕ^*. The probability density of the distribution $\mu_Q^{K_0\uparrow}$ of vertical planes hitting the plate K_0 is

$$q(d,\phi^*) = \begin{cases} L^{-1}, & 0 \leq \phi^* \leq 2\pi,\ 0 \leq d \leq l(\phi^*) \\ 0, & \text{otherwise}, \end{cases}$$

where

$$l(\varphi) = a\sqrt{1 - \sin^2\theta \sin^2(\varphi - \phi)}$$

is the support function of the ellipse of the particle projection (in vertical direction), see Fig. 6.3, and

$$L = L(a, \theta) = \int_0^{2\pi} l(\varphi) \mathrm{d}\varphi = \pi \bar{b}(a, \theta)$$

its perimeter. The basic relations between spatial and planar parameters (see [37]) are

$$\sin(\phi^* - \phi) = \cot\theta \cot\alpha, \quad \pi/2 - \theta \leq \alpha \leq \frac{\pi}{2} \tag{6.11}$$

and

$$d = \frac{\cos\theta}{\sin\alpha}\sqrt{a^2 - A^2}, \quad 0 \leq A \leq a. \tag{6.12}$$

They define a transformation between (d, ϕ^*) and (A, α) which is one-to-one for $0 \leq \phi^* < \frac{\pi}{2}$ assuming (without loss of generality) that $\phi = 0$. Its Jacobian

$$J = \begin{vmatrix} \frac{\partial d}{\partial A} & \frac{\partial d}{\partial \alpha} \\ \frac{\partial \phi^*}{\partial A} & \frac{\partial \phi^*}{\partial \alpha} \end{vmatrix} = \frac{A}{\sqrt{a^2 - A^2}} \frac{\cos^2\theta}{\sin^2\alpha\sqrt{\sin^2\alpha - \cos^2\theta}}$$

yields the conditional density

$$p(A, \alpha \mid a, \theta) = \frac{4J}{L} = \frac{4J}{\pi \bar{b}(a, \theta)},$$

independent of ϕ. The assertion follows now by using (6.5). □

Formula (6.10) is a double Abelian integral equation the theoretical solution of which with respect to h is available, see [37]:

$$N_V h(a, \theta) = \frac{N_A}{\pi \cos^2\theta \sin\theta} \frac{\partial^2}{\partial a \partial \theta} \int_a^{\infty} \int_0^{\frac{\pi}{2} - \theta} \frac{\sin^3\alpha \cos\alpha g(A, \alpha) \mathrm{d}\alpha \mathrm{d}A}{\sqrt{\cos^2\alpha - \sin^2\theta}\sqrt{A^2 - a^2}}.$$

In practical stereology, a numerical solution is prefered to the analytical one presented. There are natural reasons for this: fast algorithms are available which deal with histograms obtained directly by automatic measurement of particle profiles (sections). The method is nonparametric while an analytical solution typically needs a parametric model for either h or g with subsequent parameter estimation and model validation.

EXERCISE 6.7 *Derive formulas* (6.11) *and* (6.12).

6.2.2 Numerical solution

In formula (6.10) put $\gamma = \pi/2 - \alpha$ in $g(A, \alpha)$ and denote A_m the upper endpoint of the support of the marginal size distribution of platelike particles (finite or infinite). Then we get after this change of variables

$$g(A,\gamma) = \frac{4AN_V}{\pi N_A \cos^2\gamma} \int_A^{A_m} \int_\gamma^{\pi/2} \frac{\cos^2\theta \sin\theta h(a,\theta)\ \mathrm{d}\theta\ \mathrm{d}a}{(a^2 - A^2)^{1/2}(\cos^2\gamma - \cos^2\theta)^{1/2}}. \tag{6.13}$$

In order to present a numerical solution we transform the equation (6.13) from the relationship between the density functions to the relationship between the distribution functions according to [15]. The right hand side of (6.13) can be transformed to

$$g(A,\gamma) = \frac{4N_V}{\pi N_A \cos^3\gamma \sin\gamma} \frac{\mathrm{d}}{\mathrm{d}A} \frac{\mathrm{d}}{\mathrm{d}\gamma} T(A,\gamma) \tag{6.14}$$

with

$$T(A,\gamma) = \int_A^{A_m} \int_\gamma^{\pi/2} s(a,A)t(\theta,\gamma)h(a,\theta)\ \mathrm{d}\theta\ \mathrm{d}a$$

and

$$\begin{aligned} s(a,A) &= (a^2 - A^2)^{1/2}, \\ t(\theta,\gamma) &= \cos^2\theta \sin\theta(\cos^2\gamma - \cos^2\theta)^{1/2}. \end{aligned}$$

In the next step we will integrate equation (6.14) with respect to the variables A, γ. We can write

$$G(A,\gamma) = \int_A^{A_m} \int_\gamma^{\pi/2} g(s,\beta)\cos^3\beta \sin\beta \mathrm{d}\beta\, \mathrm{d}s. \tag{6.15}$$

Integrating the right hand side of (6.14) as in (6.15), we get the desired equation

$$N_A G(A,\gamma) = \frac{4N_V}{\pi} \int_A^{A_m} \int_\gamma^{\pi/2} \frac{\mathrm{d}}{\mathrm{d}s} \frac{\mathrm{d}}{\mathrm{d}\beta} T(s,\beta)\mathrm{d}\beta\mathrm{d}s \tag{6.16}$$

$$= \frac{4N_V}{\pi} \int_A^{A_m} \int_\gamma^{\pi/2} s(a,A)t(\theta,\gamma)h(a,\theta)\mathrm{d}\theta\mathrm{d}a \tag{6.17}$$

In fact, G is not a distribution function corresponding to g, but we can weight the data correspondingly to the weighting in (6.15) and solve equation (6.16) with respect to h numerically.

Assume that parameters of platelike particles using VUR sampling design were observed (including the radius A_m of the largest profile and N_A). Let for discretization the number of size classes be M and the number of the orientation classes be N. Thus, one can define class limits as follows:

$$A_i = a_i = i\delta, \ \delta = A_m/M, \quad i = 1, \ldots, M;$$
$$\gamma_j = \theta_j = j\omega, \ \omega = \pi/(2N), \quad j = 1, \ldots, N.$$

Under the choice of the discretatization, the plate trace with A, γ belongs to class (i, j) if $A_{i-1} \leq A < A_i$ and $\gamma_{j-1} \leq \gamma < \gamma_j$. In this way we can classify input data into bivariate histogram with class limits for the size and the orientation.

Next we suppose the function $h(a, \theta)$ to be constant within each class (i, j), $h(a, \theta) = x_{ij}$ for $a_{i-1} \leq a < a_i$ and $\theta_{j-1} \leq \theta < \theta_j$. As a discrete analogue of the stereological equation (6.16), the system of linear equations is obtained:

$$y_{kl} = \sum_{i=k}^{M} \sum_{j=l}^{N} p_{ijkl} x_{ij}, \quad k = 1, \ldots, M; \ l = 1, \ldots, N. \tag{6.18}$$

Here y_{kl} is the (weighted, see (6.15)) mean number of particles in the class (k, l) and equals

$$y_{kl} = N_A \left(G(A_{k-1}, \gamma_{l-1}) - G(A_k, \gamma_{l-1}) - G(A_{k-1}, \gamma_l) + G(A_k, \gamma_l) \right),$$

and

$$x_{ij} = N_V h(a_i, \theta_j).$$

The coefficients of the system (6.18) are given by

$$\begin{aligned} p_{ijkl} \ = \ & p(i, j, k-1, l-1) - p(i, j, k, l-1) \\ & - p(i, j, k-1, l) + p(i, j, k, l), \end{aligned} \tag{6.19}$$

where

$$p(i, j, k, l) = \frac{4}{\pi} \int_{(i-1)\delta}^{i\delta} \int_{(j-1)\omega}^{j\omega} s(a, A_k) t(\theta, \gamma_l) \mathrm{d}\theta \mathrm{d}a, \ i > k, j > l, \tag{6.20}$$

and $p(i, j, k, l) = 0$ otherwise.

In order to solve the linear equation system (6.18) the EM algorithm was used in [15]. Suppose that $\mathbf{y}$ is the matrix of incomplete data obtained by planar sampling and $\mathbf{x}$ represents the matrix of parameters to

be estimated. Let z_{ijkl} be the number of events occuring in the class (i,j) which contribute to the counts in the class (k,l). Define

$$t_{ij} = \sum_{k=1}^{M}\sum_{l=1}^{N} p_{ijkl}, \qquad r_{kl}^{(\lambda)} = \sum_{i=1}^{M}\sum_{j=1}^{N} p_{ijkl} x_{ij}^{(\lambda)},$$

where $x_{ij}^{(\lambda)}$ is the λ-th iteration of x_{ij}. Each iteration of the EM-algorithm has theoretically two steps. The E-step evaluates the expected value of z_{ijkl} given input data $\mathbf{y}$ under the current estimate $\mathbf{x}^{(\lambda)}$ of the parameter matrix $\mathbf{x}$ as

$$\bar{z}_{ijkl} = x_{ij}^{(\lambda)} y_{kl} \frac{p_{ijkl}}{r_{kl}^{(\lambda)}}. \tag{6.21}$$

The M-step yields a maximum likelihood estimate of the parameter $\mathbf{x}$ using the estimated data $\bar{z}_{ijkl}$ from the E-step, i.e.

$$x_{ij}^{(\lambda+1)} = \frac{1}{t_{ij}} \sum_{k=1}^{M}\sum_{l=1}^{N} z_{ijkl}. \tag{6.22}$$

Combining these two steps we get an EM iteration given by the updating formula

$$x_{ij}^{(\lambda+1)} = \frac{x_{ij}^{(\lambda)}}{t_{ij}} \sum_{k=1}^{M}\sum_{l=1}^{N} \frac{y_{kl} p_{ijkl}}{r_{kl}^{(\lambda)}}, \quad i = 1,\ldots,M;\ j = 1,\ldots,N. \tag{6.23}$$

Equation (6.23) produces a sequence $x_{ij}^{(\lambda)}$ of solutions for the matrix of parametres $\mathbf{x}$. As an initial iteration it is set $x_{ij}^{(0)} = y_{ij}$. This choice of nonnegative initial values ensures that each of $\mathbf{x}$ is nonnegative.

EXERCISE 6.8 *Write down the EM-algorithm for the histogram solution of the Wicksell corpuscule problem in Example 6.3.*

EXERCISE 6.9 *Simulate a realization of a Poisson process of spherical particles of equal size in a bounded window in space. Use a test plane to obtain a sample of section profiles radii. Use previous exercise to unfold the true radius distribution.*

6.2.3 Analysis of microcracks in materials

In the applications in materials science, the platelike particles can be used as a model for extremely flat particles, but also as a model for cracks in material under loading. Consider the following experiment from School of Materials Science and Engineering, Georgia Institute of

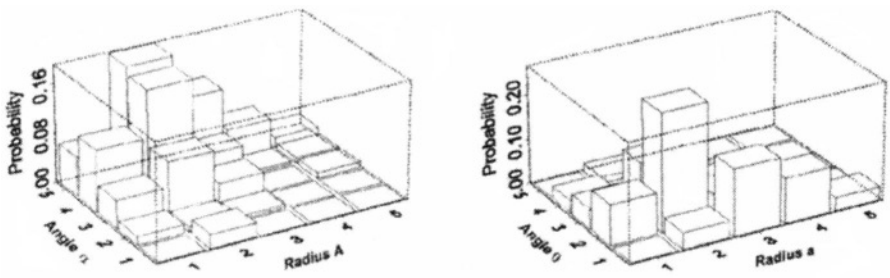

Figure 6.4. Left: The bivariate size and orientation planar distribution of observed microcrack traces in the composite Al5086 under tension. Right: The estimated bivariate size and orientation distribution of true microcrack radii with the density of microcracks $N_V = 2.52 \cdot 10^5 \mathrm{mm}^{-3}$.

Technology, Atlanta. The composites A15086 and Al6061 are described in [15]. The specimens of composites are loaded and microcracks appear in particle reinforcement. Metallographic samples were prepared and measured by means of an image analyser. Using the model of platelike microcracks, the EM algorithm is used to estimate the true bivariate size-orientation distribution. In the study, 5 classes of the radius and 5 classes of the angle (in $[0, \frac{\pi}{2})$) are chosen of equal size, the number of iterations of the EM algorithm is 16.

For the composite Al5086, a sample with tension strain 9.76% is evaluated. The total number of observed microcrack traces is 221, $N_A = 151\ \mathrm{mm}^{-2}$, radius of largest profile $A_m = 0.00238\,\mathrm{mm}$. The data and resulting estimator are in Fig. 6.4, classes are enumerated. For the composite Al6061, a sample was exposed to compression with the value of strain 70%. The total number of observed microcracks is 228, $N_A = 218\,\mathrm{mm}^{-2}$, $A_m = 0.00345\,\mathrm{mm}$. The observed and estimated bivariate size-orientation distributions are plotted in Fig. 6.5. The conclusion of this study is that expected results were obtained. The composite specimen under tensile test yields a typical graph of the marginal crack orientation with distribution concentrated at small angles θ, while the compressed specimen results in the marginal crack orientation distribution concentrated at large angles θ, see Fig. 6.6 left, right, respectively.

6.3. Trivariate unfolding

In this subsection, the integral equation for the trivariate unfolding problem of size, shape factor and orientation of spheroidal particles is derived. The method from Section 6.1 is used again, first an intersection

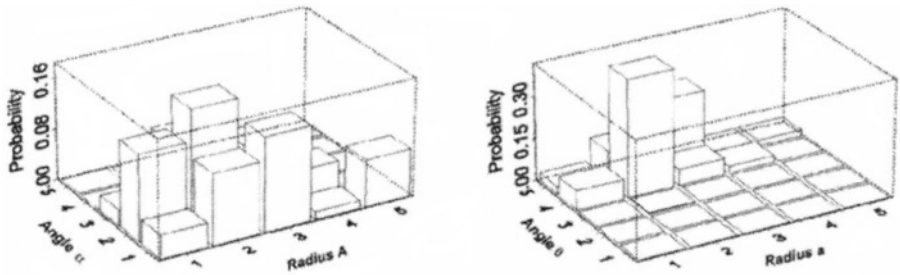

Figure 6.5. Left: The bivariate size and orientation planar distribution of observed microcrack traces in the composite Al6061 under compression. Right: The estimated bivariate size and orientation distribution of microcracks in 3D in the composite Al6061 with the density of microcracks $N_V = 3.21 \cdot 10^5 \mathrm{mm}^{-3}$.

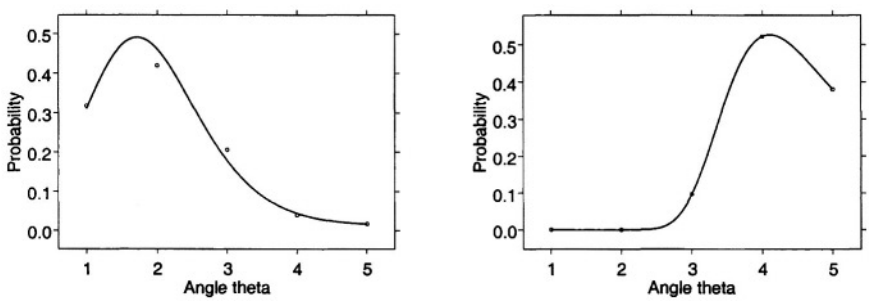

Figure 6.6. Left: Estimated and true marginal distribution of the orientation in 3D. Size and orientation distribution of microcracks of Al5086 under tension. Right: Estimated and true marginal distribution of the orientation in 3D. Size and orientation distribution of microcracks of the composite Al6061 under compression.

of a particle and planar probe is characterized. Since the orientation (direction) of particles is among parameters of interest, the IUR sampling is insufficient for this purpose. Instead, the VUR sampling design enables an elegant theoretical solution in an integral equation form (6.4). We present both the oblate and prolate case since interesting conditional dependence relations arise among parameters which lead to an application of upper, lower Frechet bound [33], respectively. Concerning the numerical solution in [13] it was recommended to proceed in steps (decomposing the trivariate equation in a sequence of two simpler integral equations), whereas here a single trivariate equation is presented which can be solved numerically easily.

An arbitrary ellipsoid in the Euclidean space $\mathbb{R}^3$ can be expressed by means of a symmetric positive definite square matrix $\mathcal{W}$ of type 3×3. The ellipsoid E attached to the matrix $\mathcal{W}$ and centred at the origin of a coordinate system is the set

$$E = \{u \in \mathbb{R}^3 : u\mathcal{W}^{-1}u' \leq 1\}, \tag{6.24}$$

where $\mathcal{W}^{-1}$ is the inverse matrix to $\mathcal{W}$ and u' is the transposed vector u. The matrix $\mathcal{W}$ can be expressed in the form $\mathcal{W} = \mathcal{O}\mathcal{D}\mathcal{O}'$ with an orthogonal matrix $\mathcal{O}$ (the columns of $\mathcal{O}$ correspond to the orientation vectors of the principal semiaxes) and a diagonal matrix $\mathcal{D}$ (the diagonal elements are the square lengths of the semiaxes of E.

Consider now an ellipsoid $x + E$, given by a matrix $\mathcal{W} = (w_{ij})$, $i, j = 1, 2, 3$, which is centred in a point $x = (x_1, x_2, x_3) \in \mathbb{R}^3$. Let L_0 denote the plane $x_1 = 0$, and consider the intersection of $x + E$ with L_0. The following result is a special case of [78, Lemma 2.1]:

LEMMA 6.10 *The intersection* $(x + E) \cap L_0$ *is nonempty if and only if*

$$e = 1 - \frac{x_1^2}{w_{11}} \geq 0. \tag{6.25}$$

Denote $y = \begin{pmatrix} x_2 \\ x_3 \end{pmatrix} - \begin{pmatrix} w_{21} \\ w_{31} \end{pmatrix} \frac{x_1}{w_{11}}$ *and*

$$\mathcal{W}_{22.3} = \begin{pmatrix} w_{22} & w_{23} \\ w_{23} & w_{33} \end{pmatrix} - \frac{1}{w_{11}} \begin{pmatrix} w_{21} \\ w_{31} \end{pmatrix} (w_{21} \; w_{31}) \; .$$

Then for $e \geq 0$ *we have*

$$(x + E) \cap L_0 = \{(0, v) : v \in \mathbb{R}^2, (v - y)\mathcal{W}_{22.3}^{-1}(v - y)' \leq e\}. \tag{6.26}$$

Moreover, the length of the orthogonal projection of $x + E$ *onto the* x_1*-axis is equal to* $2\sqrt{w_{11}}$.

6.3.1 Oblate spheroids

Let the primary grain of a particle process be an oblate spheroid E with semiaxes $a = b > c$ centred in the origin. The direction of the axis of rotation is (θ, ϕ). Let a vertical section plane F have normal orientation $(\pi/2, \phi^*)$ in spherical coordinates and distance d from the origin. Under the condition that the particle is hit by F, denote the semiaxes of the intersection ellipse (6.26) by A, C, $A \geq C$, and by α the angle between the semiaxis A and vertical axis (it is correctly defined whenever $C \neq A$), see Fig. 6.7.

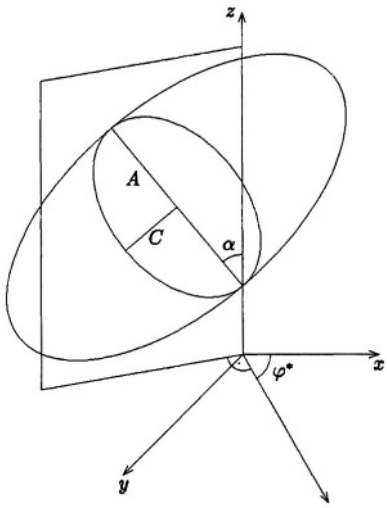

Figure 6.7. A vertical uniform random planar section of an oblate spheroid

DEFINITION 6.11 *The shape factors* s, S *of the particle, its section, are defined as*

$$s = \frac{c}{a}, \quad S = \frac{C}{A},$$

respectively.

Clearly $0 < s \leq 1$ and $0 < S \leq 1$.

LEMMA 6.12 *The spatial and planar parameters of a vertical section of a spheroid are related as*

$$\sin(\phi^* - \phi) = \cot\theta \cot\alpha \tag{6.27}$$

$$d = \frac{s\sqrt{a^2 - A^2}}{S} \tag{6.28}$$

$$A = a\sqrt{1 - \frac{d^2}{w_{11}^*}}, \tag{6.29}$$

where

$$w_{11}^* = a^2 - (a^2 - c^2)\sin^2\theta\cos^2(\phi^* - \phi). \tag{6.30}$$

Proof. Follows from Lemma 6.10 after a careful but straightforward calculation. □

We proceed by calculating the conditional densities for size-orientation and size-shape problem. Denote

$$\mathcal{E}(\beta, z) = \int_0^\beta \sqrt{1 - z^2\sin^2\varphi}\,\mathrm{d}\varphi$$

the elliptic integral of second kind, specially $\mathcal{E}(\frac{\pi}{2}, z) = \mathcal{E}(z)$.

PROPOSITION 6.2 *Under the vertical uniform random sampling design, the conditional distributions of particle section parameters for the size-orientation, size-shape unfolding problem have densities, respectively,*

$$p_1(A, \alpha \mid a, \theta, s) = \frac{4}{L} \frac{A}{\sqrt{a^2 - A^2}} \frac{\cos\theta}{\sin\alpha} \sqrt{\frac{1 - (1 - s^2)(\sin^2\theta - \cos^2\theta \cot^2\alpha)}{\sin^2\theta - \cos^2\alpha}} \quad (6.31)$$

for $\pi/2 - \theta \leq \alpha \leq \pi/2$ *and* $0 \leq A \leq a$, *and* $p_1 = 0$ *otherwise, and*

$$p_2(A, S \mid a, \theta, s) = \frac{4}{L} \frac{A}{\sqrt{a^2 - A^2}} \frac{s}{S^2} \left((1 - \frac{S^2}{s^2})(S^2 \sin^2\theta + \frac{S^2}{s^2} \cos^2\theta - 1) \right)^{-\frac{1}{2}} \quad (6.32)$$

for

$$s \leq S \leq \frac{s}{\sqrt{s^2 \sin^2\theta + \cos^2\theta}}, \quad 0 \leq A \leq a,$$

and $p_2 = 0$ *otherwise. Here*

$$L = \pi \bar{b}(a, \theta, s) = 4a\mathcal{E}(\sqrt{1 - s^2} \sin\theta)$$

is the perimeter of the ellipse of particle projection (in vertical direction) and $\bar{b}(a, \theta, s)$ *its mean width.*

Proof. Consists of the evaluation of Jacobians analogously to the proof of Theorem 6.6. For the size-orientation problem we start from formula (6.27) and

$$d = \sqrt{a^2 - A^2} \sqrt{1 - (1 - s^2)(\sin^2\theta - \cos^2\theta \cot^2\alpha)},$$

for the size-shape problem we start from formula (6.28) and

$$\sin(\phi^* - \phi) = \sqrt{1 - \frac{\frac{s^2}{S^2} - 1}{(s^2 - 1)\sin^2\theta}},$$

obtained from (6.27)-(6.30). □

The main result of this subsection is the following theorem concerning the unfolding problem (6.5) of the size-shape-orientation distribution. Let $h(a, \theta, s)$, $g(A, \alpha, S)$ be the probability densities of spatial and planar

parameters, respectively, H, G the corresponding distribution functions. Further denote

$$D(\alpha,\theta)=\frac{\sqrt{\sin^2\alpha-\cos^2\theta}}{\sin\theta\sin\alpha}$$

and

$$B(s,\theta)=\sin\theta\sqrt{1-s^2}.$$

THEOREM 6.13 *Consider the sampling design of vertical uniform random sections. Then*

$$N_A G(A,\alpha,S)=\frac{4}{\pi}N_V\int_A^\infty\int\int(a-\sqrt{a^2-A^2})K_0(\alpha,S,\theta,s)\mathrm{d}H(a,\theta,s), \tag{6.33}$$

where

$$K_0(\alpha,S,\theta,s)=\min\{K_1(\alpha,\theta,s),K_2(S,\theta,s)\}. \tag{6.34}$$

Here for each fixed θ,s,

$$K_1(\alpha,\theta,s)=\begin{cases}\mathcal{E}(\arcsin D(\alpha,\theta),B(s,\theta)), & \pi/2-\theta\le\alpha\le\pi/2,\\ 0, & \alpha<\pi/2-\theta\end{cases}$$

and

$$K_2(S,\theta,s)=$$

$$=\begin{cases}\mathcal{E}(\arcsin(\frac{1}{B(s,\theta)}\sqrt{1-\frac{s^2}{S^2}}),B(s,\theta)), & s\le S\le\frac{s}{\sqrt{s^2\sin^2\theta+\cos^2\theta}},\\ 0, & S<s,\\ \mathcal{E}(B(s,\theta)), & \textit{otherwise.}\end{cases}$$

Proof. First observe from (6.31), (6.32) the conditional independence of A and α, (A and S), respectively, given the particle parameters. On the other hand, from formulas (6.27), (6.28) in Lemma 6.12 it follows that for fixed θ,s

$$S=S(\alpha)=s[1+(s^2-1)(\sin^2\theta-\cos^2\theta\cot^2\alpha)]^{-1/2}, \tag{6.35}$$

which means that orientation and shape factor are conditionally functionally dependent (given particle parameters). Therefore, the joint conditional density $p(\alpha,S\mid\theta,s)$ is degenerate and we proceed in terms of distribution functions. Observe that the transformation $S(\alpha)$ in (6.35) is monotone increasing on $[0,\frac{\pi}{2}]$ for each fixed s,θ. Therefore (see [76]) the joint conditional distribution function

$$P(\alpha,S\mid\theta,s)=\frac{K_0(\alpha,S,\theta,s)}{\mathcal{E}(B(s,\theta))}$$

is equal to the upper Frechet bound [33] of marginal conditional distribution functions

$$\frac{K_1(\alpha,\theta,s)}{\mathcal{E}(B(s,\theta))},\quad \frac{K_2(S,\theta,s)}{\mathcal{E}(B(s,\theta))},$$

which implies (6.34). The functions K_1 and K_2 are obtained from (6.31), (6.32):

$$K_1(\alpha,\theta,s)=\int_{\frac{\pi}{2}-\theta}^{\alpha}\frac{\cos\theta}{\sin\beta}\sqrt{\frac{1-(1-s^2)(\sin^2\theta-\cos^2\theta\cot^2\beta)}{\sin^2\theta-\cos^2\beta}}\mathrm{d}\beta,$$

and

$$K_2(S,\theta,s)=\int_s^S\frac{s}{T^2}\left((1-\frac{T^2}{s^2})(T^2\sin^2\theta+\frac{T^2}{s^2}\cos^2\theta-1)\right)^{-1/2}\mathrm{d}T.$$

Although the independence does not follow from the pairwise independence, here thanks to conditional functional dependence of S and α we have the trivariate conditional distribution function

$$P(A,\alpha,S\mid a,\theta,s)=(1-\frac{\sqrt{a^2-A^2}}{a})P(\alpha,S\mid\theta,s).$$

Now from Propositions 6.1, 6.2 and formula (6.4) we obtain (6.33). □

EXERCISE 6.14 *Derive formulas* (6.27), (6.28), (6.29). *Hint: Use Lemma 6.10.*

EXERCISE 6.15 *Evaluate Jacobians for the proof of Proposition 6.2.*

6.3.2 Prolate spheroids

Consider now a system of prolate spheroids with semiaxes $a>b=c$ under the same notation as in the previous subsection. The unfolding problem for joint distribution of spatial parameters from planar parameters can be solved in an analogous way to the oblate case when replacing in the analysis a, A by the shorter semiaxes c, C. In fact, the triplet c,θ,s yields the same information as a,θ,s. Therefore, the solution of the unfolding problem between joint probability densities $h(c,\theta,s)$ and $g(C,\alpha,S)$ of spatial, planar parameters, respectively, is satisfactory for practical application.

Let the primary grain be a prolate spheroid E centred in the origin. The following lemma is derived again from Lemma 6.10.

LEMMA 6.16 *The spatial and planar parameters of a vertical section of given spheroid are related as*

$$\sin(\phi^* - \phi) = \cot\theta \tan\alpha \tag{6.36}$$

$$d = \frac{S\sqrt{c^2 - C^2}}{s} \tag{6.37}$$

$$C = c\sqrt{1 - \frac{d^2}{w_{11}}}, \tag{6.38}$$

where now

$$w_{11} = c^2 + (a^2 - c^2)\sin^2\theta\cos^2(\phi^* - \phi). \tag{6.39}$$

We proceed analogously to the previous subsection, size is represented by smaller semiaxes. Denote

$$\mathcal{Z}(s,\theta) = 1 + (s^{-2} - 1)\sin^2\theta, \quad M(s,\theta) = \sqrt{\frac{\mathcal{Z}(s,\theta) - 1}{\mathcal{Z}(s,\theta)}}.$$

PROPOSITION 6.3 *Under the vertical uniform random sampling design, the conditional distributions of particle section parameters for the size-orientation, size-shape unfolding problem have densities, respectively,*

$$p_1(C, \alpha \mid c, \theta, s) \tag{6.40}$$
$$= \frac{4}{L}\frac{C}{\sqrt{c^2 - C^2}}\frac{\cos\theta}{\cos\alpha}\sqrt{\frac{1 + (s^{-2} - 1)(\sin^2\theta - \cos^2\theta\tan^2\alpha)}{\sin^2\theta - \sin^2\alpha}},$$

for $0 \le \alpha \le \theta$ *and* $0 \le C \le c$, *and* $p_1 = 0$ *otherwise, and*

$$p_2(C, S \mid c, \theta, s) = \frac{4}{L}\frac{C}{\sqrt{c^2 - C^2}}\frac{S^2}{s}\left((S^2 - s^2)(\sin^2\theta + s^2\cos^2\theta - S^2)\right)^{-1/2}, \tag{6.41}$$

for $s \le S \le \sqrt{s^2\cos^2\theta + \sin^2\theta}$, $0 \le C \le c$, *and* $p_2 = 0$ *otherwise. Here*

$$L = \pi\bar{b}(a,\theta,s) = 4c\mathcal{Z}(s,\theta)\mathcal{E}(M(s,\theta))$$

is the perimeter of the ellipse of particle projection (in vertical orientation) and $\bar{b}(a,\theta,s)$ *its mean width.*

Proof. Consists of the evaluation of Jacobians analogously to Proposition 6.2. For the size-orientation problem we start from formula (6.36) and

$$d = \sqrt{c^2 - C^2}\sqrt{1 + (s^{-2} - 1)(\sin^2\theta - \cos^2\theta\tan^2\alpha)},$$

for the size-shape problem we start from formula (6.37) and

$$\cos(\phi^* - \phi) = \sqrt{\frac{S^2 - s^2}{(1 - s^2)\sin^2\theta}}, \tag{6.42}$$

obtained from (6.36)-(6.39). □

Concerning the unfolding problem of size-shape-orientation distribution we get the following result.

THEOREM 6.17 *Consider the sampling design of vertical uniform random sections. Then in the prolate case*

$$N_A\, G(C, \alpha, S) = \frac{4}{\pi} N_V \int_C^\infty \int\int (c - \sqrt{c^2 - C^2}) K_0(\alpha, S, \theta, s) \mathrm{d}H(c, \theta, s), \tag{6.43}$$

where

$$K_0(\alpha, S, \theta, s) = \max\{0, K_1(\alpha, \theta, s) + K_2(S, \theta, s) - \sqrt{\mathcal{Z}(s,\theta)}\mathcal{E}(M(s,\theta))\}. \tag{6.44}$$

Here for each fixed θ, s,

$$K_1(\alpha, \theta, s) = \begin{cases} \sqrt{\mathcal{Z}(s,\theta)}\mathcal{E}(\arcsin(\cot\theta\tan\alpha),\ M(s,\theta)), & 0 \le \alpha \le \theta, \\ K_1(\alpha,\theta,s) = \sqrt{\mathcal{Z}(s,\theta)}\mathcal{E}(M(s,\theta)), & \alpha > \theta, \end{cases}$$

and

$$\begin{aligned} K_2(S,\theta,s) &= \sqrt{\mathcal{Z}(s,\theta)}\mathcal{E}\left(\arcsin\left(\frac{1}{M(s,\theta)}\sqrt{1 - \frac{s^2}{S^2}}\right),\ M(s,\theta)\right) \\ &\quad - \sqrt{1 - \frac{s^2}{S^2}}\sqrt{\mathcal{Z}(s,\theta) - \frac{S^2}{s^2}} \end{aligned}$$

for

$$s \le S \le \sqrt{s^2\cos^2\theta + \sin^2\theta},$$

$K_2(S,\theta,s) = 0$ *for* $S < s$ *and* $K_2(S,\theta,s) = \sqrt{\mathcal{Z}(s,\theta)}\mathcal{E}(M(s,\theta))$ *otherwise.*

Proof. From (6.40), (6.41) we have the conditional independence of C and α, *(*C and S*)* given particle parameters, respectively.

From formulas (6.36)-(6.38) in Lemma 6.16 it follows that for fixed θ, s,

$$S = S(\alpha) = \sqrt{s^2 + (1 - s^2)(\sin^2\theta - \cos^2\theta\tan^2\alpha)}, \tag{6.45}$$

which means that orientation and shape factor are conditionally functionally dependent and the joint conditional density $p(\alpha, S \mid \theta, s)$ is degenerate. Observe that the transformation $S(\alpha)$ in (6.45) is monotone decreasing on $[0, \frac{\pi}{2}]$ for each fixed s, θ. Again by [76], the joint conditional distribution function

$$P(\alpha, S \mid \theta, s) = \frac{K_0(\alpha, S, \theta, s)}{\sqrt{Z(s,\theta)\mathcal{E}(M(s,\theta))}}$$

is equal to the lower Frechet bound of marginal conditional distribution functions

$$\frac{K_1(\alpha, \theta, s)}{\sqrt{Z(s,\theta)\mathcal{E}(M(s,\theta))}}, \quad \frac{K_2(S, \theta, s)}{\sqrt{Z(s,\theta)\mathcal{E}(M(s,\theta))}},$$

which implies (6.44). The functions K_1, K_2 follow from (6.40), (6.41):

$$K_1(\alpha, \theta, s) = \int_0^\alpha \frac{\cos\theta}{\cos\beta}\sqrt{\frac{1 + (s^{-2} - 1)(\sin^2\theta - \cos^2\theta\tan^2\beta)}{\sin^2\theta - \sin^2\beta}}\mathrm{d}\beta,$$

and

$$K_2(S, \theta, s) = \int_s^S \frac{T^2}{s}[(T^2 - s^2)(\sin^2\theta + s^2\cos^2\theta - T^2)]^{-1/2}\mathrm{d}T.$$

The last integral was found in [42], p.261. Combining this with independence of C we obtain (6.43) from (6.4) as in Theorem 6.13. □

EXERCISE 6.18 *Derive formulas* (6.36), (6.37), (6.38). *Hint: Use Lemma 6.10.*

EXERCISE 6.19 *Evaluate Jacobians for the proof of Proposition 6.3.*

6.3.3 Trivariate unfolding, EM algorithm

In Sections 6.3.1 and 6.3.2, integral equations were derived for the evaluation of the joint distribution of spatial parameters (size, shape factor, orientation) of either oblate or prolate spheroidal particles. A numerical solution of these equations is presented which is based on standard discretization techniques [19, 85]. In this way the integral equation is transformed into a system of linear equations which are solved using the EM-algorithm. The method is described further in terms of oblate spheroids, in the prolate case one can proceed analogously.

Both planar and spatial parameters will be grouped into a trivariate histogram with class limits for size, shape factors and orientations (we assume for simplicity that the number of classes for each parameter is the same, which need not be the case in general):

$$a_i, A_i, \theta_i, \alpha_i, s_i, S_i, \ i = 1, ..., r.$$

In the discrete approximation it is assumed that

$$H(i,j,k) = P(a = a_i, \theta = \theta_j, s = s_k),\ i,j,k = 1,..,r,$$

are probabilities of discrete values of spatial parameters. Denote

$$N_V(i,j,k) = N_V\, H(i,j,k);$$

thus

$$\sum_{i,j,k} N_V(i,j,k) = N_V.$$

Further, we write $N_A(i,j,k)$ for the input frequency histogram of observed particle section parameters in the class ijk

$$A_{i-1} < A \le A_i,\ \alpha_{j-1} < \alpha \le \alpha_j,\ S_k < S \le S_{k-1}$$

normalized in a way that

$$\sum_{i,j,k} N_A(i,j,k) = N_A$$

holds. Recall that N_A is the mean particle section number per unit area of VUR planar probes.

The stereological unfolding consists of the estimation of the spatial distribution $N_V(i,j,k)$ given $N_A(i,j,k)$.

Using Theorem 6.13, the function K in (6.4) for oblate spheroids is, cf. (6.33)

$$K(A,\alpha,S,a,\theta,s) = \frac{4}{\pi}(a - \sqrt{a^2 - A^2})K_0(\alpha,S,\theta,s).$$

Since K is derived from a conditional distribution function P, its discrete form for each class of section parameters given the particle parameters is

$$\begin{aligned} p_{ijklmn} &= K(A_l,\alpha_m,S_n,a_i,\theta_j,s_k) - K(A_{l-1},\alpha_{m-1},S_{n-1},a_i,\theta_j,s_k) \\ &+ K(A_l,\alpha_{m-1},S_{n-1},a_i,\theta_j,s_k) - K(A_{l-1},\alpha_m,S_n,a_i,\theta_j,s_k) \\ &- K(A_l,\alpha_m,S_{n-1},a_i,\theta_j,s_k) + K(A_{l-1},\alpha_m,S_{n-1},a_i,\theta_j,s_k) \\ &- K(A_l,\alpha_{m-1},S_n,a_i,\theta_j,s_k) + K(A_{l-1},\alpha_{m-1},S_n,a_i,\theta_j,s_k). \end{aligned}$$

Then the discrete version of formula (6.33) is

$$N_A(l,m,n) = \sum_{i,j,k} p_{ijklmn} N_V(i,j,k). \tag{6.46}$$

The EM-algorithm has **λ-th** iteration step

$$N_V^{(\lambda+1)}(i,j,k) = \frac{N_V^{(\lambda)}(l,j,k)}{t_{ijk}} \sum_{l,m,n} \frac{N_A(l,m,n)p_{ijklmn}}{r_{lmn}^{\lambda}}, \qquad (6.47)$$

where

$$t_{ijk} = \sum_{l,m,n} p_{ijklmn},$$

and

$$r_{lmn}^{\lambda} = \sum_{i,j,k} N_V^{(\lambda)}(i,j,k)p_{ijklmn}.$$

As an initial iteration $N_V^{(0)}(i,j,k) = N_A(i,j,k)$ is again appropriate. Iterations (6.47) converge rapidly to the desired estimator $\hat{N}_V(i,j,k), i,j,k = 1,\ldots,r$ of spatial size-shape-orientation distribution.

6.3.4 Damage initiation in aluminium alloys

In the materials research, the connection between microstructure and properties of materials is studied. The information about hard opaque materials is typically obtained from a single planar section of material specimen. Therefore, stereological methods described above are desired in metallography to quantify the microstructural geometry.

In the forthcoming study the developed method for the unfolding of particle size-shape-orientation distribution is used. The material under investigation is an AlSi alloy with aluminium matrix and silicon particles. The production of the material is described in detail in [13]. Except of a very small number, the particle shapes can be approximated by oblate spheroids. Uniaxial tensile tests using cylindrical specimens were carried out. Brittle particles embedded in ductile matrix do not deform plastically and particle cracking has been expected during deformation. In order to study the damage of particles metallographical samples were prepared on two levels of strain: non-deformed and deformed up to fracture (strain 20%). The samples were cut randomly parallel to tensile specimen axis to follow the VUR sampling design. Thus the orientation of the vertical axis has a clear physical interpretation here. A micrograph of the sample cut from non-deformed material is in Fig. 6.8.

Quantitative metallographical analysis has been performed in the Research Institute for Metals, **Panenské Břežany.** The input data were obtained using IBAS-Kontron image analyser connected to a light microscope. The discretization of parameters used is the following:

$$a_j = A_j = b^j,\ j \in \mathbb{Z},\ \ s_i = S_i = (1 - \frac{i}{r})^{\kappa},\ \ \gamma_i = \theta_i = i\triangle,\ i = 1,..,r. \qquad (6.48)$$

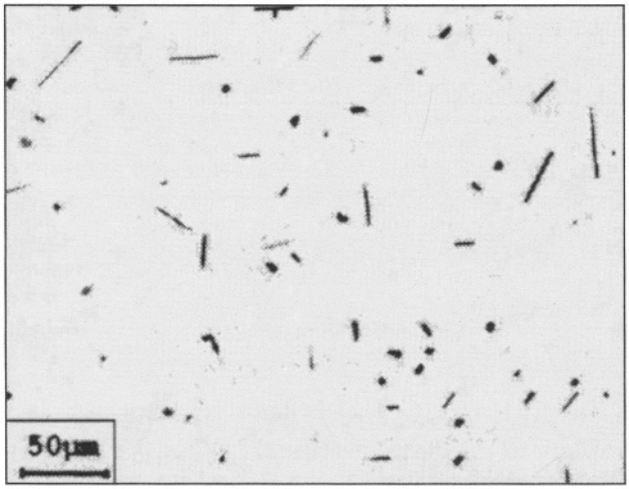

Figure 6.8. Micrograph of a polished metallographical sample of an AlSi specimen in a non-deformed state.

Here $b > 1$, $\kappa > 0$ are given constants, r the number of classes, $\Delta = \frac{\pi}{2r}$. The exponentially increasing limits for size classes have storage advantages described in [85]. Notice that classes of colatitude θ in (6.48) correspond to areas on the hemisphere of spatial orientations proportional to $(\cos\theta_{i-1} - \cos\theta_i)$.

The estimated trivariate distribution using (6.47) will be involved in the Weibull deformation model. Assume that the probability $\mathcal{P}$ of a fracture of a particle of volume $V = \frac{4}{3}\pi a^3 s$, orientation θ and shape factor s is governed by the formula

$$\mathcal{P} = 1 - \exp\left[-\frac{V}{V_0}\left(\frac{\sigma_p(s,\theta,\varepsilon,V)}{\sigma_0}\right)^m\right], \tag{6.49}$$

where σ_0, V_0 are constants, m the Weibull modulus, ε the applied strain and σ_p the stress in the particle. Assume that we know the stress function $\sigma_p(s,\theta,\varepsilon,V)$, a simplified model was suggested by Slámová [107]:

$$\sigma_p = \sigma_m(1 + \frac{a}{6s})\sin\theta, \tag{6.50}$$

where σ_m is the matrix tensile strength which is a known function of ε. The trivariate (s,θ,V) distribution for both populations of all and cracked particles (with intensities N_V, N_V^c, respectively) is estimated in a histogram form with classes indexed by i,j,k. Then we put

$$\mathcal{P}_{ijk} = \frac{2N_V^c(i,j,k)}{N_V(i,j,k)} \tag{6.51}$$

and estimate the parameters in (6.49) using regression techniques. Another stereological problem arises here since not all cracks are observed in the section plane. We model cracks as planar surfaces parallel to spheroid rotational axis, intersecting a particle. A simplest correction of this effect is based on the fact that a random chord on a disc has probability $\frac{1}{2}$ to be hit by another random chord (representing the section plane). This leads to the factor 2 in (6.51). A more detailed correction based on the assumption that the number of cracks per particle is a Poisson random variable is suggested in [13].

In numerical results, first spatial geometrical parameters of particles in the given material (AlSi alloy) are compared for samples of

a) all particles observed in nondeformed state (denoted 2L),

b) particle sections with at least one observed crack in the deformed state (strain 20%, denoted 2LC).

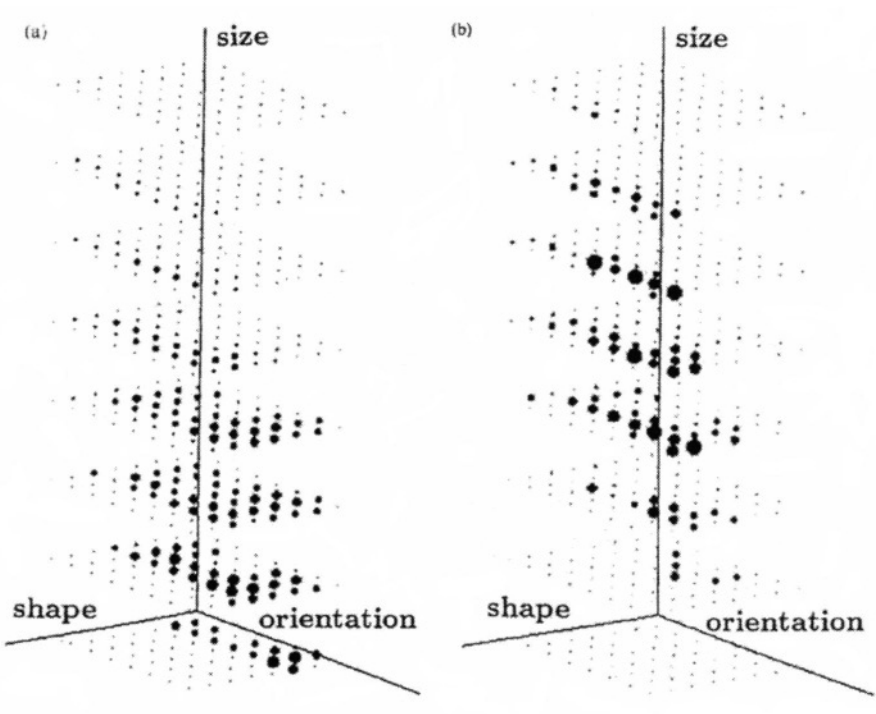

Figure 6.9. Estimated spatial size-shape-orientation histograms estimated from samples $2L$ (a), $2LC$ (b). The volume of three-dimensional balls observed is proportional to $N_V F(i, j, k)$ values. The constants of proportionality are chosen in such a way that the sums of ball volumes in each histogram coincide. The axes intersect in the point corresponding to $i = j = k = 1$.

Table 6.1. Estimated mean values, standard deviations and correlation coefficients of particle parameters

	N_V	Ea	Eθ	Es	σ_a	σ_θ	σ_s	$\varrho_{a\theta}$	ϱ_{as}	$\varrho_{\theta s}$
2L	210	2.97	1.08	0.36	2.66	0.382	0.187	-0.005	-0.431	0.07
2LC	7.25	9.22	1.15	0.122	6.89	0.34	0.116	0.018	-0.501	-0.111

The total area included in the analyses for both samples 2L, 2LC was $9.92\,\mathrm{mm}^2$. The parameters of dicretization $b = 1.75$, $\kappa = 1.5$ were chosen, number of classes $r = 8$. A sample of $n = 10,017$ particle profiles was measured among which 1,058 were observed with cracks in the deformed state. The unfolded trivariate histograms corresponding to these two samples are presented in Fig. 6.9. We observe a negative correlation between size and shape factor and comparing both histograms a natural result that larger and thinner particles tend more to cracking.

The number density N_V [mm^{-3}] estimated from measured particle sections is in Table 6.1 together with estimated expectations and standard deviations Ea [μm], Eθ, Es, σ_a, σ_θ, σ_s, of particle longer semiaxis, orientation and shape factor, respectively, and sampling correlation coefficients between pairs of these parameters: $\varrho_{a\theta}$, ϱ_{as}, $\varrho_{\theta s}$.

Finally, the probability of particle damage is evaluated. Among 1,058 particles with observed cracks only 16 times two cracks were observed and in any case more than two cracks. For the estimated spatial parameters and $\sigma_m = 45\mathrm{MPa}$ corresponding to the strain 20% using the Newton method we obtained the least squares estimator $m = 1.92$ in (6.49). This quantity is most desired by engineers to classify the damage properties of metals.

6.4. Stereology of extremes

By *stereology of extremes* we mean the unfolding problem (6.5) for particle systems with the aim to unfold extremes or quantiles of the distribution of random particle parameters. This is important in practical applications, e.g. engineers claim that the damage of materials is related to extremal rather that mean characteristics of the microstructure. While stereological relations for moments of particle parameters are known, see (6.7) and in more detail Ohser and Mücklich [86], methods for prediction of spatial extremes based on data from lower-dimensional probes still have to be developed. The first step was prediction of extreme size of spherical particles suggested by Takahashi and Sibuya [113, 114]. The theoretical background derived by Drees and Reiss [28] is based on the statistical extreme value theory (de Haan [24]). In a similar manner

recently the prediction of extremal shape factor of spheroidal particles has been investigated by Hlubinka [53].

6.4.1 Sample extremes – domain of attraction

Let K be a univariate distribution function, K^n be the n-th power of K, i.e. a distribution function of $X_{(n)}$, a maximum of n independent random variables distributed according to K.

DEFINITION 6.20 *K belongs to the domain of attraction of a distribution function $\mathfrak{K}$ if there exist normalizing constants $\{a_n\}$, $\{b_n\}$ such that for all x*

$$\lim_{n\to\infty} K^n(a_n x + b_n) = \mathfrak{K}(x), \tag{6.52}$$

where $\mathfrak{K}$ is one of the following distribution functions:

$$\mathfrak{K}_{i,\gamma}(x) = \begin{cases} \exp(-x^{-\gamma}), & x \geq 0, \quad i = 1 \ \textit{(Fréchet)} \\ \exp(-(-x)^{\gamma}), & x \leq 0, \quad i = 2 \ \textit{(Weibull)} \\ \exp(-\mathrm{e}^{-x}), & x \in \mathbb{R}, \quad i = 3 \ \textit{(Gumbel)} \end{cases} \tag{6.53}$$

and $\gamma > 0$.

We shall write $K \in \mathcal{D}(\mathfrak{K})$ if K is in the domain of attraction of $\mathfrak{K}$. $\mathfrak{K}_{3,\gamma} = \mathfrak{K}_3$ does not depend on γ.

Recall the following conditions for $K \in \mathcal{D}(\mathfrak{K})$. Denote $\omega = \sup\{x : K(x) < 1\}$ the right endpoint of the support of K. Then

$$K \in \mathcal{D}(\mathfrak{K}_{1,\gamma}) \iff \omega = +\infty, \lim_{s\to\infty} \frac{1-K(xs)}{1-K(s)} = x^{-\gamma}, x > 0$$

$$K \in \mathcal{D}(\mathfrak{K}_{2,\gamma}) \iff \omega < +\infty, \lim_{s\searrow 0} \frac{1-K(\omega - xs)}{1-K(\omega - s)} = x^{\gamma}, x > 0$$

$$K \in \mathcal{D}(\mathfrak{K}_3) \iff \lim_{s\nearrow\omega} \frac{1-K(s+xb(s))}{1-K(s)} = \mathrm{e}^{-x}, x \in \mathbb{R},$$

where b is some auxiliary function, which can be chosen such that it is differentiable for $s < \omega$, $\lim_{s\to\omega} b'(s) = 0$, and $\lim_{s\to\infty} b(s)/s = 0$ if $\omega = \infty$, or $\lim_{s\to\omega} b(s)/(\omega - s) = 0$ if $\omega < \infty$, see e.g. [24].

If the distribution K has a density k, there are sufficient conditions for K to be in $\mathcal{D}(\mathfrak{K})$. These conditions are

$$(C_{1,\gamma}): \quad x > 0, \quad \omega = +\infty, \quad \lim_{s\to\infty} \frac{k(xs)}{k(s)} = x^{-(\gamma+1)}$$

$$(C_{2,\gamma}): \quad x > 0, \quad \omega < +\infty, \quad \lim_{s\searrow 0} \frac{k(\omega - xs)}{k(\omega - s)} = x^{\gamma-1}$$

$$(C_3): \quad x \in \mathbb{R}, \quad \lim_{s\nearrow\omega} \frac{k(s+xb(s))}{k(s)} = \mathrm{e}^{-x},$$

where b is again an 'auxiliary function' which can be chosen as above.

EXERCISE 6.21 *Show that the distributions a) Gamma (with probability density* (6.65)), *b) standard Gaussian, belong to the Gumbel domain of attraction. Hint: Use condition* (C_3).

6.4.2 Normalizing constants

In the Gumbel case in (6.53) (which is followed e.g. by Gaussian, log-Gaussian or Gamma distribution), a theorem of von Mises says (see [24]):

PROPOSITION 6.4 *Let K be a distribution function with $K(x) < 1$ for all $x < \infty$, which is twice differentiable for $x > x_0$ and some x_0. Let*

$$\lim_{n\to\infty} \frac{\mathrm{d}}{\mathrm{d}x}\left[\frac{1-K(x)}{K'(x)}\right] = 0.$$

Then (6.52) *holds uniformly in $x \in \mathbb{R}$, where*

$$b_n = \inf\{x : 1 - K(x) \le 1/n\} \quad \text{and} \quad a_n = 1/nK'(b_n). \tag{6.54}$$

In general, it is not easy to express a_n, b_n by an analytical function of n. Takahashi [112] derived a simple method for the evaluation of normalizing constants in the Gumbel case which is based on finding $B > 0$, $b > 0$, $\delta > 0$ and $d \in \mathbb{R}$ such that

$$\lim_{x\to\infty} \frac{1-K(x)}{Bx^b \exp(-\delta x^d)} = 1. \tag{6.55}$$

Explicit formulas for a_n, b_n depending on B, b, δ, d are then available:

$$\begin{aligned} a_n &= \left(\frac{\log n}{\delta}\right)^{1/d-1} \frac{1}{\delta d}, \\ b_n &= \left(\frac{\log n}{\delta}\right)^{1/d} + \frac{\frac{b}{d}(\log\log n - \log\delta) + \log B}{\left(\frac{\log n}{\delta}\right)^{1-1/d} \delta d}. \end{aligned} \tag{6.56}$$

Maximum likelihood estimators (MLE) of the normalizing constants based on k largest observations are discussed in the following. Weissman [121] derived the joint density of k largest observations out of a random sample of size n. It has the form

$$f(x_1, x_2, \ldots, x_k) = a_n^{-k} \exp\left\{-\mathrm{e}^{-(x_k - b_n)/a_n} - \sum_{j=1}^{k} \frac{x_j - b_n}{a_n}\right\} \tag{6.57}$$

for Gumbel limit distribution and $x_1 \geq x_2 \geq \ldots \geq x_k$ the largest observations. Let us denote by $\bar{x}_k$ the average of k largest observations. Hence, the MLE of the normalizing constants are

$$\hat{a}_n = \bar{x}_k - x_k, \quad \hat{b}_n = \hat{a}_n \log k + x_k. \tag{6.58}$$

Based on the explicit form of normalizing constants from estimators (6.58) we can quite simply calculate the estimate from observed data. There is, however, a problem how to choose k. One should note that the Gumbel distribution is only a limit for the tail behaviour of the data and hence it should be better to use the very extremal observations. On the other hand, more observations used for the estimate usually give more precise estimate. The choice of k should be therefore balanced, taking into account these two facts.

EXERCISE 6.22 *Evaluate the normalizing constants for the distribution a) Gamma, b) standard Gaussian. Hint: Use* (6.55), (6.56).

6.4.3 Extremal size in the corpuscule problem

In the situation of Example 6.3, attention is paid to the upper tail of spherical particles radii with the distribution function H. Obviously, a large section circle radius can only be observed if the corresponding sphere radius is large, see Fig. 6.1, therefore large circle radii contain decisive information about the upper tail of H. In the model-based approach, assuming that particle centres form a stationary Poisson process marked by independent radii, Drees and Reiss [28] proved the following for the equation (6.6):

THEOREM 6.23 *Let* $\gamma > 1$, $\beta = \gamma - 1$ *if* $i = 1$ *and* $\gamma > 0$, $\beta = \gamma + \frac{1}{2}$ *if* $i = 2$. *Then we have for* $i = 1, 2, 3$*:*

(a) *if* $H \in \mathcal{D}(\mathcal{R}_{i,\gamma})$ *then* $G \in \mathcal{D}(\mathcal{R}_{i,\beta})$;

(b) *if H fulfills* $(C_{i,\gamma})$ *then G fulfills* $(C_{i,\beta})$;

(c) *if G fulfills* $(C_{i,\beta})$ *then* $H \in \mathcal{D}(\mathcal{R}_{i,\gamma})$.

A fine analysis of generalized Pareto type distributions H (Frechet class) is further derived in [28].

Theorem 6.23 (b) says that transformation (6.6) of size distribution is stable with respect to the domain of attraction. Takahashi & Sibuya ([113], [114]) tried to develop Theorem 6.23 for applications in metallography, namely for the prediction of extremal particle size based on observation of maximal profiles from planar section of a material specimen. Typically a parametric model for H is suggested which belongs to

a domain of attraction, from (b) in Theorem 6.23 G belongs to the same domain of attraction. From the observation the normalizing constants in (6.52) for G can be estimated and the aim is to get normalizing constants a_n, b_n for H. Then one can approximate the distribution $H^n(t)$ by $\mathcal{R}((t - b_n)/a_n)$.

[113] reformulated (6.6) in terms of areas (of great circle of spherical particles and of sections) and obtained results analogous to Theorem 6.23. They considered the generalized Gamma distribution for the areas of great circles and finally obtained explicit formulas for normalizing constants for both the particle and particle section limiting distribution. The p-quantile x_p of the extremal distribution and its mean $\mathrm{E}X_{(n)}$ are then estimated as

$$x_p = b_n + a_n(-\log(-\log p)), \qquad \mathrm{E}X_{(n)} = b_n + a_n C, \tag{6.59}$$

where $C = 0.5772$ is the Euler constant. The application is not completely straightforward since an optimal sampling procedure is desired. This is further discussed in [114].

6.4.4 Shape factor of spheroidal particles

In engineering applications also the extremal shape factor of particles is of great interest. In [53] the extreme value theory was applied to the unfolding problem of size and shape factor of spheroidal particles.

Consider spheroidal particles with the notation as in Subsections 6.3.1, 6.3.2. We study isotropic uniform random planar sections of the particles. The shape factor is defined in a different way than in Definition 6.11, the reason is that we deal with parametric models in the following and an unbounded support offers a larger variety of known models.

DEFINITION 6.24 *The shape factor* t, T *of a particle, its section is defined as*

$$t = \frac{a^2}{c^2} - 1, \quad T = \frac{A^2}{C^2} - 1,$$

respectively.

It is clear that $0 < c \leq a < \eta$, and $0 \leq t < \omega$, where equalities hold for balls. Values η and ω are fixed nonnegative real numbers (possibly infinity), the upper end-points of the supports of distribution of a and t, respectively. Similarly $0 < A \leq a$ and $0 \leq T \leq t$.

In what follows we restrict our attention to oblate particles only. The theory for prolate particles is analogous. All probability densities used in the following are assumed to exist. An IUR sampling design is used.

Let $h(a,t)$ be the joint probability density function of size and shape factor (a,t) of the particle. The distribution of the planar section size and shape factor (A, T) has joint density

$$N_A g(A,T) = N_V \sqrt{1+T} \int_A^\eta \int_T^\omega \frac{A\, h(a,t)\mathrm{d}t\mathrm{d}a}{\sqrt{t}\sqrt{1+t}\sqrt{t-T}\sqrt{a^2-A^2}}. \quad (6.60)$$

Here a formula of Cruz-Orive [19, (6b)] was adapted, since the shape factor of excentricity $t' = 1 - c^2/a^2 \in [0,1]$ is used there.

The joint distribution of the original size a and the profile shape factor T is needed as well.

LEMMA 6.25 *For the joint probability densities* $z(a,T)$, $h(a,t)$ *of* (a,T) *and* (a,t), *respectively, it holds in the oblate case*

$$z(a,T) = \frac{\sqrt{1+T}}{M_a} \int_T^\omega \frac{h(a,t)\mathrm{d}t}{\sqrt{t}\sqrt{1+t}\sqrt{t-T}}, \quad (6.61)$$

where

$$M_a = \int_0^\omega \left((t+1)^{-1/2} + \sqrt{\frac{t+1}{t}} \arctan\sqrt{t} \right) h(t \mid a)\mathrm{d}t.$$

Proof. Let E be a fixed spheroid (oblate) with parameters (a,t), centered in the origin, with rotational axis along vertical direction. Let F be an isotropic uniform random section plane parametrized by (r,θ,ϕ), where r is the distance from the origin and (θ,ϕ) spherical coordinates of its normal orientation. The probability density of (r,θ) given that F hits X is

$$q(r,\theta \mid a,t) = \bar{b}^{-1} \sin\theta,$$

where $-D(\theta) \le r \le D(\theta)$, $\theta \in [0,\pi/2]$, $D(\theta) = a\left(1 - \frac{t}{t+1}\cos^2\theta\right)^{\frac{1}{2}}$ is a half of width of E in direction θ (independent of ϕ), while the mean width of E is $\bar{b} = 2\pi^{-1}\int_0^\pi D(\theta)\mathrm{d}\theta$. The marginal density is

$$q(\theta \mid a,t) = \int_{-D(\theta)}^{D(\theta)} \bar{b}^{-1} \sin\theta \mathrm{d}r = \frac{2D(\theta)}{\bar{b}} \sin\theta.$$

After a transformation $T = t\sin^2\theta$ which relates the section shape factor to particle parameters we obtain

$$z(T \mid a,t) = \frac{a}{\bar{b}} \sqrt{\frac{T+1}{t+1}} \frac{1}{\sqrt{t(t-T)}}.$$

Now for a random particle of given size a it holds

$$z(T \mid a) = \int_T^\omega z(T \mid a, t) h(t \mid a, \uparrow) \mathrm{d}t,$$

where (cf. (6.9))

$$h(t \mid a, \uparrow) = h(t \mid a) \frac{\bar{b}(a,t)}{\int \bar{b}(a,t) h(t \mid a) \mathrm{d}t}$$

is the conditional probability density of t given the size a and under condition that the particle is hit by the IUR plane. Further it is

$$\begin{aligned} \bar{b}(a,t) &= 2a \int_0^{\pi/2} \left(1 - \frac{t}{t+1} \cos^2 \theta\right)^{1/2} \sin\theta \mathrm{d}\theta \\ &= 2a \int_0^t \sqrt{\frac{T+1}{t+1}} \frac{1}{2\sqrt{t(t-T)}} \mathrm{d}T. \end{aligned}$$

Denote

$$\begin{aligned} M_a &= \frac{2}{a} \int \bar{b}(a,t) h(t \mid a) \mathrm{d}t = \int_0^\omega \frac{h(t|a)}{\sqrt{t(t+1)}} \int_0^t \sqrt{\frac{T+1}{t-T}} \mathrm{d}T \mathrm{d}t \\ &= \int_0^\omega \left[(t+1)^{-1/2} + \sqrt{\frac{t+1}{t}} \arctan\sqrt{t}\right] h(t \mid a) \mathrm{d}t. \end{aligned}$$

Then for conditional probability densities we have

$$z(T \mid a) = \frac{\sqrt{1+T}}{M_a} \int_T^\omega \frac{h(t|a)\mathrm{d}t}{\sqrt{t}\sqrt{1+t}\sqrt{t-T}} \tag{6.62}$$

and since for marginals it holds $h(a) = f(a)$ for all a, also

$$z(a,T) = \frac{\sqrt{1+T}}{M_a} \int_T^\omega \frac{h(a,t)\mathrm{d}t}{\sqrt{t}\sqrt{1+t}\sqrt{t-T}}$$

and the proof is completed. □

The complementary equation which together with (6.61) yields (6.60) is

$$N_A g(A,T) = A N_V \int_A^\eta \frac{M_a z(a,T)}{\sqrt{a^2 - A^2}} \mathrm{d}a. \tag{6.63}$$

Further, denote $z(t) = h(t)$ the marginal density of the transformed shape factor. We have

$$z(T) = \sqrt{1+T} \int_T^\omega \frac{1}{\sqrt{t}\sqrt{1+t}\sqrt{t-T}} \int_0^\eta \frac{h(a,t)}{M_a} \mathrm{d}a \mathrm{d}t. \tag{6.64}$$

6.4.5 Prediction of extremal shape factor

The ideas of Drees & Reiss [28] were shown to be able to extend to extremal shape factor analysis. Let $Z_a, Z, H_a, G_A, G_T, Z_T$ be distribution functions corresponding to densities $z_a, z, h_a, g_A, g_T, z_T$. Here the lower index expresses the conditional distribution, e.g. $h_a(t) = h(t|a)$, while $Z = Z(T)$ is the marginal distribution function. Then it holds (Hlubinka [53]):

THEOREM 6.26 a) *Suppose that for any fixed size* a *the distribution function* $H_a(t)$ *satisfies condition* $C_{i,\gamma}$. *Then* $Z_a \in \mathcal{D}(L_{i,\beta})$, $i = 1, 2, 3$, *where* $\beta = \gamma$ *for* $i = 1$, *and* $\beta = \gamma + 1/2$ *for* $i = 2$.

b) *Assume that* $H_a(t)$ *satisfies the condition* $C_{i,\gamma}$ *uniformly in* a. *Then* $G_A \in \mathcal{D}(L_{i,\beta})$ *for all* A, $i = 1, 2, 3$, *where* $\beta = \gamma$ *for* $i = 1$, *and* $\beta = \gamma + 1/2$ *for* $i = 2$.

c) *Assume that* $H_a(t)$ *satisfies the condition* $C_{i,\gamma}$ *uniformly in* a. *Then* $Z(T) \in \mathcal{D}(L_{i,\beta})$, $i = 1, 2, 3$, *where* $\beta = \gamma$ *for* $i = 1$, *and* $\beta = \gamma + 1/2$ *for* $i = 2$.

Roughly speaking, the theorem says that transformations (6.62), (6.60), (6.64) of the shape factor distribution given size are stable with respect to the domain of attraction. For practical application one needs to estimate the normalizing constants a_n, b_n, a_n', b_n' such that, conditioned by the particle size a, the convergence in distribution

$$\frac{t_{(n)} - b_n}{a_n} \xrightarrow{d} \Lambda \qquad \frac{T_{(n)} - b_n'}{a_n'} \xrightarrow{d} \Lambda,$$

takes place, where $T_{(n)}$ is the maximum of n independent observations, and Λ is a random variable with extremal type of distribution.

The applicability of assertion a) in Theorem 6.26 is investigated in [53] as the case of known particle size a. Since a is in practice unknown it cannot be directly applied to measured data and it is only briefly discussed in the following.

Let us suppose that the distribution of t given a is a Gamma distribution with the density $h_a(t)$

$$h_a(t; \alpha, \mu) = \frac{t^{\alpha-1}\mu^\alpha}{\Gamma(\alpha)} e^{-\mu t}, \tag{6.65}$$

where both $\alpha = \alpha(a)$ and $\mu = \mu(a)$ possibly depend on the condition a. Recall that Gamma distribution belongs to the domain of attraction of Gumbel distribution with distribution function $L(a) = \exp\{-e^{-a}\}$.

THEOREM 6.27 *Assume that for any fixed size* $\mathbf{a}$ *the shape factor* $\mathbf{t}$ *follows Gamma distribution. Then both* $\mathbf{t}$ *and* T *(conditioned by* $\mathbf{a}$*) belong to the Gumbel domain of attraction and their normalizing constants are*

$$a_n = \frac{1}{\mu}, \qquad b_n = \frac{1}{\mu}\left[\log n + (\alpha - 1)\log\log n + \log\frac{1}{\Gamma(\alpha)}\right], \tag{6.66}$$

$$a_n' = \frac{1}{\mu}, \qquad b_n' = \frac{1}{\mu}\left[\log n + \left(\alpha - \frac{3}{2}\right)\log\log n + \log\frac{\sqrt{\pi}}{M_a\Gamma(\alpha)}\right], \tag{6.67}$$

respectively.

Proof.: Formula (6.66) is known, see e.g. [112, Proposition 4, Example 2], also Exercise 6.22. Formula (6.67) is proved in [53] as follows. The behaviour of $1 - Z_a(T)$ as $T \to \infty$ is investigated to apply (6.55). Integrating (6.62) one obtains

$$1 - Z_a(T) = \tag{6.68}$$

$$= \frac{1}{M_a}\int_T^\omega \left[\frac{\sqrt{1+T}\sqrt{t-T}}{\sqrt{t}\sqrt{1+t}} + \sqrt{\frac{1+t}{t}}\arctan\sqrt{\frac{t-T}{1+T}}\right] h_a(t)\mathrm{d}t,$$

and using (6.65) and the substitution $w = t + T$ one obtains that

$$\begin{aligned} 1 - Z_a(T) &= \frac{\mu^\alpha T^{\alpha-3/2}}{M_a\Gamma(\alpha)}\mathrm{e}^{-\mu T}\int_0^\infty \mathrm{e}^{-\mu w}\left(1 + \frac{w}{T}\right)^{\alpha-3/2} \\ &\times \left(\sqrt{\frac{1+T}{1+w+T}}\sqrt{w} + \sqrt{1+T+w}\arctan\sqrt{\frac{w}{1+T}}\right)\mathrm{d}w. \end{aligned}$$

Now since

$$\sqrt{\frac{1+T}{1+w+T}} \to 1, \quad \left(1 + \frac{w}{T}\right)^{\alpha-3/2} \to 1,$$

$$\sqrt{1+T+w}\arctan\sqrt{\frac{w}{1+T}} \to \sqrt{w}$$

as $T \to \infty$, one can conclude that for large T the tail of the distribution fulfills

$$1 - Z_a(T) \approx \frac{\mu^\alpha T^{\alpha-3/2}}{M_a\Gamma(\alpha)}\mathrm{e}^{-\mu T}\int_0^\infty 2\sqrt{w}\mathrm{e}^{-\mu w}\mathrm{d}w = \frac{2\mu^{\alpha-\frac{3}{2}}T^{\alpha-\frac{3}{2}}}{M_a\Gamma(\alpha)}\mathrm{e}^{-\mu T}\Gamma(\tfrac{3}{2}). \tag{6.69}$$

Hence we see that in (6.55)

$$B = \frac{\sqrt{\pi}\mu^{\alpha-\frac{3}{2}}}{M_a\Gamma(\alpha)}, \quad b = \alpha - \frac{3}{2}, \quad \delta = \mu, \quad d = 1,$$

and using (6.56), the proof is complete. □

A natural question arises whether it is possible to get a similar result without the assumption of known particle size. Theoretical bases are here assertions (b), (c) in Theorem 6.26, where moreover the uniformity in the conditions $(C_{1,\gamma})$ – (C_3) is assumed. This need not be satisfied in simple models, see Exercise 6.28. The use of a bivariate size-shape factor distribution model is unavoidable, and because of complexity of relations a simple model serves as a starting point in the next subsection.

EXERCISE 6.28 *Assume that*

$$(\log a,\ \log t) \sim N((\mu_1, \mu_2), \Sigma)$$

is bivariate Gaussian, $\Sigma = \begin{pmatrix} \sigma_1^2 & \rho\sigma_1\sigma_2 \\ \rho\sigma_1\sigma_2 & \sigma_2^2 \end{pmatrix}$. *We have conditionally*

$$\log t \mid a \sim N(\mu_2 + \frac{\rho\sigma_2}{\sigma_1}(\log a - \mu_1), \sigma_2^2(1-\rho^2)).$$

It follows that $t \mid a$ *is log-Gaussian for each* a *and belongs to* $\mathcal{D}(\mathcal{R}_3)$ *according to [112]. Show that the uniformity condition from (b) in Theorem 6.26 is not fulfilled.*

6.4.6 Farlie-Gumbel-Morgenstern distribution

Recall that a bivariate continuous *Farlie-Gumbel-Morgenstern* (FGM) type of distribution is given by

$$h(x,y) = h_1(x)h_2(y)\Big(1 + \lambda\big(2H_1(x) - 1\big)\big(2H_2(y) - 1\big)\Big), \qquad (6.70)$$

where $|\lambda| < 1$, h_1 and h_2 are the marginal densities of h and H_1, H_2 are the corresponding distribution functions. The uniformity condition in Theorem 6.26 is fulfilled for the FGM system of distributions, as proved in [52]:

THEOREM 6.29 *Consider that a joint density* $h(x,y)$ *is from the FGM class. If the conditional distributions* $h_x(y)$ *satisfy condition* $C_{i,\alpha}$ *for some* i *then they satisfy it uniformly in* x.

Normalizing constants of the original and section shape factor will be derived assuming that the joint distribution of (a,t) has form

$$h(a,t) = \frac{1}{\beta}\mu e^{-\mu t}[1+\lambda(2a/\beta-1)(1-2e^{-\mu t})], \quad 0 \le a \le \beta,\ t \ge 0, \quad (6.71)$$

$h(a,t) = 0$ else, that means FGM uniform/exponential with parameters $\mu > 0$, $|\lambda| < 1$, $\beta > 0$. In [53] also the exponential/exponential case is considered.

Concerning the normalizing constants for the original shape factor given size a (which belongs to the Gumbel domain of attraction) we have

$$\begin{aligned} 1 - H_a(t) &= \int_t^\infty \mu e^{-\mu u}[1 + \lambda\{2a/\beta - 1\}\{1 - 2e^{-\mu u}\}]du \\ &= \left[1 + \lambda\left\{\frac{2a}{\beta} - 1\right\}\right] e^{-\mu t} - \lambda\left\{\frac{2a}{\beta} - 1\right\} e^{-2\mu t}, \end{aligned} \tag{6.72}$$

it is easy to conclude (Exercise 6.32)

$$\begin{aligned} a_n &= \frac{1}{\mu} \\ b_n &= \frac{1}{\mu}\left[\log n + \log\{1 + \lambda(2a/\beta - 1)\}\right]. \end{aligned} \tag{6.73}$$

Next consider the observed quantities.

THEOREM 6.30 *Assume that the joint distribution of spheroid size and shape factor* (a,t) *is bivariate FGM with density* (6.71). *Then both the conditional distribution of* $(T \mid A)$ *and the marginal distribution of* T *belong to the Gumbel domain of attraction for sample maximum and their normalizing constants are given by formulas*

$$\begin{aligned} a'_n &= \frac{1}{\mu}, \\ \mu b'_n &= \log n - \frac{1}{2}\log\log n + \\ &+ \log\left\{\frac{A\sqrt{\pi}}{\bar{b}g(A)}\left(\frac{1-\lambda}{\beta}\log\left(\frac{\beta + \sqrt{\beta^2 - A^2}}{A}\right) + \frac{2\lambda}{\beta^2}\sqrt{\beta^2 - A^2}\right)\right\}, \end{aligned} \tag{6.74}$$

and

$$\begin{aligned} a''_n &= \frac{1}{\mu} \\ \mu b''_n &= \left[\log n - \frac{1}{2}\log\log n + \log\left\{\sqrt{\pi}\frac{1-\lambda}{\beta}I_1 + \frac{2\lambda}{\beta^2}I_2\right\}\right], \end{aligned} \tag{6.75}$$

respectively, where

$$I_1 = \int_0^\beta \frac{1}{M_a}da, \quad I_2 = \int_0^\beta \frac{a}{M_a}da. \tag{6.76}$$

Proof. We start with the conditional distribution with tail ($\bar{b}$ is the mean width)

$$1 - G_A(T) = \frac{A}{\bar{b}g(A)}$$
$$\times \int_A^\beta \frac{1}{\beta\sqrt{a^2 - A^2}} \int_T^\infty \left(\sqrt{\frac{(1+T)(t-T)}{t(1+t)}} + \sqrt{\frac{1+t}{t}} \arctan \sqrt{\frac{t-T}{1+T}} \right)$$
$$\times \mu e^{-\mu t} \left(1 + \lambda\{2a/\beta - 1\}\{1 - 2e^{-\mu t}\}\right) dt da. \tag{6.77}$$

Using (6.55), (6.56) we obtain (details are left to Exercise 6.32) (6.74).

Finally for the marginal distribution it holds

$$1 - G(T) = \int_T^\infty \sqrt{1+s} \int_s^\infty \frac{1}{\sqrt{t(1+t)(t-s)}} \int_0^\beta \frac{\mu e^{-\mu t}[1 + \lambda\{2a/\beta - 1\}\{1 - 2e^{-\mu t}\}]}{\beta M_a} da\, dt\, ds \tag{6.78}$$

Again using (6.55), (6.56) we obtain normalizing constants (6.75), details are left to Exercise 6.32.

□

The idea is to estimate the constants in (6.74) or (6.75) from the planar section data and then, via parameters of the model, try to calculate the normalizing constants (6.73) for original data. Thus the prediction of extremes can be realized.

EXERCISE 6.31 *Show that the correlation coefficient between the components of FGM distributed random vector lies in the range* $-\frac{1}{\pi}$ *and* $\frac{1}{\pi}$.

EXERCISE 6.32 *Derive formulas* (6.73), (6.74), (6.75). *Hint: Use* (6.55), (6.56) *and formulas in the proof of Theorem 6.30.*

6.4.7 Simulation study of shape factor extremes

In this subsection the utility of extreme value theory for the extremal shape factor prediction is tested in a simulation study. The steps of the algorithm are described in detail in [6]. A sample of N isotropic oblate spheroids is simulated according to the uniform/exponential FGM distribution. A bivariate size-shape factor histogram of IUR particle sections is the input for the estimation procedure. The transformation from the spatial to the planar distribution of the size and the shape factor given by (6.60) is observed in Fig. 6.10. To approximate the conditional

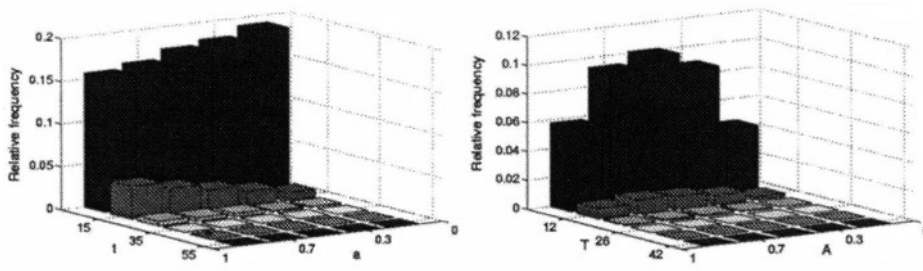

Figure 6.10. **The spatial (left) and planar (right) histogram of bivariate size-shape distribution from simulated data. The spatial parameteres: $\beta = 1$, $\mu = 0.2$, $\lambda = 0.9$.**

distribution of the section shape factor T (given size A), J size classes are used. For each $j = 1, \ldots, J$ find the vector $\boldsymbol{T}^j = (T_1^j, \ldots, T_k^j)$ of k largest observations of section shape factor and use (6.58) with T_i^j instead of x_i : calculate $\overline{T^j} = \frac{1}{k}\sum_{i=1}^{k} T_i^j$. Then the estimators of a_n', b_n' are $\hat{a}_n' = \overline{T^j} - T_k^j$ and $\hat{b}_n' = \hat{a}_n' \log k + T_k^j$. Here $n = n_j$ is the sample size of particle sections in the selected j-th class.

The goal of uniform marginal size distribution is that an asymptotically unbiased estimator $\hat{\beta} = \max_i A_i$ for β is available. From (6.60) the marginal size density $g(A)$ can be obtained, putting it into (6.74) a system of two equations for unknown λ, μ is obtained:

$$\begin{aligned} a_n' &= \tfrac{1}{\mu} \\ b_n' &= \tfrac{1}{\mu}\left[\log n - \tfrac{1}{2}\log\log n \right. \\ &\qquad \left. + \log\left\{\sqrt{\pi}\,\frac{\lambda\left[\frac{2}{\beta^2}S - \frac{1}{\beta}L\right] + \frac{L}{\beta}}{\lambda[K(\mu) - K(2\mu)]\left[\frac{2}{\beta^2}S - \frac{1}{\beta}L\right] + \frac{K(\mu)}{\beta}L}\right\}\right], \end{aligned} \tag{6.79}$$

where

$$K(\mu) = \int_0^\infty \left[(t+1)^{-1/2} + \sqrt{\frac{t+1}{t}}\arctan\sqrt{t}\right]\mu\exp\{-\mu t\}\mathrm{d}t$$

and

$$L = L(\beta, A) = \log\left(\frac{\beta + \sqrt{\beta^2 - A^2}}{A}\right), \quad S = S(\beta, A) = \sqrt{\beta^2 - A^2}.$$

The second equation of (6.79) can be solved explicitely as

Table 6.2. Simulation results for different setting of the parameter λ, the estimate of $\widehat{\beta} = \max_i A_i$, $\widehat{\mu} = 1/m \sum_{i=1}^{m} T_i$ and estimated values for a_n, b_n, $\mathrm{E}t_{(n)}$, $q_{.95}$ given $n = 10^4$, $a = 0.98$.

λ	$\hat{\lambda}$	$\hat{\beta}$	$\hat{\mu}$	$\hat{a}_n$	$\hat{b}_n$	$\widehat{\mathrm{E}t_{(n)}}$	$\hat{q}_{0.95}$
0.9	0.91	1	0.21	4.76	46.84	49.60	60.98
0.5	0.45	1	0.21	4.76	45.57	48.32	59.71
0.0	0.02	1	0.20	5.00	46.15	49.03	61.00
-0.9	-0.70	1	0.22	4.54	36.80	39.42	50.28

$$\lambda = \frac{\frac{1}{\beta} L}{\frac{2}{\beta^2} S - \frac{1}{\beta} L} \frac{\exp\left(\frac{b'_n}{a'_n}\right) \frac{\sqrt{\log n}}{n\sqrt{\pi}} K(\mu) - 1}{1 + \exp\left(\frac{b'_n}{a'_n}\right) \frac{\sqrt{\log n}}{n\sqrt{\pi}} [K(2\mu) - K(\mu)]}. \tag{6.80}$$

The conditional rather than the marginal distribution of A is used

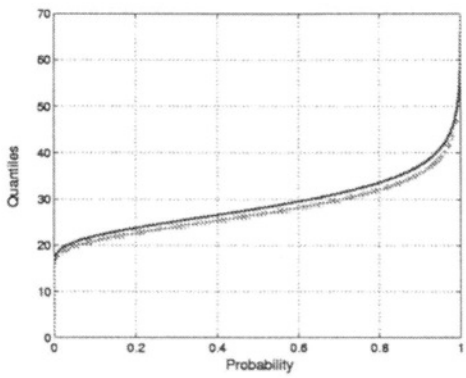

Figure 6.11. For $\lambda = 0.9$, $n = 100$, $x = 0.98$ the lower grey line indicates the limiting distribution with estimated a_n, b_n and the solid black line corresponds to the true distribution $H_a^{max}(t)$.

for the estimation of λ since it is computationally easier. Typically, a class of high j is used for this purpose, for more details see [6]. In order to estimate a_n, b_n we plug in (6.73) the estimators $\widehat{\lambda}$, $\widehat{\beta}$, $\widehat{\mu}$. Using Theorem 6.30 for the maximum conditional shape factor $(t_{(n)}|a)$ one can approximate its distribution function $H_a^{\max}(t) = (H_a(t))^n$ (independence takes place) by the Gumbel distribution. Then the quantiles of $(t_{(n)}|a)$ are estimated (cf. (6.59)) by $\hat{q}_p = \hat{b}_n + \hat{a}_n(-\log(-\log\ p))$, $0 < p < 1$, and $\widehat{\mathrm{E}t_{(n)}} = \hat{b}_n + \hat{a}_n C$. Numerical results are presented in Table 6.2 for simulations of size $N \approx 10^5$, with $\beta = 1, \mu = 0.2$ and four levels of λ. As expected when conditioning by large a the estimators of the

characteristics $Et_{(n)}$, q_p suggest decreasing tendency with decreasing λ. A comparison between the true distribution of the maximum $H_a^{\max}(t)$ (with known parameters) and its limiting version $\mathcal{K}_3(\frac{t-b_n}{a_n})$, $\mathcal{K}_3$ Gumbel, based on the reconstructed normalizing constants a_n, b_n is presented in Fig. 6.11 for the case $\lambda = 0.9$. The curves differ since the estimator $\hat{\mu}$ was employed, on the other hand the curves coincide if the true value μ is employed. A proper estimation of μ is therefore strongly needed.

References

[1] A. Baddeley. An anisotropic sampling design. In W. Nagel, editor, *Geobild'85,* pages 92–97, Jena, 1985. Friedrich–Schiller Universität.

[2] A. Baddeley. Crash course in stochastic geometry, sampling and censoring. In O.E. Barndorff-Nielsen, W.S. Kendall, and M.N.M. van Lieshout, editors, *Stochastic Geometry. Likelihood and Computation,* pages 1–78, Boca Raton, 1999. Chapman & Hall/CRC.

[3] A. Baddeley and L. M. Cruz-Orive. The Rao–Blackwell theorem in stereology and some counterexamples. *Adv. Appl. Probab.,* 27:2–19, 1995.

[4] A. J. Baddeley, H. J. G. Gundersen, and L. M. Cruz-Orive. Estimation of surface area from vertical sections. *J. Microsc.,* 142:259–276, 1986.

[5] V. Beneš. On second order formulas in anisotropic stereology. *Adv. Appl. Probab.,* 27/2:326–343, 1995.

[6] V. Beneš, K. Bodlák, and D. Hlubinka. Stereology of extremes; bivariate models and computation. *Method. Comp. Appl. Probab.,* 5:289–308, 2003.

[7] V. Beneš, K. Bodlák, J. Møller, and R. Waagepetersen. Application of log Gaussian Cox processes in disease mapping. In J. Mateu, D. Holland, and W. Gonzales-Mantiega, editors, *ISI Int. Conf. Environmental Statistics and Health,* pages 95–105. Universidade de Santiago de Compostella, 2003.

[8] V. Beneš, V. Bouše, M. Slámová, V. Suchánek, and K. Voleník. Bubble structure of enamel coatings and its determination. *Ceramics–Silikáty,* 38:4–8,1994.

[9] V. Beneš, J. Chadoeuf, and A. Kretzschmar. Properties of length estimation in spatial fibre models. *Environmetrics,* 8:397–407, 1997.

[10] V. Beneš, J. Chadoeuf, and J. Ohser. On some characteristics of anisotropic fibre processes. *Math. Nachrichten,* 169:5–17, 1994.

[11] V. Beneš and A. M. Gokhale. Planar anisotropy revisited. *Kybernetika,* 36/2:149–164, 2000.

[12] V. Beneš, M. Hlawiczková, and K. Voleník. Stereological estimation of integral mixed curvature with application. *J. Microscopy,* 200/1:26–31, 2000.

[13] V. Beneš, M. Jiruše, and M. Slámová. Stereological unfolding of the trivariate size-shape-orientation distribution of spheroidal particles with application. *Acta Mater.*, 45.3:1105-1113, 1997.

[14] V. Beneš, J. Rataj, P. Krejčíř, and J. Ohser. Projection measures and estimation variances of intensities. *Statistics,* 32:369–393, 1999.

[15] K. Bodlák, A. Balasundaram, A. M. Gokhale, and V. Beneš. Three-dimensional bivariate size-orientation distribution of microcracks. *Acta Materialia,* 51/11:3131–3143, 2003.

[16] S. Campi, D. Haas, and W. Weil. Approximation of zonoids by zonotopes in fixed directions. *Comput. Geom.,* 11:419–431, 1994.

[17] J. Chadoeuf and V. Beneš. On some estimation variances in spatial statistics. *Kybernetika,* 30/3:245–262, 1994.

[18] S. S. Chang. Role of gas atmosphere in evolution of microstructure in sintered copper powder. Technical report, University of Florida, Gainesville, PhD. thesis, 1990.

[19] L. M. Cruz-Orive. Particle size-shape distributions; the general spheroid problem. *J. Microscopy,* 107.3:235–253, 1976.

[20] L. M. Cruz-Orive. On the precision of systematic sampling: a review of Matheron's transitive methods. *J. Microscopy,* 153:315–333, 1989.

[21] L. M. Cruz-Orive, H. Hoppeler, O. Mathieu, and E. R. Weibel. Stereology analysis of anisotropic structures using directional statistics. *JRSS, Series C,* 34/1:14–32, 1985.

[22] L. M. Cruz-Orive and C. V. Howard. Estimation of individual feature surface area with the vertical spatial grid. *J. Microscopy*, 178/2:146–151, 1995.

[23] D. J. Daley and D. Vere-Jones. *Introduction to the Theory of Point Processes.* Springer–Verlag, New York, 1988.

[24] L. de Haan. On regular variation and its application to the weak convergence of sample extremes. Technical report, Math. Centre Tracks 32, Mathematisch Centrum, Amsterdam, 1975.

[25] R. T. DeHoff and F. N. Rhines. *Quantitative Microscopy.* McGraw Hill, New York, 1968.

[26] C. R. Dietrich and G. N. Newsam. A fast and exact method for multidimensional Gaussian stochastic simulation. *Water Resources Research,* 29:2861–2869, 1993.

[27] H. Digabel. Détermination practique de la rose des directions. Technical report, 15 fascicules de morphologic mathématique appliquée (6), Fontainebleau, 1976.

[28] H. Drees and R. D. Reiss. Tail behavior in Wicksell's corpuscle problem. In J. Galambos and J. Kátai, editors, *Probability Theory and Applications,* pages 205–220, Dordrecht, 1992. Kluwer.

[29] H. J. G. Gundersen et al. The new stereological tools: disector, fractionator, nucleator and point sampled intercepts and their use in pathological research and diagnostics. *Acta Pathologica Microbiol. et Immun. Scandinavica,* 96:857–881, 1988.

[30] H. J. G. Gundersen et al. Some new, simple and efficient stereological methods and their use in pathological research and diagnostics. *Acta Pathologica Microbiol. et Immun. Scandinavica,* 96:379–394, 1988.

[31] H. Federer. *Geometric Measure Theory.* Springer–Verlag, New York, 1969.

[32] A. Fellous, J. Granara, and K. Krickeberg. Statistics of stationary oriented line Poisson process in the plane. In R. Miles and J. Serra, editors, *Geometric Probability and Biological Structures: Buffon's 200th anniversary,* No 23 in LNBM, Berlin, 1978. Springer.

[33] M. Freehet. Sur les tableaux de correlation dont les marges sont donnees. *Ann. Univ. Lyon, Sec. A,* 14:53–77, 1951.

[34] D. Gamerman. *Markov Chain Monte Carlo. Stochastic Simulation for Bayesian Inference.* Chapman&Hall, London, 1997.

[35] W. Gerlach and J. Ohser. On the accuracy of numerical solutions such as the Wicksell corpuscule problem. *Biometrical J.,* 28:881–7, 1986.

[36] A. M. Gokhale. Unbiased estimation of curve length in 3D using vertical slices. *J. Microscopy,* 159:133–141, 1990.

[37] A. M. Gokhale. Estimation of bivariate size and orientation distribution of microcracks. *Acta Metall. and Mater.,* 44.2:475–485, 1996.

[38] A. M. Gokhale. Estimation of integral mixed surface curvature from vertical metallographic sections. *Acta Mater.,* 46:1741–1748, 1998.

[39] A. M. Gokhale and V. Beneš. Estimation of average particle size from vertical projections. *J. Microscopy,* 191:195–200, 1998.

[40] A. M. Gokhale and J. M. Drury. Efficient measurements of microstructural surface area using trisector. *Metall. Trans.,* 25A:919–928, 1994.

[41] P. Goodey and W. Weil. Zonoids and generalizations. In P. M. Gruber and J. M. Wills, editors, *Handbook of Convex Geometry,* pages 1297–1326, Amsterodam, 1993. North-Holland.

[42] I. S. Gradshtejn and I. M. Ryzhik. *Tables of Integrals, Sums, Series and Products (in Russian).* GIFML, Moscow, 1963.

[43] P.M. Gruber. The space of convex bodies. In P.M. Gruber and J.M. Wills, editors, *Handbook of Convex Geometry,* pages 310–318, Amsterdam, 1993. North-Holland.

[44] X. Gual-Arnau and L. M. Cruz-Orive. Systematic sampling on the circle and on the sphere. *Adv. Appl. Prob. (SGSA),* 32:628–647, 2000.

[45] H. J. G. Gundersen and E. B. Jensen. Stereological estimation of volume-weighted mean volume of arbitrary particles. *J. Microsc.,* 138:127–142, 1985.

[46] U. Hahn and D. Stoyan. Unbiased Stereological estimation of surface area density in gradient surface processes. *Adv. Appl. Probab.,* 31:315–327, 1999.

[47] E.F. Harding and D.G. Kendall (eds.). *Stochastic Geometry.* J. Wiley & Sons, 1974.

[48] H. Heyer. *Probability Measures on Locally Compact Groups.* Springer, Berlin, 1977.

[49] J. E. Hilliard. Specification and measurement of microstructural anisotropy. *Trans. Metall. Soc. AIME,* 224:1201–1211, 1962.

[50] M. Hlawiczková. On a stereological estimator of the average caliper diameter. In I, Saxl V. Beneš, **J. Janáček,** editor, *Proc. S⁴G Int. Conf. on Stereol., Spatial Stat. and Stoch. Geom.,* pages 113-118, Praha, 1999. **JČMF.**

[51] M. Hlawiczková, A. M. Gokhale, and V. Beneš. Bias of a length density estimator based on vertical projections. *J. Microsc.,* 204/3:226–231, 2001.

[52] D. Hlubinka. Shape factor extremes for spheroidal particles in fgm distributions. Technical report, KPMS Preprint 26, Charles University, Prague, 2002.

[53] D. Hlubinka. Stereology of extremes; shape factor of spheroids. *Extremes,* 6:5–24, 2003.

[54] C.V. Howard and M.G. Reed. *Unbiased Stereology. Three-dimensional Measurement in Microscopy.* Bios Scientific, Oxford, 1998.

[55] D. Hug. Contact distributions of boolean models. *Rend. Circ. Matt. Palermo II (Suppl.),* 65:137–181, 2000.

[56] D. Hug, G. Last, and W. Weil. A survey on contact distribution functions. In K. Mecke and D. Stoyan, editors, *Statistical Physics and Spatial Statistics, Lecture Notes in Physics 600,* pages 317–357, 2002.

[57] O. Kallenberg. *Random Measures.* Akademie-Verlag, Berlin, 1983.

[58] O. Kallenberg. *Foundations of modern probability.* Springer Verlag, New York, 1997.

[59] K. Kanatani. Stereological determination of structural anisotropy. *Int. J. Eng. Sci.,* 22:531–546, 1984.

[60] J. Kerstan, K. Matthes, and J. Mecke. *Unbegrenzt teilbare Punktprozesse.* Akademie-Verlag, 1974.

[61] M. Kiderlen. Non-parametric estimation of the directional distribution. *Adv. Appl. Probab. (SGSA),* 33:6–24, 2001.

[62] M. Kiderlen and E.B. Vedel-Jensen. Estimation of the directional measure of planar random sets by digitization. *Adv. Appl. Probab. (SGSA),* 35/3:583–602, 2003.

[63] K. Kieu. Three lectures on systematic geometric sampling. Technical report, University of Aarhus, 1997.

[64] K. Kieu, S. Souchet, and J. Istas. Precision of systematic sampling and transitive methods. *J. Statist. Plan. Inf.,* 77:263–279, 1999.

[65] P. Krejčíř and V. Beneš. Orientation analysis in second-order stereology. *Ada Stereol.,* 15/1:59–64, 1996.

[66] J. Lehmann. *Theory of Point Estimation.* Wadworth & Brooks, California, 1991.

[67] B. A. Mair, M. Rao, and J. M. M. Anderson. Positron emission tomography, Borel measures and weak convergence. *Inverse Problems,* 12:965–976, 1996.

[68] G. Matheron. The theory of regionalized variables and its applications. Technical report, Les Cahiers du Centre de Morphologie Mathématique de Fontainebleau 5, ENSM, Paris, 1971.

[69] G. Matheron. *Random Sets and Integral Geometry.* Wiley, New York, 1975.

[70] P. Mattila. *Geometry of Sets and Measures in Euclidean Spaces.* Cambridge Univ. Press, Cambridge, 1995.

[71] J. Mecke. Formulas for stationary planar fibre processes III - Intersections with fibre systems. *Math. Oper. Statist., Ser. Statist.,* 12:201–210, 1981.

[72] J. Mecke and W. Nagel. Stationäre raumliche Faserprozesse und ihre Schnittzahlrozen. *Elektron. Inf. Kybernet.,* 16:475–483, 1980.

[73] J. Mecke and D. Stoyan. Formulas for stationary planar fibre processes. i. general theory. *Math. Oper. Stat.,* 12:267–279, 1980.

[74] K. Mecke and D. Stoyan eds. *Statistical Physics and Spatial Statistics.* Springer, Berlin, 2000. Lecture Notes in Physics 554.

[75] S.P. Meyn and R.L. Tweedie. *Markov Chains and Stochastic Stability.* Springer, New York, 1993.

[76] P. Mikusinski, H. Sherwood, and M. Taylor. Probabilistic interpretations of copulas and their convex sums. In G. Dall Aglio et al, editor, *Advances in Probability Distributions with Given Marginals,* pages 95–112, Dordrecht, 1991. Kluwer.

[77] R. Miles. Stereological formulae based on planar curve sections of surfaces in space. *J. Microsc.,* 121:21–27, 1981.

[78] J. Møller. Stereological analysis of particles of varying ellipsoidal shape. *J. Appl. Probab.,* 25:322–335, 1988.

[79] J. Møller, A.R. Syversveen, and R.P. Waagepetersen. Log Gaussian Cox processes. *Scandinavian Journal of Statistics,* 25:451–482, 1998.

[80] J. Møller and R. Waagepetersen. *Statistical Inference and Simulation for Spatial Point Processes.* Chapman& Hall/CRC, 2003.

[81] P. Monestiez, P. Kretzschmar, and J. Chadoeuf. Modelling natural burrow systems in soil by fibre processes: Monte Carlo tests on independence of fibre characteristics. *Acta Stereol.,* 12:237–242, 1993.

[82] T. Mrkvička. Estimation variances for Poisson process of compact sets. *Adv. Appl. Prob.,* 33:765–772, 2001.

[83] W. Nagel. Dünne Schnitte von stationären räumlichen Faserprozessen. *Math. Oper. Statist.,* 14:569–576, 1983.

[84] J. Ohser. Variances of different intensity estimators of the specific line length. Technical report, Stoch. Geom., Geom. Statist., Stereol., Oberwolfach, unpublished, 1991.

[85] J. Ohser and F. Mücklich. Stereology for some classes of polyhedrons. *Adv. Appl. Prob.,* 27.2:384–396, 1995.

[86] J. Ohser and F. Mücklich. *Statistical Analysis of Microstructures in Materials Science.* Wiley, New York, 2000.

[87] J. Ohser and K. Sandau. Considerations about the estimation of size distribution in Wicksell's corpuscule problem. In K. Mecke and D. Stoyan, editors, *Statistical Physics and Spatial Statistics, Lecture Notes in Physics 554,* 1999.

[88] Z. Pawlas and V. Beneš. Central limit theorem for random measures generated by a stationary poisson point process of compact sets. *Mathematische Nachrichten,* 267, 2004.

[89] S. Pohlmann, J. Mecke, and D. Stoyan. Stereological formulas for stationary surface processes. *Math. Oper. Statist.,* 12:329–440, 1981.

[90] M. Prokešová. Bayesian MCMC estimation of the rose of directions. *Kybernetika,* 39/3:701–718, 2003.

[91] J. Rataj. On set covariance and three-point test sets. *Czech. Math. J.,* to appear.

[92] J. Rataj. Estimation of oriented direction distribution of a planar body. *Adv. Appl. Probab.,* 28:394–404, 1996.

[93] J. Rataj. Determination of spherical area measures by means of dilation volume. *Math. Nachr.,* 235:143–162, 2002.

[94] J. Rataj and I. Saxl. Analysis of planar anisotropy by means of the Steiner compact. *J. Appl. Probab.,* 26:490–502, 1989.

[95] J. Rataj and I. Saxl. Estimation of direction distribution of a planar fibre system. *Acta Stereol.,* 11/I:631–637, 1992.

[96] J. Rataj and M. Zähle. Curvatures and currents for unions of sets with positive reach ii. *Ann. Glob. Anal. Geom.,* 20:1–21, 2001.

[97] L. A. Santaló. *Integral Geometry and Geometric Probability.* Addison Wesley, Reading, MA, 1976.

[98] K. Schladitz. Estimation of the intensity of stationary flat processes. *Adv. Appl. Probab.,* 32:114–139, 2000.

[99] R. Schneider. *Convex Bodies: The Brunn-Minkowski Theory.* Cambridge University Press, 1993.

[100] R. Schneider. On the mean normal measures of a particle process. *Adv. Appl. Prob.,* 33:25–38, 2001.

[101] R. Schneider and W. Weil. Zonoids and related topics. In P. M. Gruber and J. M. Wills, editors, *Convexity and its Applications,* pages 296–317, Basel, 1983. Birkhäuser.

[102] R. Schneider and W. Weil. *Integralgeometrie.* B.G.Teubner, 1992.

[103] R. Schneider and W. Weil. *Stochaatische Geometrie.* B.G Teubner, Stuttgart - Leipzig, 2000.

[104] R. Schneider and J.A. Wieacker. Integral geometry. In *Handbook of Convex Geometry,* pages 1349–1390. North Holland, Amsterdam, 1993.

[105] B. Silverman. *Kernel Density Estimation.* Wiley, New York, 1986.

[106] B. W. Silverman, D. W. Nychka M. C. Jones, and J. D. Wilson. A smoothed EM approach to indirect estimation problems, with particular reference to stereology and emission tomography. *J. R. Statist. Soc. B,* 52:271–324, 1990.

[107] M. Slámová. Porušování kompozitních **materiálů.** Technical report, Dissertation, Charles Univ. Prague, 1996.

[108] D. Stoyan and V. Beneš. Anisotropy analysis for particle systems. *J. Microscopy,* 164/2:159–168, 1991.

[109] D. Stoyan, W.S. Kendall, and J. Mecke. *Stochastic Geometry and Its Applications.* Wiley, New York, 1995.

[110] D. Stoyan and J. Ohser. Correlations between planar random structures, with an ecological application. *Biom. J.,* 24:631–647, 1982.

[111] D. Stoyan and J. Ohser. Cross-correlation measures for weighted random measures (in Russian). *Teor. Veroyatn. Primen.,* 29:328–347, 1984.

[112] R. Takahashi. Normalizing constants of a distribution which belongs to the domain of attraction of the Gumbel distribution. *Stat. Prob. Letters,* 5:197–200, 1987.

[113] R. Takahashi and M. Sibuya. The maximum size of the planar sections of random spheres and its application to metallurgy. *Ann. Inst. Statist. Math.,* 48.1:361–377, 1996.

[114] R. Takahashi and M. Sibuya. Prediction of the maximum size in Wicksell's corpuscle problem. *Ann. Inst. Math.,* 50.2:361–377, 1998.

[115] M.N.M. van Lieshout. *Markov Point Processes and Their Applications.* World Scientific, Singapore, 2000.

[116] E.B. Vedel-Jensen. *Local Stereology.* World Scientific, Singapore, 1998.

[117] G. S. Watson. Estimating functionals of particle size distribution. *Biometrika,* 58:483–490, 1971.

[118] E.R. Weibel. *Practical Methods for Biological Morphometry. Vol. I: Stereological Methods.* Academic Press, London, 1980.

[119] W. Weil. The mean normal distribution of stationary random sets and particle process. In D. Jeulin, editor, *Advances in Theory and Applications of Random Sets,* pages 21–33, Singapore, 1997. World Scientific.

[120] W. Weil and J. A. Wieacker. Stochastic geometry. In P. M. Gruber and J. M. Wills, editors, *Handbook of Convex Geometry,* pages 1393–1438, New York, 1993. Elsevier.

[121] I. Weissman. Estimation of parameters and large quantiles based on the k largest observations. *J. American Stat. Assoc.,* 73.364:812–815, 1978.

[122] S. D. Wicksell. The corpuscule problem. A mahematical study of a biometrical problem. *Biometrika,* 17:84–88, 1925.

[123] J.A. Wieacker. Translative Poincaré formulae for Hausdorff rectifiable sets. *Geom. Dedicata,* 1984:231–248, 1984.

[124] A.T.A. Wood and G. Chan. Simulation of stationary Gaussian processes in $[0,1]^d$. *Journal of Computational and Graphical Statistics,* 3:409–432, 1994.

[125] M. Zähle. Random processes of Hausdorff rectifiable closed sets. *Math. Nachrichten,* 108:49–72, 1982.

[126] M. Zähle. Integral and current representation of Federer's curvature measures. *Arch. Math.,* 46:557–567, 1986.

[127] P. Zeman. Objective assessment of risk maps of tick-borne encephalitis and lyme boreliosis based on spatial patterns of located cases. *International Journal of Epidemiology,* 26:1121–1130, 1997.

Index